UNIVERSITY OF NATURAL RESOURCES
AND LIFE SCIENCES, VIENNA

Department of Biotechnology

Institute of Bioprocess Science and Engineering

Downstream processing of enveloped virus-like particles by polymer grafted media

To obtain the Doctor of Philosophy degree

at the University of Natural Resources and Life Sciences Vienna

Submitted by

Patrícia Pereira Aguilar, MSc.

Supervisor: Alois Jungbauer, Univ.Prof. Dipl. -Ing. Dr.nat.techn.

Vienna, January 2020

BioToP Biomolecular Technology of Proteins

VIBT Vienna Institute of Bio Technology

FWF Der Wissenschaftsfonds.

Acknowledgments

First of all, I would like to thank my supervisor and mentor Professor Alois Jungbauer, for his guidance and support throughout my PhD journey. His creativity and scientific enthusiasm have always been inspiring to me. I would also like to thank him for opening the doors to an incredible network of world-renowned scientists.

I also want to thank Professor Giorgio Carta and all his students for receiving and supporting me during my stay abroad in his "Bioseparations Engineering Group" at UVa in Charlottesville, USA.

I am thankful to the "VLP team" Petra Steppert, Viktoria Wetter, Katrin Reiter and Tobias Schneider, for all the fruitful discussions, help in the lab, scientific input and personal support. I would also like to thank Eva Berger for her help in the lab and for always knowing where everything is. Many thanks also to the entire Downstream Processing Group, especially the "5th Floor Gangstas" Susi, Mark, Stephan, Alex and Tobias, for all the scientific and specially the non-scientific support. A special thanks also to Peter Satzer for all the support in the final stretch.

Thanks to all people involved in the BioTop program, especially Christa Jakopitsch (for helping me in the cumbersome world of German-written bureaucracy) and Grete Furtmüller for their administrative support. Thanks Michael for the infinite coffee supply and friendship.

Special thanks to the "Tugas" Lídia, Catarina, Francisca, Duarte, Gonçalo and Gregory, who brought Portugal closer to Austria, to Ana Carolina, Shelly, Águas, Mari, Rita, Dani, Inês, Filipa e João, who even being far were always present, to my CrossFit partner and friend Roxie.

I am enormously grateful to my family, I especially thank my parents Zi and Paulo for their unconditional love and support, for encouraging me to always pursue my dreams. To my grandparents, Isilda and Zé, thank you for always caring for me, for always being proud of me.

Last but definitely not least, thank you Johannes for making Vienna my second home, for always being there for me, for your support, for your patience, for your love.

Abstract

Downstream processing (DSP) and analytical technologies are the limiting factors in enveloped virus-like particle (eVLP) manufacturing, especially due to the complex structure and composition of eVLPs and their contamination with host cell derived bionanoparticles, which have similar size, composition and surface properties. Nevertheless, despite the fact that productivities of currently available eVLP manufacturing platforms are still below demand, several eVLP-based products are currently under investigation in pre-clinical and clinical trials for applications in the fields of vaccine technology, gene therapy and drug delivery. Polymer-grafted chromatography media are widely used in biopharmaceuticals DSP and are known for their high binding capacity and excellent selectivity. A DSP strategy was developed for the capture and purification of HIV-1 gag VLPs directly from cell culture supernatant, using a polymer-grafted anion-exchanger. In order to accelerate DSP development, a high-throughput method for particle detection and semi-quantification was developed based on at-line multi-angle light scattering (MALS) measurements. Due to the lack of standard analytical methods for eVLP quantification and in order to allow a fair comparison between the strategy developed here, and the commonly used DSP strategies for eVLPs, four additional DSP strategies were developed for the capture and purification of HIV-1 gag VLPs, using the same starting material and the same set of analytical tools. In addition to the polymer-grafted anion-exchanger, two different anion-exchange convective supports were tested; a membrane adsorber and a monolith. Additionally, flow-through and Heparin-affinity chromatography were tested. The performance of the developed DSP strategies was evaluated regarding dynamic binding capacity, recovery, separation of different particle populations, and product purity. The membrane adsorber showed the highest binding capacity and recovery, but particle separation was not possible. Despite having a lower binding capacity, the combination of flow-through and Heparin-affinity chromatography allowed for the recovery of highly pure HIV-1 gag VLPs. The developed strategies allowed the purification of correctly assembled eVLPs and their separation from critical impurities, such as host-cell derived bionanoparticles and chromatin, in either one or two steps, thereby reducing DSP complexity and consequently improving eVLP manufacturing.

Zusammenfassung

Downstream Processing (DSP) und analytische Methoden sind die limitierenden Faktoren bei der Herstellung von umhüllten virusähnlichen Partikeln (eVLP). Dies erklärt sich aus der komplexen Struktur und Zusammensetzung von eVLPs und der Verunreinigung mit Bionanopartikeln aus den Wirtszellen. Diese weisen eine ähnliche Größe, Zusammensetzung und Oberfläche auf. Trotz der Tatsache, dass die Produktivität der derzeit verfügbaren eVLP-Produktionsplattformen immer noch unter den gewünschten Anforderungen liegt, werden derzeit mehrere auf eVLP basierende Produkte in vorklinischen und klinischen Studien für Anwendungen in den Bereichen der Impfstofftechnologie, Gentherapie und Arzneimittel geprüft. Chromatographiemedien mit Polymerbürsten zur Oberflächenvergrößerung werden häufig in der DSP von Biopharmazeutika verwendet und sie sind für ihre hohe Bindungskapazität und hervorragende Selektivität bekannt. Es wurde eine DSP-Strategie unter Verwendung eines Anionenaustauschers mit Polymerbürsten zur direkten Isolation und Reinigung von HIV-1-gag-VLPs aus Zellkulturüberstand entwickelt. Um die DSP-Entwicklung zu beschleunigen, wurde ein Hochdurchsatzverfahren basierend auf MALS-Messungen (At-Line Multi-Angle Light Scattering) zur Partikeldetektion und Quantifizierung etabliert. Da Standardanalysemethoden für die eVLP-Quantifizierung nicht vorhanden waren und um einen fairen Vergleich zwischen den entwickelten und den häufig verwendeten DSP-Strategien für eVLPs zu ermöglichen, wurden vier zusätzliche DSP-Strategien mit gleichem Ausgangsmaterial und gleichen Analysemethoden für die Isolation von HIV-1-gag-VLPs etabliert. Zusätzlich zum Anionenaustauscher mit Polymerbürsten wurden zwei verschiedene konvektive Anionenaustauscher Materialen getestet; ein Membranadsorber und ein Monolith. Zusätzlich wurden Durchfluss-Chromatographie und Heparin-Affinität getestet. Die Leistung der entwickelten DSP-Strategien wurde hinsichtlich der dynamischen Bindungskapazität, der Ausbeute, der Fähigkeit zur Trennung verschiedener Partikelpopulationen und der Produktreinheit bewertet. Der Membranadsorber zeigte die höchste Bindungskapazität und Ausbeute, jedoch war keine Partikelauftrennung möglich. Trotz der geringeren Bindungskapazität ermöglichte die Kombination von Durchfluss- und Heparin-Affinitätschromatographie die Gewinnung hochreiner HIV-1-gag-VLPs. Die entwickelten Strategien ermöglichten die Isolierung homogener eVLPs und deren Abtrennung von kritischen Verunreinigungen wie Bionanopartikeln und Chromatin aus Wirtszellen in ein oder zwei Schritten. Dadurch wurde die Komplexität des DSPs verringert und folglich die Herstellung von eVLPs verbessert.

Table of Contents

1. Introduction

Virus-like particles (VLPs) are one of the next generation biopharmaceuticals. Their potential applications include vaccines against (re)-emerging diseases, gene therapy vectors and drug delivery vehicles in cancer [1-6]. While currently available manufacturing platforms were able to bring several VLP-based vaccines to market (Table 1), and many other VLP-based products to preclinical and clinical development [3, 7-9], productivities and yields are still below demand. In VLP manufacturing, downstream processing (DSP) usually entails the most expensive and time-consuming, and least productive unit operations [2, 10]. Furthermore, VLP DSP research and development (R&D) are severely hindered by the lack of high-resolution/high-throughput analytical technologies for specific VLP detection and quantification, especially in complex mixtures [11]. Cost-reduction, simplification and acceleration of the manufacturing processes are key factors that need to be addressed.

Table 1: Examples of commercially available virus-like particle-based vaccines

Name	Manufacturer	Major antigen	Protection against	Expression system
Cervarix®	GlaxoSmithKline plc (GSK)	HPV L1 capsid protein (serotypes 16 & 18)	Human Papilloma Virus (HPV)	Baculovirus – Insect cells (*Trichoplusia ni*)
Gardasil™	Merck & Co., Inc. (MSD)	HPV L1 capsid protein (serotypes 6, 11, 16 & 18)	Human Papilloma Virus (HPV)	Yeast (*S. cerevisiae*)
Gardasil9™	Merck & Co., Inc. (MSD)	HPV L1 capsid protein (serotypes 6, 11, 16, 18, 31, 33, 45, 52 & 58)	Human Papilloma Virus (HPV)	Yeast (*S. cerevisiae*)
Hecolin®	Xiamen Innovax Biotech Co., Ltd.	Hepatitis E capsid protein	Hepatitis E (HEV)	Bacteria (*E. coli*)
MosquiRix™	GlaxoSmithKline plc (GSK)	CSP protein (*Plasmodium falciparum* malaria parasite)	Malaria	Yeast (*S. cerevisiae*)
Sci-B-Vac™	VBI Vaccines Inc.	HBV surface antigens S, Pre-S1 & Pre-S2	Hepatitis B (HBV)	Mammalian (Chinese hamster ovary cells)

Structurally, VLPs mimic the native viruses, resulting in complex bionanoparticles with sizes ranging from tens to hundreds of nanometres in diameter (Figure 1). VLP's main structural elements are viral proteins, which form the VLP capsid [11]. As for the native viruses, in the case

of enveloped VLPs (eVLPs), an additional envelope derived from a host cell lipid bi-layer surrounds the viral capsid [12]. The major difference between native viruses and VLPs is that VLPs completely lack the viral genome and are therefore non-infectious. Accordingly, VLPs have an advantageous safety profile similar to subunit vaccines [13]. Simultaneously, due to its highly organized structure and native presentation of antigenic epitopes, VLPs have an efficacy similar to conventional vaccines, such as killed or live attenuated vaccines, and are able to trigger both cellular and humoral immune response [13]. Besides the applications as prophylactic and therapeutic vaccines, VLPs have been successfully used for protein/peptide, DNA, RNA and drug delivery [14].

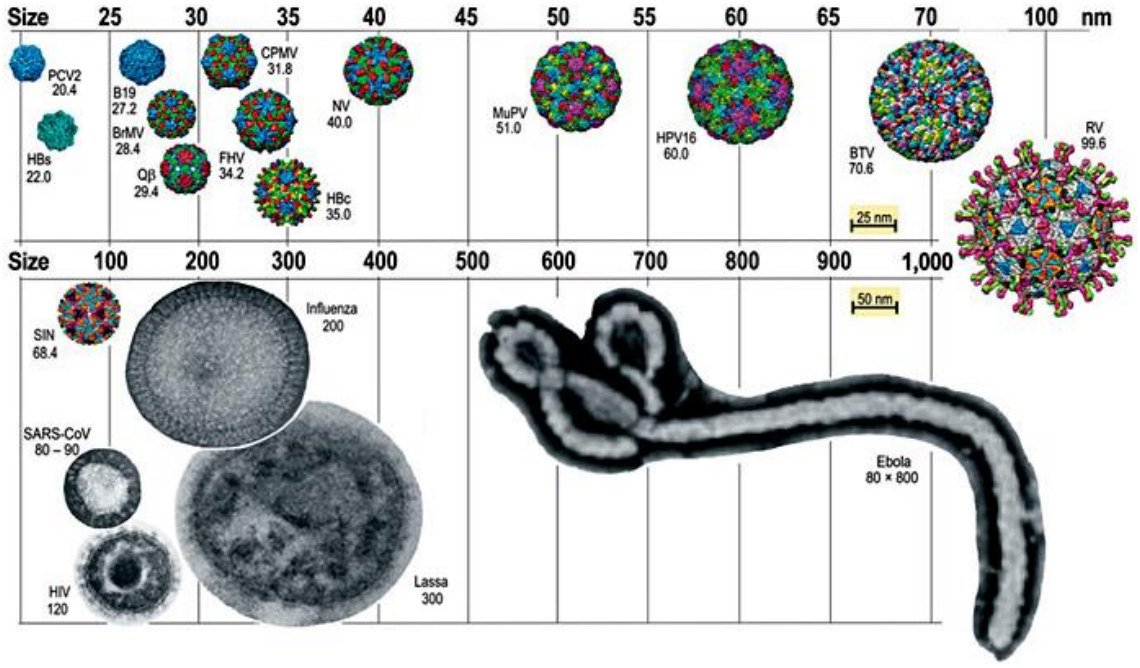

Figure 1: Size-scaled representation of crystal structures of non-enveloped viruses and experimental micrographs of complex enveloped viruses that have been used for the preparation of VLPs. Figure from Pushko *et al* 2013 (© 2013 S. Karger AG, Basel) [15].

The production of VLPs has been carried out successfully in several eukaryotic and prokaryotic expressions systems including bacteria, yeast, insect cells, mammalian cells and plants [7]. Depending on the complexity of the VLPs, different expression systems are preferred. Bacteria and yeast are cost-effective and easy to scale up production systems, however these systems lack the ability to produce adequate post-translational modification and are therefore used to

produce simple non-enveloped VLPs [8]. The insect-cell-baculovirus system offers the possibility of producing more complex, enveloped and chimeric VLPs [16]. However, the main drawback of this expression system is the co-expression of baculovirus, an enveloped virus with surface properties similar to those of the VLPs, which complicates the purification process. Mammalian cells are also very attractive expression system for VLP production, especially due to their capability of producing complex post-translational modifications which replicate human glycosylation patterns [17].

1.1. Enveloped virus-like particles

Most of the common human-threatening viruses are enveloped viruses (Figure 2) and for many, neither prophylactic nor therapeutic vaccines are available. Recent outbreaks of Influenza, Chikungunya, Ebola and Zika have reinforced the need for fast and flexible vaccine manufacturing platforms which allow the production of millions of vaccine doses in a short time [18-21]. Due to their high flexibility for tailored design, enveloped VLP (eVLP) manufacturing platforms are ideal for the fast response to pandemic and seasonal diseases [17, 19, 22]. Besides that, eVLP-based platforms are also promising for the manufacturing of chimeric VLPs carrying foreign epitopes, nucleic acids or small drugs, which can be used for the presentation of clinically-relevant antigens, for gene and cancer therapy, and drug delivery [5, 16, 23-25].

Just as the native enveloped virus, eVLPs are formed in a complex self-assembly and budding process in which, upon recombinant expression, viral proteins self-assemble at a cell's membrane and eVLPs are released, acquiring its envelope [26, 27]. The VLP envelope is therefore composed of a host cell-derived lipid bi-layer, which can carry viral and cellular membrane proteins [12]. Higher eukaryotic expression systems, such as mammalian and insect cells, are usually preferred for production of eVLPs since they allow the simultaneous expression of several complex proteins with adequate post-translational modifications [15, 28]. It has been shown that the complex assembly and budding process of eVLPs can additionally lead to the incorporation of different host cell proteins, DNA and/or RNA fragments, resulting in heterogeneous VLP populations with typically broad size distributions [29-31]. Moreover, in the last decade it was acknowledged that during enveloped virus/VLP recombinant production, cells also release other enveloped

bionanoparticles such as microvesicles and exosomes which have similar size and surface properties [11, 32, 33]. The complex structure of eVLPs, together with co-release of host cell-derived bionanoparticles, bring new challenges to the eVLP manufacturing platforms, especially regarding downstream processing and analytics [2, 10, 11].

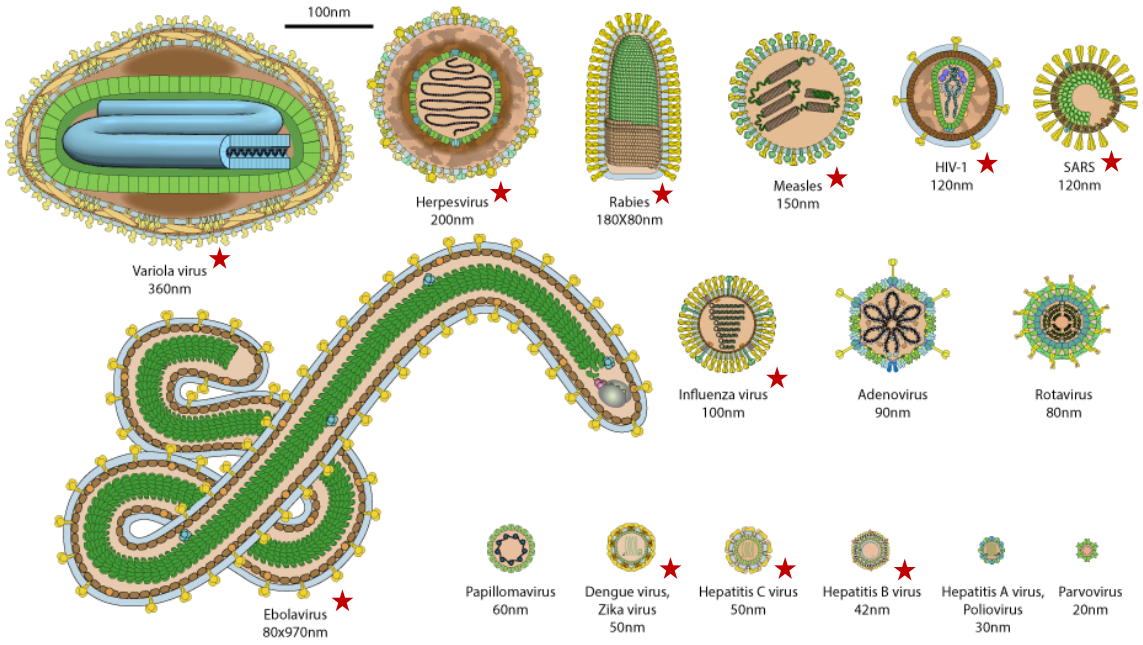

Figure 2: Representation of the most common human viruses. Red stars highlight enveloped viruses. Adapted from https://viralzone.expasy.org/ accessed on 24/12/2019.

Among different options, due to their strong immunogenicity and high flexibility, retroviral-based VLPs are often selected for the development of eVLP platforms [22, 34]. Since the recombinant expression of the HIV-1 gag polyprotein is sufficient for the production and release of eVLPs, this retroviral-protein is frequently used as scaffold for the production of chimeric eVLPs, providing an optimal platform for surface presentation of foreign envelope or transmembrane proteins, as well as for transport and delivery of proteins, nucleic acids and small drugs [35-40].

1.2. Downstream processing strategies for eVLPs

Downstream processing (DSP) of eVLPs is still a challenge and, in many cases, constitutes the main bottleneck in the development of eVLP manufacturing platforms [2, 10]. Due to the complex physicochemical properties of eVLPs, there are no general purification processes, and current

DSP strategies rely on the combination of several unit operations, most of them imported from protein and virus DSP platforms, such as ultracentrifugation, filtration and chromatography (Figure 3) [19, 41, 42]. This combination of many sub-optimal unit operations usually results in long process times, low productivities and high product loss. To ensure the fast and effective eVLP production required in pandemic and seasonal diseases, as well as to guarantee that the cost of the final product is within the expectations of the human healthcare systems, highly flexible and productive DSP strategies are required. It is therefore crucial to reduce the number of steps, decrease complexity, increase productivity and properly adjust the production scale [43].

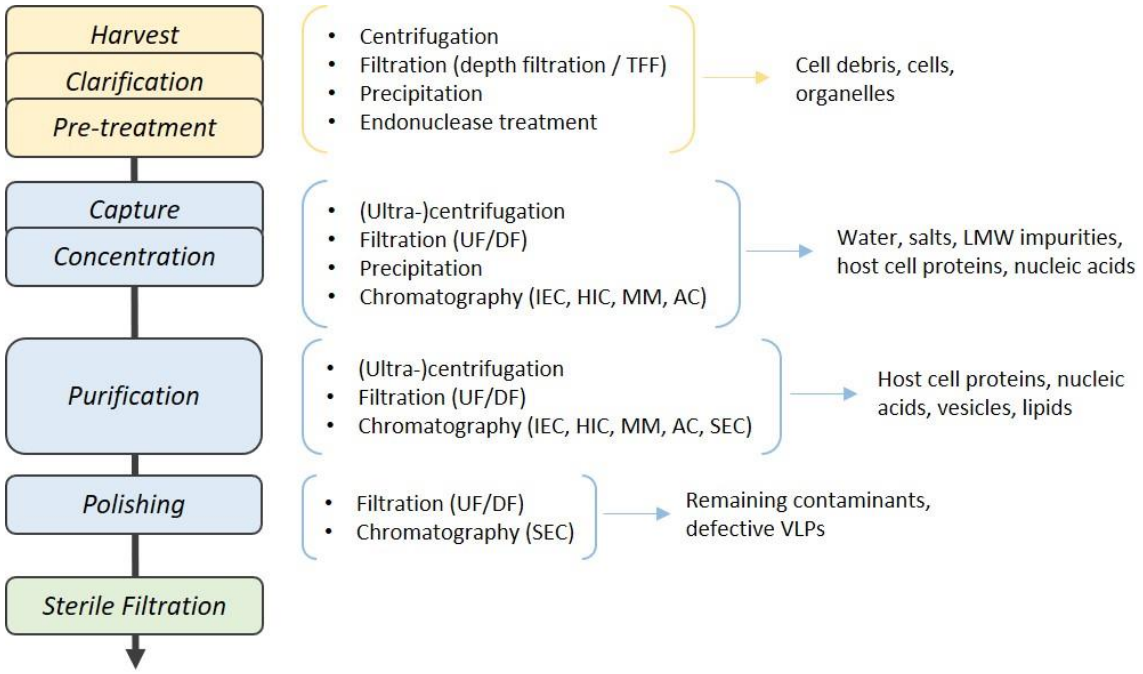

Figure 3: Example flow chart for eVLP downstream processing. Typical unit operations and major removed impurities for each DSP step are described in the middle and right-hand side respectively. [Abbreviations: LMW - low molecular weight; TFF - tangential flow filtration; UF - ultra-filtration; DF - diafiltration; IEC - ion-exchange chromatography; HIC - hydrophobic interaction chromatography; MM - mixed-mode chromatography; AC - affinity chromatography; SEC - size exclusion chromatography]. Adapted from [2, 10, 19, 41, 42]

The ultimate goal of DSP in the manufacturing of biopharmaceuticals is to remove all process- and product-related impurities generated during production, while recovering a fully active product with quality attributes that meet the guidelines from the regulatory agencies such as the

Food and Drug Administration (FDA), European Medicines Agency (EMA) and World Health Organization (WHO) [44, 45].

In eVLP production, process-related impurities derive on one hand from the up- and downstream processing (e.g., culture media components, reagents and additives, such as antibiotics, leachables, tags, stabilizers and nucleases) and on the other hand from the host cells themselves (e.g., cells and cell debris, host cell-derived DNA, proteins, lipids and vesicles). Product-related impurities result from product alterations during up- and downstream processing and include free/unassembled viral proteins and aggregated, misfolded, deformed or disassembled VLPs [2, 10, 41, 46]. Considering the similarities in shape, size and surface properties of eVLPs and host cell-derived bionanoparticles (microvesicles and exosomes), these are among the most challenging impurities to remove [32, 33]. Additionally, since many eVLPs have an overall negative charge similar to double stranded DNA (dsDNA) [47], host cell dsDNA is another challenging impurity and it is often found in eVLP samples after purification, especially when using anion-exchange chromatography [48, 49]. Figure 4 shows an example of a cell culture supernatant characterization, revealing a complex mixture, which includes eVLPs and host cell-derived bionanoparticles, proteins and DNA.

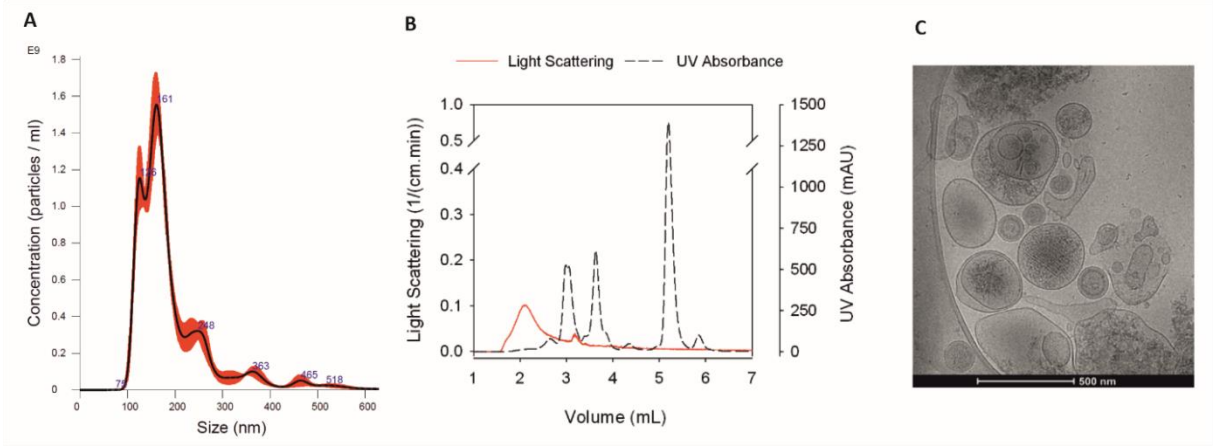

Figure 4: Composition of CHO cell culture supernatant containing HIV-1 gag VLPs and host cell-derived bionanoparticles, proteins and DNA (data from Publication III, manuscript under review in Journal of Chromatography A). A: particle size distribution measured by nanoparticle tracking analysis (particle size ranged from ~50 to 600 nm); B: chromatogram of size exclusion chromatography coupled to UV and multi-angle light scattering (MALS) detectors (particle and small molecular weight impurities detection); C: cryo-electron micrograph (visualization of different bionanoparticle populations).

The choice of unit operations for an eVLP DSP strategy is governed by the physicochemical properties of the eVLPs, such as size, isoelectric point, hydrophobicity and charge distribution. Since eVLPs are released to the extracellular space, cell lysis is not required and the downstream processing starts with the clarification step in which cells, cell debris and other insoluble components are separated from the culture supernatant by centrifugation and/or filtration techniques [2, 50, 51]. Centrifugation is one of the most commonly used unit operations for clarification of cell culture bulks in both laboratory and industrial scales. Nevertheless, the high upfront investment required, the limited scalability and the trend for using cleaning- and validation-free disposable technologies led to development and use of filtration technologies for clarification in eVLP DSP, such as dead-end and depth filters or membrane devices [51-57]. After clarification and before further processing, it is common to use nucleases in order to reduce DNA size and facilitate the subsequent unit operations by reducing the viscosity of the bulk. Additionally, this step helps achieving the host cell DNA levels required by the regulatory agencies in the final product [58].

Capture and concentration steps aim for the recovery of the product while reducing the bulk volume, exchanging the buffer, concentrating the product 10-100-fold and, in some cases, allowing simultaneous intermediate purification [41, 43]. In eVLP DSP, different unit operations can be selected for that purpose, such as ultracentrifugation, density gradient centrifugation, ultrafiltration and chromatography. Ultracentrifugation and density gradient centrifugation have been extensively used for capture, concentration and purification of viruses and VLPs [10, 19, 41, 59-61]. In large scale, density gradient continuous flow ultracentrifugation has been developed to allow the concentration and purification of viral particles from larger volumes in a single step [62, 63]. However, ultracentrifugation equipment is extremely expensive and cleaning and validation procedures are required after each run. Ultrafiltration is another unit operation commonly used for the capture, concentration and intermediate purification of eVLPs, allowing simultaneous buffer exchange and removal of low molecular weight impurities [52, 64, 65]. Since in this case the separation is based exclusively on size differences, this technique is an ideal unit operation to include in a DSP platform for different eVLPs. Moreover, recent developments in

the operation mode of ultrafiltration, such as single-pass tangential flow filtration (SPTFF), allow process intensification and processing in continuous mode [66].

The combination of capture, concentration and purification steps in a single unit operation is the most promising strategy to increase efficiency and reduce complexity in eVLP DSP. Chromatography is the most commonly used technique to capture, concentrate and purify biopharmaceuticals in a single step, in both small and large scale [67]. Chromatographic separation is achieved when product and impurities partition differently between stationary and mobile phases. The development of a chromatography-based DSP strategy requires thoughtful selection of several parameters, such as the physical structure and surface chemistry of the stationary phase, the composition of the mobile phase and the mode of operation. Additionally, despite not being directly involved in the separation process, it is important to select an adequate system hardware. Recent work has shown that by simply changing the type of column hardware, the recovery of a flow-through chromatographic step could be improved from 75 to 95% [68]. Different types of chromatographic supports have been used for VLP DSP, including traditional resins (porous beads) and modern supports, such as monoliths, membrane adsorbers, nanofibers, and nonporous and core-shell beads (Table 2) [48, 49, 68-72].

Table 2: Types of chromatography supports used for enveloped virus and VLP DSP.

Type of Support	**Features**	**Drawbacks**	**Ref.**
Porous beads	- easy and flexible scale up - no competition from particles and small impurities for the same binding sites	- low binding capacity	[48, 68]
Core-shell beads	- easy and flexible scale up - combination of size exclusion and bind-elute modes	- sample dilution - no separation of particle populations	[68, 73, 74]
Monoliths	- predominant convective mass transport - high binding capacity - high productivity - single-use / disposable	- possible binding-site competition and/or displacement effects - limited scale up - fouling and clogging	[49, 75-77]
Membrane adsorbers	- predominant convective mass transport - high binding capacity - high productivity - single-use / disposable	- limited scale up - high dead-volumes / poor resolution	[69, 78]

Due to the large size of eVLPs, convective media such as monoliths and membrane adsorbers are often preferred over conventional porous beads, since their open pore structure results in higher surface area available for binding of eVLPs, and therefore higher binding capacities can be achieved. Additionally, their predominant convective mass transfer allows the use of high flow rates, accelerating DSP [79, 80]. However, fouling and clogging of monoliths and poor resolution of membrane adsorbers have been reported as their main disadvantages [10, 41]. Moreover, although these types of chromatographic supports can be scaled-up, they are produced in a limited number of sizes and shapes reducing the desired flexibility of a DSP platform. In contrast, columns packed with bead-based resins are easily scalable to practically any dimension, allowing a flexible process design [67].

Conventional porous beads usually have a pore size between 10 and 100 nm, and macro- and giga-porous resins have recently been developed, with pore diameters of up to 400 nm [81]. As a rule of thumb, it is assumed that a pore should be 10 times larger than the molecule, to allow a fast mass transfer [82, 83]. Since eVLPs are large nanoparticles (~50-1000 nm), extremely large pores would be necessary, which is not practically feasible since the resins with such large pores may not be sufficiently stable at the high pressures and flow rates required at large scale [84]. Accordingly, porous beads are usually not considered for the purification of eVLPs due to limited pore-diffusion and pore-exclusion effects. Nevertheless, it was recently shown that polymer-grafted porous beads are suitable for the capture and purification of HIV-1 gag VLPs [48]. The determined dynamic binding capacity was only one order of magnitude lower than those usually obtained for convective media, and this setback can be easily overcome due to the easier scalability of packed columns compared to convective media supports. Polymer-grafted media have higher binding capacity compared to non-grafted media due to their ligand 3D structure formed by the long and flexible grafted polymer chains [85-89]. Additionally, the flexibility of the ligands allows multi-point ligand-biomolecule interactions, resulting in increased selectivity once the interaction involves the overall charge distribution of the eVLPs [90, 91].

In addition to conventional porous beads, new designs have been developed to support the needs in large biomolecules DSP. One example is the core bead technology developed by GE Healthcare, in which chromatography beads have a ligand-active core covered by an inactive

shell, combining the principles of size exclusion and bind-elute chromatography. These resins are used for flow-through chromatography, in which impurities bind while the target product flows through the column. Recently, many eVLP DSP strategies include one or several steps using this type of chromatography [68, 73, 74, 92].

Besides the different types of physical structures, different stationary phase surface chemistries can be selected. Several chromatographic modes have been applied in virus and VLP DSP, including ion-exchange chromatography (IEC), hydrophobic interaction chromatography (HIC), affinity chromatography (AC) and mixed-mode chromatography (MMC) [2, 10, 19, 41]. AC is often considered the most attractive chromatographic mode, due to its unique selectivity capacity, which allows the direct capture and purification of the product of interest from complex feed streams. The recovery of the product of interest with high purity levels in a single step accelerates DSP and reduces its complexity. Due the natural function of Heparin as a cell receptor for many viruses [93], Heparin and Heparin-like ligands are the most commonly used in eVLP affinity-based purification strategies [94-97]. Even though the industrial application of affinity chromatography for eVLP DSP is still uncommon, due to the high costs of ligand manufacturing, the excellent results in separation of host cell-derived bionanoparticles from eVLPs reinforce the need in continuing the development of new and more affordable affinity-based chromatographic supports [68, 94]. While affinity is the most attractive chromatographic mode, ion-exchange is the most commonly used mode of chromatography for the purification of large bionanoparticles [98]. IEC separations are based on different ionic interactions between the resin's charged ligands and the product/impurities. Depending on the product's net charge, anion- or cation-exchangers can be used. Since enveloped viruses and VLPs are surrounded by a lipid bi-layer, it is assumed that their surface contains multiple positive and negative charges. However, many viruses have an isoelectric point below 7.4, therefore having an overall negative charge [47]. Moreover, it was shown, that in a pH range from 6.5 to 8.5, HIV-1 gag VLPs bind to anion-exchange but not to cation-exchange monoliths [49]. Accordingly, anion-exchange chromatography is usually preferred and has been applied efficiently for the capture and purification of several enveloped viruses and VLPs [48, 49, 70, 75, 78, 99].

Despite its drawbacks, such as low capacity, low productivity, product dilution and high buffer consumption, SEC is still one of the methods of choice for polishing steps, allowing the removal of low molecular weight impurities and final buffer exchange [19]. Additionally, core beads and membrane adsorbers have been recently applied in negative mode as polishing steps in eVLP DSP [43]. Aside from chromatography, ultrafiltration and diafiltration are commonly used in polishing steps [2].

1.3. Analytical methods to detect, quantify and characterize eVLPs

The detection, quantification and characterization of eVLPs are essential, not only in the final product, but across the entire manufacturing process. Speed and accuracy of process development, in both up- and downstream, depend directly on the accuracy, specificity and speed of the available analytical methodologies. Most of the analytical tools currently used in eVLP manufacturing were imported from virus and protein manufacturing platforms [11]. However, on the one hand, well-established standard methods for the quantification of viruses depend on infectivity measurements and are therefore not applicable for eVLPs, which are non-infectious. On the other hand, while the quantification of viral/VLP proteins can be done with methodologies imported from protein manufacturing platforms, it is not guaranteed that all viral proteins in a sample are part of correctly assembled VLPs. Additionally, especially in complex mixtures, the presence of host cell-derived bionanoparticles, which have similar size, shape, composition and surface properties, makes eVLP quantification very cumbersome (Figure 4) [33]. Consequently, a combination of several biophysical, biochemical and biological assays is necessary in order to accurately detect, quantify and characterize eVLPs during manufacturing and in the final product, as well as to monitor product purity and activity (Figure 5).

The overall protein composition, including host cell and eVLP proteins, is usually characterized by biochemical assays such as Bradford assay, sodium dodecyl sulfate polyacrylamide gel electrophoresis (SDS-PAGE), reversed phase high performance liquid chromatography (RP-HPLC) and mass spectrometry (MS) [100-102]. Additionally, specific protein detection and quantification is done by biological assays, such as Western blot assay, enzyme-linked immunosorbent assay (ELISA) and surface plasmon resonance (SPR), via specific recognition by

antibodies [16, 103-105]. Host cell DNA quantification is mostly done by biochemical or biological assays such as Picogreen® assay, Threshold™ System and qPCR [106]. For some specific eVLPs, such as Influenza VLPs containing Hemagglutinin, cell culture based assays (hemagglutination assay in the case of Influenza VLPs) can be used to determine their biologic activity [107].

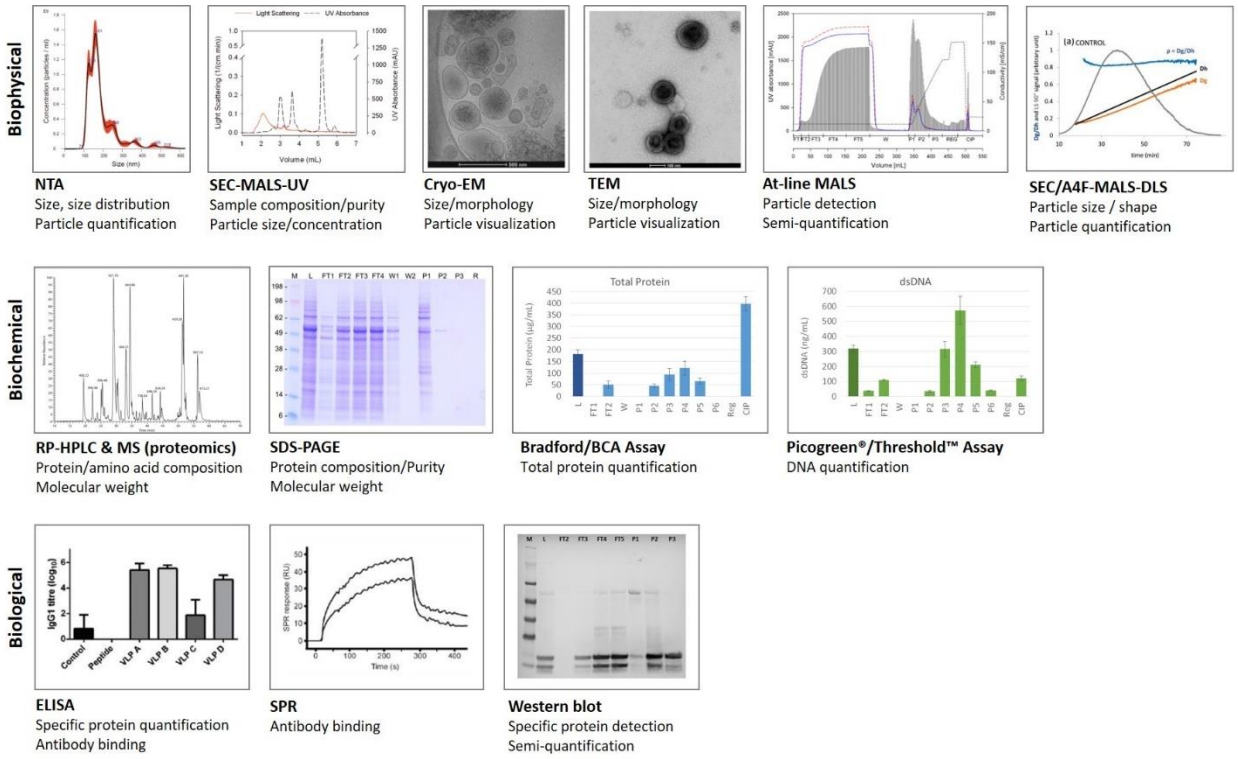

Figure 5: Schematic representation of different analytical tools used for characterization of eVLPs and impurities in eVLP manufacturing. Adapted from Lua *et al* [11].

Besides their protein composition, the structure, morphology and integrity of eVLPs have to be analysed. High-resolution microscopy techniques are the gold-standard method for particle visualization. Commonly, transmission electron microscopy (TEM), in combination with negative staining protocols, is used during process development and manufacturing for confirming the presence of spherical-like structures in the correct size range. However, it should be kept in mind that sample preparation using negative staining protocols can generate artefacts or lead to the deformation or disintegration of eVLPs, possibly affecting their size and shape. More recently, morphological and nanomechanical properties of VLPs are also being evaluated using atomic force microscopy (AFM) [108, 109]. Ultimately, cryo-electron microscopy and tomography techniques are used for the full morphological and structural characterization of eVLPs [30, 110,

111]. Since these techniques do not require staining methods, and the sample preparation is done by rapidly freezing the eVLPs in solution, it is assumed that the resulting images allow the visualization of native structures. While these methods allow the assessment of the eVLP structure with high resolution, they are not ideal for in-process product control due to their low-throughput. Additionally, particle quantification based on microscopy techniques is very difficult and often associated with low accuracy.

Quantification of eVLPs is often based on the quantification of viral proteins [11]. However, especially in early stage manufacturing, the presence of free or incorrectly assembled viral proteins usually leads to over-estimated titers. Alternatively, different techniques based on light-scattering are used for particle quantification, as well as for particle size and size distribution measurements, for example nanoparticle tracking analysis (NTA), dynamic light scattering (DLS) and multi-angle light scattering (MALS) [112-114]. In NTA, the Brownian motion of single particles is analysed by recording the light scattered by a laser-illuminated sample, using a light microscope coupled to a camera. The hydrodynamic radius of each particle is then determined using the Stoke-Einstein equation, which correlates the diffusion coefficient to the particle size. Particle concentration is determined by averaging the number of recorded particles and the analysed sample volume [115]. DLS is also used to determine hydrodynamic radii from diffusion coefficients, however, contrarily to NTA, DLS detects dynamic fluctuations in scattered light originated by the whole sample, and not by single particles, resulting in an averaged size measurement [112, 116]. In MALS, the scattered light is measured at several fixed angles. The overall measured intensity and angular dependence, known as Rayleigh ratio, combined with the appropriate mathematical models, allow the determination of particle size, molecular weight and particle concentration. In order to obtain monodisperse samples and allow accurate size measurements, MALS is usually coupled to SEC or asymmetric flow field flow fractionation (A4F) [112, 113, 115, 117]. Nevertheless, MALS has been recently used as an at- and on-line detector in biopharmaceuticals process development for rapid in-process product control [118, 119]. Although light scattering based methods allow an accurate quantification of particles, it is important to keep in mind that these methods are non-specific regarding particle composition and will consider all particles with similar radii as equals.

2. Objectives

The main objective of this work was to develop new DSP strategies for the capture and purification of eVLPs based on polymer-grafted media. In particular, it aimed to establish purification methods capable of separating different bionanoparticle populations. Due to the 3D structure and flexibility of their ligands, polymer-grafted media have increased binding capacity and selectivity, and therefore are interesting candidates for high-resolution separation of bionanoparticles. For industrial scale purification, beads are still the chromatography medium of choice due to their easy scalability. Regarding the type of chemistry involved in binding, it is known that eVLPs bind to positively charged surfaces. Therefore, anion-exchange polymer-grafted beads were selected for investigating the applicability of polymer-grafted media for the capture and purification of eVLPs. Additionally, we also aimed to develop fast high-throughput methodologies for the detection and quantification of particles in a high number of samples immediately after each purification experiment, allowing faster and more directed process development and optimization. Finally, the last aim of this work was to perform a systematic comparison of the developed and other relevant DSP strategies for the capture and purification of eVLPs. To ensure a systematic comparison, the DSP strategies had to be performed using the same starting material, and the determination of product quantity and quality had to be performed using the same analytical methods for all strategies. Different types of chromatography supports were included in the comparison, such as convective media and core-shell beads.

Accordingly, four objectives were defined for this thesis:

- Investigation of the partitioning of eVLPs in polymer grafted media and determination of the equilibrium and dynamic binding capacities.
- Development of a DSP strategy based on polymer-grafted media for the capture and purification of eVLPs, which allows the separation of different particle populations.
- Development of high-throughput methodologies for particle detection and quantification to support eVLP DSP development and optimization.
- Systematic comparison of eVLP DSP strategies regarding capacity and resolution for the separation of different particle populations.

3. Summary of the work and conclusions

In this work, the applicability of polymer grafted media for the downstream processing of enveloped virus-like particles (eVLPs) was evaluated. For that purpose, VLPs based on the HIV-1 gag polyprotein were selected as model eVLPs since they are promising candidates for chimeric eVLP manufacturing [38-40]. The challenges in process development for eVLP DSP start with the difficulties in characterizing the composition of the feed material. First, eVLPs are complex multi-component biomolecules and second, it is known that host cell-derived bionanoparticles are released to the cell culture supernatant alongside with eVLPs. All of these different bionanoparticles have overlapping sizes, compositions and surface properties, making their separation, characterization, quantification and discrimination very cumbersome [33]. Accordingly, since no standard methods are available for fast and simple quantification of eVLPs in complex mixtures, a combination of biochemical, biophysical and biological assays was used for sample characterisation, including multi-angle light scattering (MALS), nanoparticle tracking analysis (NTA), cryo-electron microscopy (cryo-EM), Western blot analysis and mass spectrometry (MS). Cryo-EM micrographs confirmed the presence of correctly assembled HIV-1 gag VLPs (Figure 6, red arrows). Additionally, several host cell-derived bionanoparticles could be observed (Figure 6, blue arrows).

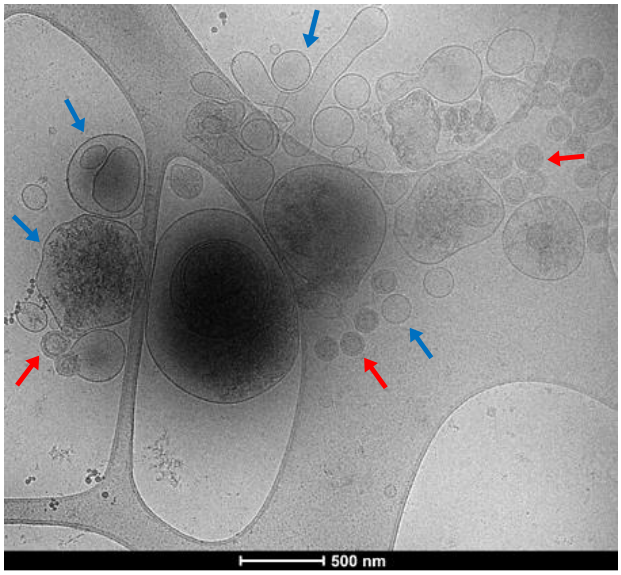

Figure 6: Cryo-EM micrograph of endonuclease treated and 0.8 µm filtered CHO cell culture supernatant containing HIV-1 gag VLPs.

The polymer-grafted chromatography resin Fractogel®-TMAE Hicap (M) from Merck was used for the capture and purification of HIV-1 gag VLPs directly from clarified cell culture supernatant or after pre-purification, using flow-through chromatography to reduce the amount of low molecular weight impurities. Porous beads, such as Fractogel®, were usually not considered for the purification of large biomolecules due to slow diffusion or pore-exclusion limitations, which often results in low binding capacities. However, in this work it was demonstrated that despite the fact that eVLPs bind exclusively on the outer surface of the porous beads (Figure 7), the obtained dynamic binding capacities (DBC) ranged from $5.5x10^{11}$ to $1.5x10^{12}$ particles/mL column, which is only one half to one order of magnitude lower than the ones usually obtained for convective chromatographic supports, such as monoliths and membrane adsorbers [49, 75, 77, 78]. Moreover, the fact that eVLPs bind exclusively on the outer surface of the beads leaves the remaining area on the interior of beads available for the binding of impurities, reducing the risk of binding competition and displacement effects.

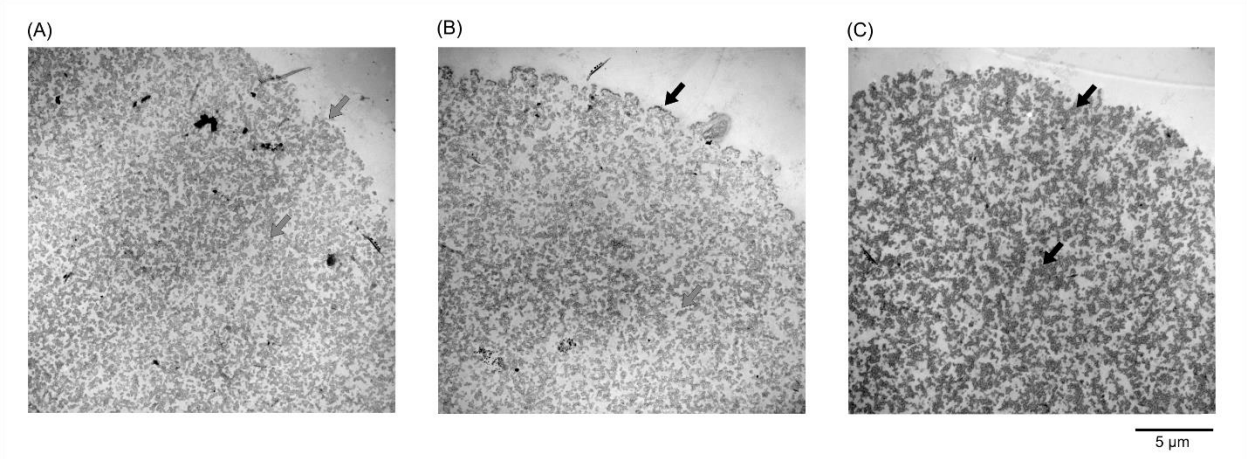

Figure 7: Transmission electron micrographs of thin slices of (A) virgin, (B) VLP-saturated and (C) BSA-saturated Fractogel®-TMAE resin beads. Black arrows point to VLP/BSA bound to the resin and grey arrows point to free resin backbone (from Publication I [48]).

In DSP it is essential to be able to detect the product at the outlet of each unit operation in order to accurately collect it for further processing and analysis. In this work, it was demonstrated that UV detectors, commonly used in biopharmaceuticals DSP, are not ideal for eVLP monitoring and often do not provide a good representation of the elution profiles, especially at small scale or in early stage development where titers are usually low (Figure 8-B). Accordingly, a high-throughput

method based on at-line measurements of light scattering by MALS was developed for in-process product monitoring, accelerating process development (Publication II [118]).

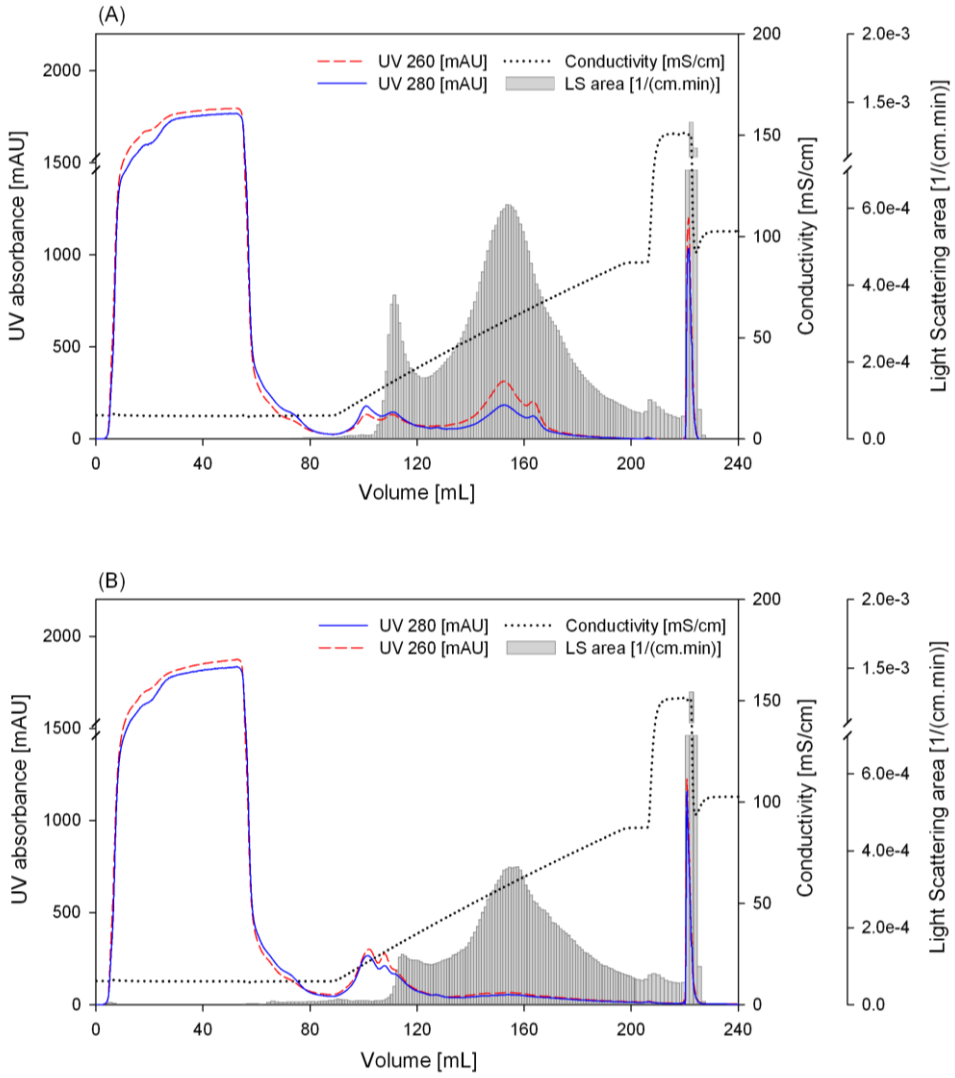

Figure 8: Comparison of the UV absorbance and light scattering elution profiles of two purification runs using (A) non-treated and (B) endonuclease-treated CHO cell culture supernatant containing HIV-1 gag VLPs. Each bar on the graphs represents the integration (area under the curve) of the light scattering signal for each collected fraction measured by at-line MALS. The light scattering signal intensity is directly proportional to the particle concentration in the respective fraction (from Publication I [48]).

In eVLP DSP, in addition to the host cell-derived bionanoparticles, DNA has been identified as a challenging impurity to remove. Moreover, due to the similar overall negative charge of dsDNA and eVLPs, there is a risk of binding competition or displacement effects when using anion-

exchange chromatography. In this work, these effects were ruled out by obtaining similar breakthrough profiles and DBCs when using endonuclease-treated and non-treated cell culture supernatant as feed material for the capture and purification of eVLPs using Fractogel® (Figure 9) [48]. However, it was shown that when non-treated cell culture supernatant is used as feed material, dsDNA and eVLPs co-elute. Accordingly, in further process development an endonuclease treatment was included in the clarification step. Moreover, in order to reach in the final product the low levels of host cell DNA requested by the regulatory agencies (<10 ng per dose [45]), it is common to apply nuclease treatments at some point during eVLP manufacturing.

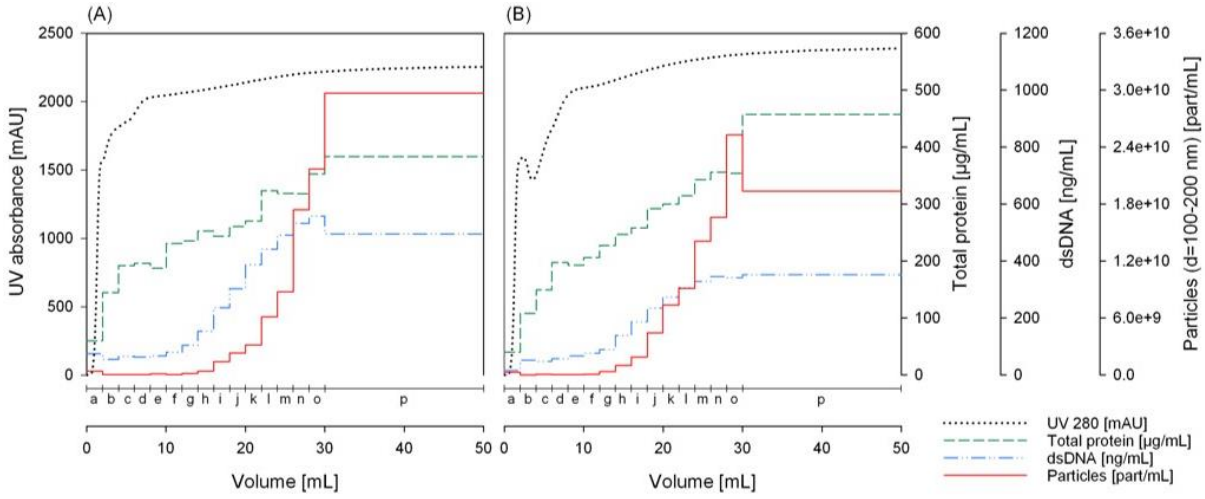

Figure 9: Breakthrough curves for the loading of (A) non-treated and (B) endonuclease-treated CHO cell culture supernatant, containing HIV-1 gag VLPs, into 1 mL Fractogel®-TMAE MiniChrom columns. Total protein, dsDNA and particle concentrations were measured offline by Bradford, Picogreen and NTA, respectively. $DBC_{10\%}$: (A) $6.6x10^{11}$ and (B) $5.5x10^{11}$ particles/mL column (from Publication I [48]).

Direct loading of cell culture supernatant into the chromatography columns was possible because the strong interaction between eVLPs and the resin ligands allowed binding at moderate conductivities. This allows for a reduction of complexity and increases productivity in eVLP DSP. Additionally, the strong eVLP interaction versus the weak interaction of host cell protein impurities is an advantage of this method, since most protein impurities are immediately excluded from the column or eluted at low salt concentrations, improving the product purity in a single step. Since the developed method uses bead-based chromatography media it can be easily scaled to practically any dimension.

Due to the lack of standard analytical methods to quantify and characterize eVLPs, researchers adapted methods from virus and protein analytics for specific eVLPs. This led to a vast variability in the methods used for determination of yields and purities in eVLP DSP. As a result, it is very difficult to systematically compare the performance of the different strategies commonly used for eVLP DSP. In order to overcome this problem, in this work, four additional DSP strategies were developed including the most commonly used chromatographic supports and modes of chromatography for eVLP DSP (Figure 10-A). For all strategies the same analytical tools as well as the same feed material were used.

The membrane adsorber NatriFlo® HD-Q Recon had the highest particle binding capacity with $5.3x10^{12}$ particles/mL membrane, followed by the monolith CIMmultus™ QA-8 with $2.9x10^{12}$ particles/mL column, the polymer-grafted resin Fractogel® EMD TMAE Hicap (M) with $1.5x10^{12}$ particles/mL column and, with the lowest binding capacity, the affinity resin Capto™ Heparin with $1.5x10^{11}$ particles/mL column.

In all capture and purification experiments using anion-exchangers (Figure 10-B: a, b and c), before breakthrough was reached, all particles and residual dsDNA bound to the columns. In contrast, for the Heparin-affinity resin (Figure 10-B: d) it was observed, as shown by the immediate partial particle breakthrough, that while some particles bound to the column, others were immediately excluded. Cryo-electron micrographs revealed that host cell-derived bionanoparticles were excluded from the column while HIV-1 gag VLPs were bound, allowing the separation of these particle populations. Interestingly, the elution of two different particle populations in two distinct peaks was indicated by the light scattering signal. Combining the results of proteomic analysis, SEC-MALS, Western blot assays and cryo-electron microscopy, it was concluded that the second particle peak eluting in the Heparin-affinity experiment was mainly composed of chromatin, while the first peak was enriched in highly pure HIV-1 gag VLPs. Separation of different particle populations was also achieved using the anion-exchangers QA-Monolith and Fractogel®, however higher salt concentrations were needed to elute the eVLPs compared to the Heparin-affinity resin.

(A)

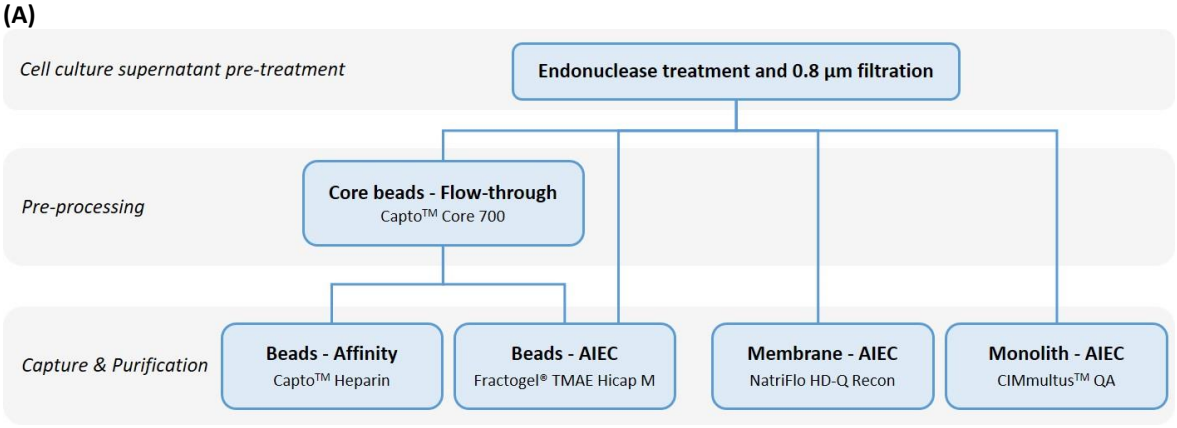

(B)

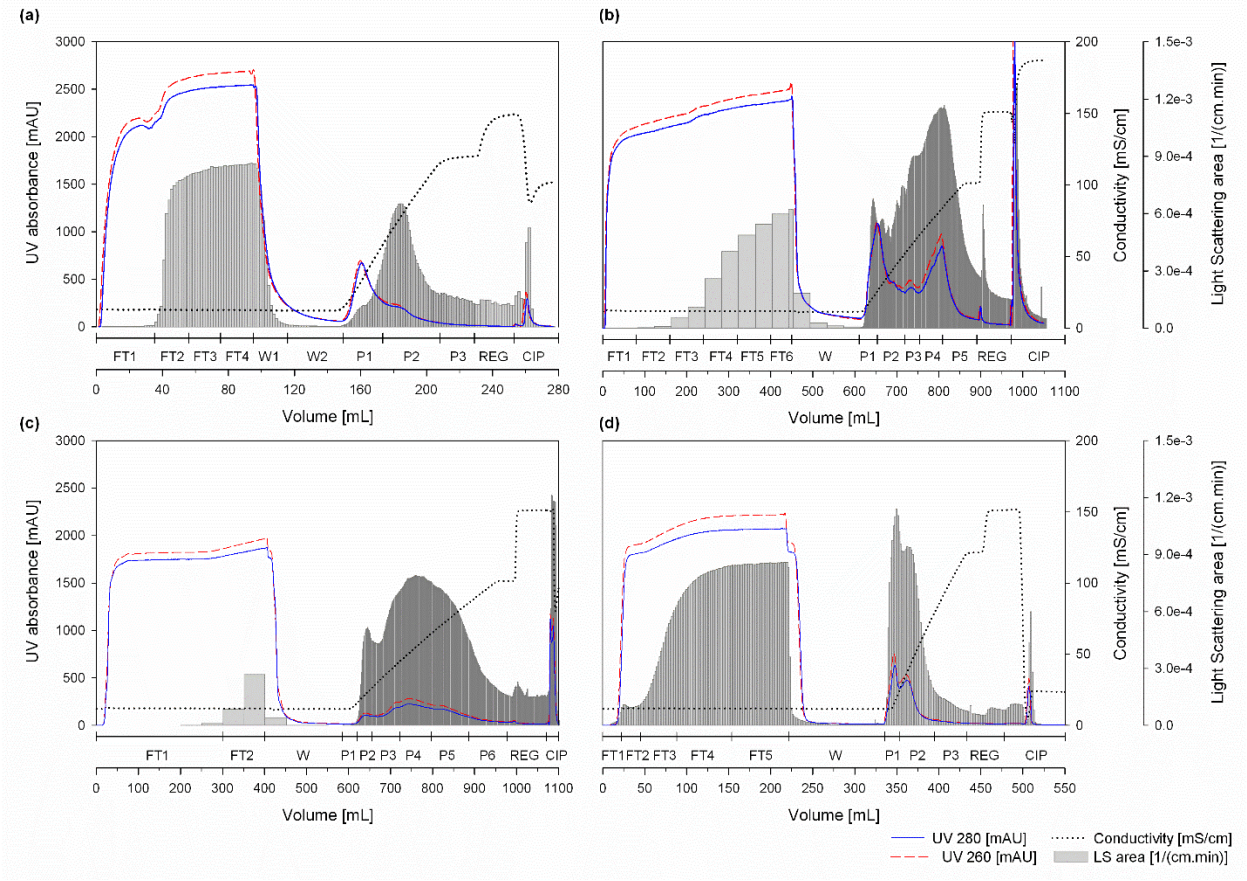

Figure 10: (A) DSP strategies for purification of HIV-1 gag VLPs produced in CHO cells. (B) Chromatograms of the capture and purification of HIV-1 gag VLPs using (a) NatriFlo® HD-Q Recon membrane adsorber, (b) CIMmultus™ QA-8 monolith, (c) Fractogel® EMD TMAE Hicap (M) column and (d) Capto™ Heparin column. FT: flow-through; W: wash; P: elution peaks; REG: regeneration with 2 M NaCl; CIP: cleaning-in-place (from Publication III, manuscript under review in Journal of Chromatography A).

These results show the importance of using a combination of several orthogonal biophysical, biochemical and biological assays to fully characterize the composition of samples in eVLP manufacturing. Additionally, these results show that besides host cell-derived bionanoparticles, chromatin affects the quantification of eVLPs, once chromatin was measured by NTA and MALS with similar results as eVLPs.

Besides binding capacity, the recovery and product purity of each developed DSP strategies was compared (Figure 11). As for the binding capacity, the membrane adsorber had the highest recovery, however since no particle separation was achieved with this method further purification steps would be necessary. Nevertheless, the high binding capacity and fast processing of the membrane adsorber make it an ideal option for direct capture steps. The highest purity was obtained using the Heparin-affinity resin Capto™ Heparin and approximately 2600 doses per liter feed material and per column volume could be purified. However, in this strategy a pre-purification step using flow-through chromatography was included.

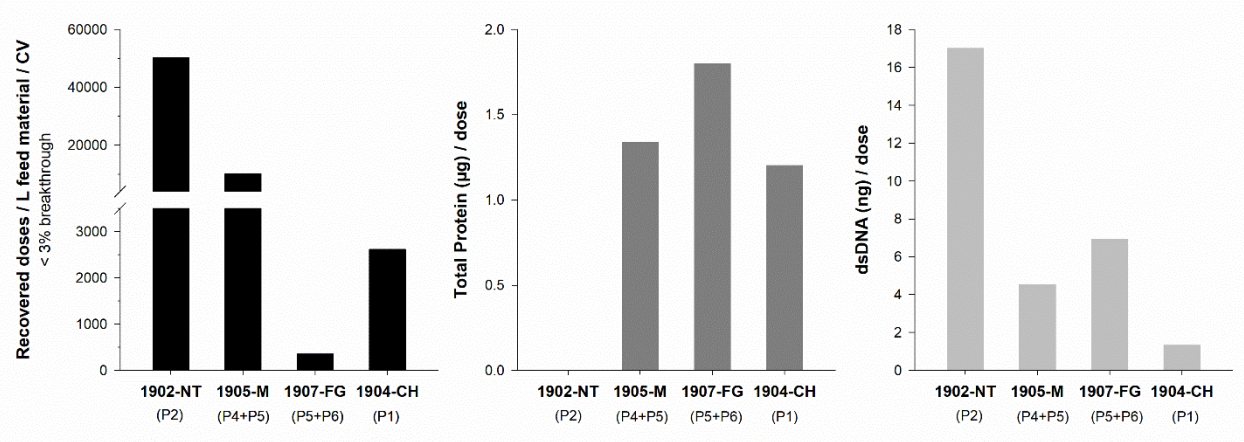

Figure 11: Comparison of recovered doses per litre of cell culture supernatant, total protein per dose and dsDNA per dose in the main product fractions. 1902-NT: NatriFlo® HD-Q Recon membrane adsorber; 1905-M: CIMmultus™ QA-8 monolith; 1907-FG: Fractogel® EMD TMAE Hicap (M); 1904-CH: Capto™ Heparin (from Publication III, manuscript under review in Journal of Chromatography A).

In conclusion this work demonstrated that polymer grafted media are suitable for the capture and purification of eVLPs. The systematic comparison between the different developed DSP strategies allowed the recognition of the strengths and weaknesses of each one of them. This

will, on one hand allow a more comprehensive selection of unit operations for an eVLP DSP train and on the other hand, serve as a guide for the development of new chromatographic materials. Moreover, the extensive sample characterization by the combination of several analytical tools increased the understanding of the complex composition of the bulk material in eVLP production and helped identify critical impurities such as host cell-derived bionanoparticles and chromatin. Finally, the development of eVLP purification strategies that allow the production of large amounts of highly pure eVLPs will contribute not only to the bioprocess engineering research but also to fundamental research addressing topics such as particle composition and biological activity.

In this thesis, the partitioning of eVLPs in polymer-grafted media was investigated and it was demonstrated that eVLPs bind on the outer surface of the polymer-grafted beads (Publication I). The equilibrium and dynamic binding capacities were determined and were higher than expected, being only one half to one order of magnitude lower than the capacities usually obtained with convective media (Publication I). A DSP strategy for the direct capture and purification of eVLPs was developed based on polymer-grafted media. This strategy allowed the separation of different bionanoparticle populations (Publication I). To accelerate process development, a high-throughput methodology for particle detection and quantification was established, using at-line MALS and fluorescence measurements (Publication II). Additionally, four different DSP strategies for eVLP purification were developed based on commonly used unit operations. Since the same starting material and the same analytical tools were used for all developed DSP strategies, it was possible to systematically compare their performance regarding capacity, recovery and resolution for the separation of different bionanoparticle populations (Publication III). Accordingly, the objectives of the thesis could be met.

4. References

[1] X. Ding, D. Liu, G. Booth, W. Gao, Y. Lu, Virus-Like Particle Engineering: From Rational Design to Versatile Applications, Biotech J, 13 (2018) 1700324.
[2] C.L. Effio, J. Hubbuch, Next generation vaccines and vectors: Designing downstream processes for recombinant protein-based virus-like particles, Biotechnology Journal, 10 (2015) 715-727.
[3] M.O. Mohsen, L. Zha, G. Cabral-Miranda, M.F. Bachmann, Major findings and recent advances in virus–like particle (VLP)-based vaccines, Seminars in Immunology, 34 (2017) 123-132.
[4] M.C. Serradell, L.L. Rupil, R.A. Martino, C.G. Prucca, P.G. Carranza, A. Saura, E.A. Fernández, P.R. Gargantini, A.H. Tenaglia, J.P. Petiti, R.R. Tonelli, N. Reinoso-Vizcaino, J. Echenique, L. Berod, E. Piaggio, B. Bellier, T. Sparwasser, D. Klatzmann, H.D. Luján, Efficient oral vaccination by bioengineering virus-like particles with protozoan surface proteins, Nature Communications, 10 (2019) 361.
[5] M.O. Mohsen, D.E. Speiser, A. Knuth, M.F. Bachmann, Virus-like particles for vaccination against cancer, Wiley Interdiscip Rev Nanomed Nanobiotechnol, 12 (2020) e1579.
[6] M. Moo-Young, Comprehensive Biotechnology, Elsevier Science, 2019.
[7] J. Fuenmayor, F. Godia, L. Cervera, Production of virus-like particles for vaccines, N Biotechnol, 39 (2017) 174-180.
[8] M.G. Masavuli, D.K. Wijesundara, J. Torresi, E.J. Gowans, B. Grubor-Bauk, Preclinical Development and Production of Virus-Like Particles As Vaccine Candidates for Hepatitis C, Front Microbiol, 8 (2017) 2413.
[9] B. Hodgins, S. Pillet, N. Landry, B.J. Ward, Prime-pull vaccination with a plant-derived virus-like particle influenza vaccine elicits a broad immune response and protects aged mice from death and frailty after challenge, Immunity & Ageing, 16 (2019) 27.
[10] M.W. Wolf, U. Reichl, Downstream processing of cell culture-derived virus particles, Expert Review of Vaccines, 10 (2011) 1451-1475.
[11] L.H. Lua, N.K. Connors, F. Sainsbury, Y.P. Chuan, N. Wibowo, A.P. Middelberg, Bioengineering virus-like particles as vaccines, Biotechnol Bioeng, 111 (2014) 425-440.
[12] S. Welsch, B. Müller, H.-G. Kräusslich, More than one door – Budding of enveloped viruses through cellular membranes, FEBS Letters, 581 (2007) 2089-2097.
[13] B. Donaldson, Z. Lateef, G.F. Walker, S.L. Young, V.K. Ward, Virus-like particle vaccines: immunology and formulation for clinical translation, Expert Review of Vaccines, 17 (2018) 833-849.
[14] Z. Shirbaghaee, A. Bolhassani, Different applications of virus-like particles in biology and medicine: Vaccination and delivery systems, Biopolymers, 105 (2015) 113-132.
[15] P. Pushko, P. Pumpens, E. Grens, Development of virus-like particle technology from small highly symmetric to large complex virus-like particle structures, Intervirology, 56 (2013) 141-165.
[16] L. Nika, J. Wallner, D. Palmberger, K. Koczka, K. Vorauer-Uhl, R. Grabherr, Expression of full-length HER2 protein in Sf9 insect cells and its presentation on the surface of budded virus-like particles, Protein Expression and Purification, 136 (2017) 27-38.
[17] A. Roldao, M.C. Mellado, L.R. Castilho, M.J. Carrondo, P.M. Alves, Virus-like particles in vaccine development, Expert Rev Vaccines, 9 (2010) 1149-1176.
[18] H.K. Charlton Hume, L.H.L. Lua, Platform technologies for modern vaccine manufacturing, Vaccine, 35 (2017) 4480-4485.
[19] T. Vicente, A. Roldão, C. Peixoto, M.J.T. Carrondo, P.M. Alves, Large-scale production and purification of VLP-based vaccines, Journal of Invertebrate Pathology, 107 (2011) S42-S48.
[20] X. Feng, X. Huo, B. Tang, S. Tang, K. Wang, J. Wu, Modelling and Analyzing Virus Mutation Dynamics of Chikungunya Outbreaks, Scientific Reports, 9 (2019) 2860.
[21] C. Adlhoch, A. Miteva, A. Zdravkova, T. Miškić, D. Kneževic, S. Perdikaris, K. Śmietanka, E. Świętoń, V. Kopriva, M. Chudý, L.J. Romero González, I. Moreno Gil, A. Wallén Norell, F. Verdonck, Estimation of

the number of exposed people during highly pathogenic avian influenza virus outbreaks in EU/EEA countries, October 2016–September 2018, Zoonoses and Public Health, 66 (2019) 874-878.
[22] F. Pitoiset, T. Vazquez, B. Bellier, Enveloped virus-like particle platforms: vaccines of the future?, Expert Review of Vaccines, 14 (2015) 913-915.
[23] R. Goswami, G. Subramanian, L. Silayeva, I. Newkirk, D. Doctor, K. Chawla, S. Chattopadhyay, D. Chandra, N. Chilukuri, V. Betapudi, Gene Therapy Leaves a Vicious Cycle, Frontiers in Oncology, 9 (2019) 297.
[24] H.K. Ong, W.S. Tan, K.L. Ho, Virus like particles as a platform for cancer vaccine development, PeerJ, 5 (2017) e4053.
[25] I.C. Schneider, J. Hartmann, G. Braun, J. Stitz, T. Klamp, M. Bihi, U. Sahin, C.J. Buchholz, Displaying Tetra-Membrane Spanning Claudins on Enveloped Virus-Like Particles for Cancer Immunotherapy, Biotechnology Journal, 13 (2018) 1700345.
[26] B.J. Chen, R.A. Lamb, Mechanisms for enveloped virus budding: Can some viruses do without an ESCRT?, Virology, 372 (2008) 221-232.
[27] G.R. Lázaro, S. Mukhopadhyay, M.F. Hagan, Why Enveloped Viruses Need Cores—The Contribution of a Nucleocapsid Core to Viral Budding, Biophysical Journal, 114 (2018) 619-630.
[28] N. Kushnir, S.J. Streatfield, V. Yusibov, Virus-like particles as a highly efficient vaccine platform: Diversity of targets and production systems and advances in clinical development, Vaccine, 31 (2012) 58-83.
[29] R. Kurg, O. Reinsalu, S. Jagur, K. Õunap, L. Võsa, S. Kasvandik, K. Padari, K. Gildemann, M. Ustav, Biochemical and proteomic characterization of retrovirus Gag based microparticles carrying melanoma antigens, Scientific Reports, 6 (2016) 29425.
[30] D.M. McCraw, J.R. Gallagher, U. Torian, M.L. Myers, M.T. Conlon, N.M. Gulati, A.K. Harris, Structural analysis of influenza vaccine virus-like particles reveals a multicomponent organization, Scientific Reports, 8 (2018) 10342.
[31] A.A. Onafuwa-Nuga, A. Telesnitsky, S.R. King, 7SL RNA, but not the 54-kd signal recognition particle protein, is an abundant component of both infectious HIV-1 and minimal virus-like particles, RNA (New York, N.Y.), 12 (2006) 542-546.
[32] D.G. Meckes, N. Raab-Traub, Microvesicles and Viral Infection, Journal of Virology, 85 (2011) 12844.
[33] E. Nolte-'t Hoen, T. Cremer, R.C. Gallo, L.B. Margolis, Extracellular vesicles and viruses: Are they close relatives?, Proceedings of the National Academy of Sciences of the United States of America, 113 (2016) 9155-9161.
[34] L. Deml, C. Speth, M.P. Dierich, H. Wolf, R. Wagner, Recombinant HIV-1 Pr55gag virus-like particles: potent stimulators of innate and acquired immune responses, Molecular Immunology, 42 (2005) 259-277.
[35] F. Pitoiset, T. Vazquez, B. Levacher, D. Nehar-Belaid, N. Dérian, J. Vigneron, D. Klatzmann, B. Bellier, Retrovirus-Based Virus-Like Particle Immunogenicity and Its Modulation by Toll-Like Receptor Activation, Journal of virology, 91 (2017) e01230-01217.
[36] H.R. Soares, R. Castro, H.A. Tomás, M.J.T. Carrondo, P.M. Alves, A.S. Coroadinha, Pseudotyping retrovirus like particles vaccine candidates with Hepatitis C virus envelope protein E2 requires the cellular expression of CD81, AMB Express, 9 (2019) 22.
[37] A. Venereo-Sanchez, M. Simoneau, S. Lanthier, P. Chahal, L. Bourget, S. Ansorge, R. Gilbert, O. Henry, A. Kamen, Process intensification for high yield production of influenza H1N1 Gag virus-like particles using an inducible HEK-293 stable cell line, Vaccine, 35 (2017) 4220-4228.
[38] J. Vidigal, B. Fernandes, M.M. Dias, M. Patrone, A. Roldão, M.J.T. Carrondo, P.M. Alves, A.P. Teixeira, RMCE-based insect cell platform to produce membrane proteins captured on HIV-1 Gag virus-like particles, Applied Microbiology and Biotechnology, 102 (2018) 655-666.

[39] V.K. Deo, T. Kato, E.Y. Park, Chimeric Virus-Like Particles Made Using GAG and M1 Capsid Proteins Providing Dual Drug Delivery and Vaccination Platform, Molecular Pharmaceutics, 12 (2015) 839-845.
[40] L. Cervera, F. Gòdia, F. Tarrés-Freixas, C. Aguilar-Gurrieri, J. Carrillo, J. Blanco, S. Gutiérrez-Granados, Production of HIV-1-based virus-like particles for vaccination: achievements and limits, Applied Microbiology and Biotechnology, 103 (2019) 7367-7384.
[41] P. Nestola, C. Peixoto, R.R.J.S. Silva, P.M. Alves, J.P.B. Mota, M.J.T. Carrondo, Improved virus purification processes for vaccines and gene therapy, Biotechnology and Bioengineering, 112 (2015) 843-857.
[42] T. Rodrigues, M.J.T. Carrondo, P.M. Alves, P.E. Cruz, Purification of retroviral vectors for clinical application: Biological implications and technological challenges, Journal of Biotechnology, 127 (2007) 520-541.
[43] M.G. Moleirinho, R.J.S. Silva, P.M. Alves, M.J.T. Carrondo, C. Peixoto, Current challenges in biotherapeutic particles manufacturing, Expert Opinion on Biological Therapy, (2019) 1-15.
[44] Annex 1. Requirments for the use of animal cells as in vitro substrates for the production of biologicals, World Health Organization 1998.
[45] Guidance for Industry: Characterization and Qualification of Cell Substrates and Other Biological Materials Used in the Production of Viral Vaccines for Infectious Disease Indications, U.S. Department of Health and Human Services Food and Drug Administration 2010.
[46] G. Raposo, W. Stoorvogel, Extracellular vesicles: exosomes, microvesicles, and friends, The Journal of cell biology, 200 (2013) 373-383.
[47] B. Michen, T. Graule, Isoelectric points of viruses, Journal of Applied Microbiology, 109 (2010) 388-397.
[48] P. Pereira Aguilar, T.A. Schneider, V. Wetter, D. Maresch, W.L. Ling, A. Tover, P. Steppert, A. Jungbauer, Polymer-grafted chromatography media for the purification of enveloped virus-like particles, exemplified with HIV-1 gag VLP, Vaccine, 37 (2019) 7070-7080.
[49] P. Steppert, D. Burgstaller, M. Klausberger, E. Berger, P.P. Aguilar, T.A. Schneider, P. Kramberger, A. Tover, K. Nobauer, E. Razzazi-Fazeli, A. Jungbauer, Purification of HIV-1 gag virus-like particles and separation of other extracellular particles, Journal of chromatography. A, 1455 (2016) 93-101.
[50] A. Jungbauer, Continuous downstream processing of biopharmaceuticals, Trends in Biotechnology, 31 (2013) 479-492.
[51] L. Besnard, V. Fabre, M. Fettig, E. Gousseinov, Y. Kawakami, N. Laroudie, C. Scanlan, P. Pattnaik, Clarification of vaccines: An overview of filter based technology trends and best practices, Biotechnology Advances, 34 (2016) 1-13.
[52] A. Negrete, A. Pai, J. Shiloach, Use of hollow fiber tangential flow filtration for the recovery and concentration of HIV virus-like particles produced in insect cells, Journal of Virological Methods, 195 (2014) 240-246.
[53] A.A. Shukla, U. Gottschalk, Single-use disposable technologies for biopharmaceutical manufacturing, Trends in Biotechnology, 31 (2013) 147-154.
[54] T. Rodrigues, A. Carvalho, M. Carmo, M.J. Carrondo, P.M. Alves, P.E. Cruz, Scaleable purification process for gene therapy retroviral vectors, J Gene Med, 9 (2007) 233-243.
[55] L. Reeves, K. Cornetta, Clinical retroviral vector production: step filtration using clinically approved filters improves titers, Gene Therapy, 7 (2000) 1993-1998.
[56] Y. Cherradi, S.L. Merdy, L.-J. Sim, T. Ito, P. Pattnaik, J. Haas, A. Boumlic, Filter-based clarification of viral vaccines and vectors, Bioprocess International, (2018) 48-53.
[57] S.B. Carvalho, R.J.S. Silva, A.S. Moreira, B. Cunha, J.J. Clemente, P.M. Alves, M.J.T. Carrondo, A. Xenopoulos, C. Peixoto, Efficient filtration strategies for the clarification of influenza virus-like particles derived from insect cells, Separation and Purification Technology, 218 (2019) 81-88.

[58] E. Gousseinov, W. Kools, P. Pattnaik, Nucleic acid impurity reduction in viral vaccine manufacturing, Bioprocess International, 12 (2014) 59-68.
[59] A.S. Coroadinha, L. Gama-Norton, A.I. Amaral, H. Hauser, P.M. Alves, P.E. Cruz, Production of retroviral vectors: review, Curr Gene Ther, 10 (2010) 456-473.
[60] C.B. Reimer, R.S. Baker, T.E. Newlin, M.L. Havens, Influenza virus purification with the zonal ultracentrifuge, Science, 152 (1966) 1379-1381.
[61] G. Tiscornia, O. Singer, I.M. Verma, Production and purification of lentiviral vectors, Nature Protocols, 1 (2006) 241-245.
[62] M. Morita, M. Aizawa, H. Toi, E. Fukuhara, K. Hashimoto, Continuous Flow Ultracentrifuge System for Production of Infection Prevention Vaccines, Hitachi Review, 60 (2011) 257-261.
[63] S. Meriño, S. Glanzman, Continuous flow centrifugation: importance in vector scale up, Cell Gene Therapy Insights, 2(5) (2016) 577-582.
[64] S.R. Wickramasinghe, B. Kalbfuß, A. Zimmermann, V. Thom, U. Reichl, Tangential flow microfiltration and ultrafiltration for human influenza A virus concentration and purification, Biotechnology and Bioengineering, 92 (2005) 199-208.
[65] M. Geraerts, M. Michiels, V. Baekelandt, Z. Debyser, R. Gijsbers, Upscaling of lentiviral vector production by tangential flow filtration, J Gene Med, 7 (2005) 1299-1310.
[66] K. Marino, P. Levison, Achieving Process Intensification with Single-Pass TFF, Genetic Engineering & Biotechnology News, 37 (2017) 30-31.
[67] G. Carta, A. Jungbauer, Protein Chromatography: Process Development and Scale-Up, Wiley-VHC Verlag GmbH & Co. KGaA, Weinheim, 2010.
[68] K. Reiter, P.P. Aguilar, V. Wetter, P. Steppert, A. Tover, A. Jungbauer, Separation of virus-like particles and extracellular vesicles by flow-through and heparin affinity chromatography, Journal of chromatography. A, 1588 (2019) 77-84.
[69] T. Vicente, M.F.Q. Sousa, C. Peixoto, J.P.B. Mota, P.M. Alves, M.J.T. Carrondo, Anion-exchange membrane chromatography for purification of rotavirus-like particles, Journal of Membrane Science, 311 (2008) 270-283.
[70] D.J. McNally, D. Darling, F. Farzaneh, P.R. Levison, N.K.H. Slater, Optimised concentration and purification of retroviruses using membrane chromatography, Journal of Chromatography A, 1340 (2014) 24-32.
[71] H.M. Oksanen, A. Domanska, D.H. Bamford, Monolithic ion exchange chromatographic methods for virus purification, Virology, 434 (2012) 271-277.
[72] J. Ruscic, C. Perry, T. Mukhopadhyay, Y. Takeuchi, D.G. Bracewell, Lentiviral Vector Purification Using Nanofiber Ion-Exchange Chromatography, Molecular Therapy - Methods & Clinical Development, 15 (2019) 52-62.
[73] Y.-F. Tseng, T.-C. Weng, C.-C. Lai, P.-L. Chen, M.-S. Lee, A.Y.-C. Hu, A fast and efficient purification platform for cell-based influenza viruses by flow-through chromatography, Vaccine, 36 (2018) 3146-3152.
[74] T. Weigel, T. Solomaier, A. Peuker, T. Pathapati, M.W. Wolff, U. Reichl, A flow-through chromatography process for influenza A and B virus purification, Journal of Virological Methods, 207 (2014) 45-53.
[75] L.M. Fischer, M.W. Wolff, U. Reichl, Purification of cell culture-derived influenza A virus via continuous anion exchange chromatography on monoliths, Vaccine, 36 (2018) 3153-3160.
[76] P. Gerster, E.-M. Kopecky, N. Hammerschmidt, M. Klausberger, F. Krammer, R. Grabherr, C. Mersich, L. Urbas, P. Kramberger, T. Paril, M. Schreiner, K. Nöbauer, E. Razzazi-Fazeli, A. Jungbauer, Purification of infective baculoviruses by monoliths, Journal of Chromatography A, 1290 (2013) 36-45.

[77] P. Steppert, D. Burgstaller, M. Klausberger, P. Kramberger, A. Tover, E. Berger, K. Nobauer, E. Razzazi-Fazeli, A. Jungbauer, Separation of HIV-1 gag virus-like particles from vesicular particles impurities by hydroxyl-functionalized monoliths, Journal of separation science, 40 (2017) 979-990.
[78] C. Ladd Effio, T. Hahn, J. Seiler, S.A. Oelmeier, I. Asen, C. Silberer, L. Villain, J. Hubbuch, Modeling and simulation of anion-exchange membrane chromatography for purification of Sf9 insect cell-derived virus-like particles, Journal of Chromatography A, 1429 (2016) 142-154.
[79] A. Zöchling, R. Hahn, K. Ahrer, J. Urthaler, A. Jungbauer, Mass transfer characteristics of plasmids in monoliths, Journal of separation science, 27 (2004) 819-827.
[80] R. Ghosh, Protein separation using membrane chromatography: opportunities and challenges, Journal of Chromatography A, 952 (2002) 13-27.
[81] M. Yu, Y. Li, S. Zhang, X. Li, Y. Yang, Y. Chen, G. Ma, Z. Su, Improving stability of virus-like particles by ion-exchange chromatographic supports with large pore size: Advantages of gigaporous media beyond enhanced binding capacity, Journal of Chromatography A, 1331 (2014) 69-79.
[82] E. Müller, Properties and Characterization of High Capacity Resins for Biochromatography, Chemical Engineering & Technology, 28 (2005) 1295-1305.
[83] G. Braas, P.F. Searle, N.K.H. Slater, A. Lyddiatt, Strategies for the isolation and purification of retroviral vectors for gene therapy, Bioseparation, 6 (1996) 211-228.
[84] A. Rathore, A. Velayudhan, Scale-Up and Optimization in Preparative Chromatography: Principles and Biopharmaceutical Applications, Taylor & Francis, 2002.
[85] A.M. Lenhoff, Protein adsorption and transport in polymer-functionalized ion-exchangers, Journal of Chromatography A, 1218 (2011) 8748-8759.
[86] B.D. Bowes, H. Koku, K.J. Czymmek, A.M. Lenhoff, Protein adsorption and transport in dextran-modified ion-exchange media. I: Adsorption, Journal of Chromatography A, 1216 (2009) 7774-7784.
[87] E.X.P. Almodóvar, Y. Tao, G. Carta, Protein adsorption and transport in cation exchangers with a rigid backbone matrix with and without polymeric surface extenders, Biotechnology Progress, 27 (2011) 1264-1272.
[88] Q. Wang, L. Yu, Y. Sun, Grafting glycidyl methacrylate to Sepharose gel for fabricating high-capacity protein anion exchangers, Journal of Chromatography A, 1443 (2016) 118-125.
[89] B.D. Bowes, A.M. Lenhoff, Protein adsorption and transport in dextran-modified ion-exchange media. III. Effects of resin charge density and dextran content on adsorption and intraparticle uptake, Journal of Chromatography A, 1218 (2011) 7180-7188.
[90] W. Müller, New ion exchangers for the chromatography of biopolymers, Journal of Chromatography A, 510 (1990) 133-140.
[91] J. Diedrich, W. Heymann, S. Leweke, S. Hunt, R. Todd, C. Kunert, W. Johnson, E. von Lieres, Multi-state steric mass action model and case study on complex high loading behavior of mAb on ion exchange tentacle resin, Journal of Chromatography A, 1525 (2017) 60-70.
[92] K.T. James, B. Cooney, K. Agopsowicz, M.A. Trevors, A. Mohamed, D. Stoltz, M. Hitt, M. Shmulevitz, Novel High-throughput Approach for Purification of Infectious Virions, Scientific reports, 6 (2016) 36826-36826.
[93] M. de las Mercedes Segura, A. Kamen, A. Garnier, Purification of Retrovirus Particles Using Heparin Affinity Chromatography, in: J.M. Le Doux (Ed.) Gene Therapy Protocols: Design and Characterization of Gene Transfer Vectors, Humana Press, Totowa, NJ, 2008, pp. 1-11.
[94] M. Zhao, M. Vandersluis, J. Stout, U. Haupts, M. Sanders, R. Jacquemart, Affinity chromatography for vaccines manufacturing: Finally ready for prime time?, Vaccine, 37 (2019) 5491-5503.
[95] A. Zahn, J.P. Allain, Hepatitis C virus and hepatitis B virus bind to heparin: purification of largely IgG-free virions from infected plasma by heparin chromatography, J Gen Virol, 86 (2005) 677-685.
[96] M. Nasimuzzaman, D. Lynn, J.C.M. van der Loo, P. Malik, Purification of baculovirus vectors using heparin affinity chromatography, Molecular Therapy - Methods & Clinical Development, 3 (2016) 16071.

[97] M.M. Segura, A. Garnier, Y. Durocher, H. Coelho, A. Kamen, Production of lentiviral vectors by large-scale transient transfection of suspension cultures and affinity chromatography purification, Biotechnology and Bioengineering, 98 (2007) 789-799.
[98] P. Kramberger, L. Urbas, A. Štrancar, Downstream processing and chromatography based analytical methods for production of vaccines, gene therapy vectors, and bacteriophages, Human Vaccines & Immunotherapeutics, 11 (2015) 1010-1021.
[99] Z. Kimia, S.N. Hosseini, S.S. Ashraf Talesh, M. Khatami, A. Kavianpour, A. Javidanbardan, A novel application of ion exchange chromatography in recombinant hepatitis B vaccine downstream processing: Improving recombinant HBsAg homogeneity by removing associated aggregates, Journal of Chromatography B, 1113 (2019) 20-29.
[100] A. Venereo-Sánchez, K. Fulton, K. Koczka, S. Twine, P. Chahal, S. Ansorge, R. Gilbert, O. Henry, A. Kamen, Characterization of influenza H1N1 Gag virus-like particles and extracellular vesicles co-produced in HEK-293SF, Vaccine, 37 (2019) 7100-7107.
[101] S. Buffin, I. Peubez, F. Barrière, M.-C. Nicolaï, T. Tapia, V. Dhir, E. Forma, N. Sève, I. Legastelois, Influenza A and B virus-like particles produced in mammalian cells are highly immunogenic and induce functional antibodies, Vaccine, 37 (2019) 6857-6867.
[102] M.M. Segura, A. Garnier, M.R. Di Falco, G. Whissell, A. Meneses-Acosta, N. Arcand, A. Kamen, Identification of Host Proteins Associated with Retroviral Vector Particles by Proteomic Analysis of Highly Purified Vector Preparations, Journal of Virology, 82 (2008) 1107.
[103] V. Lecouturier, C. Berry, A. Saulnier, S. Naville, C. Manin, Y. Girerd-Chambaz, J.E. Crowe, N. Jackson, B. Guy, Characterization of recombinant yellow fever-dengue vaccine viruses with human monoclonal antibodies targeting key conformational epitopes, Vaccine, 37 (2019) 4601-4609.
[104] F. Nasrin, A.D. Chowdhury, K. Takemura, J. Lee, O. Adegoke, V.K. Deo, F. Abe, T. Suzuki, E.Y. Park, Single-step detection of norovirus tuning localized surface plasmon resonance-induced optical signal between gold nanoparticles and quantum dots, Biosensors and Bioelectronics, 122 (2018) 16-24.
[105] R. Yazdani, M. Shams-Bakhsh, A. Hassani-Mehraban, S.S. Arab, N. Thelen, M. Thiry, J. Crommen, M. Fillet, N. Jacobs, A. Brans, A.-C. Servais, Production and characterization of virus-like particles of grapevine fanleaf virus presenting L2 epitope of human papillomavirus minor capsid protein, BMC Biotechnology, 19 (2019) 81.
[106] X. Wang, D.M. Morgan, G. Wang, N.M. Mozier, Residual DNA analysis in biologics development: Review of measurement and quantitation technologies and future directions, Biotechnology and Bioengineering, 109 (2012) 307-317.
[107] C.M. Thompson, E. Petiot, A. Lennaertz, O. Henry, A.A. Kamen, Analytical technologies for influenza virus-like particle candidate vaccines: challenges and emerging approaches, Virology Journal, 10 (2013) 141.
[108] S. Collett, J. Torresi, L. Earnest-Silveira, D. Christiansen, A. Elbourne, P.A. Ramsland, Probing and pressing surfaces of hepatitis C virus-like particles, Journal of Colloid and Interface Science, 545 (2019) 259-268.
[109] I. González-Domínguez, S. Gutiérrez-Granados, L. Cervera, F. Gòdia, N. Domingo, Identification of HIV-1-Based Virus-like Particles by Multifrequency Atomic Force Microscopy, Biophysical journal, 111 (2016) 1173-1179.
[110] J.L. Martin, S. Cao, J.O. Maldonado, W. Zhang, L.M. Mansky, Distinct Particle Morphologies Revealed through Comparative Parallel Analyses of Retrovirus-Like Particles, Journal of virology, 90 (2016) 8074-8084.
[111] S. Liu, Y. Luo, Y. Wang, S. Li, Z. Zhao, Y. Bi, J. Sun, R. Peng, H. Song, D. Zhu, Y. Sun, S. Li, L. Zhang, W. Wang, Y. Sun, J. Qi, J. Yan, Y. Shi, X. Zhang, P. Wang, H.-J. Qiu, G.F. Gao, Cryo-EM Structure of the African Swine Fever Virus, Cell Host & Microbe, 26 (2019) 836-843.e833.

[112] M. Klein, M. Menta, T.G. Dacoba, J. Crecente-Campo, M.J. Alonso, D. Dupin, I. Loinaz, B. Grassl, F. Séby, Advanced nanomedicine characterization by DLS and AF4-UV-MALS: Application to a HIV nanovaccine, Journal of Pharmaceutical and Biomedical Analysis, 179 (2020) 113017.
[113] Z. Wei, M. McEvoy, V. Razinkov, A. Polozova, E. Li, J. Casas-Finet, G.I. Tous, P. Balu, A.A. Pan, H. Mehta, M.A. Schenerman, Biophysical characterization of influenza virus subpopulations using field flow fractionation and multiangle light scattering: Correlation of particle counts, size distribution and infectivity, Journal of Virological Methods, 144 (2007) 122-132.
[114] R.A. Dragovic, C. Gardiner, A.S. Brooks, D.S. Tannetta, D.J.P. Ferguson, P. Hole, B. Carr, C.W.G. Redman, A.L. Harris, P.J. Dobson, P. Harrison, I.L. Sargent, Sizing and phenotyping of cellular vesicles using Nanoparticle Tracking Analysis, Nanomedicine: Nanotechnology, Biology and Medicine, 7 (2011) 780-788.
[115] P. Steppert, D. Burgstaller, M. Klausberger, A. Tover, E. Berger, A. Jungbauer, Quantification and characterization of virus-like particles by size-exclusion chromatography and nanoparticle tracking analysis, Journal of chromatography. A, 1487 (2017) 89-99.
[116] J. Stetefeld, S.A. McKenna, T.R. Patel, Dynamic light scattering: a practical guide and applications in biomedical sciences, Biophysical Reviews, 8 (2016) 409-427.
[117] S. Podzimek, Multi-Angle Light Scattering: An Efficient Tool Revealing Molecular Structure of Synthetic Polymers, Macromolecular Symposia, 384 (2019) 1800174.
[118] P. Pereira Aguilar, I. Gonzalez-Dominguez, T.A. Schneider, F. Godia, L. Cervera, A. Jungbauer, At-line multi-angle light scattering detector for faster process development in enveloped virus-like particle purification, Journal of separation science, 42 (2019) 2640-2649.
[119] H. Amartely, D. Some, A. Tsadok, M. Lebendiker, Ion Exchange Chromatography (IEX) Coupled to Multi-angle Light Scattering (MALS) for Protein Separation and Characterization, JoVE, (2019) e59408.

5. Publications

Publication I

"Polymer-grafted chromatography media for the purification of enveloped virus-like particles, exemplified with HIV-1 gag VLP"

***Patricia Pereira Aguilar**, Tobias Amadeus Schneider, Viktoria Wetter, Daniel Maresch, Wai Li Ling, Andres Tover, Petra Steppert, Alois Jungbauer*, Vaccine, 37(47), 2019, 7070-7080

https://doi.org/10.1016/j.vaccine.2019.07.001

Publication II

"At-line multi-angle light scattering detector for faster process development in enveloped virus-like particle purification"

***Patricia Pereira Aguilar**, Irene González-Domínguez, Tobias Amadeus Schneider, Francesc Gòdia, Laura Cervera, Alois Jungbauer*, Journal of Separation Science, 42(16), 2019, 2640-2649

https://doi.org/10.1002/jssc.201900441

Publication III

"Capture and purification of HIV-1 gag virus-like particles: convective media vs porous beads"

***Patricia Pereira Aguilar**, Katrin Reiter, Viktoria Wetter, Petra Steppert, Daniel Maresch, Wai Li Ling, Peter Satzer, Alois Jungbauer*, Submitted to Journal of Chromatography A (under review since 24/12/2019)

Publication IV

"Purification of HIV-1 gag virus-like particles and separation of other extracellular particles"

Journal of Chromatography A 2016, 1455, 93-101

Petra Steppert, Daniel Burgstaller, Miriam Klausberger, Eva Berger, ***Patricia Pereira Aguilar**, Tobias A. Schneider, Petra Kramberger, Andres Tover, Katharina Nöbauer, Ebrahim Razzazi-Fazeli, Alois Jungbauer*, Journal of Chromatography A, 1455, 2016, 93-101

https://doi.org/10.1016/j.chroma.2016.05.053

Publication V

"Separation of virus-like particles and extracellular vesicles by flow-through and heparin affinity chromatography"

Katrin Reiter, ***Patricia Pereira Aguilar****, Viktoria Wetter, Petra Steppert, Andres Tover, Alois Jungbauer*, Journal of Chromatography A, 1588, 2019, 77-84,

https://doi.org/10.1016/j.chroma.2018.12.035

Publication VI

"Separation of influenza virus-like particles from baculovirus by polymer grafted anion-exchanger"

Katrin Reiter, ***Patricia Pereira Aguilar****, Dominik Grammelhofer, Judith Joseph, Petra Steppert, Alois Jungbauer*, Submitted to Journal of Separation Science (submitted on 30/11/2019, currently under review)

Contributions for the publications:

For publication I, Patricia Aguilar designed, operated and evaluated all experiments, except proteomic and microscopy analysis. Patricia Aguilar wrote the manuscript and revised it together with Prof. Alois Jungbauer.

For publication II, Patricia Aguilar evaluated all chromatographic and analytical experiments and conducted them together with Irene González-Domínguez and Tobias Amadeus Schneider. Patricia Aguilar wrote and revised the manuscript.

For publication III, Patricia Aguilar designed, operated and evaluated all chromatographic experiments and designed and evaluated all of the analytical experiments. Patricia Aguilar wrote the manuscript and revised it together with Dr. Peter Satzer and Prof. Alois Jungbauer.

For publication IV, Patricia Aguilar performed part of the chromatographic and analytical experiments.

For publication V, Patricia Aguilar helped evaluating the data of some of the experiments and helped writing and revising the manuscript.

For publication VI, Patricia Aguilar helped designing and evaluating the chromatographic experiments and helped writing and revising the manuscript.

PUBLICATION I

Vaccine 37 (2019) 7070–7080

Contents lists available at ScienceDirect

Vaccine

journal homepage: www.elsevier.com/locate/vaccine

Polymer-grafted chromatography media for the purification of enveloped virus-like particles, exemplified with HIV-1 gag VLP

Patricia Pereira Aguilar [a], Tobias Amadeus Schneider [b], Viktoria Wetter [b], Daniel Maresch [a], Wai Li Ling [c], Andres Tover [d], Petra Steppert [a], Alois Jungbauer [a,b,*]

[a] Department of Biotechnology, University of Natural Resources and Life Sciences Vienna, Austria
[b] Austrian Centre of Industrial Biotechnology, Vienna, Austria
[c] Univ. Grenoble Alpes, CEA, CNRS, IBS, F-38000 Grenoble, France
[d] Icosagen AS, Tartumaa, Estonia

ARTICLE INFO

Article history:
Available online 9 July 2019

Keywords:
Fractogel®
Dynamic binding capacity
HIV-1 gag variants
Nanoparticle tracking analysis
Multi-angle light scattering

ABSTRACT

Polymer-grafted chromatography media, especially ion exchangers, are high performance materials for protein purification. However, due to the pore size limitation, conventional chromatography beads are usually not considered for the downstream processing of large biomolecules such as virus-like particles (VLPs). Contrariwise, since the outer surface of the chromatography beads provides satisfactory binding capacity for VLPs and impurities of smaller size can bind inside of the beads, conventional porous beads should be considered for VLP capture and purification. We used HIV-1 gag VLPs with a diameter of 100–200 nm as a model to demonstrate that polymer-grafted anion exchangers are suitable for the purification of bionanoparticles. The equilibrium binding capacity was 1×10^{13} part/mL resin. Moderate salt concentration up to 100 mM NaCl did not affect binding, allowing direct loading of cell culture supernatant onto the column for purification. Dynamic binding capacity at 10% breakthrough, when loading cell culture supernatant, was approximately 6×10^{11} part/mL column; only 1-log lower than for monoliths. Endonuclease treatment of the cell culture supernatant did not increase the dynamic binding capacity, suggesting that dsDNA does not compete for the binding sites of VLPs. Nevertheless, due to simultaneous elution of particles and dsDNA, endonuclease treatment is required to reduce dsDNA contamination in the product. Proteomic analysis revealed that HIV-1 gag VLPs contain different host cell proteins in their cargo. This cargo is composed of conserved proteins and other proteins that vary from one particle population to another, as well as from batch to batch. This process allowed the separation of different particle populations. HIV-1 gag VLPs were directly captured and purified from cell culture supernatant with a total particle recovery in the elution of about 35%. Columns packed with beads can be scaled to practically any dimension and therefore a tailored design of the process is possible.
© 2019 The Authors. Published by Elsevier Ltd. This is an open access article under the CC BY license (http://creativecommons.org/licenses/by/4.0/).

1. Introduction

Polymer-grafted chromatography media are rigid porous backbone supports containing polymer chains grafted on their surface. In ion exchange chromatography, these polymer chains are functionalized with charged ligands, which are responsible for interacting with biomolecules [1]. Ion-exchange chromatography is a highly efficient unit operation for the purification of biopharmaceuticals such as proteins, DNA and bionanoparticles [2–4]. Currently emerging biopharmaceuticals include very large and complex molecules, with hydrodynamic radius ranging from tens to hundreds of nanometers, such as virus-like particles (VLPs), viral vectors, extracellular vesicles (EVs) and liposomes [5–11]. New generation matrices have been developed for the capture and purification of such large bionanoparticles including monoliths, membrane adsorbers, fibers and gigaporous resins [8,12,13]. Monoliths', membrane adsorbers' and fibers' open pore structure results in higher surface area available for the binding of large biomolecules and the predominant convective mass transfer allows the use of high flow rates [14–16]. However, monoliths are prone to fouling and clogging and membrane adsorbers tend to have poor resolution [12,17]. Additionally, although these type of matrices can be scaled-up, they are produced in a limited number of sizes reducing the flexibility of the scale-up. Conversely, conventional

* Corresponding author at: Department of Biotechnology, University of Natural Resources and Life Sciences Vienna, Muthgasse 18, 1190 Vienna, Austria.
E-mail address: alois.jungbauer@boku.ac.at (A. Jungbauer).

https://doi.org/10.1016/j.vaccine.2019.07.001
0264-410X/© 2019 The Authors. Published by Elsevier Ltd.
This is an open access article under the CC BY license (http://creativecommons.org/licenses/by/4.0/).

chromatography media (beads) have the advantage of easy and flexible scalability to industrial scale [18]. Porous beads are usually not considered for the purification of large biomolecules in bind-elute mode due to pore size limitations. As a rule of thumb, it is assumed that to guarantee fast mass transfer, a pore size 10 times larger than the molecule size is required [19,20]. Macro- and giga-porous chromatography beads were developed to overcome the mass transfer limitation of conventional porous beads. Yu et al. showed that increasing the resin's pore diameter (up to 280 nm) increases both, binding capacity and mass transfer rate of HB-VLPs (50 nm diameter) [21]. Still, the estimated effective pore diffusivity (D_e) was one or two orders of magnitude lower than the D_e of most proteins in similar conditions [22]. Moreover, larger biomolecules (diameter >50 nm) are usually excluded from the resin pores, binding as thin layers on the surface of the beads and consequently resulting in lower binding capacities [23,24]. Nevertheless, the expected reduced binding capacity of large biomolecules onto porous chromatography beads can be balanced by the easy scalability of this type of chromatography. In addition, binding sites in the interior of the beads are available for binding of impurities such as host cell proteins, DNA and RNA, reducing the probability of binding site competition and displacement effects.

Polymer-grafted ion exchangers are widely used for protein purification and have higher binding capacity when compared to non-grafted resins [25,26]. This is explained by the increase in surface area and ligand density upon grafting (up to a certain limit), as well as by the 3D structure of the ligands which allows multilayer adsorption [26–28]. To investigate the applicability of ion exchange chromatography beads for the purification of large and complex biomolecules we used Fractogel® EMD TMAE Hicap (M) resin from Merck (Darmstadt, Germany), hereinafter referred as Fractogel®-TMAE. Fractogel®-TMAE beads have a crosslinked polymethacrylate backbone grafted with long linear polymer chains ("tentacles") which are functionalized with trimethylaminoethyl groups (strong anion exchanger). Ligands in tentacle-type ion exchangers have high flexibility allowing multipoint ligand-biomolecule interactions. This increases selectivity as the interaction involves the overall steric charge distribution of the biomolecules [29,30]. According to the manufacturer, Fractogel®-TMAE beads have a particle size distribution of 40–90 μm and a pore size of 80 nm.

Within the new emerging biopharmaceuticals, we selected enveloped virus-like particles (eVLPs) as model for large and complex biomolecules. VLPs have proven their value in several applications such as vaccines, drug delivery and medical diagnostics [5,6,9,31]. VLPs have the advantageous safety profile of subunit vaccines (lack of viral genetic material) while keeping the same efficacy of the conventional ones, such as killed or live attenuated vaccines [7,31]. Enveloped virus-like particles are formed in a complex process which includes the self-assembly of recombinant viral proteins while budding at a host cell membrane. It has been shown that, besides the plasma membrane, several intracellular membranes, such as endosomes, nuclear envelope, endoplasmic reticulum and Golgi, serve as viral budding platforms [32]. Due to the complexity of the assembly and budding processes, the recombinant production of eVLPs often results in heterogeneous particle population's, which may include in their cargo (incorporated molecular components) different host cell proteins, DNA and/or RNA fragments [33–35]. Additionally, cells naturally release extracellular vesicles (EVs) with similar surface properties, size, structure and cargo to eVLPs because both, eVLPs and EVs, share some biogenesis pathways [36]. The result is a very complex mixture containing different bionanoparticle populations that need to be separated in order to allow their characterization and understanding of their biologic activity. Since eVLPs are surrounded by the host cell lipid-bilayer it is assumed that they have multiple positive and negative charges on their surface [37]. We used HIV-1 gag VLPs, produced in CHO cells, which have a diameter of about 100–200 nm. Steppert et al. showed that HIV-1 gag VLPs bind to anion exchange monoliths but do not bind to cation exchange monoliths, revealing that these VLPs have an overall negative net charge (in a pH range from 6.5 to 8.5) [38]. Therefore, HIV-1 gag VLPs are suitable for investigating the capability of polymer-grafted anion exchangers, such as Fractogel®-TMAE, to capture and purify eVLPs.

A remaining challenge in the development and optimization of downstream processes is the lack of high throughput methodologies for specific detection and quantification of eVLPs in complex mixtures, as well as for the in-process control of product quality and quantity [6,39]. Additionally, there are no simple and accurate bioassay for differentiating between different particle populations [40,41]. So far the available methods for EV and VLP discrimination depend on modifications at the cellular level, for example by incorporating fluorescent tags in VLPs [42,43]. Thus, we used a combination of methods for particle detection, quantification and visualization (multi-angle light scattering, MALS; nanoparticle tracking analysis, NTA; TEM and cryo-TEM), total and specific protein detection and quantification (SDS-PAGE, Bradford assay, Western blot analysis and ELISA) and dsDNA quantification (Picogreen assay). Proteomic analysis (mass spectrometry) was performed to characterize the cargo of the particles and differentiate different particle populations.

We developed a downstream processing strategy based on polymer-grafted chromatography media (Fractogel®-TMAE) for the direct capture and purification of HIV-1 gag VLPs and separation of different particle populations.

2. Materials and methods

2.1. Chemicals and reagents

Chemicals and reagents used in the experiments were purchased from Merck KGaA (Darmstadt, Germany) or Sigma Aldrich (St. Louis, MO, USA).

2.2. HIV-1 gag VLPs

Cell culture supernatant containing HIV-1 gag VLPs was kindly provided by Icosagen (Tartumaa, Estonia). The VLPs were produced in a CHOEBNALT85 cell line using a stable episomal expression system, as previously described by Steppert et al. [1].

2.3. Endonuclease treatment

The digestion of double stranded DNA (dsDNA) was performed using Benzonase® purity grade II (Merck KGaA, Darmstadt Germany) according to the manufacturer's instructions. Briefly, the clarified cell culture supernatant was treated with 150 U/mL Benzonase® and 2 mM $MgCl_2$ for 2 h at 37 °C.

2.4. Adsorption isotherms

Adsorption isotherms were determined by equilibrating 10 μL of Fractogel®-TMAE (Fractogel® EMD TMAE Hicap (M) resin, Merck, Darmstadt, Germany) with 250 μL HIV-1 gag VLP solutions, at different initial concentrations, in 96 well filter plates (AcroPrep™ Advance, 350 μL, 1.2 μm Supor® membrane, Pall Corporation, New York, USA). For this purpose, HIV-1 gag VLPs were purified by preparative anion exchange chromatography using an 8 mL CIMmultus QA monolith (BIA Separations, Ajdovščina, Slovenia) as previously described by Steppert et al. [38]. Purified VLPs were

buffer exchanged to 50 mM HEPES, pH 7.2 buffer containing 0 or 100 mM NaCl using Slide-A-Lyzer™ Dialysis Cassettes (Thermo Fisher Scientific, Waltham, MA, USA) with a 10 K molecular weight cut off. Fractogel®-TMAE was equilibrated with the same buffer conditions as the VLPs. All isotherms were conducted at 22 °C and 350 rpm during 24 h. After equilibration, a filtration step was used to separate the resin from the equilibrium VLP solution (containing the unbound VLPs). VLP quantification before and after equilibration with the resin was performed by measuring the UV absorbance at 280 nm. A calibration curve relating the particle concentration measured by Nanoparticle Tracking Analysis (NTA) and the UV absorbance at 280 nm was used to access the VLP concentration in particles/mL.

2.5. Chromatographic experiments

2.5.1. Equipment

Chromatographic experiments were performed on an Äkta pure 25 M2 equipped with a 1.4 mL mixer chamber, a S9 sample pump and a F9-C fraction collector (GE Healthcare, Uppsala, Sweden). System control and data acquisition were performed using the Unicorn 6.4.1 software. UV absorbance (280, 260 and 214 nm), conductivity and pH were continuously monitored during the chromatographic runs.

2.5.2. Chromatographic stationary and mobile phases

Fractogel®-TMAE (Fractogel® EMD TMAE Hicap (M) resin) was used as stationary phase (Merck KGaA, Darmstadt, Germany). Buffer A, containing 50 mM HEPES, pH 7.2 and buffer B, containing 50 mM HEPES, 2 M NaCl, pH 7.2 were used as mobile phases. To obtain different concentration of the modifier (NaCl), buffer A and B were mixed. During cleaning-in-place procedures, 0.5 M NaOH was used. All buffers were prepared with ultra-pure water and filtered using MF-Millipore™ 0.22 μm MCE Membranes (Sigma Aldrich, St. Louis, MO, USA).

2.5.3. Breakthrough curves and dynamic binding capacity

Breakthrough experiments were performed in prepacked Mini-Chrom columns 8 × 20 mm (Merck KGaA, Darmstadt, Germany) containing 1 mL of Fractogel®-TMAE. Clarified cell culture supernatant was 0.8 μm filtered (Millex AA filter, Millipore Bedford, USA) and, without further preconditioning, loaded into the column. The used method consisted of a 10 CV equilibration step at 5% B, followed by the injection of 50 mL loading material via sample pump. The flow rate was 0.2 mL/min (24 cm/h, 5 min residence time). Flow-through fractions were collected and pooled according to the chromatogram. The same method was used for the breakthrough curve of endonuclease treated cell culture supernatant. The dynamic binding capacity ($DBC_{10\%}$) was calculated at 10% breakthrough of particles in the range of 100–200 nm (measured with NTA). $DBC_{10\%}$ was calculated using the following equation $DBC_{10\%} = (C_F \cdot V_{b,10\%})/CV$, where C_F is the feed concentration, $V_{b,10\%}$ is the load volume at 10% breakthrough and CV is the column volume [18].

2.5.4. Purification of HIV-1 gag VLPs

For preparative purification of HIV-1 gag VLPs form CHO cell culture supernatant, a XK 16/20 column (GE Healthcare, Uppsala, Sweden) packed with 5.43 mL of Fractogel®-TMAE was used. Clarified cell culture supernatant (or clarified and Benzonase® treated cell culture supernatant) was 0.8 μm filtered (Millex AA filter, Millipore Bedford, USA) and, without further preconditioning, loaded into the column. The used method consisted of a 2 CV equilibration step at 5% B, followed by the injection of 50 mL loading material via sample pump. After loading, the column was washed with 5% B buffer for 6 CV. Elution was achieved by a salt linear gradient from 5 to 50% B in 20 CV, including a 10 mL hold step at 50% B at the end of the gradient. The column was regenerated with 100% B in a 3 CV step. Cleaning-in-place (CIP) was performed with 0.5 M NaOH in a 5 CV step. The flow rate was 1.0 mL/min (29.8 cm/h, 5.4 min residence time). Small fractions were collected in 96-well plates during the whole run and pooled according to the chromatogram.

2.6. Multi-angle light scattering (MALS)

Light scattering intensity (LS) measurements were performed using a MALS detector (DAWN HELEOS, 18-angle, Wyatt, Santa Barbara, CA, USA) connected to an Ultimate 3000 HPLC system equipped with a 3000TSL autosampler (Thermo Fisher, Waltham, MA, USA). Chromeleon® 7 software (Thermo Fisher, Waltham, MA, USA) was used to control the HPLC system. LS data was acquired and processed using the ASTRA software, version 6.1.2 (Wyatt, Santa Barbara, CA, USA). A sample volume of 20 μL was directly injected into the MALS detector using the HPLC in bypass mode. All samples were measured in duplicates. A flow rate of 0.3 mL/min was used.

2.7. Nanoparticle tracking analysis (NTA)

Particle concentration and particle size distribution were determined by NTA using a NanoSight NS300 instrument (Malvern Instruments Ltd., Worcestershire, UK), equipped with a blue laser module (488 nm) and a neutral density filter. The NanoSight NTA software version 3.2 (Malvern Instruments Ltd., Worcestershire, UK) was used for instrument control, data acquisition and data processing. Each sample was serially diluted in particle-free water in order to obtain a particle concentration in the range of 20–100 particles/frame. For each sample, three dilutions were measured. Per dilution, five videos of 30 s were recorded and analysed. All measurements were performed at 25 °C. The camera level was manually adjusted to values between 12 and 16. For the data processing, detection thresholds between 3 and 5 were used. Remaining analysis parameters were automatically selected by the software and kept constant for all samples.

2.8. Total protein and double stranded DNA (dsDNA) quantification

Total protein was quantified by Bradford assay using Coomassie blue G-250-based protein dye reagent (Bio-Rad Laboratories, Hercules, CA, USA). Bovine serum albumin (BSA) standards (Thermo Fisher Scientific, Waltham, MA, USA) diluted in 1x PBS buffer were used to obtain a calibration curve in the range of 25–200 μg/mL. Total dsDNA was quantified using Quant-iT™ PicoGreen® dsDNA kit (Life Technologies, Waltham, MA, USA). Both quantifications were performed in a microtiter plate format according to the manufacturer's instructions. A Genius Pro plate reader (Tecan, Männedorf, Switzerland) was used to measure the signals in both assays.

2.9. Protein identification and peptide analysis using LC-ESI-MS

Relevant samples were digested with sequencing grade modified trypsin (Promega, Madison, Wisconsin, EUA). The samples were analysed using a Dionex Ultimate 3000 system (Thermo Fischer Scientific, Waltham, MA, USA) directly linked to a QTOF instrument (maXis 4G ETD, Bruker, Billerica, Massachusetts, USA) equipped with the standard ESI source (CaptiveSpray nanoBooster, respectively) in the positive ion, DDA mode (=switching to MSMS mode for eluting peaks). MS-scans were recorded (range: 150–2200 m/z) and the 6 highest peaks were selected for fragmentation. Instrument calibration was performed using ESI calibration mixture (Agilent Technologies, Santa Clara, California, EUA). For separation of the peptides a Thermo BioBasic C18 separation

column (5 μm particle size, 150 × 0.320 mm) was used. A gradient from 95% solvent A and 5% solvent B (Solvent A: 65 mM ammonium formiate buffer, B: 100% ACN) to 32% B in 45 min was applied, followed by a 15 min gradient from 32% B to 75% B, at a flow rate of 6 μL/min. For the measurements in nano-mode a Thermo Acclaim PepMap300 RSLC C18 separation column (2 μm particle size, 150 × 0.075 mm) was used with a Thermo Acclaim PepMap μ-precolumn. A gradient from 5% solvent B (solvent A: 0.1% formic acid in HQ-water, solvent B: 0.1% formic acid in ACN) to 32% B in 60 min was applied, followed by a 10 min gradient from 32% B to 70% B that facilitates elution of large peptides, at a flow rate of 0.3 μL/min. The analysis files were converted using Data Analysis 4.0 (Bruker, Billerica) to XML files, which are suitable to perform MS/MS ion searches with MASCOT (embedded in ProteinScape 3.0, Bruker) for protein identification. Only proteins identified with at least 2 peptides with a protein score higher than 80 were accepted. For the searches, the reviewed UniProt database and the Reference proteome of Cricetulus griseus (UP000001075) were used.

2.10. Enzyme-linked immunosorbent assay (ELISA)

The HIV-1 p24 Capsid Protein p24 ELISA Kit (Sino Biological, Wayne, USA) was used for the quantification of HIV-1 p24, which is part of the HIV-1 gag polyprotein, according to the manufacturer's instructions. In order to release the gag protein from the enveloped VLPs, samples were incubated with SNCR buffer [44] at 70 °C for 10 min, followed by an incubation with 1.5% Triton X-100 at 100 °C for another 10 min. A linear calibration curve for the p24 protein (10 to 1000 pg/mL) was obtained using the HIV-1 p24 standard provided in the kit. A SIGMAFAST™ OPD substrate tablet (Sigma Aldrich, St. Louis, MO, USA) dissolved in 20 mL deionized water was used as substrate solution. The enzymatic reaction was stopped adding 1.25 N H_2SO_4. Absorbance was measured at 492 nm with a reference wavelength at 630 nm using an Infinite 200 Pro plate reader (Tecan, Männedorf, Switzerland).

2.11. Sodium dodecyl sulfate-polyacrylamide gel electrophoresis (SDS-PAGE) and Western blot analysis

Electrophoresis (200 V, 400 mA, 50 min) was performed in an X-cell SureLock® Mini-Cell electrophoresis chamber (Invitrogen, Carlsbad, CA, USA), using NuPAGE® Bis/Tris 4–12% gels (Invitrogen, Carlsbad, CA, USA) and reduced MES-SDS running conditions. Samples were prepared with NuPAGE® LDS sample buffer (Invitrogen, Carlsbad, CA, USA) and reduced at 99 °C for 15 min in the presence of 182 mM dithiothreitol (DTT). For each sample, a volume of 20 μL was loaded in a gel lane. SeeBlue® Plus2 Pre-stained Protein Standard (Invitrogen, Carlsbad, CA, USA) was used as molecular weight marker. Protein bands in the gel were stained using Coomassie Brilliant Blue G-250 based EZBlue™ Gel Staining Reagent (Sigma Aldrich, St. Louis, MO, USA). For Western blot analysis, after SDS-PAGE, proteins were transferred from the gel to a 0.2 μm nitrocellulose membrane using the Trans-Blot® Turbo™ Transfer System (Bio-Rad Laboratories, Hercules, CA, USA) according to the manufacturer's instructions. Membrane was blocked overnight with 3% w/v BSA in PBS-T (0.1% w/v Tween-20 in PBS). HIV-1 p24 detection was performed using a two-step procedure. First, the membrane was incubated with primary mouse monoclonal antibody against HIV-1 p24 (Icosagen AS, Tartumaa, Estonia), diluted 1:1000 in PBS-T containing 1% w/v BSA for 2 h. The second step was the incubation of the membrane with anti-mouse IgG conjugated with alkaline phosphatase (Sigma Aldrich, St. Louis, MO, USA), diluted 1:1000 in PBS-T with 1% w/v BSA for 1 h. Premixed BCIP®/NBT solution (Sigma Aldrich, St. Louis, MO, USA) was used as substrate for visualizing the alkaline phosphatase conjugates.

2.12. Transmission electron microscopy (TEM)

For nanoparticle visualization using TEM, relevant samples were prepared using the negative staining method. Briefly, 30 μL of sample were incubated on 400-mesh copper grids (coated with pioloform film and stabilized by carbon evaporation) for 1 min at room temperature. After the incubation, excess liquid was removed and samples were fixed incubating the grids with 2.5% glutaraldehyde solution (in 100 mM cacodylate buffer, pH 7.0) for 15 min. The grids were then washed with water and stained with 1% uranyl acetate solution for 30 s. After the staining, excess liquid was removed and the grids were air-dried. A Tecnai G^2 200 kV transmission electron microscope (FEI, Eindhoven, The Netherlands) was used for visualization of the specimens.

For cryo-TEM, approximately 4 μL of the sample were applied to a glow-discharged holey carbon grid and plunged frozen in liquid ethane using a FEI Vitrobot mark IV. Imaging was performed on an FEI F20 microscope at 200 kV and recorded on an FEI Ceta detector.

For observation of the internal structure of virgin and saturated beads, resin samples were washed and equilibrated with binding buffer (50 mM HEPES, pH 7.2). Saturated resins were prepared by incubating the resin beads with BSA or HIV-1 gag VLP in binding buffer, during 24 h at room temperature. After the incubation, beads were washed with binding buffer and chemically fixed with 2% glutaraldehyde for 20 min at room temperature. For the preparation of the specimens for TEM, resin samples were dehydrated with increasing ethanol concentrations (0–100% anhydrous ethanol), embedded in LRWhite resin (London Resin Company, Ltd., London, UK) and ultramicrotomed into 80 nm sections. The sections were then stained with lead citrate followed by uranyl acetate and imaged with a JEOL 1230 instrument (JEOL, Tokyo, Japan).

3. Results and discussion

3.1. Adsorption isotherms

HIV-1 gag VLP equilibrium binding capacity on Fractogel®-TMAE was determined and adsorption isotherms were constructed (Fig. 1). The Langmuir isotherm model [18] was applied to fit the experimental data. The obtained values for the maximum binding capacity (q_{max}) and equilibrium constant (K) are summarized in Table 1. Under strong binding conditions (50 mM HEPES, pH 7.2), a maximum binding capacity ($q_{max,0}$) of 1.6×10^{13} part/mL resin

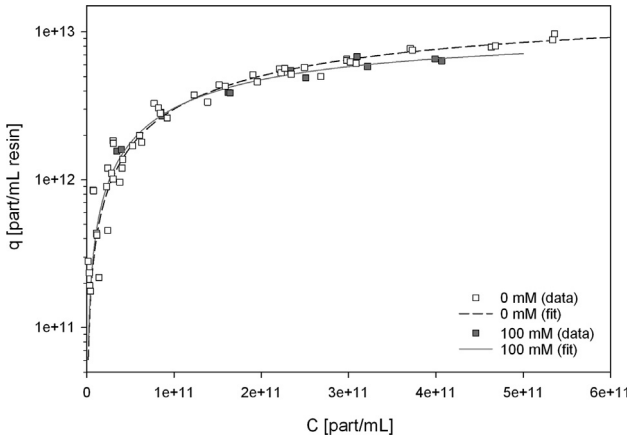

Fig. 1. Adsorption isotherms of HIV-1 gag VLPs on Fractogel®-TMAE after 24 h of incubation, using 0 or 100 mM NaCl in the binding buffer (50 mM HEPES, pH 7.2). Squares represent the data points and lines the fitting of the Langmuir isotherm model. C: equilibrium constant; q: surface concentration or binding capacity.

Table 1
Langmuir isotherm model parameters determined for the adsorption isotherms represented in Fig. 1. K: equilibrium constant; q_{max}: maximum binding capacity.

NaCl [mM]	K [mL/particles]	q_{max} [particles/mL resin]
0	2.4×10^{-12}	1.6×10^{13}
100	4.0×10^{-12}	1.1×10^{13}

was predicted. In order to evaluate the effect of moderate conductivity on binding, isotherms were also performed adding 100 mM NaCl to the binding buffer. This results in a conductivity similar to cell culture supernatants with 9.5–10.0 mS/cm. In this case, a maximum binding capacity ($q_{max,100}$) of 1.1×10^{13} part/mL resin was obtained. Despite $q_{max,100mM}$ value is 30% lower than $q_{max,0}$ it is important to note that particle concentrations measured by NTA have an accepted error of 20% [45,46]. Accordingly, no significant difference on binding capacity is observed under moderate conductivity conditions, allowing the direct loading of cell culture supernatant without compromising the binding capacity of the VLPs.

3.2. Breakthrough and dynamic binding capacity

The performance of Fractogel®-TMAE for the capture of HIV-1 gag VLPs was evaluated by the dynamic binding capacity ($DBC_{10\%}$) when directly loading 50 mL of 0.8 μm filtered cell culture

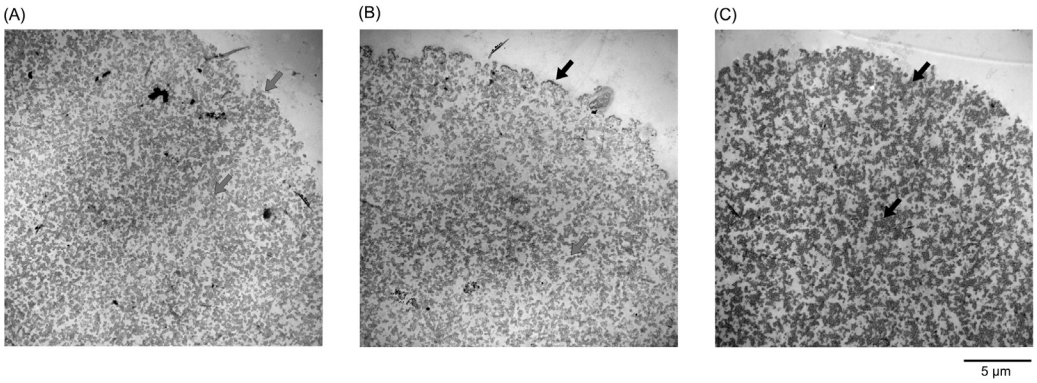

Fig. 2. Transmission electron micrographs of thin slices of (A) virgin, (B) VLP-saturated and (C) BSA-saturated Fractogel®-TMAE resin beads. Black arrow point to VLP/BSA bound to the resin and grey arrows point to free resin backbone.

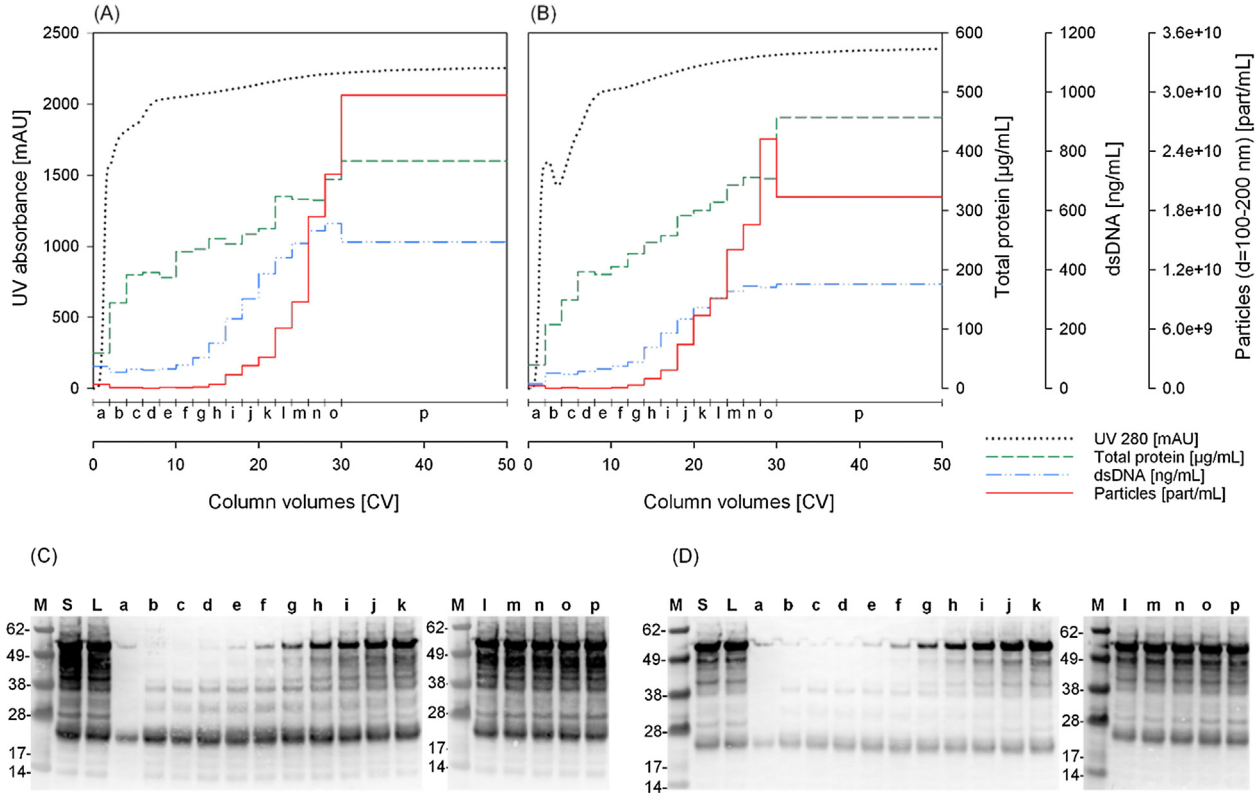

Fig. 3. (A) and (B) Breakthrough curves for the loading of CHO cell culture supernatant, containing HIV-1 gag VLPs, into 1 mL Fractogel®-TMAE MiniChrom columns. Total protein, dsDNA and particle concentrations were measured offline by Bradford, Picogreen and NTA, respectively; (C) and (D) Western blots for the detection of HIV-1 p24 corresponding to the breakthrough curves (A) and (B) respectively; (A) Loading material: 0.8 μm filtered CHO cell culture supernatant containing 710 μg/mL of total protein, 17594 ng/mL of dsDNA and 3.0×10^{10} part/mL of 100–200 nm particles; (B) Loading material: endonuclease treated and 0.8 μm filtered CHO cell culture supernatant containing 630 μg/mL of total protein, 441 ng/mL of dsDNA and 2.8×10^{10} part/mL of 100–200 nm particles; a-p: collected and analysed fractions.

supernatant onto a 1 mL column (Fig. 3A). In order to investigate the potential competition of dsDNA for the VLP binding sites, breakthrough experiments were also performed with endonuclease pretreated cell culture supernatant. The endonuclease digestion breaks down nucleic acids (DNA and RNA) into small oligonucleotides (3–5 bases) which can enter the resin pores, leaving the outer surface area of the beads available for VLP binding. dsDNA content was reduced by 97.9% (Fig. 3B). Collected flow-through fractions denoted as a-p (Fig. 3A and B) were analysed by NTA, Bradford assay and Picogreen assay for the quantification of particles, total protein and dsDNA respectively. In both cases, non-pretreated and endonuclease pretreated supernatant, proteins start to breakthrough immediately at 2 CV loading and 46–57% of the total protein did not bind to the column. This result was confirmed by the SDS-PAGE analysis (Fig. S1, Supplementary material A). This can be explained by the exclusion of positively-charged and non-charged proteins by the anion exchange ligands, as well as by the weak interaction with some negatively-charged proteins due to the moderate conductivity in the cell culture supernatant [3]. Nevertheless, full protein breakthrough was not achieved because the concentration at the outlet did not reach the feed concentration. In the non-pretreated supernatant (Fig. 3A), breakthrough of dsDNA and particles starts after about 12 and 14 CV loading respectively. Full breakthrough of particles is achieved at the end of the loading. However, only a 3% breakthrough of dsDNA is observed, indicating that the maximum binding capacity of Fractogel®-TMAE for dsDNA was not reached. Similar results were obtained for the endonuclease-pretreated supernatant (Fig. 3B). Western blot analysis (Fig. 3C and D) confirm the breakthrough of HIV-1 gag VLPs measured by NTA (bands at

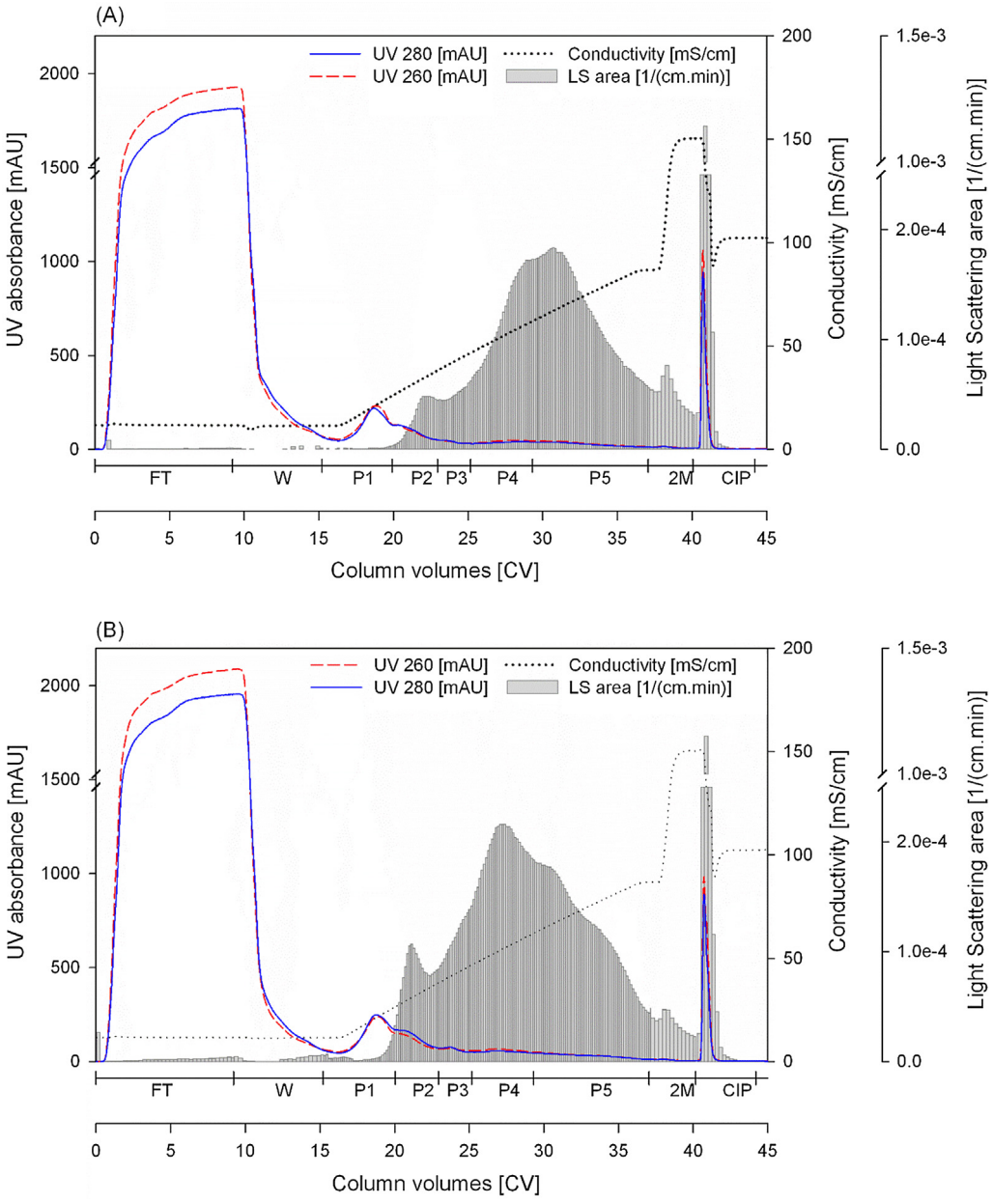

Fig. 4. Chromatograms of HIV-1 gag purification with Fractogel®-TMAE using a linear gradient elution from 100 to 1000 mM NaCl (Buffer A: 50 mM HEPES, pH 7.2; Buffer B: 50 mM HEPES, 2 M NaCl, pH 7.2). (A) Run 1: batch A. (B) Run 2: batch B. In both cases, the loading material was endonuclease pretreated and 0.8 μm filtered CHO cell culture supernatant. Bars represents the area under the curve of the light scattering intensity (LS) measurements for each collected fraction, using a MALS detector. FT: flow-through; W: wash; P1-5: peaks 1 to 5; 2 M: regeneration with 2 M NaCl; CIP: cleaning-in-place with 0.5 M NaOH.

55 kDa corresponding to HIV-1 gag polyprotein). $DBC_{10\%}$ was similar for both non-pretreated and endonuclease-pretreated supernatants with 6.6×10^{11} and 5.5×10^{11} part/mL column respectively, indicating that VLPs and dsDNA do not compete for the same binding sites.

Due to their large size, VLPs are expected to bind exclusively at the outer surface of the chromatography beads. Consequently, very low binding capacity would be expected. The exclusive binding of VLPs on the beads' outer surface was confirmed by transmission electron micrographs of VLP-saturated Fractogel®-TMAE beads (Fig. 2B). In Fig. 2, the uniform light grey area (outside and inside the beads) is the LRWhite embedding matrix, which fills the empty spaces. The medium-dark grey areas present in all images correspond to the resin backbone. When beads are incubated with a small protein (BSA), binding can be observed across the entire bead by the darker grey colour around the resin backbone (Fig. 2C). On the other hand, it is possible to observe that VLPs form a thin layer at the surface of the bead and no binding can be observed in the interior of the bead (Fig. 2B). This was also confirmed by confocal laser scanning microscopy when using fluorescently labelled VLPs (data not shown). Furthermore, it is possible to observe that despite being spherical, the beads have a rough surface, which increases the available surface area for VLP binding and is the explanation for obtaining a binding capacity higher than expected. The obtained dynamic binding capacity is only one order of magnitude smaller compared to the values reported for enveloped virus and VLPs on monoliths [38,47,48]. Additionally, since chromatography packed beds are scalable to hundreds of litres, the lower capacity of polymer-grafted media can be easily compensated by increasing the unit operation scale.

3.3. Purification of HIV-1 gag VLPs

Purification of HIV-1 gag VLPs produced in CHO cells was performed using a XK 16/20 column packed with 5.4 mL of Fractogel®-TMAE. Since the equilibrium binding capacity was not affected by moderate salt concentrations, clarified and 0.8 μm filtered cell culture supernatant was directly loaded onto the column. A loading volume of 50 mL was used to avoid column overloading and product loss. Elution was achieved using a 20 CV salt linear gradient from 100 to 1000 mM NaCl. The flow rate was 1 mL/min, ensuring a residence time of 5.4 min. Small fractions (0.8–1.5 mL) were collected throughout the entire chromatographic run and directly injected into a MALS detector using an HPLC in bypass mode (Fig. 4 and Fig. S2 (Supplementary material A)). The UV absorbance peak at 260 and 280 nm at the fractions were the majority of the particles elute is significantly reduced when the supernatant is pretreated with endonuclease (Fig. S2B). This indicates that the amount of dsDNA co-eluting with particles was reduced. Although pre-treatment of the supernatant with endonuclease does not increase the dynamic binding capacity, it is still required to reduce dsDNA contamination of the product. Consequently, further process development was performed with endonuclease pretreated supernatant.

Chromatograms in Fig. 4A and B represent two purification runs of HIV-1 gag VLPs from two different CHO cell culture batches (run 1/batch A and run 2/batch B respectively). Supernatant (S) from batch B had slightly higher content in particles and dsDNA and double the amount of total protein (Table 2). Before loaded onto the column both supernatants were pretreated with endonuclease and 0.8 μm filtered. Reductions of 98.2% and 97.1% in dsDNA content were achieved for batch A and B respectively. As before, small fractions were collected throughout the entire chromatographic runs and, directly after the run, analysed using a MALS detector. Fractions were later pooled, considering both UV absorbance and light scattering signals (Fig. 4A and B). To evaluate the purification process in terms of recovery, yield and host cell protein and dsDNA depletion, all collected fractions as well as loading materials were analysed for particle quantity, particle size distribution, total protein content, dsDNA content and HIV-1 gag protein content (Table 2). Additionally, the purity of the samples at the protein level was semi-quantitatively determined by SDS-PAGE (Fig. 5A

Table 2
Mass balance of HIV-1 gag purification with Fractogel®-TMAE represented in Fig. 4 (batch A: Fig. 4A; batch B: Fig. 4B). Particle, total protein, dsDNA and p24 concentrations measured by NTA, Bradford, Picogreen and p24 ELISA respectively. Recovery was calculated based on the particle concentration measured by NTA. S: supernatant; L: load; FT: flow-through; W: wash; P1-5: peaks 1 to 5; 2 M: regeneration with 2 M NaCl; CIP: cleaning-in-place with 0.5 M NaOH; < LLOQ: lower than the lower limit of quantification.

	Volume [mL]	Particles d: 100–200 nm [particles/mL]	Recovery [%]	Total Protein [μg/mL]	dsDNA [ng/mL]	p24 [ng/mL]
Batch A						
S	50.0	4.6×10^{10}	–	383.5	12096.9	2589.9
L	50.0	3.0×10^{10}	100.0	323.5	218.4	2473.9
FT	50.0	5.3×10^{08}	1.8	123.6	35.5	4.5
W	32.6	4.4×10^{08}	1.0	59.2	12.3	134.3
P1	25.5	<LLOQ	–	108.9	10.8	<LLOQ
P2	16.5	3.1×10^{09}	3.5	151.6	25.2	21.5
P3	12.0	2.6×10^{09}	2.1	40.6	31.6	140.2
P4	22.5	6.8×10^{09}	10.3	<LLOQ	384.2	324.8
P5	42.1	7.3×10^{09}	20.7	<LLOQ	61.1	274.1
2M	16.3	2.6×10^{09}	2.8	<LLOQ	13.3	102.8
CIP	26.0	1.9×10^{10}	32.6	81.8	<LLOQ	0.5
Total			74.7			
Batch B						
S	50.0	5.1×10^{10}	–	669.0	13720.5	2624.6
L	50.0	4.9×10^{10}	100.0	649.5	400.3	2342.0
FT	50.0	<LLOQ	–	172.7	47.9	893.7
W	32.6	<LLOQ	–	71.4	17.3	179.7
P1	26.3	<LLOQ	–	163.5	14.0	0.6
P2	15.8	3.7×10^{09}	2.4	312.1	60.8	130.0
P3	12.0	7.0×10^{09}	3.4	88.8	608.9	244.7
P4	22.5	1.2×10^{10}	11.4	<LLOQ	762.2	496.6
P5	42.1	1.0×10^{10}	17.8	<LLOQ	82.5	218.5
2M	16.3	3.1×10^{09}	2.1	<LLOQ	17.4	58.0
CIP	26.0	1.7×10^{10}	18.6	93.0	18.6	0.6
Total			55.8			

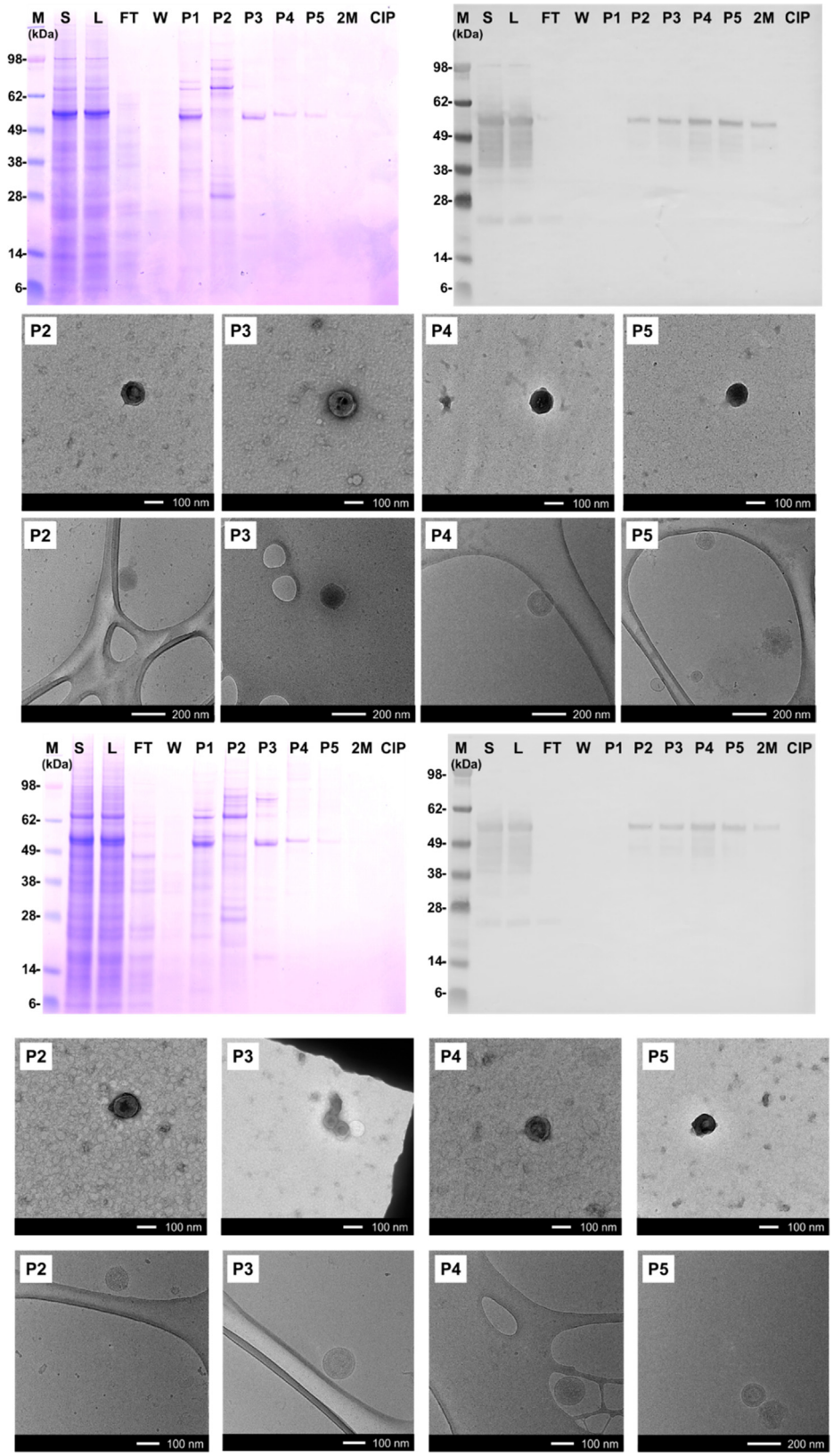

Fig. 5. (A) SDS-PAGE, (B) Western blot analysis, (C) TEM pictures and (D) cryo-TEM pictures of the pooled fractions from the purification run represented in Fig. 4A. (E) SDS-PAGE, (F) Western blot analysis, (G) TEM pictures and (H) cryo-TEM pictures of the pooled fractions from the purification run represented in Fig. 4B. M: molecular weight marker; S: supernatant; L: load; FT: flow-through; W: wash; P1-5: peaks 1 to 5; 2 M: regeneration with 2 M NaCl; CIP: cleaning-in-place with 0.5 M NaOH.

and E). MALS showed that almost all particles bound to the column. No significant light scattering signal is observed during column loading and washing, indicating no particle breakthrough (Fig. 4A and B). This was confirmed by NTA measurements of the flow-through and wash samples (Table 2). Majority of the host cell proteins did not bind to the column and were found in the flow-through and wash fractions. Bound proteins started to elute immediately at the beginning of the salt linear gradient and no particles were found in the first peak (P1). Particles were eluted in peaks 2 to 5 over a broad range of salt concentrations, starting from 320 mM NaCl (26 mS/cm) until the end of the linear gradient (1000 mM, 88 mS/cm). VLPs are large biomolecules and expose multiple host cell glycoproteins on their membrane. This complex surface allows the interaction with multiple ligands, resulting in a strong adsorption which requires high salt concertation for elution. This is different to protein elution, which requires lower salt concentrations, and lot of protein already eluted at binding conditions for VLPs. The non- or weakly-binding of protein impurities at moderate-high conductivities is one of the advantages of the use of polymer-grafted media to capture enveloped VLPs, which still bind to the column under these conditions.

HIV-1 gag polyprotein (55 kDa) was detected by Western blot analysis (Fig. 5B and F) in all particle-containing fractions, indicating the presence of HIV-1 gag VLPs. The presence of spherical particles in these fractions was confirmed by TEM (Fig. 5C and G). Cryo-TEM was used to investigate the inner structure of the particles (Fig. 5D and H). The majority of the particles had an outer membrane and appeared to be full. In some cases (Figs. 5D-P4 and 5H-P3) a second inner layer typical of HIV-1 gag VLPs was visible [49]. However, due to the concentration limitation of the scale, a low number of particles was found in the cryo-EM experiments therefore we can only speculate that structurally different particles are eluted in different fractions. Most particles in all peaks have a diameter of about 150 nm expressed as the statistical mode of the particle size distribution. The diameter of 150 nm is typical for HIV-1 gag VLPs [50]. However, peak 2 has a wider size distribution which is typical of EV samples [51]. Considering particle size distribution, SDS-page profile and p24 content, we assume that HIV-1 gag VLPs are enriched in the later fractions of the elution gradient in peaks 4 and 5. These two peaks contain the majority of the eluted particles and present a high purity at the protein level (Table 2, Fig. 5A and E). Yet, the depletion of dsDNA did not meet the requirements of the regulatory agencies (<10 ng/dose, dose: 10^9 particles).

3.4. Particle variants by proteomic analysis

Proteomic analysis of the different elution peaks was performed using LC-ESI-MS. The generated data were analysed by UnitProt database (detailed results are presented in Supplementary material B). Considering peaks 2 to 5, in total 214 and 227 proteins were identified in runs 1 and 2 respectively. Peak 2 had the highest number of total and unique proteins when compared with peaks 3 to 5. This is in agreement with the SDS-PAGE (Fig. 5A and E) as well as with the total protein concentration measured by Bradford. Nonetheless, Peak 2 is excluded from the proteomic interpretation, because it is contaminated by host cell proteins as seen in TEM and cryo-TEM. Peaks 3 to 5 have a substantial number of unique proteins (Table 3). Therefore, we assume that VLP variants are eluted. This is also supported by the particle size distribution measured for the different elution fractions. Previously it has been shown that HIV-1 uses different biogenesis pathways for budding [32]. This explains the presence of different particle variants. Moreover, peaks 2 and 3 have a wider particle size distribution than 4 and 5. Finally, we assume that numerous particle variants with similar surface properties and cargo are present and it is almost impossible to isolate single variants.

Table 3
Number of proteins identified by proteomic analysis using LC-ESI-MS.

Batch	Total P2-P5	Total P3-P5	Peak	Total	Unique	In P3-P5
A	214	111	**2**	145	103	21
			3	78	33	
			4	49	7	
			5	50	11	
B	227	129	**2**	163	98	30
			3	71	14	
			4	74	10	
			5	78	15	

High-resolution separation between different particle variants is crucial to allow the development of new analytical tools for high throughput particle quantification, characterisation and discrimination.

4. Conclusion

Our work demonstrates that polymer-grafted ion exchangers are suitable for the direct capture and purification of eVLPs. The developed method also allowed the separation of different HIV-1 gag VLP variants. Despite the binding capacity is one order of magnitude lower than the one for monoliths, chromatography columns can be packed in any size and geometry, allowing an easy and flexible scale-up. The strong VLP interaction versus the weak interaction of protein impurities is an advantage of this method because loading can be done at moderated salt concentrations, allowing direct loading of cell culture supernatants. The fact that VLPs bind exclusively on the outer surface leaves space on the interior of the beads available for the binding of highly negatively charged small impurities. Non-charged and positively charged proteins are immediately excluded from the column in the flow-through and wash steps, significantly improving product purity in a single step. This method can be easily implemented either in existing processes or adapted for the capture and purification of other enveloped VLPs produced in any type of expression system.

Declaration of Competing Interest

The authors declared that there is no conflict of interest.

Acknowledgements

This project has been supported by the Austrian Science Fund (project BioToP; FWF W1224). Schneider and Wetter have been supported by the Austrian BMWD, BMVIT, SFG, Standortagentur Tirol, Government of Lower Austria and Business Agency Vienna through the Austrian FFG-COMET-Funding Program. This work used the platforms of the Grenoble Instruct-ERIC Center (ISBG: UMS 3518 CNRS-CEA-UGA-EMBL) with support from FRISBI (ANR-10-INSB-05-02) and GRAL (ANR-10-LABX-49-01) within the Grenoble Partnership for Structural Biology (PSB). The electron microscope facility is supported by the Auvergne Rhône-Alpes Region, the Fondation Recherche Medicale (FRM), the fonds FEDER and the GIS-Infrastrutures en Biologie Sante et Agronomie, France (IBISA). The funding agencies had no influence on the conduct of this research. The authors would like to specially thank Professor Giorgio Carta for the great scientific collaboration and Preston Fuks for the help in the laboratory, especially regarding the imaging of resin beads.

Appendix A. Supplementary material

Supplementary data to this article can be found online at https://doi.org/10.1016/j.vaccine.2019.07.001.

References

[1] Lenhoff AM. Protein adsorption and transport in polymer-functionalized ion-exchangers. J Chromatogr A 2011;1218(49):8748–59. https://doi.org/10.1016/j.chroma.2011.06.061.

[2] Abdulrahman A, Ghanem A. Recent advances in chromatographic purification of plasmid DNA for gene therapy and DNA vaccines: A review. Anal Chim Acta 2018;1025:41–57. https://doi.org/10.1016/j.aca.2018.04.001.

[3] Zhu M, Fuks P, Carta G. Protein adsorption in anion exchange resins – effects of polymer grafting, support structure porosity, and protein size. Chem Technol Biotechnol 2018;93(7):1948–58. https://doi.org/10.1002/jctb.5410.

[4] Jungbauer A. Chromatographic media for bioseparation. J Chromatogr A 2005;1065(1):3–12. https://doi.org/10.1016/j.chroma.2004.08.162.

[5] Brune KD, Howarth M. New routes and opportunities for modular construction of particulate vaccines: stick, click, and glue. Front Immunol 2018;9(1432). https://doi.org/10.3389/fimmu.2018.01432.

[6] Ding X, Liu D, Booth G, Gao W, Lu Y. Virus-like particle engineering: from rational design to versatile applications. Biotech J 2018;13(5):1700324. https://doi.org/10.1002/biot.201700324.

[7] Donaldson B, Lateef Z, Walker GF, Young SL, Ward VK. Virus-like particle vaccines: immunology and formulation for clinical translation. Expert Rev Vaccines 2018;17(9):833–49. https://doi.org/10.1080/14760584.2018.1516552.

[8] Effio CL, Hubbuch J. Next generation vaccines and vectors: Designing downstream processes for recombinant protein-based virus-like particles. Biotech J 2015;10(5):715–27. https://doi.org/10.1002/biot.201400392.

[9] Pitoiset F, Vazquez T, Bellier B. Enveloped virus-like particle platforms: vaccines of the future? Expert Rev Vaccines 2015;14(7):913–5. https://doi.org/10.1586/14760584.2015.1046440.

[10] Watson DS, Endsley AN, Huang L. Design considerations for liposomal vaccines: Influence of formulation parameters on antibody and cell-mediated immune responses to liposome associated antigens. Vaccine 2012;30(13):2256–72. https://doi.org/10.1016/j.vaccine.2012.01.070.

[11] Hardcastle N, Boulis NM, Federici T. AAV gene delivery to the spinal cord: serotypes, methods, candidate diseases, and clinical trials. Expert Opin Biol Ther 2018;18(3):293–307. https://doi.org/10.1080/14712598.2018.1416089.

[12] Wolf MW, Reichl U. Downstream processing of cell culture-derived virus particles. Expert Rev Vaccines 2011;10(10):1451–75. https://doi.org/10.1586/erv.11.111.

[13] Turnbull J, Wright B, Green NK, Tarrant R, Roberts I, Hardick O, et al. Adenovirus 5 recovery using nanofiber ion-exchange adsorbents. Biotechnol Bioeng 2019;116(7):1698–709. https://doi.org/10.1002/bit.26972.

[14] Zöchling A, Hahn R, Ahrer K, Urthaler J, Jungbauer A. Mass transfer characteristics of plasmids in monoliths. J Sep Sci 2004;27(10–11):819–27. https://doi.org/10.1002/jssc.200401777.

[15] Marcus RK. Use of polymer fiber stationary phases for liquid chromatography separations: Part II – applications. J Sep Sci 2009;32(5–6):695–705. https://doi.org/10.1002/jssc.200800645.

[16] Ghosh R. Protein separation using membrane chromatography: opportunities and challenges. J Chromatogr A 2002;952(1):13–27. https://doi.org/10.1016/S0021-9673(02)00057-2.

[17] Nestola P, Peixoto C, Silva RRJS, Alves PM, Mota JPB, Carrondo MJT. Improved virus purification processes for vaccines and gene therapy. Biotechnol Bioeng 2015;112(5):843–57. https://doi.org/10.1002/bit.25545.

[18] Carta GA. Jungbauer Protein Chromatography: Process Development and Scale-Up. Weinheim: Wiley-VHC Verlag GmbH & Co. KGaA; 2010.

[19] Müller E. Properties and Characterization of High Capacity Resins for Biochromatography. Chem Eng Tech 2005;28(11):1295–305. https://doi.org/10.1002/ceat.200500161.

[20] Braas G, Searle PF, Slater NKH, Lyddiatt A. Strategies for the isolation and purification of retroviral vectors for gene therapy. Bioseparation 1996;6(4):211–28.

[21] Yu M, Li Y, Zhang S, Li X, Yang Y, Chen Y, et al. Improving stability of virus-like particles by ion-exchange chromatographic supports with large pore size: Advantages of gigaporous media beyond enhanced binding capacity. J Chromatogr A 2014;1331:69–79. https://doi.org/10.1016/j.chroma.2014.01.027.

[22] Yamamoto S, Miyagawa E. Retention behavior of very large biomolecules in ion-exchange chromatography. J Chromatogr A 1999;852(1):25–30. https://doi.org/10.1016/S0021-9673(99)00594-4.

[23] Wu Y, Simons J, Hooson S, Abraham D, Carta G. Protein and virus-like particle adsorption on perfusion chromatography media. J Chromatogr A 2013;1297:96–105. https://doi.org/10.1016/j.chroma.2013.04.062.

[24] Trilisky EI, Lenhoff AM. Sorption processes in ion-exchange chromatography of viruses. J Chromatogr A 2007;1142(1):2–12. https://doi.org/10.1016/j.chroma.2006.12.094.

[25] Bowes BD, Koku H, Czymmek KJ, Lenhoff AM. Protein adsorption and transport in dextran-modified ion-exchange media. I: Adsorption. J Chromatogr A 2009;1216(45):7774–84. https://doi.org/10.1016/j.chroma.2009.09.014.

[26] Almodóvar EXP, Tao Y, Carta G. Protein adsorption and transport in cation exchangers with a rigid backbone matrix with and without polymeric surface extenders. Biotechnol Prog 2011;27(5):1264–72. https://doi.org/10.1002/btpr.643.

[27] Bowes BD, Lenhoff AM. Protein adsorption and transport in dextran-modified ion-exchange media. III. Effects of resin charge density and dextran content on adsorption and intraparticle uptake. J Chromatogr A 2011;1218(40):7180–8. https://doi.org/10.1016/j.chroma.2011.08.039.

[28] Wang Q, Yu L, Sun Y. Grafting glycidyl methacrylate to Sepharose gel for fabricating high-capacity protein anion exchangers. J Chromatogr A 2016;1443:118–25. https://doi.org/10.1016/j.chroma.2016.03.033.

[29] Müller W. New ion exchangers for the chromatography of biopolymers. J Chromatogr A 1990;510:133–40. https://doi.org/10.1016/S0021-9673(01)93746-X.

[30] Diedrich J, Heymann W, Leweke S, Hunt S, Todd R, Kunert C, et al. Multi-state steric mass action model and case study on complex high loading behavior of mAb on ion exchange tentacle resin. J Chromatogr A 2017;1525:60–70. https://doi.org/10.1016/j.chroma.2017.09.039.

[31] Shirbaghaee Z, Bolhassani A. Different applications of virus-like particles in biology and medicine: Vaccination and delivery systems. Biopolymers 2015;105(3):113–32. https://doi.org/10.1002/bip.22759.

[32] Welsch S, Müller B, Kräusslich H-G. More than one door – Budding of enveloped viruses through cellular membranes. FEBS Lett 2007;581(11):2089–97. https://doi.org/10.1016/j.febslet.2007.03.060.

[33] Kurg R, Reinsalu O, Jagur S, Õunap K, Võsa L, Kasvandik S, et al. Biochemical and proteomic characterization of retrovirus Gag based microparticles carrying melanoma antigens. Sci Rep 2016;6:29425. https://doi.org/10.1038/srep29425.

[34] McCraw DM, Gallagher JR, Torian U, Myers ML, Conlon MT, Gulati NM, et al. Structural analysis of influenza vaccine virus-like particles reveals a multicomponent organization. Sci Rep 2018;8(1):10342. https://doi.org/10.1038/s41598-018-28700-7.

[35] Onafuwa-Nuga AA, Telesnitsky A, King SR. 7SL RNA, but not the 54-kd signal recognition particle protein, is an abundant component of both infectious HIV-1 and minimal virus-like particles. RNA 2006;12(4):542–6. https://doi.org/10.1261/rna.2306306.

[36] Nolte-'t Hoen E, Cremer T, Gallo RC, Margolis LB. Extracellular vesicles and viruses: Are they close relatives? Proc Natl Acad Sci USA 2016;113(33):9155–61. https://doi.org/10.1073/pnas.1605146113.

[37] Michen B, Graule T. Isoelectric points of viruses. J Appl Microbiol 2010;109(2):388–97. https://doi.org/10.1111/j.1365-2672.2010.04663.x.

[38] Steppert P, Burgstaller D, Klausberger M, Berger E, Aguilar PP, Schneider TA, et al. Purification of HIV-1 gag virus-like particles and separation of other extracellular particles. J Chromatogr A 2016;1455:93–101. https://doi.org/10.1016/j.chroma.2016.05.053.

[39] Vicente T, Roldão A, Peixoto C, Carrondo MJT, Alves PM. Large-scale production and purification of VLP-based vaccines. J Invertebr Pathol 2011;107:S42–8. https://doi.org/10.1016/j.jip.2011.05.004.

[40] Thompson CM, Petiot E, Lennaertz A, Henry O, Kamen AA. Analytical technologies for influenza virus-like particle candidate vaccines: challenges and emerging approaches. Virol J 2013;10(1):141. https://doi.org/10.1186/1743-422x-10-141.

[41] Tengattini S. Chromatographic approaches for purification and analytical characterization of extracellular vesicles: recent advancements. Chromatographia 2018. https://doi.org/10.1007/s10337-018-3637-7.

[42] Tang VA, Renner TM, Fritzsche AK, Burger D, Langlois M-A. Single-particle discrimination of retroviruses from extracellular vesicles by nanoscale flow cytometry. Sci Rep 2017;7(1):17769. https://doi.org/10.1038/s41598-017-18227-8.

[43] Gutiérrez-Granados S, Cervera L, Gòdia F, Carrillo J, Segura MM. Development and validation of a quantitation assay for fluorescently tagged HIV-1 virus-like particles. J Virol Methods 2013;193(1):85–95. https://doi.org/10.1016/j.jviromet.2013.05.010.

[44] Schüpbach J, Tomasik Z, Knuchel M, Opravil M, Günthard HF, Nadal D, et al. Optimized virus disruption improves detection of HIV-1 p24 in particles and uncovers a p24 reactivity in patients with undetectable HIV-1 RNA under long-term HAART. J Med Virol 2006;78(8):1003–10. https://doi.org/10.1002/jmv.20655.

[45] U.S. Department of Health and Human Services Food and Drug Administration Guidance for Industry, Bioanalytical Method Validation. In: Center for Drug Evaluation and Research (CDER) Center for Veterinary Medicine (CVM); 2001.

[46] Kramberger P, Ciringer M, Štrancar A, Peterka M. Evaluation of nanoparticle tracking analysis for total virus particle determination. Virol J 2012;9(1):265. https://doi.org/10.1186/1743-422x-9-265.

[47] Gerster P, Kopecky E-M, Hammerschmidt N, Klausberger M, Krammer F, Grabherr R, et al. Purification of infective baculoviruses by monoliths. J Chromatogr A 2013;1290:36–45. https://doi.org/10.1016/j.chroma.2013.03.047.

[48] Steppert P, Burgstaller D, Klausberger M, Kramberger P, Tover A, Berger E, et al. Separation of HIV-1 gag virus-like particles from vesicular particles impurities

by hydroxyl-functionalized monoliths. J Sep Sci 2017;40(4):979–90. https://doi.org/10.1002/jssc.201600765.
[49] Wang B-Z, Liu W, Kang S-M, Alam M, Huang C, Ye L, et al. Incorporation of high levels of chimeric human immunodeficiency virus envelope glycoproteins into virus-like particles. J Virol 2007;81(20):10869–78. https://doi.org/10.1128/jvi.00542-07.
[50] Steppert P, Burgstaller D, Klausberger M, Tover A, Berger E, Jungbauer A. Quantification and characterization of virus-like particles by size-exclusion chromatography and nanoparticle tracking analysis. J Chromatogr A 2017;1487:89–99. https://doi.org/10.1016/j.chroma.2016.12.085.
[51] Raposo G, Stoorvogel W. Extracellular vesicles: exosomes, microvesicles, and friends. J Cell Biol 2013;200(4):373–83. https://doi.org/10.1083/jcb.201211138.

Supplementary material A

Polymer-grafted chromatography media for the purification of enveloped virus-like particles, exemplified with HIV-1 gag VLP

Patricia Pereira Aguilar[1], Tobias Amadeus Schneider[2], Viktoria Wetter[2], Daniel Maresch[1], Wai-Li Ling[3], Andres Tover[4], Petra Steppert[1], Alois Jungbauer[1,2]

[1] Department of Biotechnology, University of Natural Resources and Life Sciences Vienna, Austria

[2] Austrian Centre of Industrial Biotechnology, Vienna, Austria

[3] Univ. Grenoble Alpes, CEA, CNRS, IBS, F-38000 Grenoble, France

[4] Icosagen AS, Tartumaa, Estonia

Figure S1

SDS-PAGE analysis of the fractions collected in the breakthrough experiments represented in (A) Figure 2A and (B) Figure 2B. M: molecular weight marker; S: supernatant; L: load; a-p: flow-through fractions.

(A)

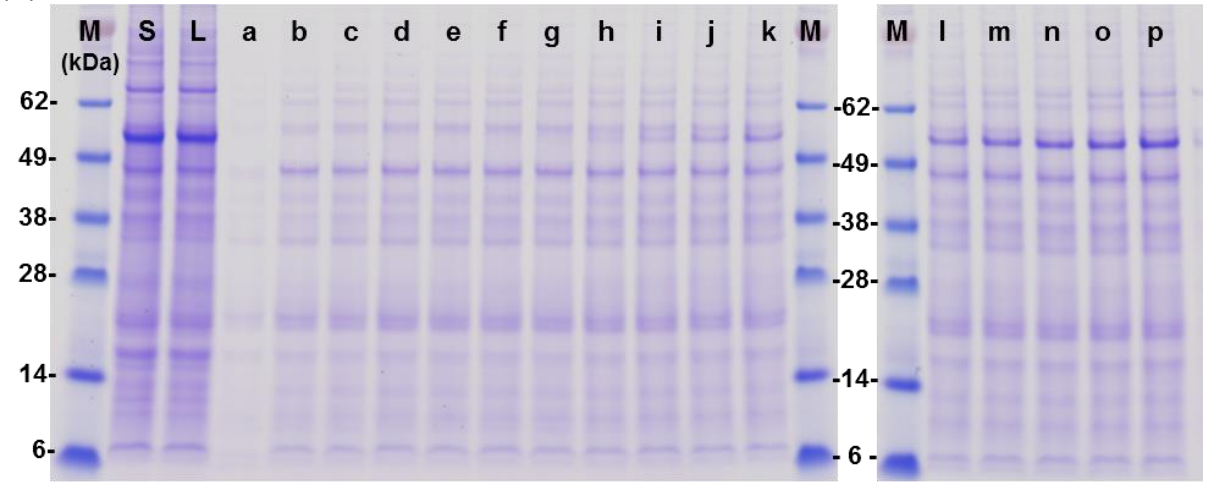

(B)

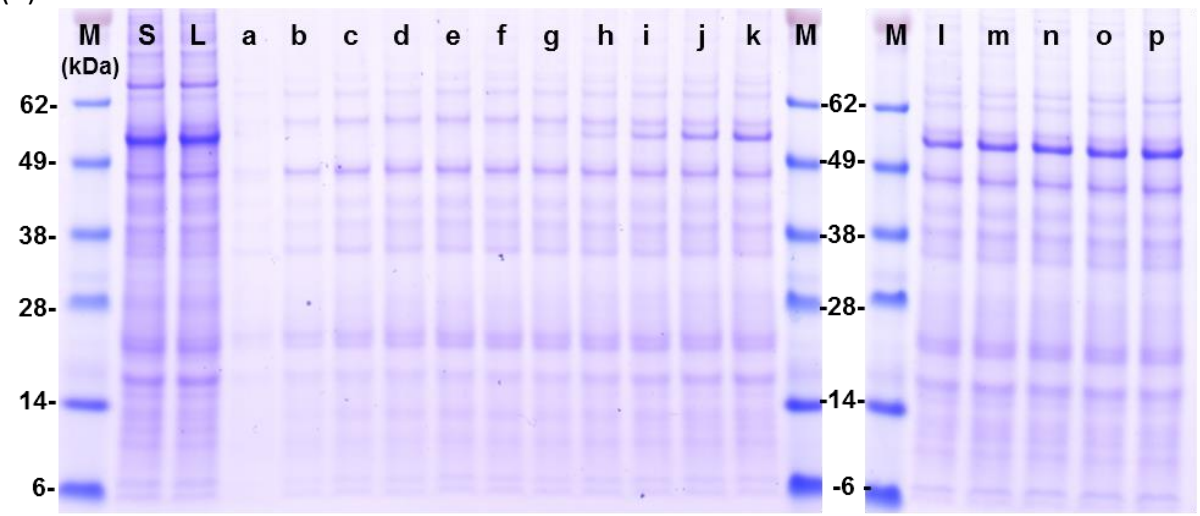

Figure S2

Comparison of the UV absorbance and light scattering elution profiles of two purification runs using non-treated (A) and endonuclease-treated (B) CHO cell culture supernatants containing HIV-1 gag VLPs. In both cases, the supernatants were 0.8 µm filtered before loaded into the column. Each bar on the graphs represents the integration (area under the curve) of the light scattering signal for each collected fraction.

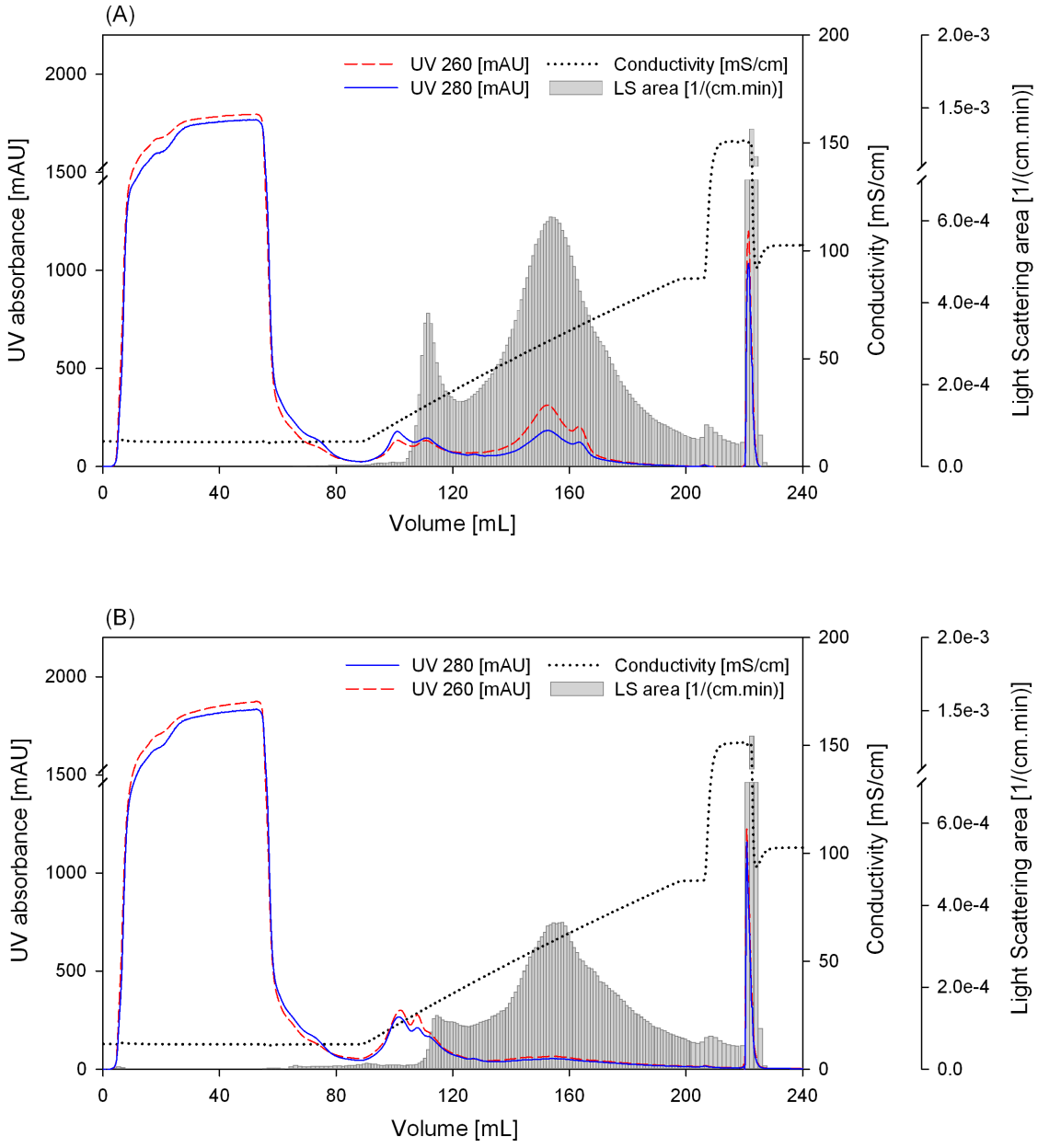

Figure S3

Particle size distribution measured by NTA. Particle concentration was normalized by the peak maximum. (A) run 1, (B) run 2.

(A)

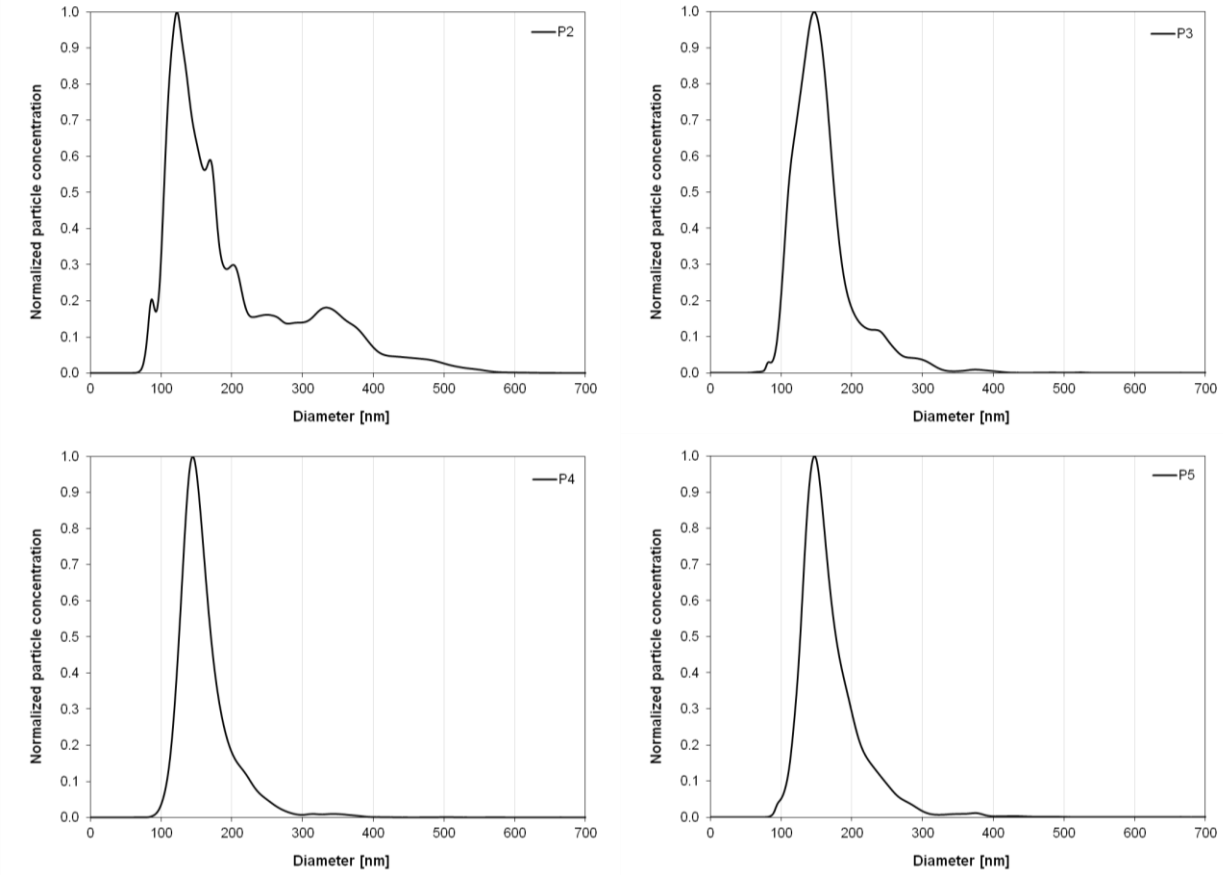

(B)

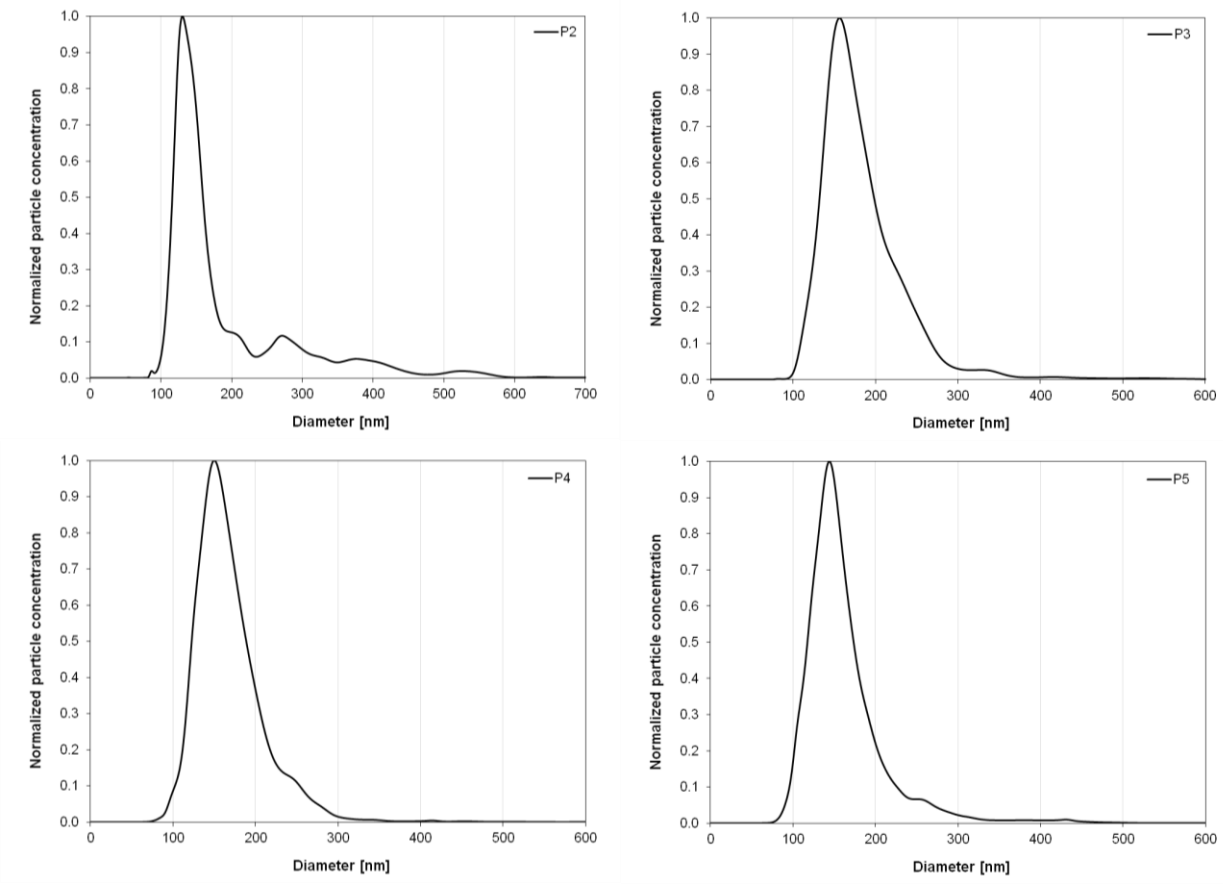
P2
Normalized particle concentration
Diameter [nm]
P3
Normalized particle concentration
Diameter [nm]
P4
Normalized particle concentration
Diameter [nm]
P5
Normalized particle concentration
Diameter [nm]

PUBLICATION II

Received: 6 May 2019 | Revised: 4 June 2019 | Accepted: 4 June 2019

DOI: 10.1002/jssc.201900441

RESEARCH ARTICLE

JOURNAL OF SEPARATION SCIENCE

At-line multi-angle light scattering detector for faster process development in enveloped virus-like particle purification

Patricia Pereira Aguilar[1]* | **Irene González-Domínguez**[2]* | **Tobias Amadeus Schneider**[3] | **Francesc Gòdia**[2] | **Laura Cervera**[2] | **Alois Jungbauer**[1,3]

[1]Department of Biotechnology, University of Natural Resources and Life Sciences, Vienna, Austria

[2]Department d'Enginyeria Química Biològica i Ambiental, Universitat Autònoma de Barcelona, Bellaterra, Barcelona, Spain

[3]Austrian Centre of Industrial Biotechnology, Vienna, Austria

Correspondence
Professor Dipl.-Ing. Dr.nat.techn. Alois Jungbauer, Department of Biotechnology, University of Natural Resources and Life Sciences Vienna, Muthgasse 18, 1190 Vienna, Austria.
Email: alois.jungbauer@boku.ac.at

*Both authors contributed equally to this paper.

At-line static light scattering and fluorescence monitoring allows direct in-process tracking of fluorescent virus-like particles. We have demonstrated this by coupling at-line multi-angle light scattering and fluorescence detectors to the downstream processing of enveloped virus-like particles. Since light scattering intensity is directly proportional to particle concentration, our strategy allowed a swift identification of product containing fractions and rapid process development. Virus-like particles containing the Human Immunodeficiency Virus-1 Gag protein fused to the Green Fluorescence protein were produced in Human Embryonic Kidney 293 cells by transient transfection. A single-column anion-exchange chromatography method was used for direct capture and purification. The majority of host-cell protein impurities passed through the column without binding. Virus-like particles bound to the column were eluted by linear or step salt gradients. Particles recovered in the step gradient purification were characterized by nanoparticle tracking analysis, size exclusion chromatography coupled to multi-angle light scattering and fluorescence detectors and transmission electron microscopy. A total recovery of 66% for the fluorescent particles was obtained with a 50% yield in the main product peak. Virus-like particles were concentrated 17-fold to final a concentration of 4.45×10^{10} particles/mL. Simple buffers and operation make this process suitable for large scale purposes.

KEYWORDS
enveloped bionanoparticles, fluorescent virus-like particles, monoliths, nanoparticle tracking analysis

1 | INTRODUCTION

The majority of the analytical techniques used in virus-like particle (VLP) downstream processing (DSP) were imported from protein DSP [1]. Typically, colorimetric methods such as Bradford assay and SDS-PAGE are used to gain insights into the total protein content. In addition, assays such as Western blot and ELISA allow the specific detection and quantification of VLP specific proteins. However, none of these methods confirms the presence of correctly assembled VLPs, but

Article Related Abbreviations: CV, column volume; DSP, downstream processing; FL, fluorescence; Gag, group specific antigen; GFP, green fluorescence protein; HEK 293, Human Embryonic Kidney 293 cells; HIV-1, Human Immunodeficiency Virus 1; LS, light scattering; MALS, multi-angle light scattering; NTA, nanoparticle tracking analysis; PEI, polyethilenimine; SEC-MALS-FL, SEC coupled to MALS and fluorescence detectors; VLP, virus-like particle.

This is an open access article under the terms of the Creative Commons Attribution License, which permits use, distribution and reproduction in any medium, provided the original work is properly cited.

© 2019 The Authors. *Journal of Separation Science* published by WILEY-VCH Verlag GmbH & Co. KGaA, Weinheim.

only the presence of specific viral proteins, which, when in their free state, represent one of the product related impurities. Particle morphology is usually confirmed by high-resolution microscopy techniques such as TEM and multi-frequency atomic force microscopy [2]. Particle number and size distributions are frequently measured by nanoparticle tracking analysis (NTA) and dynamic or static light scattering [3–5]. However, these methods are non-specific regarding the particle's composition and consider all structures with the same hydrodynamic or geometric radius as equals. As a result, a combination of biochemical, biophysical, and biological analytical methods is required to ensure an accurate detection and quantification of VLPs. This results in very laborious and time-consuming process analytics and hinders DSP process development, which is strongly dependent on the ability to detect, quantify and characterize the product of interest as well as on the capacity to discriminate the product from its related impurities.

Multi-angle light scattering (MALS) is one of the most used techniques for quantification and characterization of different nanoparticles [6]. Usually, monodisperse samples are required to allow for structural characterization based on light scattering. Typically, SEC or asymmetric flow field-flow fractionation are used to first separate the samples before the measurement [4,7]. Nevertheless, the intensity of scattered light by particles in solution is directly proportional to the particle concentration [8,9]. Thus, an at-line MALS detector can be used for fast detection and semi-quantification of particles without the requirement of monodisperse samples. This rapid method could be used as an in-process control to speed up process development and optimization.

Outbreaks of Flu, Ebola, and Zika in the last decade reinforced the need for faster process development and flexible manufacturing platforms which enable the production of millions of vaccine doses in a short time [10,11]. Among different candidates, retroviral-based VLPs are promising towards the development of vaccines and drug delivery systems [12,13]. Enveloped virus-like particles (eVLPs) are produced by recombinantly expressing one or more viral proteins [10–12]. As a model, we used eVLPs produced in Human Embryonic Kidney (HEK) 293 cells by recombinantly expressing the Human Immunodeficiency Virus-1 (HIV-1) group specific antigen (Gag) protein which was fused to Green Fluorescence protein (GFP) [2,14–16]. Similar to the native HIV-1 production process, upon recombinant expression, Gag polyprotein self-assembles underneath the cell membrane and VLPs bud to the extracellular space as spherical particles [17]. The resulting particles are enveloped by a host-cell derived lipid bilayer and have a diameter of 100–200 nm [4,18,19]. The integration of GFP permits the use of fluorescence-based techniques as an orthogonal method for detection and quantification of HIV-1 Gag-GFP VLPs.

Different DSP strategies have been developed for the purification of bionanoparticles [5,11,20–22]. Monolithic columns have been often used for the direct capture and purification of enveloped virus and VLPs from cell culture supernatant [23–27]. Due to its convective pore structure, high binding capacities can be achieved in monolithic columns while maintaining high flow rates. This results in higher productivities when compared with traditional VLP purification methods such as density gradient centrifugation [28]. As a model purification strategy, we used anion exchange monolithic columns for the direct capture and purification of HIV-1 Gag-GFP VLPs directly from cell culture supernatant. We show how at-line MALS and fluorescence detectors simplified DSP process development and optimization. Furthermore, size exclusion chromatography coupled to multi-angle light scattering and fluorescence (SEC-MALS-FL) is an effective method for particle quantification and characterization.

2 | MATERIALS AND METHODS

2.1 | Chemicals

The chemicals used for all experiments were acquired from Merck (Darmstadt, Germany) or Sigma Aldrich (St. Louis, MO, USA).

2.2 | Production of virus-like particles

2.2.1 | Cell line, media, and culture conditions

A serum-free suspension-adapted Human Embryonic Kidney 293 cells (HEK 293) cell line (HEK293SF-3F6, National Research Council, Montreal, Canada) kindly provided by Dr. Amine Kamen from McGill University (McGill, Montreal, Canada) was used. Cells were cultured in Freestyle 293® medium supplemented with 0.1% Pluronic® (both Invitrogen, Carlsbad, CA, USA), 1.6 mg/L of r-transferrin (Merck Millipore, Kankakee, IL, USA), 19.8 mg/L of r-insulin (Novo Nordisk Pharmatek, Køge, Denmark), and 0.9X of an in-house developed lipid mixture to maximize cell growth [8]. Cells were routinely maintained in 20 mL of culture medium. Flasks were shaken at 130 rpm using an orbital shaker (Stuart, Stone, UK) placed in an incubator maintained at 37°C in a humidified atmosphere of 5% CO_2 in air.

2.2.2 | Plasmids

The pGag-eGFP plasmid used in this work codes for a Rev-independent HIV-1 Gag protein fused in frame to the enhanced GFP [27]. The plasmid from the NIH AIDS Reagent Program (Cat 11468) was constructed by cloning the Gag sequence from pCMV55M1-10 [28] into the pEGFP-N1 plasmid (Clontech, Takara Bio, Mountain View, CA, USA). The plasmids were prepared and purified as previously described with Endofree Plasmid Mega kit (Qiagen, Hilden,

Germany) [29]. Snap Gene Viewer was used to analyse the plasmid features (GSL Biotech, Chicago, IL, USA).

2.2.3 | DNA/polyethilenimine complex formation and transient transfection of HEK 293 cells

HEK 293 suspension cells were transiently transfected using 25 kDa linear polyethilenimine (PEI) (PolySciences, Warrington, FO, USA). Transfections were performed using a final DNA concentration of 1 μg/mL. PEI/DNA complexes were formed by adding PEI to plasmid DNA (1:2 w/w DNA:PEI ratio) diluted in fresh culture medium (10% of the total culture volume to be transfected) [8].

Cells were cultured for 72 h post transfection to maximize VLP yields [30]. Cell culture supernatants were primary harvested by centrifugation at 4000 g for 30 min at 4°C. Recovered supernatants were stored at 4°C before purification.

2.3 | Chromatographic purification

2.3.1 | Chromatographic equipment and mobile phases

Chromatographic experiments were performed using an Äkta pure 25 M2 with a sample pump S9 and fraction collector F9-C (GE Healthcare, Uppsala, Sweden). During the purification runs, pH, conductivity and UV absorbance at 280 and 260 nm wavelengths were monitored. Unicorn software versions 5.10 or 6.4.1 (GE Healthcare, Uppsala, Sweden) were used for method programming, system control, and data acquisition.

Mobile phase A and B consisted in 50 mM HEPES, pH 7.2 and 50 mM HEPES, 2 M NaCl, pH 7.2 respectively. Sanitization buffer consisted in 1 M NaOH.

2.3.2 | Preparative scale purification

Clarified cell culture supernatant containing HIV-1 Gag-GFP VLPs was 0.8 μm filtered (Millex AA syringe filter, Millipore Bedford, MA, USA) and 100 mL were loaded into a 1 mL radial flow monolith (CIMmultus^{TM} QA, BIA Separations, Ajdovščina, Slovenia). Before loading, the column was equilibrated with 50 mM HEPES, 100 mM NaCl, pH 7.2 (5% buffer B). After the loading phase, the column was washed with equilibration buffer (5% buffer B) for 15 column volumes (CV). In the linear gradient purification, a salt linear gradient from 100 to 1000 mM NaCl (5 to 50% buffer B) in 50 CV was used. For the step gradient purification, three steps of 300, 520 and 1000 mM NaCl (15, 26 and 50% buffer B) with 15 CV each were used for elution. In both purification strategies, the column was regenerated with 100% buffer B in a 10 CV step. After regeneration, the column was sanitized using 10 CV of 1 M NaOH. All preparative purification runs were performed using a flow rate of 1 mL/min. The sample was loaded into the column using the sample pump. Fractions of 1 mL were collected in 96 deep-well plates and pooled according to the chromatograms.

2.4 | Nanoparticle tracking analysis

Particle concentration and particle size distribution were determined by NTA using a NanoSight NS300 (Malvern Instruments, Worcestershire, UK) equipped with a blue laser module (488 nm), a neutral density filter and a 500 nm fluorescence filter. To obtain a particle concentration of 20 to 80 particles per video frame in the measuring chamber, samples were serially diluted using particle-free water or 0.1 μm filtered 50 mM HEPES pH 7.2 buffer. Each sample was measured with both scattering (LS) and fluorescence (FL) modes in three different dilutions in triplicates. In total, nine videos of 60 s were recorded per sample. The camera level varied between 14 and 16 and it was manually adjusted prior to each measurement. Recorded videos were analysed using the NanoSight NTA software version 3.2 (Malvern Instruments, Worcestershire, UK). Detection thresholds between 3 and 5 were used.

2.5 | Total protein and double stranded DNA quantification

Total protein concentration was determined by Bradford assay using Coomassie blue G-250-based protein dye reagent (Bio-Rad Laboratories, Hercules, CA, USA). The calibration curve was obtained using BSA standards (Thermo Fisher Scientific, Waltham, MA, USA) diluted in TE-Buffer to a concentration range of 50–200 μg/mL. Double stranded DNA (dsDNA) quantification was performed using the Quant-iTTM PicoGreen® dsDNA kit (Life Technologies, Waltham, MA, USA). Protein and dsDNA assays were performed according to the respective instructions from the manufacturer in a 96-well plate format. Since HIV-1 Gag-GFP VLPs emit at the same range as the Quant-iTTM PicoGreen® reagent, the native fluorescence was measured prior to the reagent addition and later subtracted to the fluorescence after the reaction.

2.6 | Sodium dodecyl sulfate-polyacrylamide gel electrophoresis and Western blot analysis

Precast NuPAGE Bis/Tris gels 4–12% (Invitrogen, Carlsbad, CA, USA) were used in a MES-SDS buffer system. The protocol was adapted from manufacturer's instructions. Briefly: 40 μL of sample were mixed with 20 μL of 4x LDS buffer and 2 M DTT to a final concentration of 1% v/v. Each sample incubated at 95°C for 20 min. SeeBlue® Plus2 Pre-stained Protein Standard (Invitrogen, Carlsbad, CA, USA) was used as protein marker. Gels were run at 200 V, 400 mA. Coomassie Brilliant Blue G-250 based EZBlue^{TM} Gel Staining Reagent

(Sigma Aldrich, St. Louis, MO, USA) was used for protein staining. After SDS-PAGE, proteins were blotted using Trans-Blot® turbo system (Bio-Rad Laboratories, Hercules, CA, USA) with 0.2 μm nitrocellulose membranes and blocked with 3% BSA in PBS with 0.1% w/v Tween-20 overnight. Detection of HIV-1 Gag-GFP protein was performed by incubation with primary mouse monoclonal antibody against HIV-1 p24 (Icosagen AS, Tartumaa, Estonia), diluted 1:1000 in PBS-T containing 1% BSA for 2 h. Anti-mouse IgG conjugated with alkaline phosphatase (Sigma Aldrich, St. Louis, MO, USA), diluted 1:1000 in PBS-T with 1% w/v BSA was used as secondary antibody. Premixed BCIP®/NBT solution (Sigma Aldrich, St. Louis, MO, USA) was used as substrate solution.

2.7 | At-line multi-angle light scattering and fluorescence

At-line MALS and fluorescence measurements were performed using an Ultimate 3000 system (Thermo Fisher, Waltham, MA, USA). A sample of all collected fractions during the purification runs was directly injected into the detectors bypassing the column. The HPLC system was equipped with a LPG-3400SD quaternary pump, WPS-3000TSL analytical autosampler, DAD 3000 UV-detector and FLD 3100 fluorescence detector (Thermo Fisher, Waltham, MA, USA). Additionally, the system was connected to a multi-angle light scattering detector DAWN HELEOS 18-angle and a differential refractive index detector Optilab rEX (both Wyatt, Santa Barbara, CA, USA). Chromeleon 7 (Thermo Fisher Scientific, Waltham, MA, USA) and Astra 5.3.4 Wyatt, (Santa Barbara, CA, USA) software were used for method programming, system control and data acquisition. GFP fluorescence was monitored with an excitation wavelength of 480 nm and emission of 505 nm. Analysis time was 3 min/sample. Light scattering intensity was accessed by calculating the peak area of the light scattering signal obtained with the 90° angle.

2.8 | Size exclusion chromatography coupled to multi-angle light scattering and fluorescence

SEC-MALS-FL measurements were performed using the same HPLC system, detectors and software as described in Section 2.7.

A TSKgel G5000PWXL 300.0 mm × 7.8 mm i.d. in combination with a TSKgel PWXL guard column 40.0 mm × 6.0 mm i.d. (both Tosoh Bioscience, Stuttgart, Germany) were used for size exclusion chromatography. The method was previously described by Steppert et al. [20]. Data analysis was done in Astra 6.1.2 using the number density procedure and the sphere model fit with a particle refractive index of 1.46 [29].

2.9 | TEM

HIV-1 Gag-GFP VLP samples were prepared by air-dried negative staining method. Briefly, 8 μL of sample was placed on discharged carbon-coated copper or holly carbon 200 mesh grids and incubated at room temperature for 1 min. Excess sample was drained carefully off the grid with filter paper. Samples were stained negatively with 8 μL of uranyl acetate (2%) by incubation for 1 min at room temperature. Excess stain was drained off as before, and grids were dried. Micrographs were taken with a JEM-400 transmission electron microscope (JEOL USA, Pleasanton, CA, USA) equipped with an ES1000W Erlangshen charge-coupled device camera (Model No. 785; Gatan, Pleasanton, CA, USA).

3 | RESULTS AND DISCUSSION

In this work, we aimed to streamline the process development for enveloped virus-like particle purification by including at-line multi-angle light scattering and fluorescence detectors for high-throughput particle detection and semi-quantification. Since it has been shown that strong anion-exchange monoliths allow the simultaneous capture and purification of enveloped bionanoparticles such as eVLPs and exosomes [22,23], we used a QA monolith to capture and purify HIV-1 Gag-GFP VLPs directly from HEK 293 cell culture supernatant in a single step. As a starting point, a salt linear gradient was used for VLP elution. Later, the data obtained in the at-line MALS and fluorescence measurements were used to develop a salt step elution strategy, providing a base for potential scale-up.

3.1 | Linear gradient purification

HIV-1 Gag-GFP VLPs were produced by transient transfection in HEK 293 cells. For VLP capture and purification in a single step, 100 mL of clarified and filtered cell culture supernatant were loaded into a 1 mL QA monolith. Elution was achieved by a 50 CV salt linear gradient from 100 to 1000 mM NaCl. Fractions of 1 mL were collected in 96 deep-well plates and directly injected into the at-line MALS and fluorescence detectors. For each elution fraction, the total light scattering intensity and the total fluorescence were calculated by integrating the signals measured by the MALS and fluorescence detectors, respectively. Data were plotted together with the purification run chromatogram (Figure 1). Since light scattering intensity is directly proportional to particle concentration [8] and the main structural element of the VLPs (Gag-GFP protein) is fluorescent [30], this method allows a fast detection and semi-quantification of HIV-1 Gag-GFP VLPs and subsequently a fast identification of the fractions containing the product of interest is possible. Considering the total

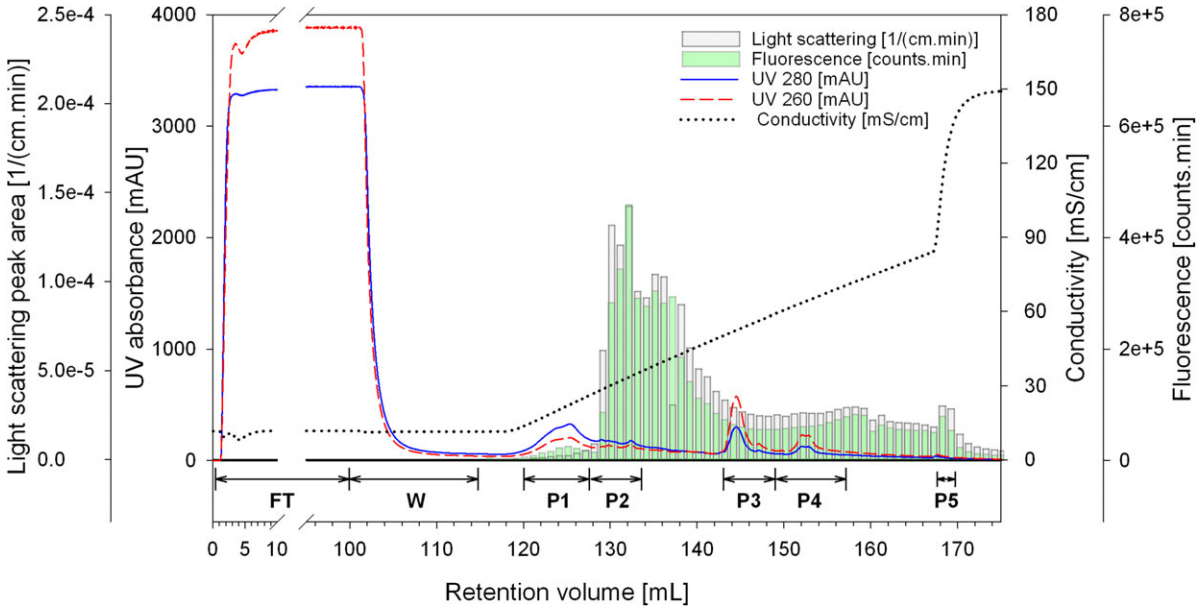

FIGURE 1 Chromatogram of the linear gradient purification of HIV-1 Gag-GFP VLP using a QA monolith. The loading material was 100 mL of clarified and 0.8 µm filtered HEK 293 cell culture supernatant. Bars represent the area under the curve of the light scattering intensity (grey) and fluorescence (green) at-line measurements. FT: flow-through; W: wash; P1-P5: polled fractions for peaks 1–5

TABLE 1 Total protein and dsDNA mass balance of the purification of HIV-1 Gag-GFP VLPs using a linear gradient elution (Figure 1). S: supernatant; L: loading material; FT: flow-through; W: wash; P1-P5: peaks 1-5

Sample	Volume [mL]	Total protein [µg/mL]	Total protein %	dsDNA [ng/mL]	dsDNA %
S	100	310.9	–	1387.5	–
L	100	313.1	100.0	1289.4	100.0
FT	100	134.9	43.1	37.5	2.9
W	15	<LLOQ	–	<LLOQ	–
P1	7	367.6	8.2	10.2	0.1
P2	5	275.1	4.4	310.5	1.2
P3	6	<LLOQ	–	5114.5	23.8
P4	6	<LLOQ	–	3129.6	14.6
P5	2	<LLOQ	–	1108.3	1.7
Recovery			55.7		44.3

<LLOQ: lower than the lower LOQ

light scattering intensity and the total fluorescence data, the majority of VLPs eluted from approximately 130 to 142 mL, corresponding to a conductivity range of 27–49 mS/cm. It is important to note that neither UV 280 nor UV 260 signals provide a good representation of the VLPs elution profile. This fact is one of the challenges in bionanoparticles process development, especially in early stage development where titers are usually low.

In order to determine the total protein and dsDNA composition of the fractions, samples were pooled according to the chromatogram (Figure 1) and analysed by Bradford and Picogreen assays respectively (Table 1). Due to the relatively high conductivity of the cell culture supernatant (11.8 mS/cm), 43% of the protein impurities did not bind to the column and were collected during column loading in the flow-through fraction (FT). Additionally, weakly bound proteins eluted immediately at the beginning of the salt linear gradient (fraction P1). Comparable results were obtained when using conditioned media harvested prior to transfection as loading material (data not shown). Contrariwise, the majority of the dsDNA bound to the column and only 3% was recovered in the FT fraction. Elution of dsDNA was achieved at conductivities higher than 50 mS/cm and collected in the fractions P3 and P4, in which the total protein content was very low (Table 1 and Figure 2A). Western blot analysis detecting HIV-1 p24 confirmed the presence of the Gag-GFP protein in all elution fractions (band at approximately 88 kDa, Figure 2B, P1-P5). Little or no

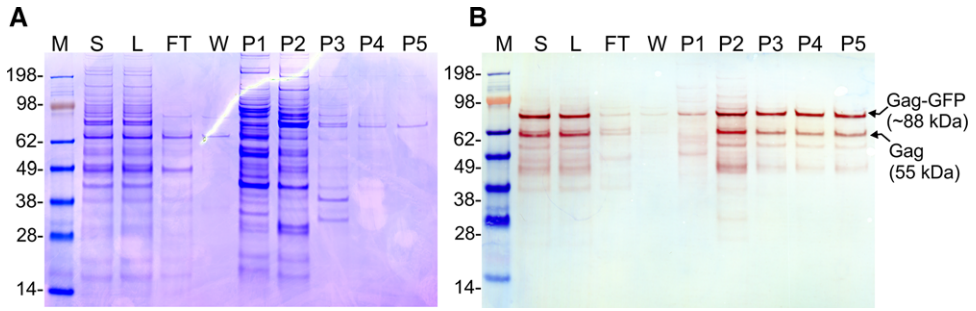

FIGURE 2 (A) SDS-PAGE and (B) Western blot analysis of the pooled fractions from the linear gradient purification (Figure 1). M: molecular weight marker; S: cell culture supernatant; L: loading material; FT: flow-through; W: wash; P1-P5: pooled fractions for peaks 1–5

FIGURE 3 Chromatogram of the step gradient purification of HIV-1 Gag-GFP VLP using a QA monolith. The loading material was 100 mL of clarified and 0.8 µm filtered HEK 293 cell culture supernatant. FT: flow-through; W: wash; P1-P4: pooled fractions for peaks 1–4

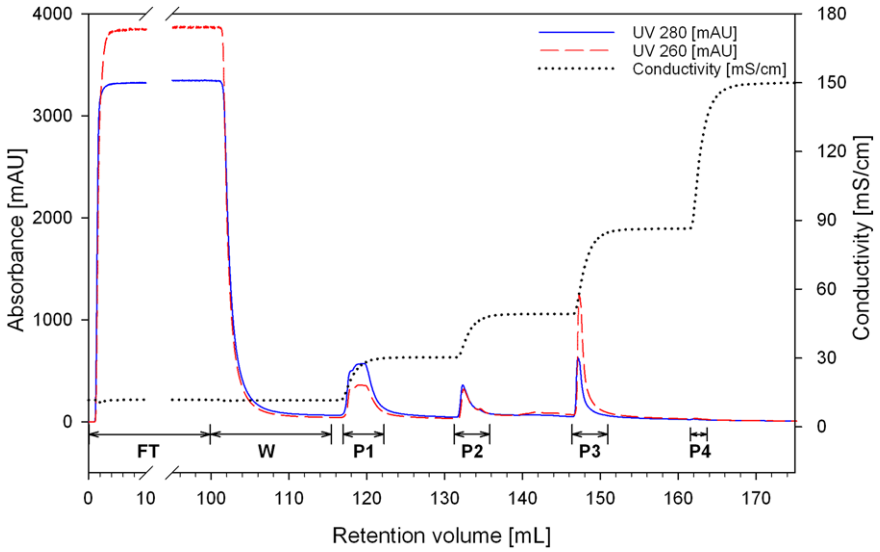

signal was obtained for the fractions FT and W in the Western blot, confirming the successful binding of the VLPs to the column. According to the light scattering and fluorescence data, the fraction P2 contains the majority of the HIV-1 Gag-GFP VLPs. Comparing the total protein and dsDNA content of P2 with the loading material (L), a depletion of approximately 96% of total protein and 99% of dsDNA was achieved. In P3 and P4, VLPs and host cell dsDNA co-eluted. Enveloped VLPs and dsDNA co-elution during purification using anion-exchange chromatography has been previously reported [23].

The at-line MALS and fluorescence monitoring allowed a fast identification of the VLP containing fractions and a direct transfer from the linear gradient to a step gradient elution. In the next chapter, we describe the step gradient purification.

3.2 | Step gradient purification

The step gradient purification was designed based on the results obtained by the at-line MALS and fluorescence monitoring of the linear gradient purification. The same column and loading material were used. Column equilibration, loading and regeneration conditions were also kept constant. Elution was designed targeting the recovery of the VLPs eluted in the linear gradient purification in a conductivity range of 27–49 mS/cm, as well as targeting the separation of VLPs from weakly bound protein impurities and from strongly bound dsDNA. Therefore, elution consisted in three steps of 15 CV each, using 300, 520, and 1000 mM NaCl (15, 26 and 50% B), corresponding to approximately 30, 49, and 86 mS/cm. In order to characterize the fractions collected in each step, samples were pooled according to the chromatogram (Figure 3). Protein content was analyzed by SDS-PAGE and Western blot and total protein was quantified by Bradford analysis (Figures 4A and B, Table 2). Picogreen assay was used to determine the dsDNA content (Table 2). Particles were visualized by transmission electron microscopy (Figures 4C–E) and quantified by NTA in scattering and fluorescence modes (Table 2).

As in the linear gradient purification, most of the protein impurities (55%) did not bind to the column or were eluted in fraction P1 using 300 mM NaCl (30 mS/cm). Western blot analysis confirmed the presence of Gag-GFP protein in fraction P1, however only a small number of particles were recovered in this fraction (3–5% measures by NTA in scattering or fluorescence mode). This indicates the presence of

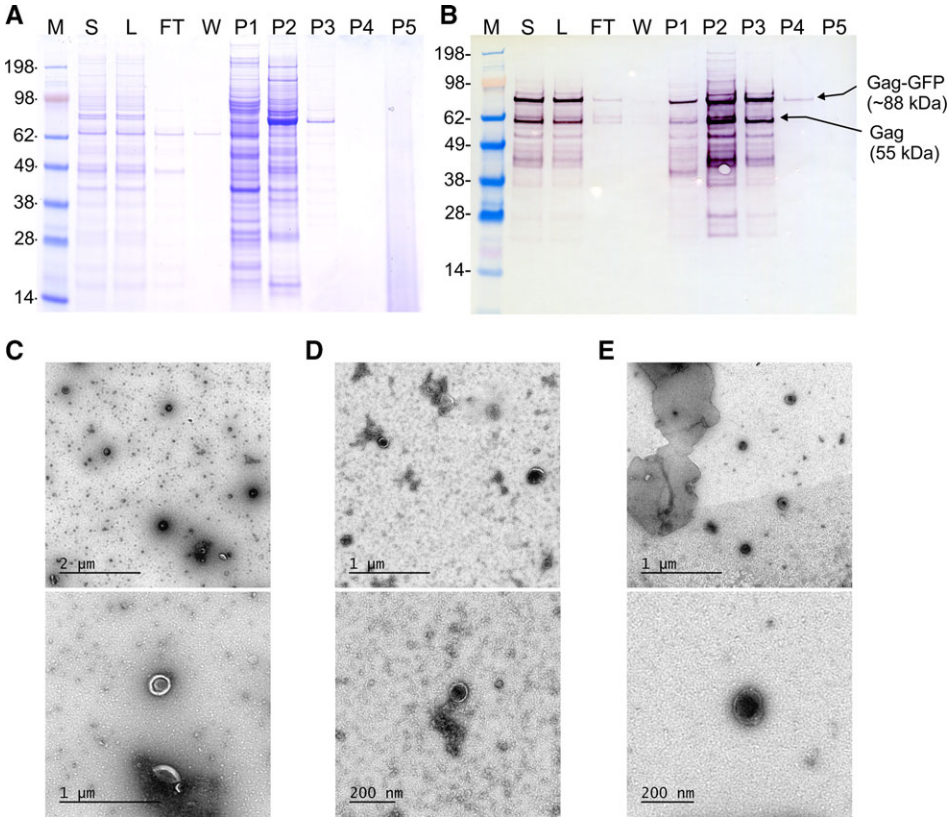

FIGURE 4 A: SDS-PAGE and B: Western blot analysis of the pooled fractions from the step gradient purification (Figure 3). (C), (D), and (E) electron microscopy micrographs of loading material (L) and fractions P2 and P3, respectively. M: molecular weight marker; S: cell culture supernatant; L: loading material; FT: flow-through; W: wash; P1-P4: pooled fractions for peaks 1–4

TABLE 2 Particles (diameter: 100–200 nm), total protein and dsDNA mass balance of the purification of HIV-1 Gag-GFP VLPs using a step gradient elution (Figure 3). L: loading material; FT: flow-through; W: wash; P1-P4: peaks 1-4; CIP: cleaning-in-place

Sample	Volume [mL]	Particles (LS)[a] d: 100-200 nm [particles/mL]	Particles (LS)[a] d: 100-200 nm %	Particles (FL)[b] d: 100-200 nm [particles/mL]	Particles (FL)[b] d: 100-200 nm %	Total Protein [µg/mL]	Total Protein %	dsDNA [ng/mL]	dsDNA %
L	100	2.4×10^{10}	100.0	2.7×10^{09}	100.0	297.8	100.0	448.0	100.0
FT	100	<LLOQ	–	<LLOQ	–	126.7	42.5	39.2	8.8
W	15	<LLOQ	–	<LLOQ	–	41.0	2.1	645.5	21.6
P1	5	2.2×10^{10}	4.5	1.5×10^{09}	2.8	632.2	10.6	91.5	1.0
P2	3	1.3×10^{11}	16.5	4.5×10^{10}	49.9	510.3	5.1	975.4	6.5
P3	3	2.7×10^{10}	3.3	1.2×10^{10}	13.6	62.4	0.6	12747.8	85.4
P4	1	5.0×10^{09}	0.2	<LLOQ	–	<LLOQ	–	691.6	1.5
CIP	15	n.d.	–	n.d.	–	456.8	23.0	<LLOQ	–
Recovery			24.5		66.3		83.9		124.8

[a]Particles measured in light scattering (LS) mode
[b]Particles measured in fluorescence (FL) mode
<LLOQ: lower than the lower LOQ
n.d.: not determined

fragmented particles or free Gag-GFP protein, which did not form a correctly assembled VLP. No particles were found in the flow-through (FT) and wash (W) fractions, confirming the efficient capture of the VLPs by the monolithic column. As expected, most particles were recovered and concentrated in fraction P2 (17–50%) and Western blot analysis confirmed the presence of the Gag-GFP protein. TEM micrographs confirmed the presence of correctly assembled spherical particles. Comparing the total protein and dsDNA content of P2 with the loading material (L), a depletion of approximately

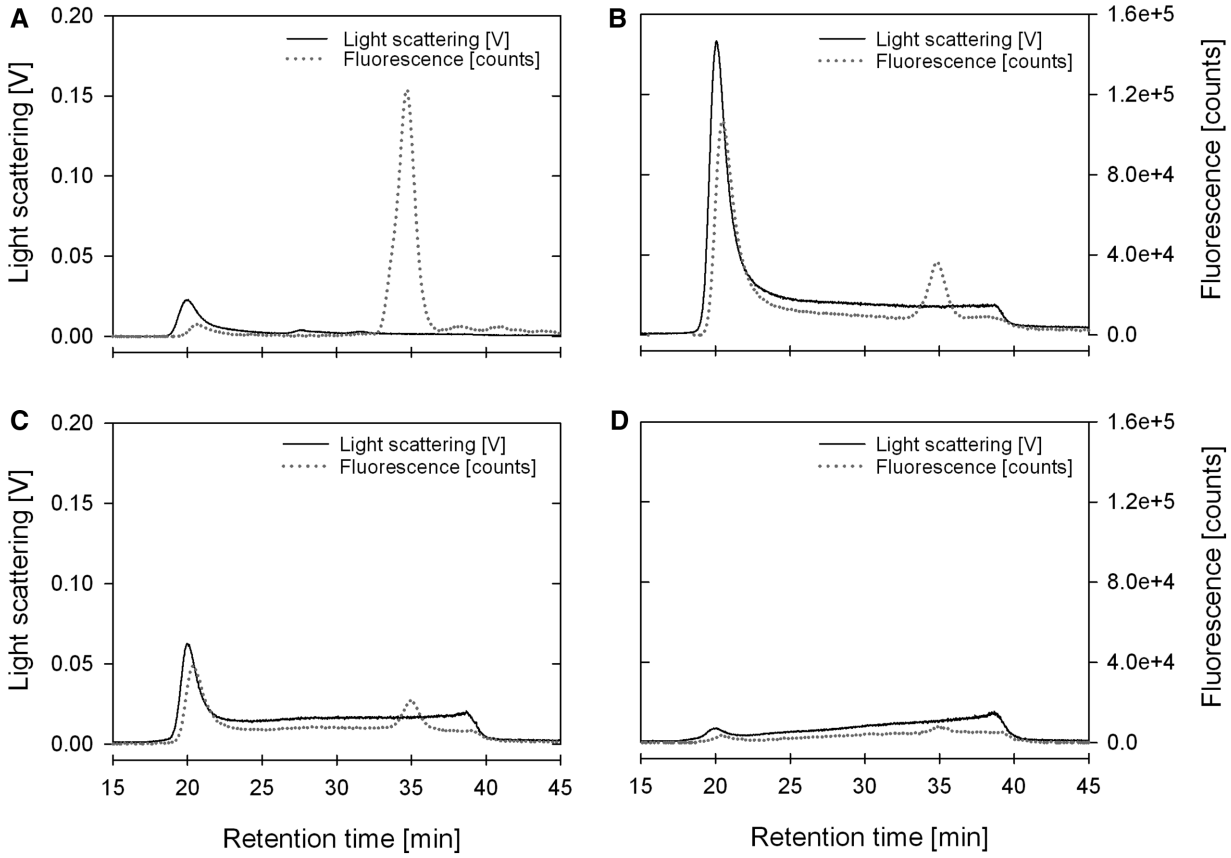

FIGURE 5 Analysis of the fractions P1-P4 from the step gradient purification (Figure 3) by analytical size exclusion chromatography coupled to MALS and fluorescence detectors (SEC-MALS-FL). (A) P1; (B) P2; (C) P3; (D) P4

95% of total protein and 94% of dsDNA was achieved for the main product fraction during the step gradient purification. Lastly, as in the linear gradient purification, the majority of dsDNA (85%) was eluted using higher ionic strength (1000 mM NaCl) and collected in fraction P3 together with strongly bound particles (3–14%).

In order to further characterize the samples, size exclusion chromatography coupled to MALS and fluorescence detectors (SEC-MALS-FL) was used. This strategy allows the separation of correctly assembled HIV-1 Gag-GFP VLPs from free Gag-GFP proteins and/or protein aggregates smaller than 100 nm, which are still identified when using Western blot analysis as detection method. As VLP reference, HIV-1 gag VLPs produced in CHO cells and purified as described by Steppert et al [23] were used. As free protein reference, GFP standard was used. VLPs standard eluted in the void volume of the SEC column (approximately 20 min) while GFP standard elutes at approximately 35 min post injection (data not shown). Fractions P1, P2, P3, and P4 were analysed by SEC-MALS-FL (Figures 5A–D respectively). As expected, in fraction P1 (Figure 5A) a very small light scattering peak was measured at the void volume due to the very low number of particles in this fraction. On the other hand, a significant fluorescence signal was obtained at 35 min, confirming the presence of free Gag-GFP protein already indicated by the Western blot analysis (Figure 3B). Conversely, in fraction P2 (Figure 5B) a significant light scattering signal together with a significant fluorescence signal were observed at the void volume confirming the presence of correctly assembled HIV-1 Gag-GFP VLPs. The small fluorescence peak observed at 35 min indicates that the sample still contains a small amount of product related impurities (free Gag-GFP). Similarly to fraction P2, fraction P3 SEC-MALS-FL analysis (Figure 5C) indicates the presence of correctly assembled particles, however in lower concentration due to the lower light scattering signal intensity. This could also be observed in the measurements done by NTA (Table 2).

MALS data was also used to calculate the geometric radius of particles in fractions P2 and P3, using the Rayleigh-Gans-Debye approximation. Geometric radii of approximately 70 nm (140 nm of diameter) and 69 nm (138 nm of diameter) were obtained for fractions P2 and P3, respectively. These values are in agreement with the values obtained for the hydrodynamic radii of 126 and 140 nm for fractions P2 and P3, respectively, calculated using the Stokes-Einstein equation and the diffusion constant measured by NTA.

SEC-MALS-FL validated at-line MALS results as a robust analytical tool to DSP development. Furthermore, VLP

integrity was confirmed by traditional TEM micrographs, where VLPs were clearly distinguished from product-related impurities.

4 | CONCLUDING REMARKS

The use of at-line multi-angle light scattering and fluorescence monitoring of a purification strategy for fluorescent VLPs allowed not only in-process monitoring and control but also faster process development. Product-containing fractions were quickly identified, allowing a swift transition from a linear gradient to a step gradient elution, providing a base for potential scale-up.

The single-step purification using a QA-monolith effectively captured and purified HIV-1 Gag-GFP VLPs produced in HEK 293 cells directly from the clarified cell culture supernatant. A VLP yield of 50% (measured by NTA in fluorescence mode) was obtained with a 17-fold concentration factor regarding the loading material. Assuming a dose of 10^9 particles, more than 44 doses can be captured per mL column.

This strategy streamlines VLP DSP process development and optimization and minimizes the need for several time-consuming and laborious analytical techniques during severe viral outbreaks.

ACKNOWLEDGMENTS

The authors wish to thank Dr. Amine Kamen (McGill, Montreal, Canada) for providing the HEK 293 SF-3SF6. The following reagent was obtained through the NIH AIDS reagent Program, Division AIDS, NIAID, NIH: pGag-EGFP (Cat# 11468) from Dr. Merilyn Resh. We would like to thank Dr. Dieter Palmberger, Dr. Reingard Grabherr and Dr. David Reinhart from BOKU (Vienna, Austria) for providing their cell culture equipment for the production of HEK 293 cells. This work was supported by the Generalitat de Catalunya under project 2014 SGR 1216 and 2017 SGR 898. I.G-D. would like to thank the Spanish Ministry of Education Culture and Sport for its support with a PhD grant (FPU16/02555). This work was also supported by the Austrian Science Fund (project BioToP; FWF W1224) and by the Austrian BMWD, BMVIT, SFG, Standortagentur Tirol, Government of Lower Austria and Business Agency Vienna through the Austrian FFG-COMET- Funding Program. The funding agencies had no influence on the conduct of this research.

CONFLICT OF INTEREST

The authors have declared no conflict of interest.

ORCID

Alois Jungbauer https://orcid.org/0000-0001-8182-7728

REFERENCES

1. Lua, L. H., Connors, N. K., Sainsbury, F., Chuan, Y. P., Wibowo, N., Middelberg, A. P., Bioengineering virus-like particles as vaccines. *Biotechnol. Bioeng.* 2014, *111*, 425–440.
2. Gonzalez-Dominguez, I., Gutierrez-Granados, S., Cervera, L., Godia, F., Domingo, N., Identification of HIV-1-based virus-like particles by multifrequency atomic force microscopy. *Biophys. J.* 2016, *111*, 1173–1179.
3. Kramberger, P., Ciringer, M., Strancar, A., Peterka, M., Evaluation of nanoparticle tracking analysis for total virus particle determination. *Virol. J.* 2012, *9*, 265.
4. Steppert, P., Burgstaller, D., Klausberger, M., Tover, A., Berger, E., Jungbauer, A., Quantification and characterization of virus-like particles by size-exclusion chromatography and nanoparticle tracking analysis. *J. Chromatogr. A* 2017, *1487*, 89–99.
5. Bagheri, M., Norouzi, H. R., Hossienizadeh, S. M. J., Es-Haghi, A., Ghassempour, A., Development and modeling of two-dimensional fast protein liquid chromatography for producing nonstructural protein-free food-and-mouth diseases virus vaccine. *J. Chromatogr. B* 2018, *1096*, 113–121.
6. Wyatt, P. J., Measurement of special nanoparticle structures by light scattering. *Anal. Chem.* 2014, *86*, 7171–7183.
7. Chen, Y., Zhang, Y., Zhou, Y., Luo, J., Su, Z., Asymmetrical flow field-flow fractionation coupled with multi-angle laser light scattering for stability comparison of virus-like particles in different solution environments. *Vaccine* 2016, *34*, 3164–3170.
8. Podzimek, S., Light Scattering, Size Exclusion Chromatography and Asymmetric Flow Field Flow Fractionation, John Wiley & Sons, Inc.2011.
9. Kamide, K., Dobashi, T., in: K., Kamide, T., Dobashi (Eds.), Physical Chemistry of Polymer Solutions, Elsevier Science, Amsterdam 2000, 377–442.
10. Charlton Hume, H. K., Lua, L. H. L., Platform technologies for modern vaccine manufacturing. *Vaccine* 2017, *35*, 4480–4485.
11. Vicente, T., Roldao, A., Peixoto, C., Carrondo, M. J., Alves, P. M., Large-scale production and purification of VLP-based vaccines. *J. Invertebr. Pathol.* 2011, *107*, S42–S48.
12. Pitoiset, F., Vazquez, T., Bellier, B., Enveloped virus-like particle platforms: Vaccines of the future? *Expert. Rev. Vaccines* 2015, *14*, 913–915.
13. Pitoiset, F., Vazquez, T., Levacher, B., Nehar-Belaid, D., Derian, N., Vigneron, J., Klatzmann, D., Bellier, B., Retrovirus-based virus-like particle immunogenicity and its modulation by toll-like receptor activation. *J. Virol.* 2017, *91*.
14. Cervera, L., Gutierrez-Granados, S., Martinez, M., Blanco, J., Godia, F., Segura, M. M., Generation of HIV-1 Gag VLPs by transient transfection of HEK 293 suspension cell cultures using an optimized animal-derived component free medium. *J. Biotechnol.* 2013, *166*, 152–165.
15. Venereo-Sanchez, A., Simoneau, M., Lanthier, S., Chahal, P., Bourget, L., Ansorge, S., Gilbert, R., Henry, O., Kamen, A., Process intensification for high yield production of influenza H1N1 Gag virus-like particles using an inducible HEK-293 stable cell line. *Vaccine* 2017, *35*, 4220–4228.
16. Cervera, L., Gonzalez-Dominguez, I., Segura, M. M., Godia, F., Intracellular characterization of Gag VLP production by transient transfection of HEK 293 cells. *Biotechnol. Bioeng.* 2017, *114*, 2507–2517.

17. Welsch, S., Muller, B., Krausslich, H. G., More than one door - Budding of enveloped viruses through cellular membranes. *FEBS Lett*. 2007, *581*, 2089–2097.
18. Gutierrez-Granados, S., Cervera, L., Segura Mde, L., Wolfel, J., Godia, F., Optimized production of HIV-1 virus-like particles by transient transfection in CAP-T cells. *Appl. Microbiol. Biotechnol.* 2016, *100*, 3935–3947.
19. Fuenmayor, J., Cervera, L., Gòdia, F., Kamen, A., Extended gene expression for Gag VLP production achieved at bioreactor scale. *J. of Chem. Technol. & Biotechnol.* 2019, *94*, 302–308.
20. Kramberger, P., Urbas, L., Strancar, A., Downstream processing and chromatography based analytical methods for production of vaccines, gene therapy vectors, and bacteriophages. *Hum. Vaccin. Immunother.* 2015, *11*, 1010–1021.
21. Effio, C. L., Hubbuch, J., Next generation vaccines and vectors: Designing downstream processes for recombinant protein-based virus-like particles. *Biotechnol. J.* 2015, *10*, 715–727.
22. Heath, N., Grant, L., De Oliveira, T. M., Rowlinson, R., Osteikoetxea, X., Dekker, N., Overman, R., Rapid isolation and enrichment of extracellular vesicle preparations using anion exchange chromatography. *Sci. Rep.* 2018, *8*, 5730.
23. Steppert, P., Burgstaller, D., Klausberger, M., Berger, E., Aguilar, P. P., Schneider, T. A., Kramberger, P., Tover, A., Nobauer, K., Razzazi-Fazeli, E., Jungbauer, A., Purification of HIV-1 gag virus-like particles and separation of other extracellular particles. *J. Chromatogr. A* 2016, *1455*, 93–101.
24. Gerster, P., Kopecky, E. M., Hammerschmidt, N., Klausberger, M., Krammer, F., Grabherr, R., Mersich, C., Urbas, L., Kramberger, P., Paril, T., Schreiner, M., Nobauer, K., Razzazi-Fazeli, E., Jungbauer, A., Purification of infective baculoviruses by monoliths. *J. Chromatogr. A* 2013, *1290*, 36–45.
25. Steppert, P., Burgstaller, D., Klausberger, M., Kramberger, P., Tover, A., Berger, E., Nobauer, K., Razzazi-Fazeli, E., Jungbauer, A., Separation of HIV-1 gag virus-like particles from vesicular particles impurities by hydroxyl-functionalized monoliths. *J. Sep. Sci.* 2017, *40*, 979–990.
26. Burden, C. S., Jin, J., Podgornik, A., Bracewell, D. G., A monolith purification process for virus-like particles from yeast homogenate. *J. Chromatogr. B* 2012, *880*, 82–89.
27. Zaveckas, M., Snipaitis, S., Pesliakas, H., Nainys, J., Gedvilaite, A., Purification of recombinant virus-like particles of porcine circovirus type 2 capsid protein using ion-exchange monolith chromatography. *J. Chromatogr. B* 2015, *991*, 21–28.
28. Jungreuthmayer, C., Steppert, P., Sekot, G., Zankel, A., Reingruber, H., Zanghellini, J., Jungbauer, A., The 3D pore structure and fluid dynamics simulation of macroporous monoliths: High permeability due to alternating channel width. *J. Chromatogr. A* 2015, *1425*, 141–149.
29. Hu, Y., Cheng, X., Daniel Ou-Yang, H., Enumerating virus-like particles in an optically concentrated suspension by fluorescence correlation spectroscopy. *Biomed. Opt. Express* 2013, *4*, 1646–1653.
30. Gutiérrez-Granados, S., Cervera, L., Gòdia, F., Carrillo, J., Segura, M. M., Development and validation of a quantitation assay for fluorescently tagged HIV-1 virus-like particles. *J. Virol. Meth.* 2013, *193*, 85–95.

How to cite this article: Pereira Aguilar P, González-Domínguez I, Schneider TA, Gòdia F, Cervera L, Jungbauer A. At-line multi-angle light scattering detector for faster process development in enveloped virus-like particle purification. *J Sep Sci* 2019;42:2640–2649. https://doi.org/10.1002/jssc.201900441

PUBLICATION III

For submission to Journal of Chromatography A

Capture and purification of HIV-1 gag virus-like particles: convective media vs porous beads

Patricia Pereira Aguilar[1,2], Katrin Reiter[2], Viktoria Wetter[2], Petra Steppert[1], Daniel Maresch[1], Wai Li Ling[3], Peter Satzer[2*], Alois Jungbauer[1,2]

[1] Department of Biotechnology, University of Natural Resources and Life Sciences, Vienna, Austria

[2] Austrian Centre of Industrial Biotechnology, Vienna, Austria

[3] Univ. Grenoble Alpes, CEA, CNRS, IBS, F-38000 Grenoble, France

*Corresponding author

Dipl.Ing Peter Satzer, Ph.D

Austrian Centre of Industrial Biotechnology, Vienna, Austria

Muthgasse 18, 1190 Vienna

Phone: +43 1 47654-79114

Fax: +43 1 47654-79009

E-mail: peter.satzer@boku.ac.at

Abstract

Downstream processing (DSP) of enveloped virus-like particles (eVLPs) is still a challenge. Capture and purification of enveloped bionanoparticles still relies on the combination of several sub-optimal unit operations, most of them imported from virus or protein production platforms. Most of the technologies currently in discussion are underdeveloped and it is not clear which of the novel capture and purification strategies are the best for eVLP purification. Four different DSP strategies were tested for the capture and purification of eVLPs. As a model, HIV-1 gag VLPs produced in CHO cells were used. An anion-exchange monolith and a membrane adsorber were used for the capture and purification of HIV-1 gag VLPs directly from clarified cell culture supernatant. A polymer-grafted anion-exchange resin and a heparin-affinity resin were tested for eVLP purification after a first flow-through step using core-shell beads with multimodal ligands to remove small impurities. The performance of the different strategies was evaluated regarding binding capacity, ability to separate different particle populations and product purity. Several analytical methods such as multi-angle light scattering, Western blot, nanoparticle tracking analysis, mass spectrometry and cryo electron microscopy, were used in order to detect, characterize and quantify the eVLPs. It was possible to capture HIV-1 gag VLPs directly from endonuclease-treated and filtered CHO cell culture supernatant using ion exchange membrane adsorbers. Another viable identified option was the Heparin-affinity chromatography which is also suitable for purification of eVLP and in comparison to ion exchange allowed the separation of HIV-1 gag VLPs from host cell derived bionanoparticles and chromatin on the expense of necessary pre-processing.

Keywords: Enveloped VLP; Affinity chromatography; Ion exchange chromatography; Polymer-grafted media; Convective media; Downstream processing.

1 Introduction

The growing interest in the use of enveloped virus-like particles (eVLPs) as novel vaccines or vectors for gene and cancer therapy applications lead to an increase demand for efficient and scalable production platforms [1-3]. Current downstream processing (DSP) strategies in eVLP production still rely on the combination of several unit operations, including ultracentrifugation, filtration and chromatography [4-6]. Here we compare different DSP strategies for eVLP purification including the use of monoliths, membrane adsorbers, polymer-grafted media and core-shell beads. Drawbacks of the combination of several sub-optimal unit operations in a DSP strategy include long process times, low productivity and high product losses. Furthermore, the lack of standard methods for detection and quantification of eVLPs leads to the use of methodologies imported from protein biotechnology, which are non-optimal for eVLPs, consequently hindering process development and optimization [2, 7]. Besides that, the use of protein-based methods for quantification of specific proteins of different eVLPs makes a systematic comparison between the currently available eVLP DSP strategies unfeasible. In this work, we compared the performance of four different chromatography-based DSP strategies for capture and purification of a model eVLP, using the same starting material. Several works have shown that anion-exchange chromatography allows the efficient capture and purification of enveloped viruses and VLPs [8-11]. Therefore, we selected three different types of anion exchangers: a monolithic support, a membrane absorber and a polymer-grafted bead resin. Monoliths and membrane adsorbers are attractive options as unit operation for bionanoparticle's DSP due to their convective flow properties and large surface area accessible for binding of large molecules [12-14]. In contrast, in porous-bead based chromatography, mass transfer mainly occurs through pore diffusion and usually pores are too small to allow VLP diffusion into the pores. Nevertheless, even when eVLPs are completely excluded from the resin's pores, the bead's outer surface area still provides satisfactory binding capacity, which is only one order of magnitude smaller than the one obtained with convective media [8]. Moreover, the scalability of conventional chromatography resins easily overcomes its lower biding capacity as current monolith technology is limited in column size to a couple liters. Besides anion-exchange chromatography, affinity chromatography has great potential for capture and purification of eVLPs, once it allows the direct capture of the product of interest

from complex feed streams, resulting in high levels of purity in a single step [4]. This increases DSP productivity and accelerates R&D. Since heparin is a natural cell receptor for many viruses [15], we selected a heparin-affinity resin. Moreover, it was already reported that heparin-affinity can separate eVLPs from host cell derived bionanoparticles [16]. However, due to the possible presence of heparin-binding proteins in the cell culture supernatant, a first pre-processing step is required to avoid reduction in binding capacity or co-elution of protein impurities with the eVLP product. For that purpose, we use flow-through chromatography with core-shell beads in which the VLPs flow-through the column without reaching the active core of the beads where the proteins can bind [17, 18]. As model eVLP, we used HIV-1 gag VLPs (100-200 nm in diameter) produced in Chinese Hamster ovary (CHO) cells. Structurally VLPs mimic their native viruses, resulting in complex bionanoparticles containing several copies of one or more viral proteins. These proteins typically self-assemble in spherical-like structures with sizes ranging from tens to hundreds of nanometers in diameter. In the case of eVLPs, as for enveloped viruses, an additional lipid bi-layer composed of the host cell membrane is part of their structure [7, 19]. These complex structural features of eVLPs bring new challenges to the production platforms. Especially in DSP development and analytics additional challenges arise from the simultaneous release of host cell derived nanoparticles, such as exosomes and extracellular vesicles, which have similar structure, size and composition as the eVLPs [20]. Besides that, dsDNA is another challenging impurity due to its overall negative charge, which is similar to the charge of many enveloped viruses and VLPs [21]. Especially when using anion-exchange based methods, co-elution of eVLPs and dsDNA was observed [8, 9].

Efficient DSP development requires fast and high-resolution analytical methods for in-process product quality and quantity control. However, there are no methods which allow the direct quantification of eVLPs in complex mixtures. Consequently, eVLP titers are often measured based on the quantification of a single viral protein or total particle count, which leads to under- or over-estimated titers[5, 22, 23]. Detection and quantification methods based on infectivity assays are not applicable for VLPs once they lack viral genome and are therefore non-infectious. Accordingly, we used a combination of several biochemical and biophysical analytical methods to detect, quantify and characterize particle populations, including multi-angle light scattering (MALS), nanoparticle tracking analysis (NTA), cryo transmission electron microscopy (cryo-TEM), Western blot analysis and mass spectrometry (MS). The use of the same

analytical methodologies to access product quantity and quality as well as the use of the same starting material, allowed a systematic comparison of the binding capacity and resolution for particle separation of an anion-exchange monolith, a membrane adsorber, a polymer-grafted anion-exchange resin and a heparin-affinity resin.

2 Material and methods

2.1 Chemicals and standards

All chemicals were acquired from Sigma Aldrich (St. Louis, MO, USA), Merck (Darmstadt, Germany) or Abcam (Cambridge, England) and were of analytical grade, if not otherwise stated.

2.2 Enveloped VLP production

HIV-1 gag VLPs, kindly provided by Icosagen (Tartumaa, Estonia), were used as an enveloped VLP model. VLP production was carried out in CHOEBNALT85 cells using a stable episomal system as described by Steppert *et al* [9]. Cell culture was harvested by centrifugation (1000 g, 30 min) and 0.01% NaN_3 was added to the supernatant.

2.3 Endonuclease treatment

Benzonase® purity grade II (Merck KGaA, Darmstadt, Germany) was used for the digestion of double stranded DNA (dsDNA). The digestion was performed by incubating cell culture supernatant with 150 U/mL Benzonase® and 2 mM $MgCl_2$ for 2 h at 37°C.

2.4 Preparative chromatography

2.4.1 Chromatographic system

All chromatographic experiments were performed on an Äkta pure 25 M2 equipped with a 1.4 mL mixer chamber, a S9 sample pump and a F9-C fraction collector (GE Healthcare, Uppsala, Sweden). System control and data acquisition were performed using the Unicorn 6.4.1 software. UV absorbance (280, 260 and 214 nm) and conductivity were continuously monitored.

2.4.2 Chromatography media and mobile phases

All preparative chromatographic experiments for capture and purification of eVLPs were performed using 50 mM HEPES, pH 7.2 as mobile phase A and 50 mM HEPES, 2 M NaCl, pH 7.2 as mobile phase B. Different concentrations of the modifier were obtained by mixing mobile phases A and B using the chromatography system. If not further stated, cleaning in place was performed using 0.5 M NaOH solution. The used chromatography media are summarized in Table 1.

2.4.3 Capture and purification of HIV-1 gag VLPs

For the capture and purification of HIV-1 gag VLPs, clarified CHO cell culture supernatant was endonuclease treated and either directly loaded onto the column or pre-processed using flow-through chromatography (Capto-Core). Direct loading was used for Natrix-Membrane and QA-Monolith devices. Fractogel-TMAE and Capto-Heparin columns were loaded with the flow-through fractions of the pre-processing runs. For the packed columns (Fractogel-TMAE and Capto-Heparin) flow rates were defined in order to achieve a 5 min residence time. For the pre-packed devices (Natrix-Membrane and QA-Monolith) flow rates recommended by the manufacturers were used. In all chromatographic experiments, equilibration of the stationary phase was performed before loading using equilibration buffer (50 mM HEPES, 100 mM NaCl, pH 7.2 / 5 % B). After loading, columns were washed with equilibration buffer to ensure the removal of unbound material from the column. In the capture and purification experiments, elution was achieved by salt linear gradients. Details of flow rates, loading volumes and elution gradients are summarized in Table 2. After the elution phase, columns were regenerated using 100 % B buffer. Fractions were collected and pooled according to the chromatograms, considering both, the light scattering intensity and the UV absorbance signals.

2.5 Particle detection and quantification

Particle detection of collected fractions from the chromatographic experiments was performed by at-line multi-angle light scattering (MALS) measurements as described in [24]. Briefly, an Ultimate 3000 system (Thermo Fisher, Waltham, MA, USA) was used in bypass mode for the direct injection of each collected fraction into the MALS detector (DAWN HELEOS 18-angle, Wyatt, Santa Barbara, CA, USA). The peak area of the light scattering signal measured at 90° angle was used to access the light scattering intensity which is proportional to the particle concentration. This information together with the UV data was used to decide on sample pooling.

Particle concentration of pooled samples was accessed by nanoparticle tracking analysis (NTA) using a NanoSight NS300 (Malvern Instruments Ltd., Worcestershire, UK) equipped with a blue laser module (488 nm). For the NTA measurements, samples were diluted using particle-free water in order to achieve a concentration of 20 to 80 particles per video frame. In total 15 videos of 30 seconds were recorded per

sample. NanoSight NTA software version 3.2 (Malvern Instruments Ltd., Worcestershire, UK) was used to record and analyse the data.

Transmission electron microscopy (TEM) was used to visualize the structure of the particles in relevant samples. Negative staining was used to prepare grids with native or antibody labelled samples. For native samples, 30 µL of sample were incubated on coated 400-mesh copper grids for 1 min at room temperature. Fixation was performed by incubating the grids in 2.5 % glutaraldehyde solution (in 100 mM cacodylate buffer, pH 7.0) for 15 min. Finally, grids were stained with 1 % uranyl acetate for 30 seconds. Specimens were visualized using a Tecnai G2 200 kV transmission electron microscope (FEI, Eindhoven, The Netherlands). For cryo-TEM, 4 µL of the sample were applied to a glow-discharged holey carbon grid and plunge frozen in liquid ethane using a FEI Vitrobot™ mark IV (ThermoFisher Scientific, Oregon, USA). Imaging was performed on an FEI F20 microscope at 200 kV and recorded on an FEI Ceta detector (ThermoFisher Scientific, Oregon, USA).

2.6 Protein and DNA detection and quantification

Total protein was quantified by Bradford assay using Coomassie blue G-250-based protein dye reagent (Bio-Rad Laboratories, Hercules, CA, USA. Double stranded DNA (dsDNA) was quantified by Quant-iT™ PicoGreen® dsDNA kit (Life Technologies, Waltham, MA, USA). Both quantifications were performed according to the manufacturer's instructions in a microtiter plate format.

Total protein content was also qualitatively evaluated by sodium dodecyl sulphate polyacrylamide gel electrophoresis (SDS-PAGE) as described in [8]. Specific proteins (HIV-1 gag p24 and H3 histone) were detected by Western blot analysis as described in [8].

Proteomic analysis was used for protein identification. For that purpose, relevant samples were digested in solution. Proteins were S-alkylated with iodoacetamide and digested with Trypsin (Promega, Madison, WI, USA). Digested samples were analysed as described before in [8].

2.7 Analytical chromatography

Size exclusion chromatography coupled to multi-angle light scattering (SEC-MALS) was used to access sample composition and purity. An Ultimate 3000 HPLC system (Thermo Fisher, Waltham, MA, USA) with a quaternary LPG-3400SD pump, a WPS-

3000TSL autosampler and a DAD 3000 UV-detector was used as chromatography system. A TSKgel G5000PWxl 30.0 cm × 7.8 mm i.d. column in combination with a TSKgel PWxl guard column 4.0 cm × 6.0 mm i.d. or a TSKgel SuperMultiporePW-H 15.0 cm × 6.0 mm column (Tosoh Bioscience, Stuttgart, Germany) were used as SEC columns. A DAWN HELEOS 18-angle (Wyatt, Santa Barbara, CA, USA) was used as multi-angle light scattering detector. Mobile phase consisted of 50 mM HEPES, 100 mM NaCl, pH 7.2. Flow rate was 0.3 mL/min for the G5000PWxl column and 0.175 mL for the SupermultiporePW-H column. In both cases, sample volume was 50 µL. HPLC was controlled by Chromeleon 7 software (Thermo Fisher, Waltham, MA, USA). MALS data collection and analysis was performed with ASTRA software, version 6.1.2 (Wyatt, Santa Barbara, CA, USA).

3 Results and discussion

3.1 Feed material composition before and after pre-processing

After clarification by centrifugation, CHO cell culture supernatant contained approximately $1x10^{11}$ part/mL, 830 µg/mL of total protein and 22 µg/mL of dsDNA, determined by NTA, Bradford assay and Picogreen assay, respectively. Cryo-electron microscopy revealed the presence of several enveloped bionanoparticle populations including HIV-1 gag VLPs and host cell derived vesicles such as microvesicles and exosomes (Figure 1a). To be suited as feed material for direct loading of anion-exchange monoliths and membrane adsorbers, clarified CHO cell culture supernatant was endonuclease pre-treated and 0.8 µm filtered. Resulting feed material contained approximately $1x10^{11}$ part/mL, 800 µg/mL of total protein and 0.5 µg/mL of dsDNA (98% reduction in dsDNA content). To be suited as feed material for the heparin-affinity resin, endonuclease pre-treated and 0.8 µm filtered CHO cell culture supernatant was further pre-processed by flow-through chromatography. For that purpose, a HiScale 26/20 column packed with 50.4 mL of Capto-Core resin was used. A recovery of approximately 82% of particles with a reduction of 76% in total protein and 34% in dsDNA was obtained (Supplementary material A, Figures SA7 and SA8) during the pre-processing of the feed material for the heparin-affinity experiment. Similar results were obtained while preparing the feed material for the polymer-grafted anion-exchanger. While the pre-processing with flow-through chromatography allowed the reduction of host cell protein and dsDNA content, separation between different bionanoparticle populations was not possible using this method (Figure 1b). Further purification of this material was done using heparin-affinity and anion-exchange chromatography.

3.2 Binding capacity

When using cell culture supernatant as feed material (with or without pre-processing), it is not possible to accurately determine the concentration of HIV-1 gag VLPs due to the presence of other bionanoparticles and the lack of specific analytical methods to quantify eVLPs in these complex mixtures. Subsequently, it is no possible to determine the dynamic binding capacity for the HIV-1 gag VLPs directly. However, since it was possible to identify the particle breakthrough by the light scattering signal (Figure 2,

LS area) we used this signal to estimate a binding capacity for all bionanoparticles. For comparison reasons, the estimation of the binding capacity was done considering the loading volume that led to less than 3% particle breakthrough in each one of the four tested strategies (measured by NTA, Table SA1-SA4). Taking this into account, the following capacities were estimated: Natrix-Membrane: $5.3x10^{12}$ particles/mL membrane (loading of 35 mL or 44 CV); QA-Monolith: $2.9x10^{12}$ particles/mL column (loading of 240 mL or 30 CV); Fractogel-TMAE: $1.5x10^{12}$ particles/mL column (loading of 400 mL or 17 CV) and Capto-Heparin: $1.5x10^{11}$ particles/mL column (loading of 45 mL or 2 CV). Anion-exchange based chromatography materials had the higher binding capacities for bionanoparticles. As expected, due their larger surface area accessible for binding of large molecules, membrane adsorber and monolith had slightly higher binding capacity than the porous-bead resin, in which bionanoparticles can only bind at the outer surface of the beads [8]. Nevertheless, all three materials had binding capacities in the same range (2-$5x10^{12}$ particles/mL column or membrane) and the easy scalability of packed columns compensates for the lower binding capacity. The obtained values are also comparable to previously reported data [8, 9, 25]. For all three anion-exchangers a salt linear gradient was used as elution strategy (Table 2, Figure 2).

3.3 Capture and purification of eVLPs using anion-exchange monoliths, membrane adsorbers and polymer-grafted porous beads

The membrane adsorber, Natrix-Membrane, showed the highest binding capacity and allowed the capture and semi-purification of HIV-1 gag VLPs directly from endonuclease treated and filtered CHO cell culture supernatant. At the beginning of the loading phase, while bionanoparticles bound to the membrane adsorber, part of the proteins and dsDNA flowed through the column (Figure 2a, Table SA1: FT1). Bound proteins (P1) were separated from bound particles (P2) during the elution gradient. SDS-PAGE analysis (Figure 3a) shows a significant reduction in protein content from the loading material (L) to the elution fraction P2. This was confirmed by Bradford assay, in which the total protein content in P2 was lower than the lower limit of quantification (Table SA1). The presence of HIV-1 gag VLPs in P2 was confirmed by cryo-electron microscopy (Figure 3d) in combination with the p24 Western blot assay (Figure 3b) and proteomic analysis (Supplementary material B). However, co-elution of different particle populations was also observed by cryo-electron microscopy

(Figure 3d) and co-elution of dsDNA and chromatin was confirmed by Picogreen assay, H3-histone Western blot assay and proteomic analysis (Table SA1, Figure 3c, Supplementary material B). Nevertheless, a two-fold reduction in dsDNA content from the feed material to the fraction P2 was already achieved.

The QA-Monolith was also used for the direct capture HIV-1 gag VLPs directly from endonuclease treated and filtered CHO cell culture supernatant (Figure 2b). As for the Natrix-Membrane, at the beginning of loading phase of the QA-Monolith, part of the host cell proteins and dsDNA passed through the monolith while bionanoparticles bound (Table SA2). In contrast with the Natrix-Membrane, for the QA-Monolith light scattering signal and NTA measurements revealed that particles elute across the entire elution gradient (Figure 2b). Despite in all elution fractions the presence of HIV-1 gag polyprotein was confirmed by p24 Western blot (Figure SA2b), SDS-PAGE and proteomic analysis revealed that the different elution fractions (P1-P5) contained different proteins in their composition. Picogreen assay and H3-histone Westernblot showed that most of the bound dsDNA and chromatin eluted in fractions P2 and P3 (Table SA2, Figure SA2c). Cryo-electron micrographs showed the presence of HIV-1 gag VLPs in all elution fractions (Figure SA2d). Fractions P4 and P5 were considered the main product fractions due to the higher particle concentration and simultaneous lower total protein and dsDNA content per dose (hypothetical vaccination dose of 10^9 particles, Figure SA3). Despite that cryo-electron micrographs showed an enrichment of HIV-1 gag VLPs in fractions P4 and P5, some host cell derived bionanoparticles could still be found as well as disrupted VLPs. Additionally, according to H3-histone Western blot, proteomic analysis and Picogreen assay dsDNA and chromatin are still present in fractions P4 and P5. Nevertheless, reductions of 13.3-fold for host cell protein and 2.9-fold for dsDNA, together with partial particle separation, were achieved using the QA-monolith.

Capture and purification of HIV-1 gag VLPs directly from CHO cell culture supernatant using Fractogel^{-}TMAE was recently reported [8]. Aiming to increase the binding capacity for eVLPs, endonuclease treated and 0.8 µm filtered cell culture supernatant was pre-processed by flow-through chromatography using Capto-Core. Even though pre-processing of the feed material allowed a reduction of 73% of the total protein and 15% of dsDNA content (data not shown), the binding capacity increase was only 0.4-log. This strengthens the hypothesis that when using porous beads, small protein impurities bind to the ligands inside of the chromatography beads which are not

accessible for VLPs, reducing the risk of binding competition or displacement effects. Similarly to the QA-Monolith, particle elution from the Fractogel-TMAE column occurred across the entire elution gradient (Figure 2c, Table SA3). Moreover, according to SDS-PAGE and proteomic analysis, late elution fractions of QA-Monolith (P3-P5) and Fractogel-TMAE (P3-P6) contained similar proteins (Figures SA2 and SA4 and Supplementary material B). Despite HIV-1 gag VLPs were identified in all elution fractions by cryo-electron microscopy (Figure SA4d), considering particle concentration together with the total protein and dsDNA per dose (Figure SA5) only fractions P5 and P6 were considered as main product fractions.

3.4 Purification of eVLPs and removal of host cell derived bionanoparticles and chromatin using heparin-affinity chromatography

Purification of HIV1- gag VLPs by heparin affinity was performed using Capto-Heparin. In order to remove potential heparin-binding host cell proteins, endonuclease treated and 0.8 µm filtered CHO cell culture supernatant was also pre-processed by flow-through chromatography using Capto-Core as described in section 3.1 (Figures SA7 and SA8).

Contrarily to the anion-exchange based strategies, in which at the beginning of the loading phase all particles bound to the column/membrane, during the Capto-Heparin loading, particle breakthrough started immediately after the column void volume (light scattering signal, Figure 2d). This indicates that, while some particles bound to the heparin ligands, others passed directly through the column. Similar behaviour was already reported for the purification HIV-1 gag VLPs produced in HEK 293 cells [16]. Cryo-electron micrographs showed that, despite of the presence of some HIV-1 gag VLPs, the majority of the particles eluting in the first flow-through fractions (FT2 and FT3) are host cell derived vesicles (Figure 4d). Flow-through fractions FT4 and FT5 had a composition similar to the feed material indicating full breakthrough and column overloading (Table SA4, Figures 1b and 4a-4d). Bound particles were eluted using a salt linear gradient (Table 2). Although no complete resolution was achieved, two elution peaks could be clearly distinguished, indicating the elution of different particle populations (Figure 2d). SDS-PAGE and proteomic analysis showed that the protein composition of fractions P1 and P2 was different. Picogreen assay showed that fraction P2 contained 7 times more dsDNA than fraction P1 and proteomic analysis revealed that fraction P2 contained several histones while in P1 only histone H4 was

found. Cryo-electron micrographs confirmed the different nature of the particles eluting in fractions P1 and P2 (Figure 4d). Fraction P1 was enriched in HIV-1 gag VLPs, while fraction P2 contained mostly other particulate structures. Considering the identification of several histones by proteomic analysis and the confirmation of the presence of H3-histone by Western blot analysis, the particulate structures in fraction P2 were identified as chromatin. This was additionally confirmed by immunogold labelling of H3-histones and negative staining TEM (data not shown). Moreover, similar structures were previously reported in cryo-electron micrographs as chromatin [26]. It is important to note than in both fractions, P1 and P2, nearly the same number of particles were quantified by NTA (Table SA4) and an average diameter of approximately 150 nm was measured also for both. These results clearly show the need for combining several biophysical, biochemical and high-resolution imaging methods for the quantification and characterization of eVLPs. Moreover, these results show that with the available methodologies specific quantification of eVLPs in complex mixtures such as cell culture supernatants is very difficult and impossible without advanced methodology.

3.5 Purity and recovery of main product fractions

Size exclusion analytical chromatography coupled to multi-angle light scattering (SEC-MALS) was used to semi-quantitatively access the purity of all elution fractions (Figure SA9). As an example, SEC-MALS chromatograms of relevant fractions from the DSP strategy with higher binding capacity (Natrix-Membrane: 1902NT) and the DSP strategy with better bionanoparticle separation (Capto-Heparin: 1904CH) are shown in Figure 5. In all tested DSP strategies, significant reduction of UV absorbance signal of impurities eluting not at the same time as eVLPs could be observed from the feed material to the main product fractions, indicating an increase in purity. As discussed in 3.4, in the Capto-Heparin experiment, fraction P1 contained mainly HIV-1 gag VLPs while fraction P2 contained mainly chromatin. SEC-MALS chromatogram of fraction P1 showed that HIV-1 gag VLPs elute in the void volume of the SEC column (light scattering signal starting at approximately 1.5 mL and with peak maximum at 2.1 mL). SEC-MALS chromatogram of fraction P2 (chromatin rich fraction) showed that despite particle elution (light scattering signal) also started at approximately 1.5 mL, the peak maximum was shifted to approximately 3.2 mL indicating the elution of smaller molecules or particle retention by interaction with the SEC column. Interestingly, this was not observed in the SEC-MALS chromatograms of the feed material or flow-

through fractions. The reason for that is that chromatin structure is disrupted at moderate-high salt concentrations [27] as the ones used during elution, resulting in smaller and more flexible structures that are longer retained in the SEC column.

Specific quantification of HIV-1 gag VLPs in the feed material by particle quantification methods, such as NTA or SEC-MALS, was not possible due to the presence of other particulate structures such as host cell derived bionanoparticles and chromatin. Likewise, HIV-1 gag VLP concentration could not be estimated by quantifying the HIV-1 gag polyprotein due to the presence of free HIV-1 gag protein in solution which was produced by the cells but did not assemble into VLPs. Consequently, direct determination of the yield of HIV-1gag VLPs was not possible. In order to compare the performance of the tested DSP strategies for the capture and purification of HIV-1 gag VLPs we determined the recovered doses in the main product fractions considering a hypothetical vaccination dose of 10^9 particles (Figure 6) under the assumption that particles in this main fraction are exclusively product. Additionally, we normalized the calculated recoveries considering the volume of feed material loaded in each experiment before 3% particle breakthrough was reached and considering the column/membrane volume. This product yield can only serve as an estimate due to the lack of proper analytics, but as TEM micrographs show that the main component in all selected product peaks is indeed intact VLP attributing the whole particle fraction of those peaks to being product is justified. Taking this into account, convective media (membrane adsorber and monolith) allowed the recovery of higher number of doses than the porous-bead resins but less than the Natrix-Membrane. Nevertheless, scalability of bead-based resins easily overcomes the lower recovery as monolithic columns are currently restricted to a couple of litres. For assessment and comparison of the purity of the main product fractions, total protein and dsDNA contents were normalized by the number of recovered doses (Figure 6). Natrix-Membrane had the highest recovery, however HIV-1 gag VLPs could not be separated from host cell derived bionanoparticles. Highest overall purity was achieved using Capto-Heparin which allowed not only the separation of HIV-1 gag VLPs from host cell derived bionanoparticles but also the separation of VLPs from chromatin. Polymer-grafted beads (Fractogel-TMAE) and monoliths (QA-Monolith) main product fractions had similar final composition. Despite QA-Monolith had a significantly higher recovery than Fractogel-TMAE, packed beads can be easily scaled up to hundreds of litres while monoliths have been successfully scaled up only up to 8 L.

4 Conclusion

Anion-exchange chromatography is suitable for capture and semi-purification of enveloped VLPs directly from cell culture supernatant. A fast capture of HIV-1 gag VLPs directly from endonuclease-treated and filtered CHO cell culture supernatant was possible using the membrane adsorber, NatriFlo® HD-Q Recon. Heparin-affinity chromatography is suitable for purification of eVLPs as well. Capto™ Heparin allowed the separation of HIV-1 gag VLPs from host cell derived bionanoparticles and chromatin. The best performer including factors like scalability, removal of host cell bionanoparticles, protein and dsDNA was the strategy combining flow-through chromatography using Capto™ Core 700 and Heparin-affinity chromatography using Capto™ Heparin. Regardless of the significant recent advances in eVLP DSP, development and optimization are still severely hindered by the lack of high-resolution methodologies for eVLP detection and quantification in complex mixtures, especially due to the presence of host cell derived bionanoparticles and chromatin. While we successfully showed the use of cryo-electron micrographs for particle identification, this methodology is not suited for rapid process development and significant amounts of highly pure eVLPs are required to allow the development and validation of novel analytical technologies. At the same time, to obtain highly pure eVLPs, DSP development and optimization are required. Therefore, a simultaneous development and optimization of both DSP and analytical technologies is essential in the future.

Acknowledgements

This project has been supported by the Austrian Science Fund (project BioToP; FWF W1224). Reiter and Wetter have been supported by the Austrian BMWD, BMVIT, SFG, Standortagentur Tirol, Government of Lower Austria and Business Agency Vienna through the Austrian FFG-COMET-Funding Program. This work used the platforms of the Grenoble Instruct-ERIC Center (ISBG: UMS 3518 CNRS-CEA-UGA-EMBL) with support from FRISBI (ANR-10-INSB-05-02) and GRAL (ANR-10-LABX-49-01) within the Grenoble Partnership for Structural Biology (PSB). The electron microscope facility is supported by the Auvergne Rhône-Alpes Region, the Fondation Recherche Medicale (FRM), the fonds FEDER and the GIS-Infrastrutures en Biologie Sante et Agronomie (IBISA). The funding agencies had no influence on the conduct of this research.

Additionally the authors would like to acknowledge Icosagen (Tartumaa, Estonia) for producing the HIV-1 gag VLPs and providing the cell culture supernatant.

Tables

Table 1

Chromatography media used for preparative chromatography.

Type of chromatography		Name	Referred in the text as	Manufacturer	Column volume (mL)
Anion exchange	Membrane adsorber / hydrogel (porous polyacrylamide)	NatriFlo® HD-Q Recon	Natrix-Membrane	Merck, Darmstadt, Germany	0.8
	Poly-methacrylate based monolithic column	CIMmultus™ QA-8 2 µm	QA-Monolith	BIA Separations, Ajdovščina, Slovenia	8.0
	Methacrylate based polymer grafted beads	Fractogel® EMD TMAE Hicap (M)	Fractogel-TMAE	Merck, Darmstadt, Germany	23.0
Affinity (Heparin)	Agarose based beads	Capto™ Heparin	Capto-Heparin	GE Healthcare, Uppsala, Sweden	22.0
Flow-through	Agarose based core beads	Capto™ Core 700	Capto-Core	GE Healthcare, Uppsala, Sweden	50.4

Table 2

Flow rates, loading volumes and elution gradients of chromatographic experiments.

Run code	Chromatography media	Flow rate (mL/min)	Residence time (min)	Loading volume (mL)	Linear gradient elution
1902-NT	NatriFlo® HD-Q Recon	4.0	0.2	95	5 – 75% B in 75 CV (60 mL)
1904-CH	Capto™ Heparin	4.4	5.0	212	5 – 75% B in 4 CV (88 mL)
1903-CC	Capto™ Core 700	10.0	5.0	350	n.a.
1905-M	CIMmultus™ QA-8 2 µm	8.0	1.0	450	5 – 60% B in 30 CV (240 mL)
1906-CC	Capto™ Core 700	10.0	5.0	450	n.a.
1907-FG	Fractogel® EMD TMAE Hicap (M)	4.6	5.0	400	5 – 60% B in 15 CV (345 mL)

Figure legends

Figure 1:

Cryo-TEM micrographs showing HIV-1 gag VLPs and several host cell derived particles from (a) endonuclease treated and 0.8 µm filtered CHO cell culture supernatant used for the capture and purification experiments with the NatriFlo® HD-Q Recon membrane adsorber or the CIMmultus™ QA-8 monolith; (b) collected flow-through from the pre-processing experiments with Capto™ Core 700, later used for the capture and purification experiments using Fractogel® EMD TMAE Hicap (M) or Capto™ Heparin media.

Figure 2:

Chromatograms of the capture and purification of HIV-1 gag VLPs using (a) NatriFlo® HD-Q Recon membrane adsorber, (b) CIMmultus™ QA-8 monolith, (c) Fractogel® EMD TMAE Hicap (M) column and (d) Capto™ Heparin column. FT: flow-through; W: wash; P: elution peaks; REG/2M: regeneration with 2 M NaCl; CIP: cleaning-in-place.

Figure 3:

SDS-PAGE (a), HIV-1 p24 (b) and H3-histone (c) Western blots and cryo-TEM micrographs (d) of relevant fractions from the capture and purification experiments using NatriFlo® HD-Q Recon membrane adsorber. M: molecular weight marker; FT: flow-through; W: wash; P: elution peaks; REG: regeneration with 2 M NaCl; CIP: cleaning-in-place.

Figure 4:

SDS-PAGE (a), HIV-1 p24 (b) and H3-histone (c) Western blots and cryo-TEM micrographs (d) of relevant fractions from the capture and purification experiments using Capto™ Heparin. M: molecular weight marker; FT: flow-through; W: wash; P: elution peaks; REG: regeneration with 2 M NaCl; CIP: cleaning-in-place.

Figure 5:

Chromatograms of analytical size exclusion chromatography experiments of relevant fractions from the capture and purification experiments using NatriFlo® HD-Q Recon membrane adsorber (1902NT) and Capto™ Heparin (1904CH). Light scattering

signal: 90° angle detector; UV absorbance at 280 nm. L: loading material; P: elution peaks.

Figure 6:

Comparison of recovered doses per litre of cell culture supernatant, total protein per dose and dsDNA per dose in the main product fractions. 1902-NT: NatriFlo® HD-Q Recon membrane adsorber; 1905-M: CIMmultus™ QA-8 monolith; 1907-FG: Fractogel® EMD TMAE Hicap (M); 1904-CH: Capto™ Heparin.

Figures

Figure 1

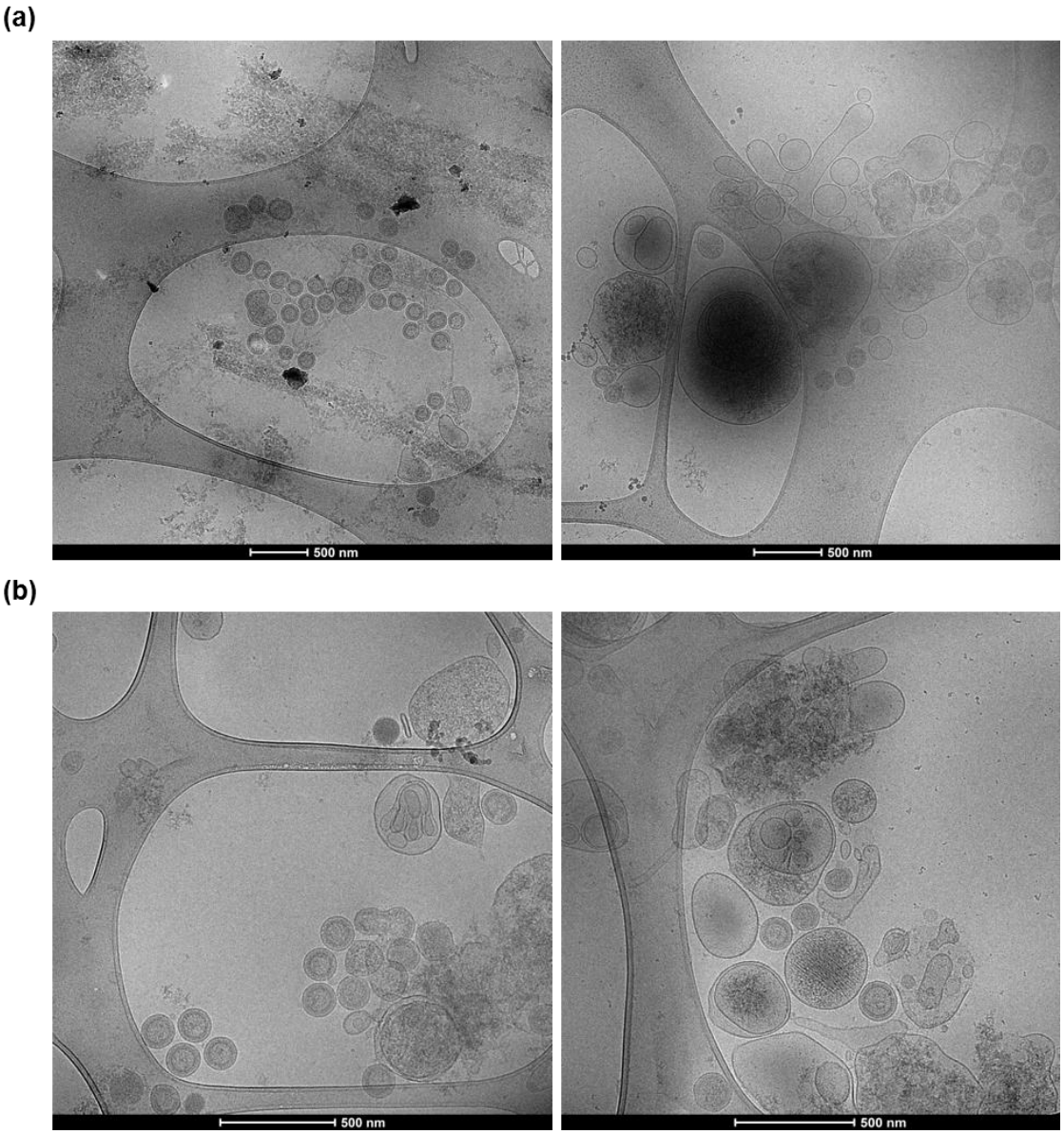

Figure 2

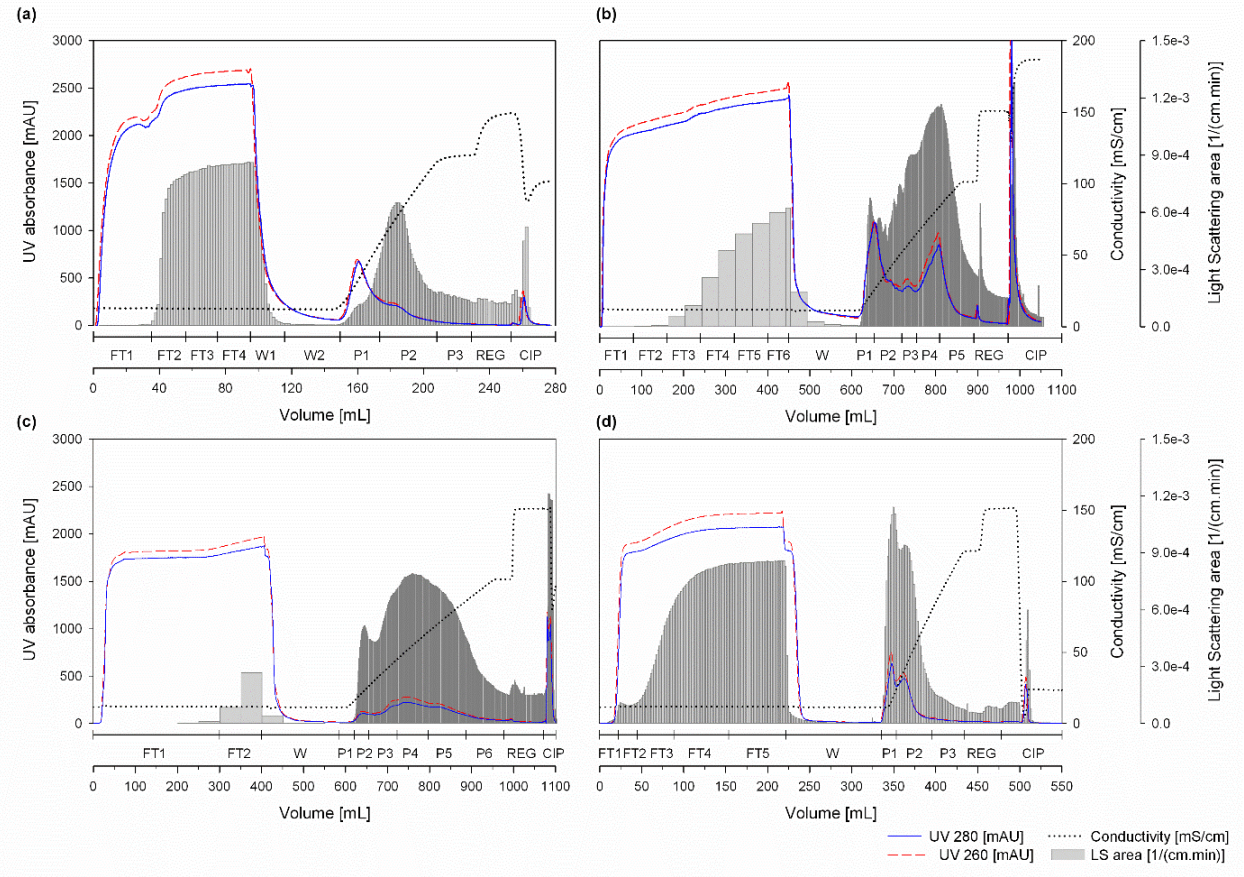
(a)
(b)
(c)
(d)
UV absorbance [mAU]
Conductivity [mS/cm]
Light Scattering area [1/(cm.min)]
Volume [mL]
FT1 FT2 FT3 FT4 W1 W2 P1 P2 P3 REG CIP
FT1 FT2 FT3 FT4 FT5 FT6 W P1 P2 P3 P4 P5 REG CIP
FT1 FT2 W P1 P2 P3 P4 P5 P6 REG CIP
FT1 FT2 FT3 FT4 FT5 W P1 P2 P3 REG CIP
UV 280 [mAU]
UV 260 [mAU]
Conductivity [mS/cm]
LS area [1/(cm.min)]

Figure 3

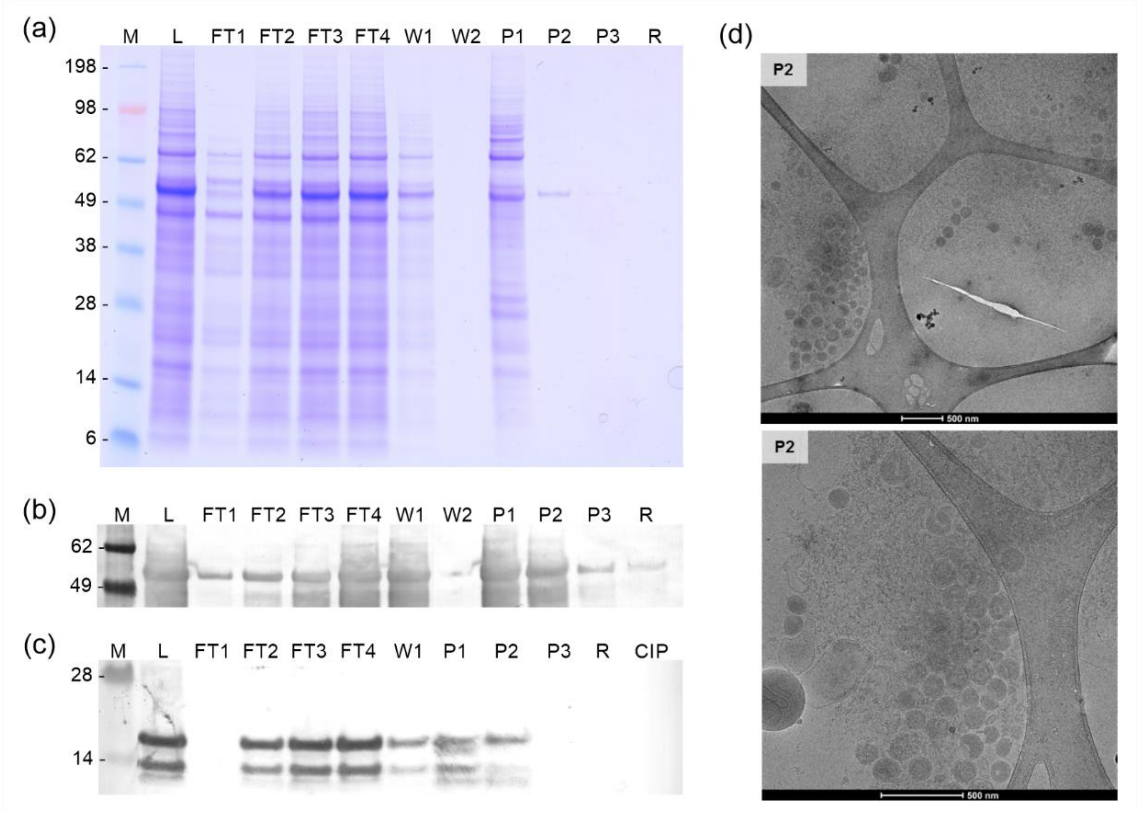
(a)
M L FT1 FT2 FT3 FT4 W1 W2 P1 P2 P3 R
198
98
62
49
38
28
14
6
(b)
M L FT1 FT2 FT3 FT4 W1 W2 P1 P2 P3 R
62
49
(c)
M L FT1 FT2 FT3 FT4 W1 P1 P2 P3 R CIP
28
14
(d)
P2
500 nm
P2
500 nm

Figure 4

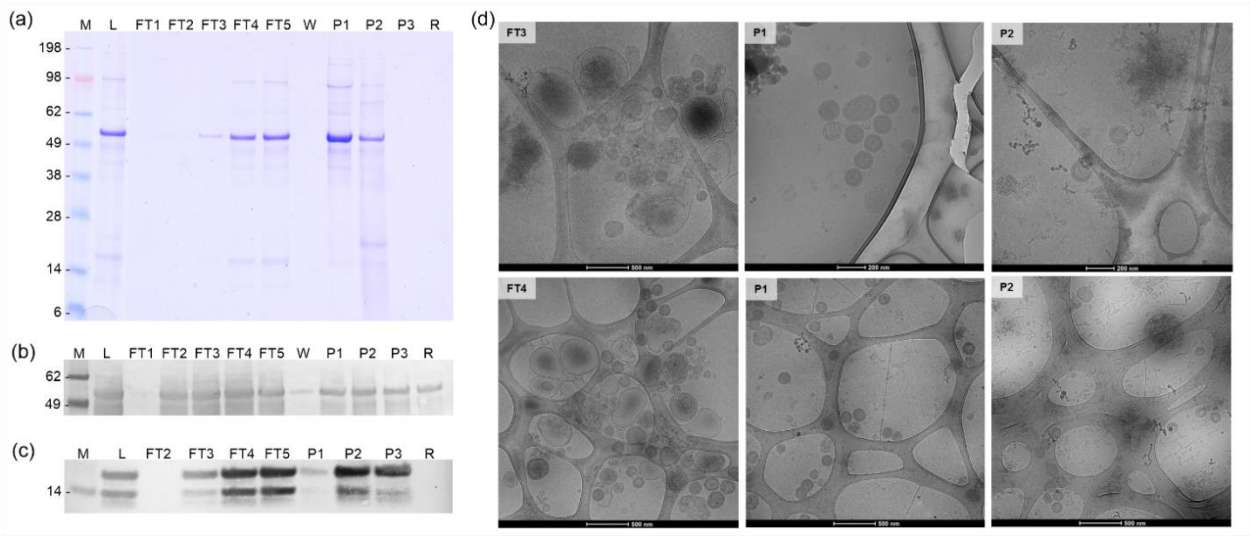
(a)
M L FT1 FT2 FT3 FT4 FT5 W P1 P2 P3 R
198
98
62
49
38
28
14
6
(b)
M L FT1 FT2 FT3 FT4 FT5 W P1 P2 P3 R
62
49
(c)
M L FT2 FT3 FT4 FT5 P1 P2 P3 R
14
(d)
FT3
P1
P2
FT4
P1
P2

Figure 5

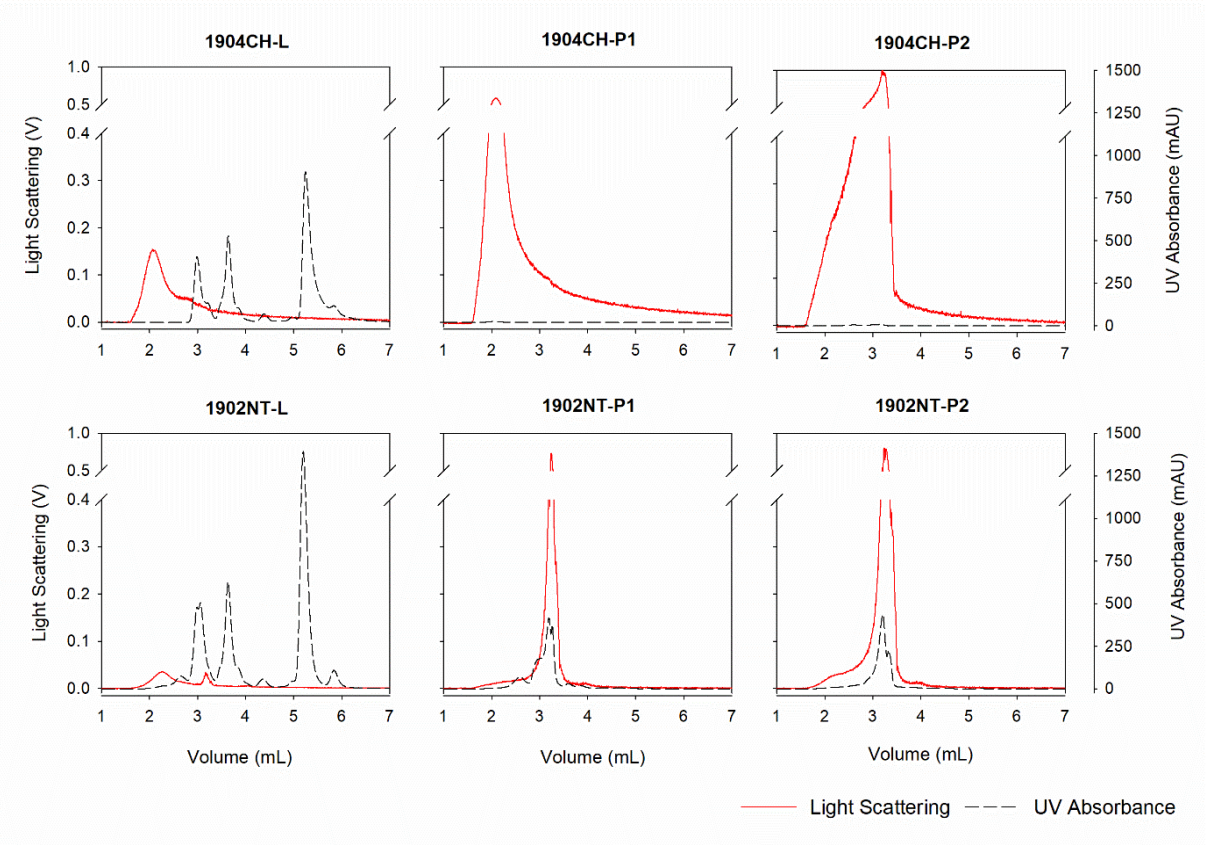
1904CH-L
1904CH-P1
1904CH-P2
1902NT-L
1902NT-P1
1902NT-P2
Light Scattering (V)
UV Absorbance (mAU)
Volume (mL)
Light Scattering
UV Absorbance

Figure 6

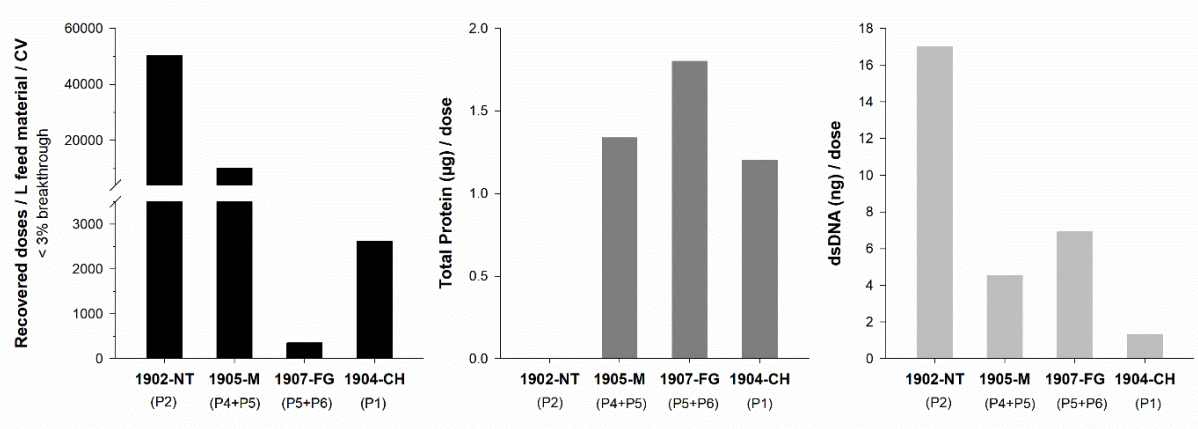
Recovered doses / L feed material / CV
< 3% breakthrough
60000
40000
20000
3000
2000
1000
0
1902-NT (P2)
1905-M (P4+P5)
1907-FG (P5+P6)
1904-CH (P1)
Total Protein (µg) / dose
2.0
1.5
1.0
0.5
0.0
1902-NT (P2)
1905-M (P4+P5)
1907-FG (P5+P6)
1904-CH (P1)
dsDNA (ng) / dose
18
16
14
12
10
8
6
4
2
0
1902-NT (P2)
1905-M (P4+P5)
1907-FG (P5+P6)
1904-CH (P1)

References

[1] S.H. Wong, A. Jassey, J.Y. Wang, W.C. Wang, C.H. Liu, L.T. Lin, Virus-Like Particle Systems for Vaccine Development against Viruses in the Flaviviridae Family, Vaccines, 7 (2019).
[2] L. Cervera, F. Gòdia, F. Tarrés-Freixas, C. Aguilar-Gurrieri, J. Carrillo, J. Blanco, S. Gutiérrez-Granados, Production of HIV-1-based virus-like particles for vaccination: achievements and limits, Applied Microbiology and Biotechnology, 103 (2019) 7367-7384.
[3] M.O. Mohsen, L. Zha, G. Cabral-Miranda, M.F. Bachmann, Major findings and recent advances in virus–like particle (VLP)-based vaccines, Seminars in Immunology, 34 (2017) 123-132.
[4] M. Zhao, M. Vandersluis, J. Stout, U. Haupts, M. Sanders, R. Jacquemart, Affinity chromatography for vaccines manufacturing: Finally ready for prime time?, Vaccine, 37 (2019) 5491-5503.
[5] T. Vicente, A. Roldão, C. Peixoto, M.J.T. Carrondo, P.M. Alves, Large-scale production and purification of VLP-based vaccines, Journal of Invertebrate Pathology, 107 (2011) S42-S48.
[6] P. Nestola, C. Peixoto, R.R.J.S. Silva, P.M. Alves, J.P.B. Mota, M.J.T. Carrondo, Improved virus purification processes for vaccines and gene therapy, Biotechnology and Bioengineering, 112 (2015) 843-857.
[7] L.H. Lua, N.K. Connors, F. Sainsbury, Y.P. Chuan, N. Wibowo, A.P. Middelberg, Bioengineering virus-like particles as vaccines, Biotechnol Bioeng, 111 (2014) 425-440.
[8] P. Pereira Aguilar, T.A. Schneider, V. Wetter, D. Maresch, W.L. Ling, A. Tover, P. Steppert, A. Jungbauer, Polymer-grafted chromatography media for the purification of enveloped virus-like particles, exemplified with HIV-1 gag VLP, Vaccine, 37 (2019) 7070-7080.
[9] P. Steppert, D. Burgstaller, M. Klausberger, E. Berger, P.P. Aguilar, T.A. Schneider, P. Kramberger, A. Tover, K. Nobauer, E. Razzazi-Fazeli, A. Jungbauer, Purification of HIV-1 gag virus-like particles and separation of other extracellular particles, Journal of chromatography. A, 1455 (2016) 93-101.
[10] Z. Kimia, S.N. Hosseini, S.S. Ashraf Talesh, M. Khatami, A. Kavianpour, A. Javidanbardan, A novel application of ion exchange chromatography in recombinant hepatitis B vaccine downstream processing: Improving recombinant HBsAg homogeneity by removing associated aggregates, Journal of Chromatography B, 1113 (2019) 20-29.
[11] L.M. Fischer, M.W. Wolff, U. Reichl, Purification of cell culture-derived influenza A virus via continuous anion exchange chromatography on monoliths, Vaccine, 36 (2018) 3153-3160.
[12] G. Carta, A. Jungbauer, Protein Chromatography: Process Development and Scale-Up, Wiley-VHC Verlag GmbH & Co. KGaA, Weinheim, 2010.
[13] A. Zöchling, R. Hahn, K. Ahrer, J. Urthaler, A. Jungbauer, Mass transfer characteristics of plasmids in monoliths, Journal of separation science, 27 (2004) 819-827.
[14] R. Ghosh, Protein separation using membrane chromatography: opportunities and challenges, Journal of Chromatography A, 952 (2002) 13-27.

[15] M. de las Mercedes Segura, A. Kamen, A. Garnier, Purification of Retrovirus Particles Using Heparin Affinity Chromatography, in: J.M. Le Doux (Ed.) Gene Therapy Protocols: Design and Characterization of Gene Transfer Vectors, Humana Press, Totowa, NJ, 2008, pp. 1-11.
[16] K. Reiter, P.P. Aguilar, V. Wetter, P. Steppert, A. Tover, A. Jungbauer, Separation of virus-like particles and extracellular vesicles by flow-through and heparin affinity chromatography, Journal of chromatography. A, 1588 (2019) 77-84.
[17] N. An, P. Gong, H. Hou, W. Chi, H. Jin, L. Zhao, Q. Tan, X. Tang, F. Wang, H. Jin, R. Zhang, Fabrication of macroporous microspheres with core-shell structure for negative chromatography purification of virus, Journal of Chromatography A, (2019) 460578.
[18] K.T. James, B. Cooney, K. Agopsowicz, M.A. Trevors, A. Mohamed, D. Stoltz, M. Hitt, M. Shmulevitz, Novel High-throughput Approach for Purification of Infectious Virions, Scientific Reports, 6 (2016) 36826.
[19] X. Ding, D. Liu, G. Booth, W. Gao, Y. Lu, Virus-Like Particle Engineering: From Rational Design to Versatile Applications, Biotech J, 13 (2018) 1700324.
[20] E. Nolte-'t Hoen, T. Cremer, R.C. Gallo, L.B. Margolis, Extracellular vesicles and viruses: Are they close relatives?, Proc Natl Acad Sci USA, 113 (2016) 9155-9161.
[21] B. Michen, T. Graule, Isoelectric points of viruses, J Appl Microbiol, 109 (2010) 388-397.
[22] S.B. Carvalho, R.J.S. Silva, M.G. Moleirinho, B. Cunha, A.S. Moreira, A. Xenopoulos, P.M. Alves, M.J.T. Carrondo, C. Peixoto, Membrane-Based Approach for the Downstream Processing of Influenza Virus-Like Particles, Biotechnol J, 14 (2019) e1800570.
[23] M.W. Wolf, U. Reichl, Downstream processing of cell culture-derived virus particles, Expert Rev Vaccines, 10 (2011) 1451-1475.
[24] P. Pereira Aguilar, I. Gonzalez-Dominguez, T.A. Schneider, F. Godia, L. Cervera, A. Jungbauer, At-line multi-angle light scattering detector for faster process development in enveloped virus-like particle purification, Journal of separation science, 42 (2019) 2640-2649.
[25] T. Vicente, C. Peixoto, M.J. Carrondo, P.M. Alves, Purification of recombinant baculoviruses for gene therapy using membrane processes, Gene Ther, 16 (2009) 766-775.
[26] Q. Fang, P. Chen, M. Wang, J. Fang, N. Yang, G. Li, R.M. Xu, Human cytomegalovirus IE1 protein alters the higher-order chromatin structure by targeting the acidic patch of the nucleosome, Elife, 5 (2016).
[27] A. Gansen, J. Langowski, Nucleosome Dynamics Studied by Förster Resonance Energy Transfer, in: D.P. Bazett-Jones, G. Dellaire (Eds.) The Functional Nucleus, Springer International Publishing, Cham, 2016, pp. 329-356.

Supplementary material A

Capture and purification of HIV-1 gag virus-like particles: convective media vs porous beads

Patricia Pereira Aguilar[1,2], Katrin Reiter[2], Viktoria Wetter[2], Petra Steppert[1], Daniel Maresch[1], Wai Li Ling[3], Peter Satzer[2*], Alois Jungbauer[1,2]

[1] Department of Biotechnology, University of Natural Resources and Life Sciences, Vienna, Austria

[2] Austrian Centre of Industrial Biotechnology, Vienna, Austria

[3] Univ. Grenoble Alpes, CEA, CNRS, IBS, F-38000 Grenoble, France

Table SA1

Mass balance of HIV-1 gag capture and purification using a NatriFlo® HD-Q Recon membrane adsorber. Particle, total protein and dsDNA concentrations were measured by NTA, Bradford and Picogreen assays respectively. L: Load; FT: flow-through; W: wash; P: elution peaks; REG: regeneration with 2M NaCl; CIP: cleaning-in-place.

Sample	**Volume**	**Total Protein**				**dsDNA**				**Particles 100-200 nm**			
	(mL)	**(µg/mL)**	**SD**	**(mg)**	**(%)**	**(ng/mL)**	**SD**	**(µg)**	**(%)**	**(part/mL)**	**SD**	**(part)**	**(%)**
L	95.0	817.9	72.8	77.7	100.0	492.7	7.6	46.8	100.0	1.2E+11	1.8E+10	1.2E+13	100.0
FT1	35.2	218.4	13.8	7.7	9.9	41.2	5.8	1.4	3.1	LLOQ	-	-	-
FT2	20.8	536.5	60.0	11.2	14.4	200.2	27.0	4.2	8.9	4.1E+10	6.4E+09	8.6E+11	7.5
FT3	19.2	729.8	103.0	14.0	18.0	335.1	27.6	6.4	13.7	6.8E+10	8.4E+09	1.3E+12	11.3
FT4	19.8	723.3	83.7	14.3	18.4	365.5	36.8	7.2	15.5	7.8E+10	1.1E+10	1.5E+12	13.3
W1	20.8	239.5	31.2	5.0	6.4	89.1	16.7	1.9	4.0	2.3E+10	3.6E+09	4.7E+11	4.1
W2	33.6	<LLOQ	-	-	-	<LLOQ	-	-	-	1.5E+08	1.9E+07	5.0E+09	0.0
P1	24.0	352.3	11.0	8.5	10.9	686.8	102.3	16.5	35.2	1.7E+10	1.0E+09	4.0E+11	3.5
P2	**34.4**	**<LLOQ**	**-**	**-**	**-**	**700.3**	**108.0**	**24.1**	**51.5**	**4.1E+10**	**5.6E+09**	**1.4E+12**	**12.3**
P3	20.8	<LLOQ	-	-	-	95.5	11.2	2.0	4.2	4.1E+09	7.8E+08	8.5E+10	0.7
REG	24.0	<LLOQ	-	-	-	<LLOQ	-	-	-	3.0E+09	5.6E+08	7.3E+10	0.6
CIP	24.0	63.9	0.9	1.5	2.0	<LLOQ	-	-	-	n.d.	-	-	-

Table SA2

Mass balance of HIV-1 gag capture and purification using a CIMmultus™ QA-8 monolith. Particle, total protein and dsDNA concentrations were measured by NTA, Bradford and Picogreen assays respectively. L: Load; FT: flow-through; W: wash; P: elution peaks; REG: regeneration with 2M NaCl; CIP: cleaning-in-place.

Sample	Volume	Total Protein				dsDNA				Particles 100-200 nm			
	(mL)	(µg/mL)	SD	(mg)	(%)	(ng/mL)	SD	(µg)	(%)	(part/mL)	SD	(part)	(%)
L	450.0	768.2	66.5	345.7	100.0	566.8	48.1	255.0	100.0	9.8E+10	1.5E+10	4.4E+13	100.0
FT1	80.0	249.4	21.0	20.0	5.8	53.5	4.4	4.3	1.7	<LLOQ	-	-	-
FT2	80.0	311.7	16.6	24.9	7.2	65.7	8.3	5.3	2.1	3.4E+08	6.5E+07	2.7E+10	0.1
FT3	80.0	359.6	18.9	28.8	8.3	85.0	4.0	6.8	2.7	4.8E+09	8.6E+08	3.8E+11	0.9
FT4	80.0	439.3	28.5	35.1	10.2	140.8	7.8	11.3	4.4	1.9E+10	4.1E+09	1.5E+12	3.5
FT5	80.0	511.1	20.8	40.9	11.8	198.4	15.9	15.9	6.2	3.4E+10	5.0E+09	2.7E+12	6.1
FT6	50.1	535.2	25.8	26.8	7.7	231.7	19.2	11.6	4.5	4.2E+10	6.9E+09	2.1E+12	4.7
W	160.0	<LLOQ	-	-	-	-	-	-	-	1.9E+09	2.8E+08	3.1E+11	0.7
P1	43.2	521.5	27.6	22.5	6.5	80.2	9.5	3.5	1.4	5.9E+10	7.1E+09	2.6E+12	5.8
P2	65.6	582.7	64.9	38.2	11.1	2740.1	123.1	179.8	70.5	7.0E+10	1.5E+10	4.6E+12	10.3
P3	35.2	243.2	21.8	8.6	2.5	3564.0	421.4	125.5	49.2	1.5E+11	2.3E+10	5.1E+12	11.6
P4	**54.4**	**286.3**	**15.5**	**15.6**	**4.5**	**1216.7**	**155.0**	**66.2**	**26.0**	**2.2E+11**	**2.9E+10**	**1.2E+13**	**27.3**
P5	**81.6**	**128.0**	**14.9**	**10.4**	**3.0**	**266.1**	**18.0**	**21.7**	**8.5**	**9.1E+10**	**1.9E+10**	**7.4E+12**	**16.8**
REG	80.0	<LLOQ	-	-	-	36.5	2.8	2.9	1.1	1.1E+10	1.7E+09	8.8E+11	2.0
CIP	80.0	547.8	22.3	43.8	12.7	69.3	7.9	5.5	2.2	n.d.	n.d.	n.d.	n.d.

Table SA3

Mass balance of HIV-1 gag capture and purification using Fractogel® EMD TMAE Hicap (M) (Figure 5). Particle, total protein and dsDNA concentrations were measured by NTA, Bradford and Picogreen assays respectively. L: Load; FT: flow-through; W: wash; P: elution peaks; REG: regeneration with 2M NaCl; CIP: cleaning-in-place.

Sample	**Volume**	**Total Protein**				**dsDNA**				**Particles 100-200 nm**			
	(mL)	**(µg/mL)**	**SD**	**(mg)**	**(%)**	**(ng/mL)**	**SD**	**(µg)**	**(%)**	**(part/mL)**	**SD**	**(part)**	**(%)**
L	400.0	182.2	16.7	72.9	100.0	318.2	23.5	127.3	100.0	8.6E+10	1.0E+10	3.4E+13	100.0
FT1	300.0	<LLOQ	-	-	-	37.3	2.9	11.2	8.8	1.0E+08	1.3E+07	3.1E+10	0.1
FT2	100.0	50.8	15.3	5.1	7.0	110.0	5.2	11.0	8.6	6.1E+08	1.5E+08	6.1E+10	0.2
W	150.0	<LLOQ	-	-	-	<LLOQ	-	-	-	1.3E+08	2.9E+07	2.0E+10	0.1
P1	35.2	<LLOQ	-	-	-	<LLOQ	-	-	-	1.3E+08	2.4E+07	4.6E+09	0.0
P2	35.2	46.0	8.1	1.6	2.2	35.6	7.5	1.3	1.0	9.6E+09	1.1E+09	3.4E+11	1.0
P3	67.2	94.2	24.6	6.3	8.7	315.5	52.1	21.2	16.7	8.9E+08	5.3E+08	6.0E+10	0.2
P4	73.6	121.4	30.3	8.9	12.3	572.5	93.1	42.1	33.1	1.1E+10	2.0E+09	7.9E+11	2.3
P5	**89.6**	**65.8**	**13.0**	**5.9**	**8.1**	**211.8**	**19.5**	**19.0**	**14.9**	**3.2E+10**	**4.1E+09**	**2.8E+12**	**8.3**
P6	**91.0**	**<LLOQ**	**-**	**-**	**0.0**	**39.8**	**3.7**	**3.6**	**2.8**	**4.9E+09**	**1.3E+09**	**4.4E+11**	**1.3**
REG	92.5	<LLOQ	-	-	-	<LLOQ	-	-	-	1.6E+09	4.1E+08	1.4E+11	0.4
CIP	33.6	397.7	30.1	13.4	18.3	121.7	16.2	4.1	3.2	7.5E+10	1.2E+10	2.5E+12	7.4

Table SA4

Mass balance of HIV-1 gag capture and purification using Capto™ Heparin (Figure 7). Particle, total protein and dsDNA concentrations were measured by NTA, Bradford and Picogreen assays respectively. L: Load; FT: flow-through; W: wash; P: elution peaks; REG: regeneration with 2M NaCl; CIP: cleaning-in-place.

*table in separate file

Sample	Volume	Total Protein				dsDNA				Particles 100-200 nm			
	(mL)	(µg/mL)	SD	(mg)	(%)	(ng/mL)	SD	(µg)	(%)	(part/mL)	SD	(part)	(%)
L	212.0	166.3	13.3	35.3	100.0	337.4	17.7	71.5	100.0	7.3E+10	1.2E+10	1.5E+13	100.0
FT1	22.4	LLOQ	-	-	-	LLOQ	-	-	-	3.6E+09	7.3E+08	8.0E+10	0.5
FT2	22.4	LLOQ	-	-	-	51.5	0.7	1.2	1.6	1.4E+10	1.9E+09	3.2E+11	2.1
FT3	43.2	LLOQ	-	-	-	145.3	6.1	6.3	8.8	1.3E+10	1.4E+09	5.8E+11	3.8
FT4	65.6	118.9	9.0	7.8	22.1	287.0	3.3	18.8	26.3	4.0E+10	4.9E+09	2.6E+12	17.2
FT5	68.0	139.2	11.7	9.5	26.8	308.7	5.1	21.0	29.3	6.9E+10	7.2E+09	4.7E+12	30.6
W	113.8	LLOQ	-	-	-	LLOQ	-	-	-	1.5E+08	2.6E+07	1.7E+10	0.1
P1	**17.6**	**176.0**	**21.3**	**3.1**	**8.8**	**194.8**	**29.1**	**3.4**	**4.8**	**1.5E+11**	**9.7E+09**	**2.6E+12**	**16.7**
P2	41.6	141.6	7.0	5.9	16.7	577.1	26.3	24.0	33.6	7.1E+10	1.3E+10	3.0E+12	19.3
P3	38.5	LLOQ	-	-	-	61.1	0.7	0.0	0.0	7.0E+08	2.2E+08	2.7E+10	0.2
REG	44.2	LLOQ	-	-	-	LLOQ	-	-	-	8.6E+08	1.8E+08	3.8E+10	0.2
CIP	38.4	LLOQ	-	-	-	121.6	10.9	4.7	6.5	n.d.	n.d.	n.d.	n.d.

Figure SA1

Comparison of recovered doses per millilitre of cell culture supernatant, total protein per dose and dsDNA per dose in the elution fractions from 1902-NT (NatriFlo® HD-Q Recon membrane adsorber).

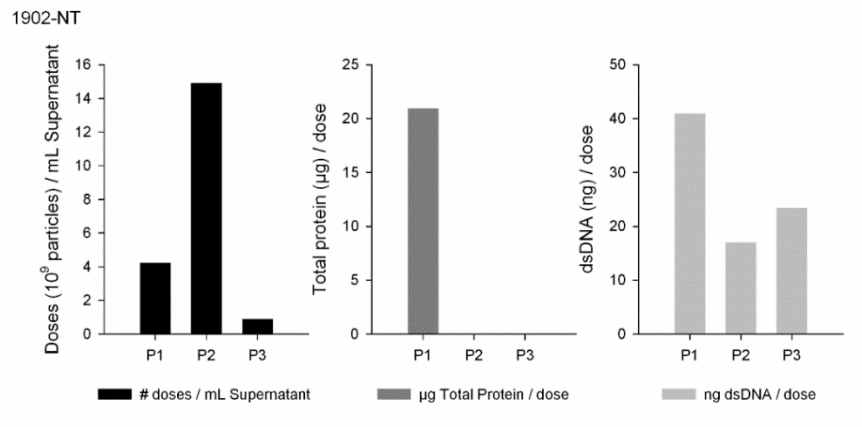

Figure SA2

SDS-PAGE (a), HIV-1 p24 (b) and H3-histone (c) Western blots and cryo-TEM micrographs (d) of relevant fractions from the capture and purification experiments using CIMmultus™ QA-8 monolith. M: molecular weight marker; FT: flow-through; W: wash; P: elution peaks; REG: regeneration with 2M NaCl; CIP: cleaning-in-place.

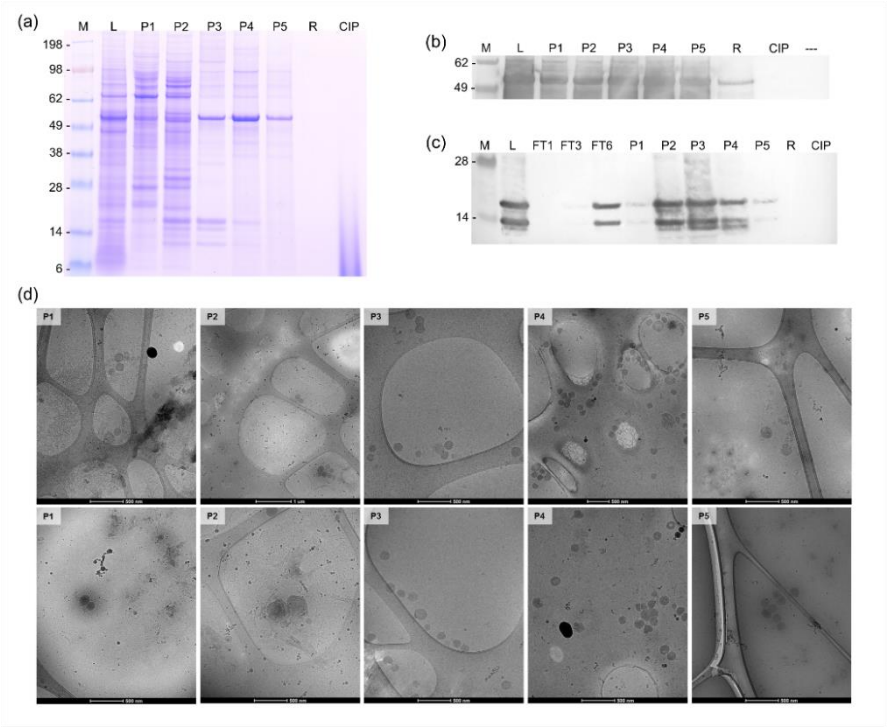

Figure SA3

Comparison of recovered doses per millilitre of cell culture supernatant, total protein per dose and dsDNA per dose in the elution fractions from 1905-M (CIMmultus™ QA-8 monolith).

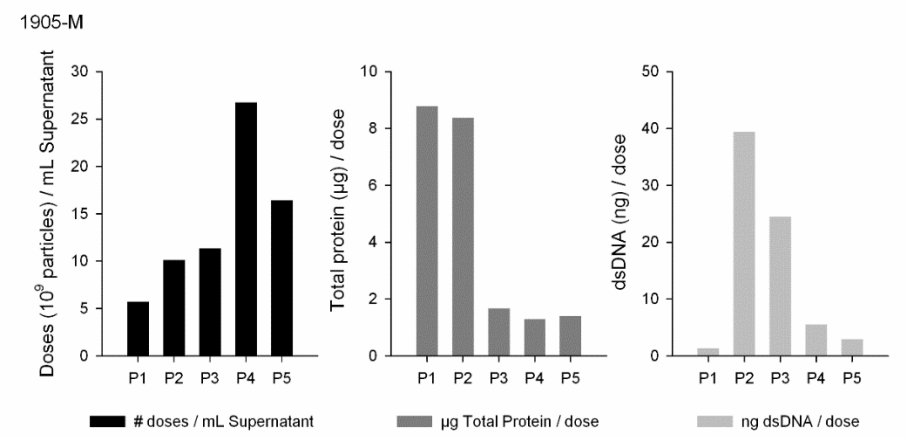

Figure SA4

SDS-PAGE (a), HIV-1 p24 (b) and H3-histone (c) Western blots and cryo-TEM micrographs (d) of relevant fractions from the capture and purification experiments using Fractogel® EMD TMAE Hicap (M). M: molecular weight marker; FT: flow-through; W: wash; P: elution peaks; REG: regeneration with 2M NaCl; CIP: cleaning-in-place.

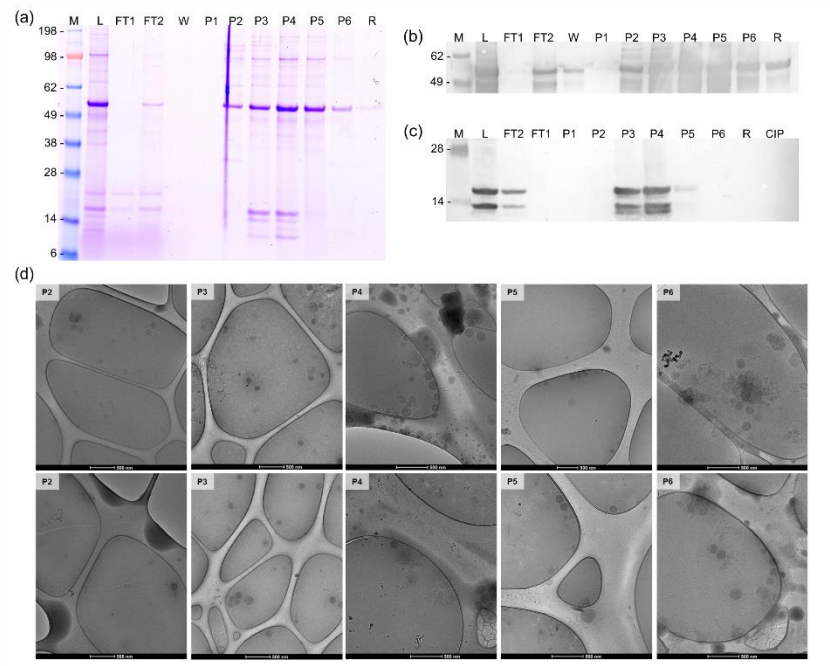

Figure SA5

Comparison of recovered doses per millilitre of cell culture supernatant, total protein per dose and dsDNA per dose in the elution fractions from 1907-FG (Fractogel® EMD TMAE Hicap (M)).

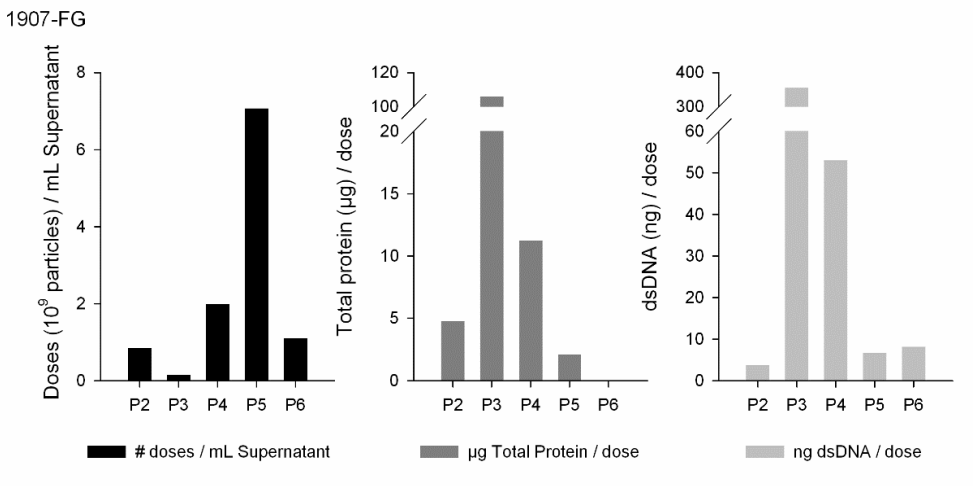

Figure SA6

Comparison of recovered doses per millilitre of cell culture supernatant, total protein per dose and dsDNA per dose in the elution fractions from 1904-CH (Capto™ Heparin).

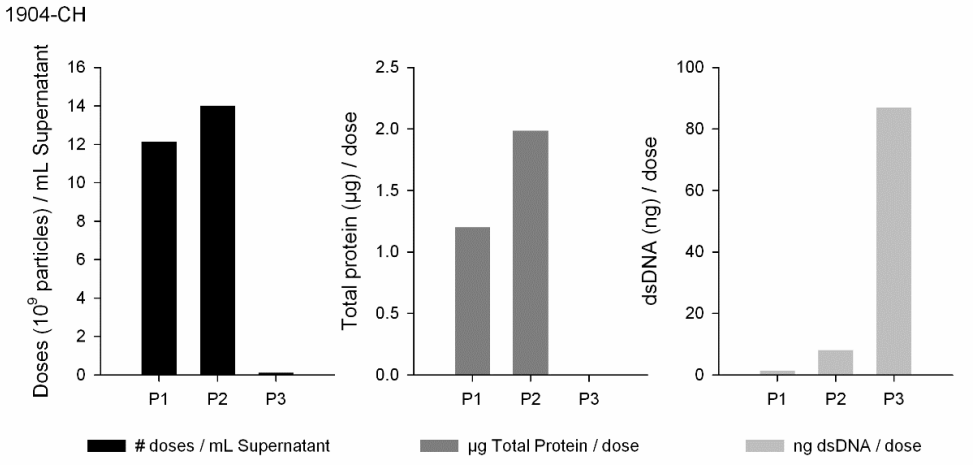

Figure SA7

Representative chromatogram of pre-processing step using Capto™ Core 700 in flow-through mode. Loading material: endonuclease treated and 0.8 µm filtered CHO cell culture supernatant. FT: flow-through; W: wash; P: elution peak; CIP: cleaning-in-place with 30% isopropanol in 1 M NaOH.

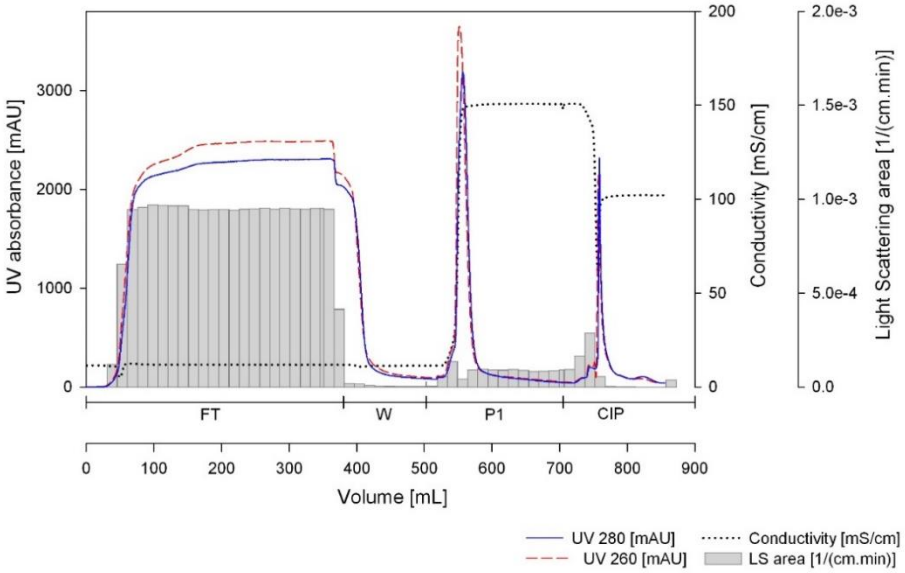

Figure SA8

Analytical results of the flow-through fraction (FT) from the pre-processing run represented in Figure S1. (a) Negative staining TEM, (b) SDS-PAGE, (c) particle recovery measured by NTA, (d) total protein content measured by Bradford assay and (e) dsDNA content measured by Picogreen assay.

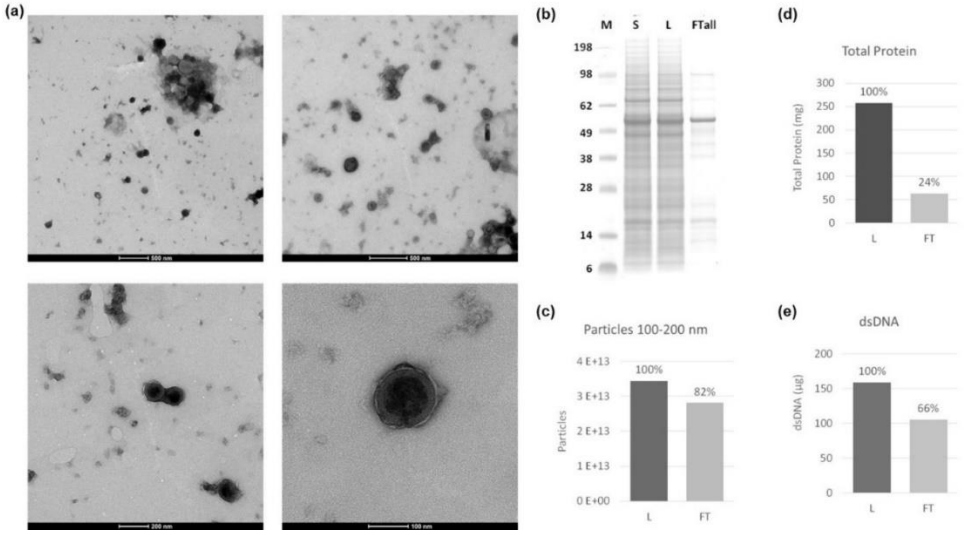

Figure SA9

Chromatograms of analytical size exclusion chromatography of feed material and elution fractions of NatriFlo® HD-Q Recon membrane adsorber (1902NT), CIMmultus™ QA-8 monolith (1905M), Fractogel® EMD TMAE Hicap (M) (1907FG) and Capto™ Heparin (1904CH). Light scattering signal: 90° angle detector; UV absorbance at 280 nm. L: loading material; P: elution peaks.

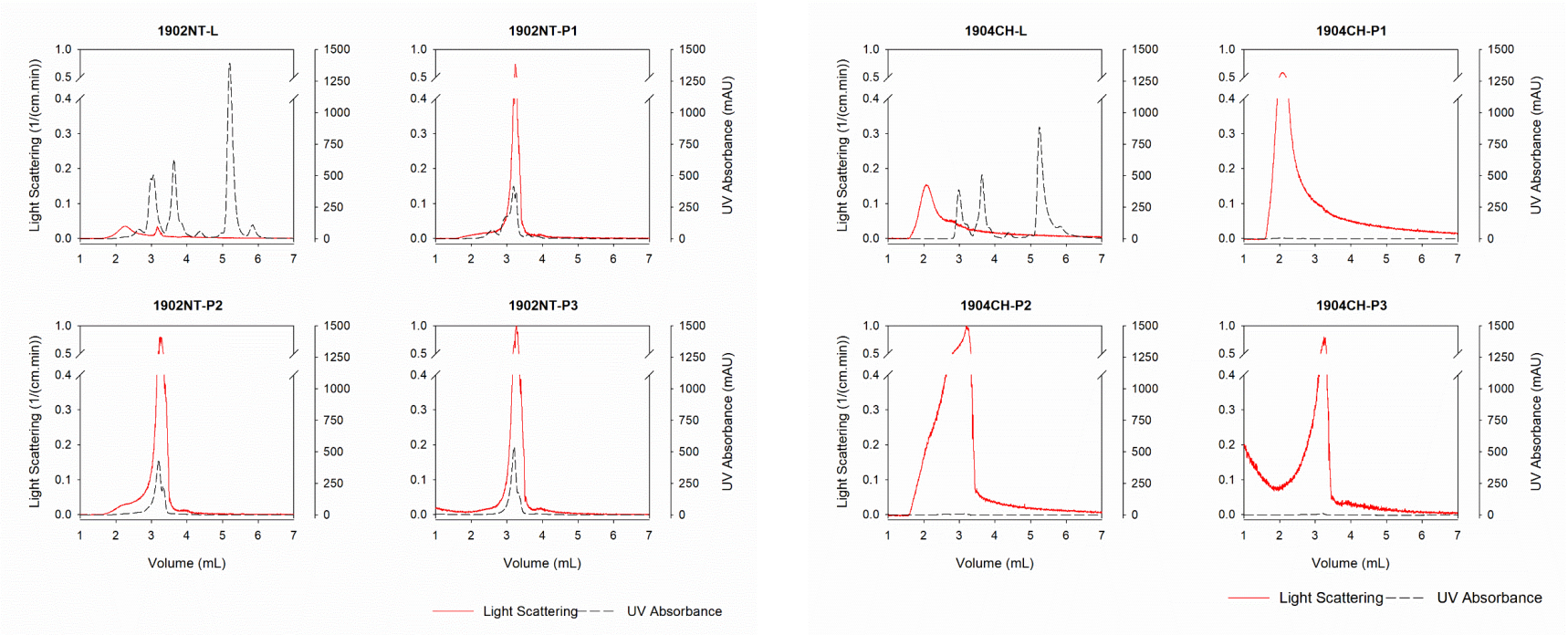

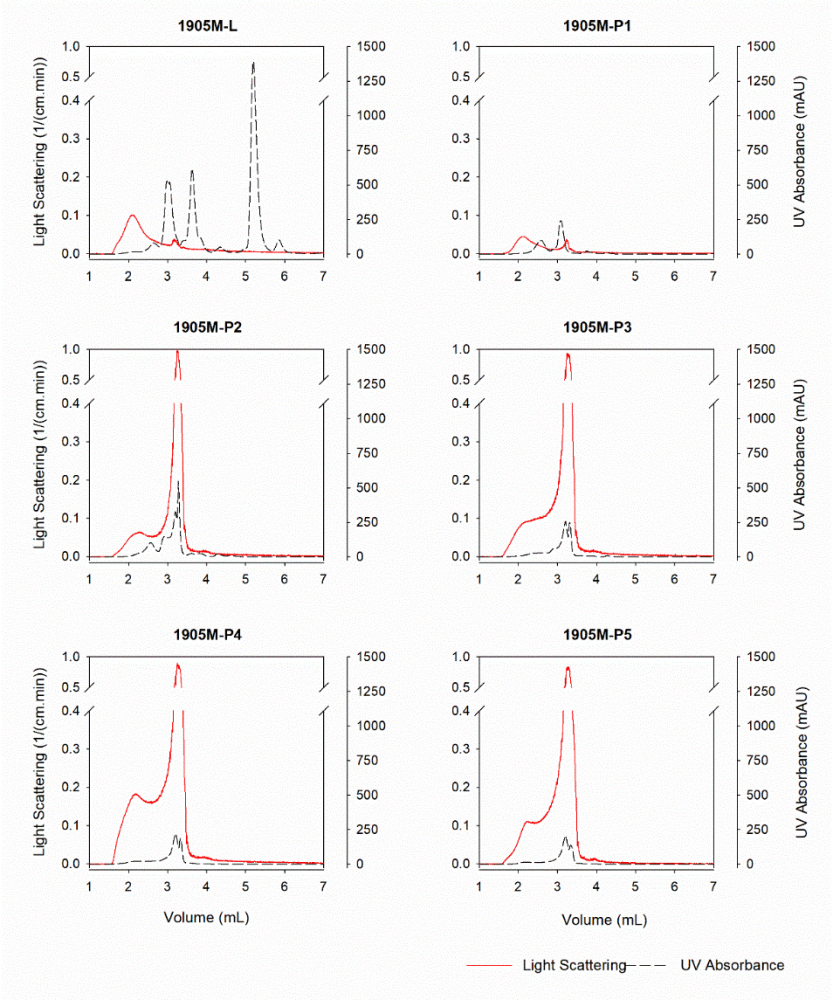
1905M-L
1905M-P1
1905M-P2
1905M-P3
1905M-P4
1905M-P5
Light Scattering (1/(cm.min))
UV Absorbance (mAU)
Volume (mL)
Light Scattering
UV Absorbance

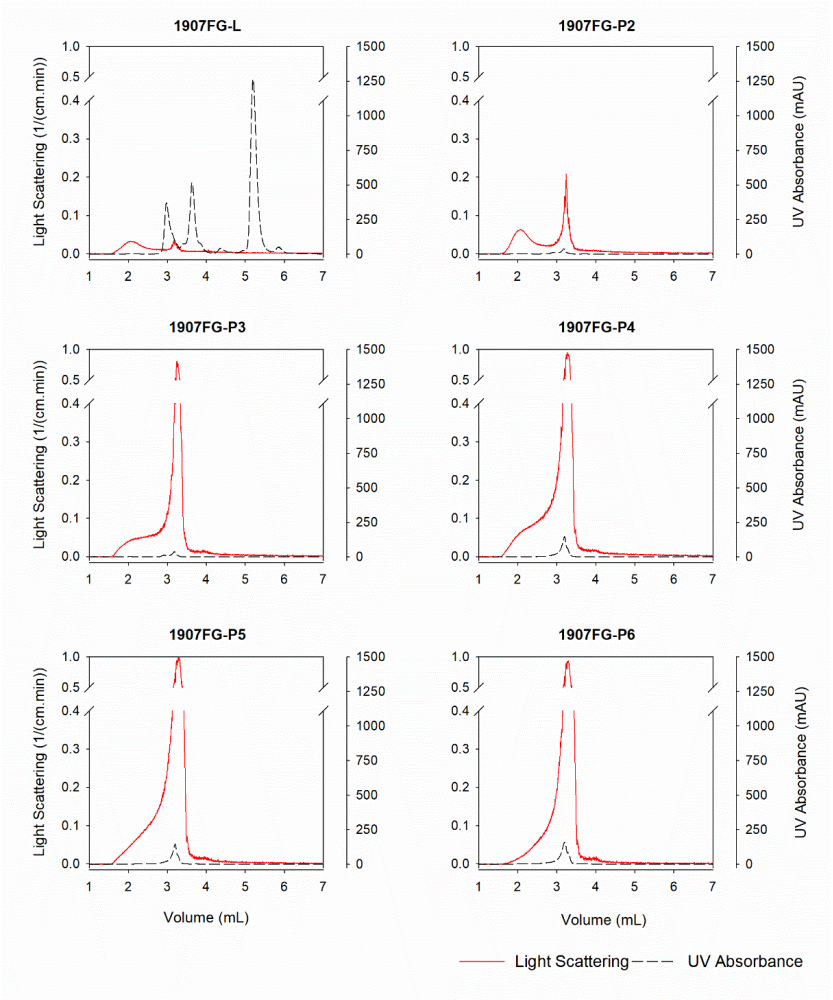
1907FG-L
1907FG-P2
1907FG-P3
1907FG-P4
1907FG-P5
1907FG-P6
Light Scattering (1/(cm.min))
UV Absorbance (mAU)
Volume (mL)
Light Scattering
UV Absorbance

PUBLICATION IV

Journal of Chromatography A, 1455 (2016) 93–101

Contents lists available at ScienceDirect

Journal of Chromatography A

journal homepage: www.elsevier.com/locate/chroma

Purification of HIV-1 gag virus-like particles and separation of other extracellular particles

Petra Steppert[a], Daniel Burgstaller[a], Miriam Klausberger[a], Eva Berger[b], Patricia Pereira Aguilar[a], Tobias A. Schneider[b], Petra Kramberger[c], Andres Tover[d], Katharina Nöbauer[e], Ebrahim Razzazi-Fazeli[e], Alois Jungbauer[a,b,*]

[a] Department of Biotechnology, University of Natural Resources and Life Sciences Vienna, Vienna, Austria
[b] ACIB GmbH, Vienna, Austria
[c] BIA Separations d.o.o., Ajdovščina, Slovenia
[d] Icosagen AS, Tartumaa, Estonia
[e] VetCore Facility for Research, University of Veterinary Medicine Vienna, Vienna, Austria

ARTICLE INFO

Article history:
Received 2 December 2015
Received in revised form 4 May 2016
Accepted 13 May 2016
Available online 18 May 2016

Keywords:
Vaccines
Chromatography
Extracellular particles
Host cell DNA
Host cell protein
Density gradient centrifugation

ABSTRACT

Enveloped virus-like particles (VLPs) are increasingly used as vaccines and immunotherapeutics. Frequently, very time consuming density gradient centrifugation techniques are used for purification of VLPs. However, the progress towards optimized large-scale VLP production increased the demand for fast, cost efficient and scale able purification processes. We developed a chromatographic procedure for purification of HIV-1 gag VLPs produced in CHO cells. The clarified and filtered cell culture supernatant was directly processed on an anion-exchange monolith. The majority of host cell impurities passed through the column, whereas the VLPs were eluted by a linear or step salt gradient; the major fraction of DNA was eluted prior to VLPs and particles in the range of 100–200 nm in diameter could be separated into two fractions. The earlier eluted fraction was enriched with extracellular particles associated to exosomes or microvesicles, whereas the late eluting fractions contained the majority of most pure HIV-1 gag VLPs. DNA content in the exosome-containing fraction could not be reduced by Benzonase treatment which indicated that the DNA was encapsulated. Many exosome markers were identified by proteomic analysis in this fraction. We present a laboratory method that could serve as a basis for rapid downstream processing of enveloped VLPs. Up to 2000 doses, each containing 1×10^9 particles, could be processed with a 1 mL monolith within 47 min. The method compared to density gradient centrifugation has a 220-fold improvement in productivity.

© 2016 The Author(s). Published by Elsevier B.V. This is an open access article under the CC BY-NC-ND license (http://creativecommons.org/licenses/by-nc-nd/4.0/).

1. Introduction

Enveloped virus-like particles (VLPs) are promising candidates for vaccination, gene therapy, and cancer immunotherapy [1–7]. Purification of VLPs is in its infancy and used methods often have been adopted from virus purification procedures, mostly density gradient centrifugation and combinations of filtration and flow through chromatography [8–11]. It is often overlooked that enveloped VLPs and viruses are secreted together with extracellular vesicles such as microvesicles and exosomes [12,13]. Such mixtures are difficult to separate and often the presence of microvesicles in VLP and virus preparations are ignored and their biological relevance is not understood [14,15]. Monoliths are well suited for purification of large bio-particles, such as plasmid DNA, viruses and VLPs [16–22]. For plasmids, large scale processes have already been established [23]. Pretreatment of the feedstock before purification by such methods as multiple depth and membrane filtration steps and polishing of viruses and VLPs often accounts for not only reduction in yield but also contributes to the costs of the process [8,24]. Thus, it is desirable to directly load the culture supernatant onto the chromatography column with minimum efforts of pretreatment.

In this study we focus on HIV-1 gag VLPs as a model system. These VLPs, using the structural protein gag of HIV-1, are produced in CHO cells. Such an expression system secretes the VLPs into the supernatant and high productivity can be obtained [25–28]. Thus such a system would be suited for production of pandemic vaccines or requirements for treatment of large patient population [3].

* Correspondence to: Muthgasse 18, 1190 Vienna, Austria.
E-mail address: alois.jungbauer@boku.ac.at (A. Jungbauer).

http://dx.doi.org/10.1016/j.chroma.2016.05.053
0021-9673/© 2016 The Author(s). Published by Elsevier B.V. This is an open access article under the CC BY-NC-ND license (http://creativecommons.org/licenses/by-nc-nd/4.0/).

However, the studied system must be strictly considered as a model system.

The HIV-1 gag VLPs are composed of a lipid bilayer, which originate from the host cell, in our case the CHO cells. The gag polyprotein drives the self-assembly of spherical particles, buttressing the lipid bilayer, and once assembled, bud from the cell membrane [29]. The biophysical properties which are important for purification development are not exactly known. The physical size is in the range of 100–150 nm in diameter [29], with density around 1.18 g/cm^3 [10]. It has been assumed that enveloped viruses have multiple positive and negative charges distributed on the surface [30]. This is the most important property to design an ion-exchange chromatography step either in flow through or binding and eluting mode. The processes for such particles must be developed in an empirical manner, because their properties are not fully known.

A further complication of purification of VLPs is the potential contamination of the feedstock with extracellular vesicles such as microvesicles and exosomes [12,13]. These particles usually range from 40 to 1000 nm in diameter although a lot of these particles have a size between 40 and 100 nm which is very close to enveloped VLPs [13]. The large vesicles are easily separated during the clarification steps by centrifugation or filtration while the vesicles of the same size as VLPs have to be separated during a chromatographic purification step based on the particles structure. Studies with HIV viruses have shown that these vesicles carry similar membrane proteins [15]. Budding processes for the virus and the extracellular vesicles are similar, or at least have been shown to be for HIV [12,15]. It is not clear to what extent CHO budding of VLPs and extracellular vesicles follow the same route. It is well know that CHO cells secrete such vesicles, because they have been considered for use as a measure of the quality of the cell [31]. A mixture of VLPs or viruses and extracellular vehicles is extremely difficult to separate [14]. In addition, the analysis and discrimination of VLPs from extracellular vesicles is very challenging since they are similar in size and are in a large part composed of the same structural proteins. Usually, analytical methods for characterization of VLPs are based on identification of structural proteins and evaluation of the particle number and particle size [32]. Evaluation of the particle number and size can be done by nanoparticle tracking analysis (NTA). However, this method cannot distinguish between different particle structures and is associated with a variability of measurements up to 15–20%, which is still in the acceptable error range for accuracy of bioanalytical methods recommended by the FDA [33,34]. TEM is used as an orthogonal method for NTA, to corroborate the particle size and as a visual proof for particle formation but does not provide any information about the particle composition. Biochemical methods such as Western blotting and mass spectrometry (MS) are used for detection of structural proteins and peptides and suggests information about the particle composition, but also detect unstructured protein impurities that are not assembled into particles. Impurities, such as dsDNA, frequently packaged in extracellular vesicles [35] can be detected by fluorescent nucleic acid stains in combination with endonuclease treatment procedures. Only the combination of multiple complementary analytical methods can gather conclusions about the particle structure [36].

VLP separation can be managed by a combination of flow through chromatography, membrane chromatography, micro-/ultrafiltration steps, and size exclusion chromatography [8,37,38]. We have focused on monoliths with channels of 2 μm in diameter. In previous work, we were able to purify baculovirus by monoliths. These rod-shape infective viruses have a completely different physical shape compared to the enveloped VLPs. For VLPs, we assumed a homogenous distribution of charged membrane proteins on the surface whereas baculoviruses have a head region that accumulates virus protein gp64 and is distinct from the tail [17].

We aimed to directly load the cell free culture supernatant on a monolith column and the exclusive pretreatment, after cell and cell debris removal by centrifugation, should consist only of 0.8 μm membrane filtration. Optional endonuclease pretreatment was tested to reduce the dsDNA content before chromatography. Binding and elution conditions must be found which allow removal of host cell impurities and concentrate VLPs to a particle number which would be equivalent to a vaccine. The pretreated culture supernatant was loaded and respective gradients were applied for elution. A combination of multiple complementary methods (NTA, TEM, Western blotting) were applied to detect VLPs. For discrimination between VLPs and other extracellular particles proteomic analysis was performed and potentially encapsulated dsDNA was detected after endonuclease treatment. We also wanted to benchmark our process with the most common method, density ultracentrifugation.

2. Material and methods

2.1. Chemicals

All chemicals were purchased from Merck (Darmstadt, Germany) or Sigma Aldrich (St. Louis, MO, USA).

2.2. Expression of HIV-1 gag VLPs

For production of VLPs based on HIV-1 gag protein, a pQMCF expression vector expressing HIV-1 gag protein under the control of the CMV promoter was constructed. For production CHOEBNALT85 cell line (Icosagen, Tartumaa, Estonia) grown at 37 °C was used. Cells (6×10^6) were transfected by electroporation with 1 μg of VLP expression vector pQMCF-HIVgag. Forty eight h after transfection 700 μg/mL of G418 Geneticin® (Gibco/Thermo Fischer, Waltham, MA) was added to the selected plasmid-containing cell population. After selection, on day 10, the temperature of the cell culture was shifted to 30 °C and fed with CHO CD Efficient FeedB (Thermo Fisher Scientific, Waltham, MA USA) for 9 days. Cell culture media was a mixture of CDCHO and 293SFM (Thermo Fisher Scientific, Waltham, MA USA) including HT Supplement and Glutamax (Thermo Fisher Scientific, Waltham, MA USA). Production of HIV-1 gag VLPs was confirmed by Western blot analysis detecting HIV-1 p24. After production of the HIV-1 gag VLPs, cells were removed by centrifugation (1000*g*, 30 min) and 0.01% NaN_3, was added.

2.3. Density gradient centrifugation

The HIV-1 gag VLPs were pelleted from the VLP containing cell culture supernatant through a 20% (w/v) sucrose cushion at 77,100*g* for 2.5 h at 4 °C by a Beckmann L8–80 M ultracentrifuge using a SW41Ti rotor (Brea, CA, USA). The VLP-containing pellet was resuspended in PBS buffer and loaded onto a 20% – 60% (w/v) sucrose gradient and centrifuged at 93,500*g* for 17.5 h at 4 °C. The gradient was fractionated from the top in 300 μL aliquots at 22 °C. Density was determined gravimetrically (Sartorius, Göttingen, Germany) and absorbance at 280 nm was measured by NanoDropND-1000 (Thermo Fisher Scientific, Waltham, MA USA) at 22 °C.

2.4. Chromatographic experiments

2.4.1. Chromatographic equipment

Preliminary chromatographic experiments were conducted on an Agilent Series 1100 System (Agilent, Waldbronn, Germany) consisting of a well plate automatic liquid sampler (WP ALS) for injection, a degasser, a quaternary pump, and a diode array detector (DAD). The ChemStation for LC 3D systems (Rev. B. 04.03) software was used for data acquisition and control. UV

absorbances were monitored at 280 and 260 nm simultaneously. Elution fractions were collected manually and pooled according to the chromatograms.

Chromatographic experiments on preparative scale were performed on an ÄKTA explorer 100 equipped with a P-960 sample-pump and fraction collector (Frac-950) (GE Healthcare, Uppsala, Sweden). For control and data acquisition Unicorn software 10.1 was used. Conductivity, pH, and absorbance at 280 and 260 nm were monitored simultaneously. Elution fractions of 1 mL were collected by fraction collector and pooled according to the chromatograms.

2.4.2. Preliminary chromatographic experiments

Preliminary chromatographic experiments were performed on an analytical scale using quaternary amine (QA), diethylamine (DEAE) and sulfate (SO3) CIMac™ analytical monoliths (V = 0.1 mL) (BIA Separations, Ajdovščina, Slovenia). For anion-exchange chromatography, 20 mM Tris and 50 mM HEPES buffer systems were tested over the pH range from 7.2 to 8.5 and for cation-exchange chromatography 20 mM phosphate buffer was used over the pH range from 6.0 to 8.0. Optional 150 mM NaCl was added to equilibration buffers (mobile phase A) for anion-exchange chromatography and all elution buffers (mobile phase B) contained 2 M NaCl. Analytical monoliths were equilibrated for 15 bed volumes with appropriate equilibration buffer. Aliquots (100 μL to 500 μL) of HIV-1 gag VLP standard material obtained by density gradient centrifugation or clarified and 0.8 μm filtered (Millex AA filter, Millipore Bedford, MA, USA) CHO supernatant were loaded onto the monolith and eluted by a linear gradient 0–50% B in 50 bed volumes followed by a regeneration step to 100% B for 30 bed volumes and sanitization with 1 M NaOH for 30 bed volumes. Flow rate during chromatography was 1 mL/min.

2.4.3. Preparative chromatographic purification of HIV-1 gag VLPs

Preparative purifications of HIV-1 gag VLPs from clarified and 0.8 μm filtered (Millex AA filter, Millipore Bedford, MA, USA) culture supernatant were conducted by anion-exchange with the 1 mL radial flow monoliths CIMmultus QA or CIMmultus DEAE (BIA Separations, Ajdovščina, Slovenia). Equilibration buffer (mobile phase A) was 50 mM HEPES, 100 mM NaCl pH 7.2 for linear gradient elution and 50 mM HEPES, 350 mM NaCl pH 7.2 for stepwise elution. A wash step of 20 bed volumes was introduced after loading and before linear gradient elution. For step gradient elution the wash step length was reduced to 15 bed volumes. Elution and regeneration was performed with 50 mM HEPES, 2 M NaCl pH 7.2 (mobile phase B). Linear gradients were conducted from 0 to 50% B in 50 bed volumes and stepwise elution was achieved by 0–25–45% B steps with a hold of 15 bed volumes each. After regeneration, sanitization was performed with 1 M NaOH. Equilibration was performed for 15 bed volumes, regeneration for 15 bed volumes and sanitization for 60 bed volumes. Flow rate during development of the purification process was 1 mL/min. After optimization of purification procedure the flow rate was adjusted to 5 mL/min.

2.5. Sodium dodecyl sulfate-polyacrylamide gel electrophoresis (SDS-PAGE) and Western blot analysis

NuPAGE Bis/Tris gels 4–12% (Invitrogen, Carlsbad, CA, USA) and MES-SDS running conditions were used to perform electrophoresis under reducing conditions in accordance to manufacturer's instructions. If required, samples were diluted in deionized water to obtain similar protein concentrations. SeeBlue® Plus2 Pre-stained Protein Standard (Invitrogen, Carlsbad, CA, USA) was used as the protein molecular weight ladder. Protein bands were stained by Coomassie Brilliant Blue G-250 based EZBlue™ Gel Staining Reagent (Sigma Aldrich, St. Louis, MO, USA). After SDS-PAGE, proteins were electroblotted onto a nitrocellulose membrane (Whatman, Dassel, Germany). The membrane was blocked with 3% BSA in PBS-T (0.1% w/v Tween-20 in PBS) for 2 h. Detection was performed by incubation of primary mouse monoclonal antibody against HIV-1 p24 (Icosagen AS, Tartumaa, Estonia), diluted 1:1000 in PBS-T containing 1% BSA for 2 h, followed by secondary antibody incubation with anti-mouse IgG conjugated with alkaline phosphatase (Sigma Aldrich, St. Louis, MO, USA), diluted 1:1000 in PBS-T with 1% BSA for 1 h. Visualization was carried out by Lumi Phos™ (Thermo Fisher Scientific, Waltham, MA USA) on Lumi Imager (Boehringer Ingelheim, Ingelheim, Germany).

2.6. Protein concentration and dsDNA content

Protein concentration was determined by Bradford assay using Coomassie blue G-250-based protein dye reagent (Bio-Rad Laboratories, Hercules, CA, USA). The calibration curve was obtained by bovine serum albumin (BSA) standards diluted in TE-Buffer. DNA content was determined by Quant-iT™ PicoGreen® dsDNA kit (Life technologies, Waltham, MA, USA). Protein and DNA assays were performed according to the particular manufacturer's instructions in 96-well plate format. Signals were measured by Genius Pro plate reader (Tecan, Männedorf, Switzerland).

2.7. Nanoparticle tracking analysis (NTA)

For determination of particle concentration NTA measurements were performed by a NanoSight LM-10 (Malvern Instruments Ltd., Worcestershire, UK) equipped with a blue laser (405 nm). Samples were serially diluted in particle-free water to reach a suitable particle concentration (60–100 particles per video frame) for analysis. Videos (60 s) of three dilution steps for each sample were captured at room temperature. The videos were analysed and evaluated by NTA 2.0 software. Camera level was adjusted manually and optimized analysis parameters were kept constant during all measurements. Particle number was evaluated for particles with diameters between 100 and 200 nm.

2.8. Mass spectrometric analysis of proteins

Bands of interest were excised manually from Coomassie blue stained 1D-gels. After washing and destaining [39] spots were reduced with dithiothreitol and alkylated with iodoacetamide [40]. In-gel digestion was performed with trypsin (Trypsin Gold) with a final trypsin concentration of 20 ng/μl in 50 mM aqueous ammonium bicarbonate and 5 mM $CaCl_2$. Digest proceeded for 8 h at 37 °C [41]. Afterwards, peptides were extracted with three changes of 30 μL of 5% TFA in 50% aqueous CH_3CN supported by ultrasonication for 10 min per change. Extracted peptides were dried down in a vacuum concentrator (Eppendorf AG, Hamburg, Germany). Desalted peptides were dissolved in 10 μL 0.1% TFA and 1 μL was injected into the nano-HPLC Ultimate 3000 RSLC system (Thermo Fisher Scientific, Waltham, MA, USA). Sample pre-concentration and desalting was accomplished with a 5 mm Acclaim PepMap μ-Precolumn (300 μm inner diameter, 5 μm particle size, and 100 Å pore size) (Thermo Fisher Scientific, Waltham, MA, USA). Separation was performed on a 25 cm Acclaim PepMap C18 column (75 μm inner diameter, 3 μm particle size, and 100 Å pore size) with a flow rate of 300 nl/min. The gradient started with 4% B (80% ACN with 0.1% formic acid) and increased to 35% B in 90 min. It was followed by a washing step with 90% B. Mobile Phase A consisted of mQ H_2O with 0.1% formic acid. For mass spectrometric analysis a Triple TOF 6600 instrument (Sciex, Framingham, MA, USA) was used. MS1 spectra were collected in the range 400–1500 *m/z*. The 20 most intense precursors with charge

state 2–4 which exceeded 100 counts per second were selected for fragmentation, and MS2 spectra were collected in the range 100–1800 m/z for 150 ms. The precursor ions were dynamically excluded from reselection for 10 s. The nano-HPLC system was regulated by Chromeleon 8.8 (Thermo Fisher Scientific, Waltham, MA, USA) and the MS by Analyst Software 1.7. Processed spectra were searched via the software Protein Pilot (Sciex, Framingham, MA, USA) in a UniProt database containing all proteins from *Cricetulus griseus* (identifier: 10029) as well as all proteins from Human immunodeficiency virus 1 (identifier: 11676) using the following search parameters: Global modification: Cysteine alkylation with iodoacetamide, Species: *Mus musculus*, Search effort: rapid, FDR analysis: Yes.

Proteins with more than 2 matching peptides at 95% confidence were selected.

2.9. Endonuclease treatment

Clarified and filtered cell culture supernatant was treated for 1 h with Benzonase purity grade II (Merck KgA, Darmstadt Germany) at a final concentration of 150 U/mL at 22 °C before 0.8 μm filtration and chromatographic purification. For all analytical purposes, samples were diluted in Benzonase buffer (1 M Tris-HCl, 30 mM $MgCl_2$, pH 8.0) before being treated with Benzonase at a final concentration of 150 U/mL at 37 °C for 1 h. For analytical purposes digestion was stopped by addition of 50 mM EDTA.

2.10. Transmission electron microscopy (TEM)

The samples were incubated for 1 min on 400-mesh copper grids, coated with Pioloform film and shaded with carbon. After fixation with 2.5% glutaraldehyde solution for 15 min and three wash steps with water, samples were stained with 1% uranyl acetate solution for 30 s followed by air drying step [42]. The negatively stained specimens were analysed in a Tecnai G2 200 kV transmission electron microscope (FEI, Eindhoven, The Netherlands), operating at 80 keV.

3. Results and discussion

VLPs were first purified by density gradient ultracentrifugation in order to produce a reference standard and to obtain material for development of a chromatographic purification method. This experiment also served to allow comparison of the new process with the well-established density gradient ultracentrifugation method.

3.1. Purification of HIV-1 gag VLPs by density gradient centrifugation

Two high speed ultracentrifugation steps were performed to enrich HIV-1 gag VLPs at densities between 1.16 and 1.18 g/cm^3 (Fig. 1A) which are similar to values reported in literature for HIV-1 VLPs [10]. Density gradient fractions were analysed by Western blot detecting HIV-1 gag specific p24, SDS-PAGE (Fig. 1B and C) and the presence of VLP-like structures was confirmed by TEM (Fig. 2 A). Quantification of particles was made by NTA and showed that 6.6×10^{10} to 9.1×10^{10} part/mL were present in the pooled VLP fractions, resulting in yields between 22.8–48.0%.

3.2. Purification process

Screening experiments for development of a chromatographic purification process for HIV-1 gag VLPs were performed on an analytical scale. A strong (QA) and a weak (DEAE) anion-exchange as well as a strong cation-exchange (SO3) monoliths were tested in order to bind and elute HIV-1 gag VLPs. Purified standard material or clarified and filtered cell culture supernatant containing HIV-1 gag VLPs were injected. Different buffer systems with pH ranges from 6.0 to 8.5 were tested to elute HIV-1 gag VLPs by a linear gradient from 0 to 1000 mM NaCl. HIV-1 gag VLPs did not bind to the SO3 monolith, whereas QA and DEAE monoliths resulted in similar performances and a 50 mM HEPES buffer system at pH 7.2 was identified to provide optimal conditions for elution of VLPs between 560 and 770 mM NaCl (45–90 mS/cm). The complex surface structure of enveloped viruses and VLPs has not been well defined. However, a lot of enveloped viruses are negatively charged with isoelectric points between 1.9 and 8.4 and viruses with very basic isoelectric points have not been reported so far [30]. The phospholipid bilayer originated from the host cell membrane during the VLP budding processes and the associated membrane proteins contribute to the binding. The polar head groups of the most common phospholipids provide a negative net charge at physiological pH and are oriented outside, towards the membrane surface [43]. Thus, it is reasonable that the HIV-1 gag VLPs bind to anion-exchangers.

Purification experiments were scaled up to 1 mL radial flow QA and DEAE monoliths and clarified and filtered cell culture supernatant (50 mL) was directly loaded onto the monoliths and eluted by a linear gradient from 100 mM to 1000 mM NaCl at flow rates of 1 mL/min. A representative chromatogram obtained by QA monolith is presented in Fig. 3A. Both monoliths were tested and compared in terms of process recovery, yield, host cell (hc) protein, and dsDNA depletion. Results obtained from the strong anion-exchanger (Fig. 3, Table 1 and Table 2) and weak anion-exchanger showed comparable purity (1.2 μg total protein/10^9 particles and 15.0 ng dsDNA/10^9 particles purified by DEAE) and yield (20.8% for DEAE). Further process development was done with the strong anion-exchanger, because a higher operational stability can be expected, because pH-shifts are smaller in strong ion-exchangers [44]. Analysis of flow through fraction (FT) by Western blot detecting p24, (Fig. 3C) showed that nearly all HIV-1 gag VLPs bound to the monolith which was confirmed when measuring particle concentration by NTA (Table 1) and by representative pictures generated by TEM (data not shown). About 50% of hc proteins did not bind and consequently were present in the flow through fractions. VLPs were eluted over a broad range of salt concentrations between 100 and 1000 mM (Fig. 3, Table 1) where about 15% of particles were eluted at the beginning of the gradient at low salt concentrations with conductivities between 12 and 32 mS/cm. Majority of dsDNA (65.6%) was co-eluted with about one third of particles at an intermediate salt concentration equivalent to 32–48 mS/cm but the majority of particles (43.5%) were eluted at the end of the gradient between 48 and 89 mS/cm.

All three particle-containing fractions were examined by TEM and the presence of particles was confirmed but no remarkable visible differences between particles could be observed (Fig. 2). However, different particle size distributions were measured by NTA (Fig. 4), indicating that particles eluting in fraction P1 were slightly smaller than particles eluted in P2 and P3. Particles eluting in P3 were characterized by a broader particle size distribution compared to particles eluted in P2. Additionally, a different protein band pattern in SDS-PAGE (Fig. 3B) for these fractions was observed. With focus on the main band at 55 kDa representing the gag protein and a semi-quantitative evaluation of the band thickness, intermediate and late eluting fractions P2 and P3 were more dominant compared to P1. Furthermore, when the SDS-PAGE band profile of standard material obtained from density gradient centrifugation (Fig. 1B) was compared to those of chromatographic eluting fractions P1 to P3 (Fig. 3B) nearly no similarities were noted between P1 and the standard material, but several analogous components between P2, P3 and the standard material were identified. Particles eluting in P1 were composed of a variety of contaminant proteins,

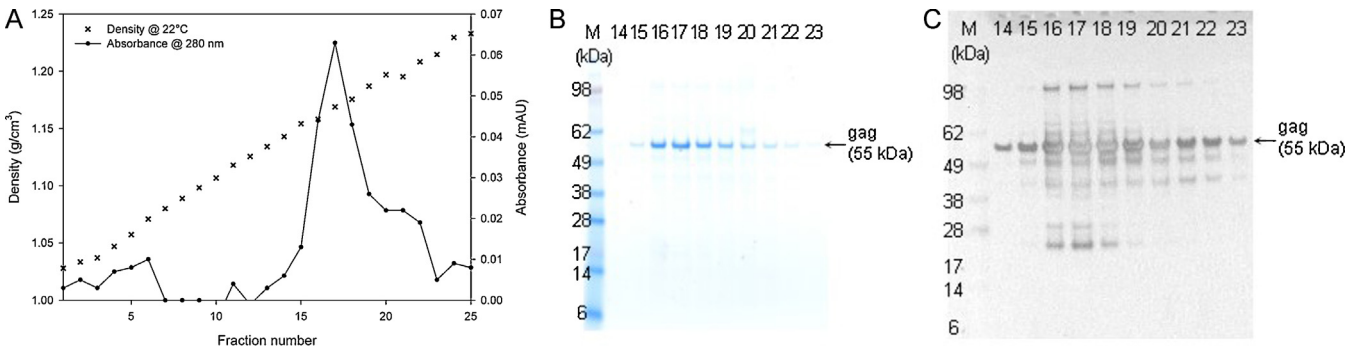

Fig. 1. Absorbance and density profile of sucrose gradient centrifugation of HIV-1 gag VLPs (A) and corresponding Coomassie stained SDS-PAGE (B) and Western blot analysis (C). 5 μL of each sample were loaded. Western blot detection was performed using a primary mouse monoclonal antibody against HIV-1 p24 (1:1000) and anti-mouse IgG conjugated with alkaline phosphatase (1:1000) as secondary antibody. Visualization of bands was carried out by a chemiluminescent substrate detecting alkaline phosphatase. Lane numbers indicate fraction number in (A), M: molecular mass marker.

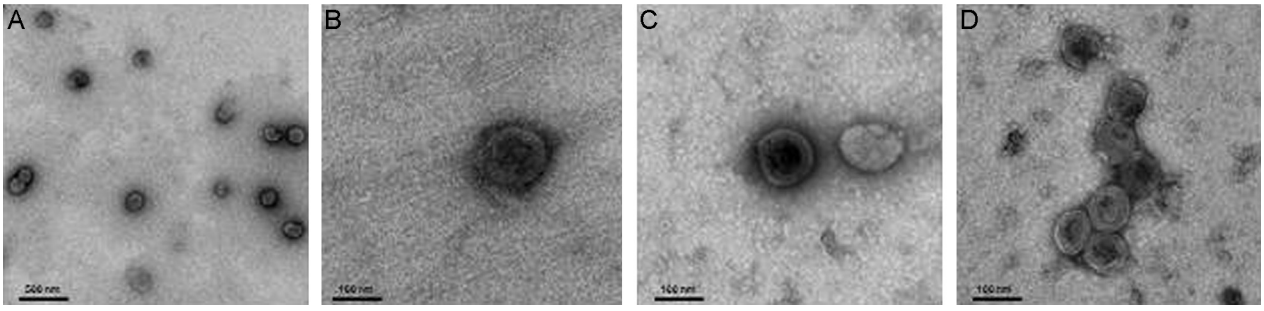

Fig. 2. Transmission electron microscopy from HIV-1 gag VLPs purified by (A) sucrose density gradient centrifugation and anion-exchange chromatography eluted at low (B) intermediate (C) or high salt concentration (D). The scale bar corresponds to 500 nm in (A) and to 100 nm in (B) to (D).

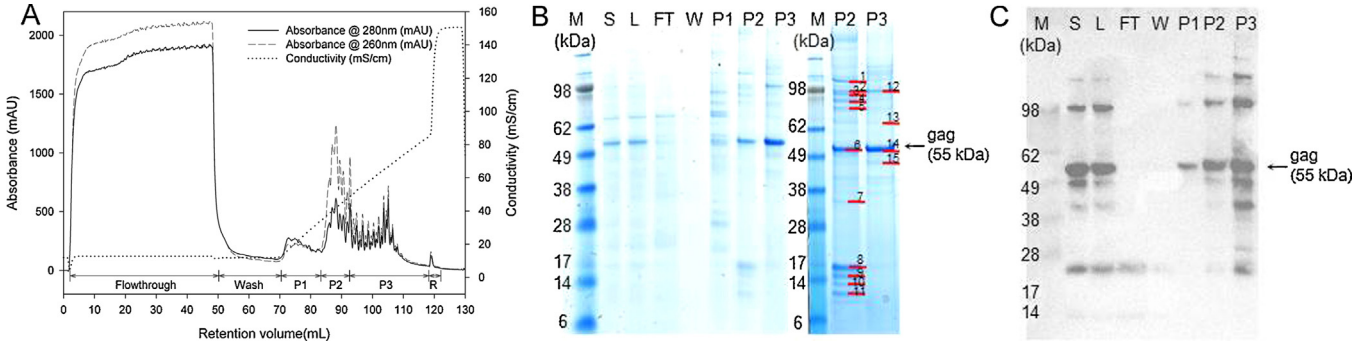

Fig. 3. (A) Chromatogram of HIV-1 gag VLP purification from 50 mL 0.8 μm filtered CHO cell culture supernatant applied to a 1 mL QA radial flow monolith. Equilibration buffer was 50 mM HEPES, pH 7.2 and linear gradient elution was performed from 100 to 1000 mM NaCl in 50 bed volumes at a flowrate of 1 mL/min. (B) SDS-PAGE and (C) Western blot analysis of collected fractions. The amount of loaded protein per lane was 785 ± 23 ng. Western blot detection was performed using a primary mouse monoclonal antibody against HIV-1 p24 (1:1000) and anti-mouse IgG conjugated with alkaline phosphatase (1:1000) as secondary antibody. Visualization of bands was carried out by a chemiluminescent substrate detecting alkaline phosphatase. M: molecular mass marker, S: cell culture supernatant; L: load, filtered cell culture supernatant; FT: flow through; W: wash; P1-P3: fractions of eluting peaks; R: regenerate. Marked bands in (B) were analysed by MS.

but gag protein (band at 55 kDa in Fig. 3B) was not the main structural component or, conceivably, a great number of free hc proteins were also aggregated with these particles. Analysis of significant protein bands (marked bands 1–15 in Fig. 3B) by MS (results are presented in the supplementary information) indicated that particles eluting in P3 consisted mainly of hc membrane-associated proteins (bands 12, 13 and 15 in Fig. 3B) and HIV-1 gag (band 14 in Fig. 3 B). The hc proteins were part of the VLPs and were incorporated into the particle during the budding process. Proteome analysis of particles eluting in P2 showed that a large number of histones (bands 8–11 in Fig. 3 B) and an increased number of exosome marker proteins (results are presented in the supplementary information) were present in this fraction. Histones are usually present in the cell nucleus to package DNA and should not be incorporated into correctly assembled VLPs. Therefore, we assume that we are eluting a portion of particles enriched with extracellular vesicles which partially carry encapsulated DNA. DNA digestion by Benzonase, done after the chromatographic method has been converted to stepwise elution, showed that dsDNA content could be minimized by enzymatic treatment in the VLP-containing fraction to 0.9 ng dsDNA/10^9 particles but not in the fraction containing the DNA (32.4 ng dsDNA/10^9 particles). This observation supports the assumption that DNA must be encapsulated in these particles. It is known that CHO cells produce a larger number of exosomes [31] which bud simultaneously together with VLPs and carry encapsulated DNA [35].

An endonuclease treatment step with 150 U/mL of Benzonase for 1 h at room temperature was introduced before chromatogra-

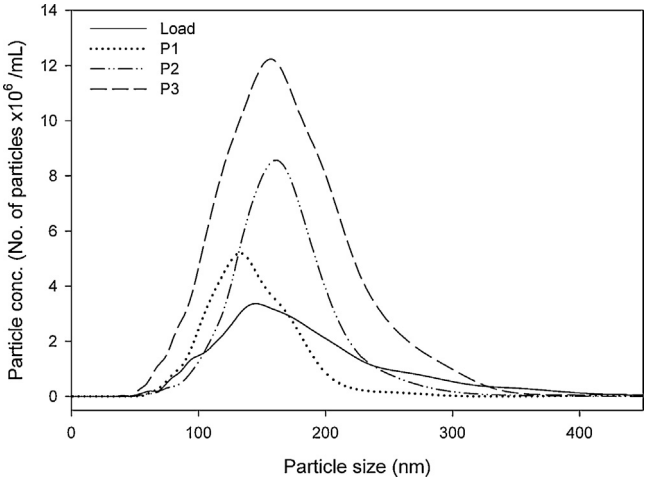

Fig. 4. Particle size distribution measured by NTA. Fractions, corresponding to Fig. 3, were eluted form 1 mL QA radial flow monolith by a linear gradient from 100 to 1000 mM NaCl in 50 bed volumes.

phy to optimize and improve DNA removal and to avoid potential competitive binding of DNA on the AIEX surface. The dsDNA content of the cell culture supernatant was reduced 22.8 times (95.6%) before 0.8 μm filtration and loading onto the anion-exchange monoliths. The elution profile of endonuclease treated supernatant changed (compare Fig. 3 with Fig. 5). According to our expectations, signals of intermediate eluting fraction were reduced because the majority of DNA had been already digested into oligonucleotide fragments before loading. Elution order of particles, particle yield and particle concentration of elution fractions were not significantly affected by enzymatic treatment of starting material (Table 1, Table 2). Changes are explained by different fraction sizes because of differently pooled fractions and were within the methodical error of measurement using NTA. The majority of HIV-1 gag VLPs (49.1%) were eluted at high salt concentrations but residual dsDNA content of main HIV-1 gag VLP fraction was 3.2 times reduced (Table 1, Table 2). The enzymatic pretreatment of the feedstock resulted in a HIV-1 gag VLP fraction with an increased purity compared to purification of non-treated supernatant (Table 2). However, an additional process step is required subsequently to remove the Benzonase. Furthermore, it is commonly known that Benzonase is a huge cost factor and usage of high concentrations during early process steps might increase the total process costs. We did not focus on the optimization of the endonuclease treatment step and arrived at a reasonable concentration of Benzoase for 1 h incubation time. This short incubation time makes the process more robust and the whole process sequence can be performed within one working day. Benzonase seems expensive at first glance, but also labour cost and plant utilization are an important cost factor. When the process time is reduced the plant can be more efficiently utilized. Only a professional cost analysis using modelling tools such as BioSolve (Biopharm Services, Chesham, UK) or SuperProDesigner (Intelligen Inc., Scotch Plains, NJ, USA) could give information about the cost effectiveness of the process operated with or without endonuclease treatment.

Often stepwise elution facilitates purification processes, especially for use on a large scale. The equilibration buffer was adapted

Table 1
Mass balance of HIV-1 gag VLP purification with a 1 mL radial flow QA monolith by linear gradient elution. Loading material was 0.8 μm filtered and optional endonuclease treated CHO cell culture supernatant. (Buffer A: 50 mM HEPES, 100 mM NaCl, pH 7.2; Buffer B: 50 mM HEPES, 2 M NaCl, pH 7.2; 0–50% B in 50 bed volumes).

Linear gradient elution

	Volume (mL)	Particles D 100–200 nm (part/mL)	Distribution of particles %	Total protein (μg/mL)	dsDNA (ng/mL)
Load	50	5.7E + 10	100	448	12988
FT	50	4.5E + 08	0.8	232	43
Wash	20	2.9E + 08	0.2	38	nd
P1	11	3.9E + 10	15.1	229	46
P2	14	6.3E + 10	30.7	241	30450
P3	20	6.E + 10	43.5	117	1281
Recovery			90.3		

Benzonase treatment before linear gradient elution

	Volume (mL)	Particles D 100–200 nm (part/mL)	%	Total protein (μg/mL)	dsDNA (ng/mL)
Load	50	9.5E + 10	100	379	717
FT	50	3.0E + 07	0	190	46
Wash	20	4.9E + 07	0	45	nd
P1	13	7.7E + 10	20.9	353	201
P2	6	1.8E + 10	2.2	164	2136
P3	13	2.1E + 10	5.8	59	1961
P4	20	1.2E + 11	49.1	131	755
Recovery			78.2		

nd: not detectable.

Table 2
Comparison of purification strategies and characterisation of purified HIV-1 gag VLPs.

	Loading volume (mL)	Flow rate (mL/min)	Yield (%)	Total protein /10^9 part. (μg/1×10^9 part.)	dsDNA /10^9part. (ng/1×10^9part.)	Productivity (1×10^9part./mL/min)
Linear gradient elution	50	1	43.5	1.9	21	8
Benzonase treatment before linear gradient elution	50	1	49.1	1.1	6	11
Step gradient elution (n=3)	50	1	41.9 ± 9.6	1.8 ± 0.3	11 ± 2	8
Step gradient elution	160	1	21.8	2.4	14	9
Step gradient elution	160	5	20.4	2.4	13	44
Density gradient centrifugation	10.2	–	48.1	1.6	3	0

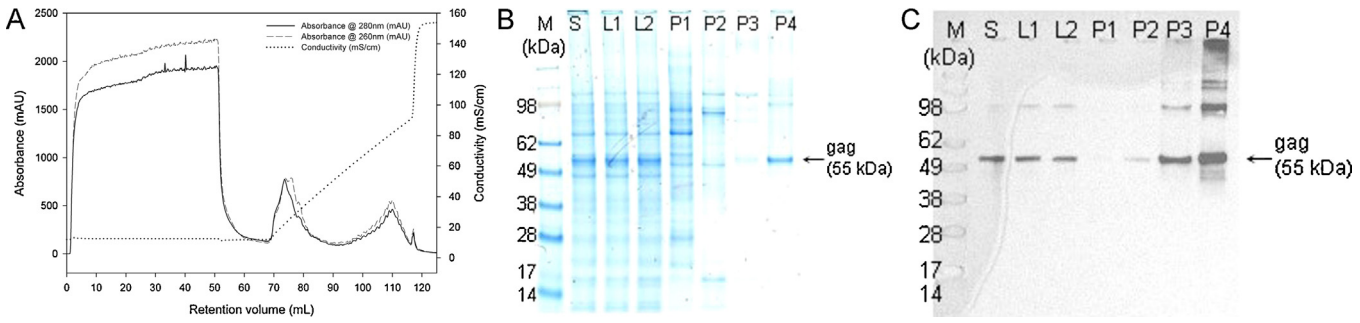

Fig. 5. (A) Chromatogram of HIV-1 gag VLP purification from 50 mL endonuclease treated and 0.8 μm filtered CHO cell culture supernatant by 1 mL QA radial flow monolith. Equilibration buffer was 50 mM HEPES, pH 7.2 and linear gradient elution was performed from 100 to 1000 mM NaCl in 50 bed volumes at a flowrate of 1 mL/min. (B) SDS-PAGE and (C) Western blot analysis of collected fractions. The amount of loaded protein per lane was 643 ± 33 ng. Western blot detection was performed using a primary mouse monoclonal antibody against HIV-1 p24 (1:1000) and anti-mouse IgG conjugated with alkaline phosphatase (1:1000) as secondary antibody. Visualization of bands was carried out by a chemiluminescent substrate detecting alkaline phosphatase. M: molecular mass marker; S: cell culture supernatant; L1: endonuclease treated cell culture supernatant; L2: endonuclease treated and filtered cell culture supernatant; P1-P4: fractions of eluting peaks; R: regenerate.

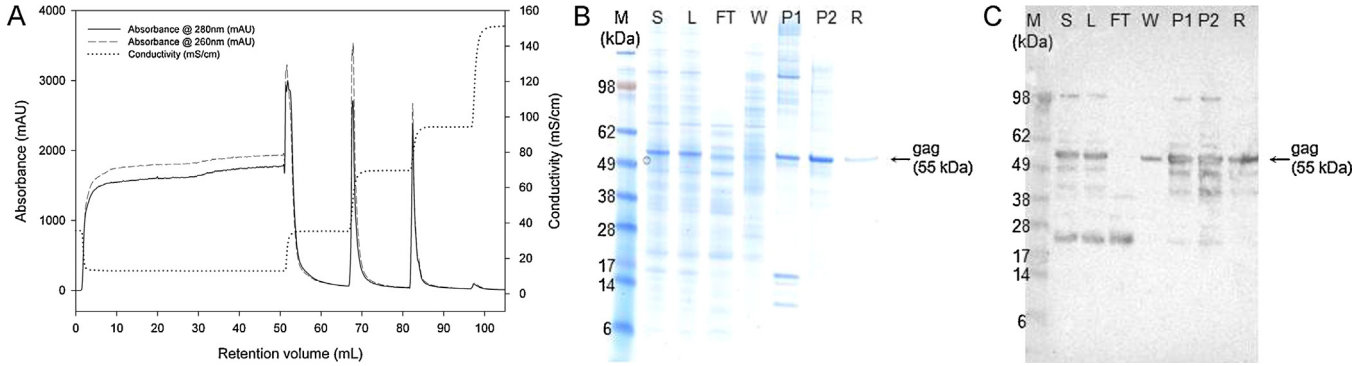

Fig. 6. (A) Chromatogram of HIV-1 gag VLP purification eluted by a step gradient (0–25–45% B with a hold volume of 15 bed volumes) at a flowrate of 1 mL/min. 50 mL of 0.8 μm filtered CHO cell culture were loaded. Equilibration buffer was 50 mM HEPES, 350 mM NaCl, pH 7.2 and elution buffer 50 mM HEPES, 2 M NaCl, pH 7.2. (B) SDS-PAGE and (C) Western blot analysis of collected fractions. The amount of loaded protein per lane was 1234 ± 66 ng and 289 ng for the regenerate. Western blot detection was performed using a primary mouse monoclonal antibody against HIV-1 p24 (1:1000) and anti-mouse IgG conjugated with alkaline phosphatase (1:1000) as secondary antibody. Visualization of bands was carried out by a chemiluminescent substrate detecting alkaline phosphatase. M: molecular mass marker, S: cell culture supernatant; L: load, filtered cell culture supernatant; FT: flow through, W: wash, P1-P2: fractions of eluting peaks, R: regenerate.

Table 3
Mass balance of HIV-1 gag VLP purification with a 1 mL radial flow QA monolith step gradient elution. (Buffer A: 50 mM HEPES, 350 mM NaCl, pH 7.2; Buffer B: 50 mM HEPES, 2 M NaCl, pH 7.2; 0–25–45% B with a hold volume of 15 bed volumes).

	Volume (mL)	Particles D 100–200 nm (part/mL)	Distribution of particles %	Total protein (μg/mL)	dsDNA (ng/mL)
Load	50.0	10	100.0	349	10008
FT	50.0	2.3E + 07	0.1	171	40
Wash	15.0	9.2E + 09	7.5	371	65
P1	15.0	3.0E + 10	24.2	175	24652
P2	15.0	4.8E + 10	38.8	98	602
Recovery			70.5		

to contain 350 mM NaCl, the length of the wash step was reduced to 15 bed volumes, and elution was performed by 0–25–45% B steps with a hold volume of 15 bed volumes each with elution buffer containing 2 M NaCl. In Fig. 6, step elution profile and corresponding SDS-PAGE and Western blot results are shown and mass balance is presented in Table 3. Robustness and reproducibility of the purification performance were demonstrated by three independent purification cycles with two different supernatant batches. The total process recovery of particles in all fractions were between 70.5 and >99.9%. Consistently, 50.3 ± 1.3% of hc proteins did not bind to the monolith and were present in the flow through fractions and 33.6 ± 3.3% of hc proteins and about 14 ± 8.1% of particles could be removed during the wash step. Particles eluting during the wash step, initially eluted in P1 during the linear gradient elution (compare Fig. 3B, P1 with Fig. 6B, W), were either aggregated to free hc proteins or were not mainly assembled from the gag protein (Fig. 6B, C). In peak one (P1, Fig. 6) generated by 25% B an average of 80.8 ± 7.3% of dsDNA co-eluted with about one third of particles (32.7 ± 9.4%) mainly consisting of extracellular vesicles. However, co-elution of a noteworthy portion of correctly assembled HIV-1 gag VLPs cannot be excluded. Whereas, majority and most pure HIV-1 gag VLPs eluted during the 45% B step resulting in a process yield of 41.9 ± 9.6% (P2, Fig. 6 and Table 2). In summary, an average over-all hc protein depletion of 90.9% and an average dsDNA depletion of 98.2% was achieved.

3.3. Dynamic binding capacity (DBC)

DBC was determined by direct loading of the filtered culture supernatant (Fig. 7). After about 100 mL loading, the particles start to breakthrough and after 200 mL (equivalent to a total particle load of 8.6×10^{12} part/mL QA) the breakthrough of particles reached

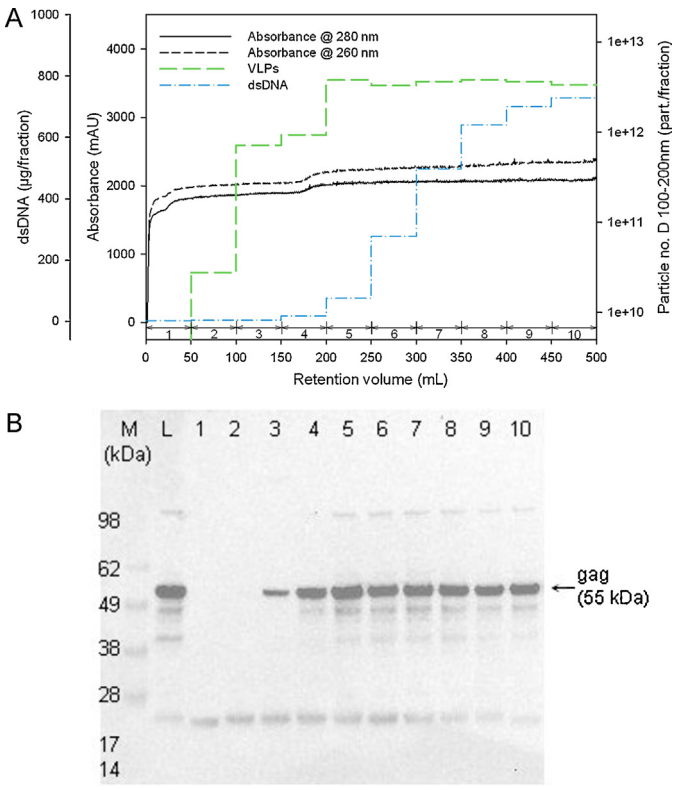

Fig. 7. (A) Dynamic binding capacity of filtered CHO cell culture supernatant containing HIV-1 gag VLPs. Flow through fractions (1–10) were measured by NTA to monitor the VLP breakthrough and analysed by Picogreen assay to monitor dsDNA breakthrough. (B) Western blot analysis of collected flow through fractions (5 µL of fractions 1–10 in (A) were loaded). Western blot detection was performed using a primary mouse monoclonal antibody against HIV-1 p24 (1:1000) and anti-mouse IgG conjugated with alkaline phosphatase (1:1000) as secondary antibody. Visualization of bands was carried out by a chemiluminescent substrate for detecting alkaline phosphatase.

the starting concentration (4.3×10^{10} part/mL). This result could be observed by the increase of UV signals and was confirmed by Western blot analysis (Fig. 7B). The early breakthrough contained only a minimal fraction of the total load (0.1%). Slightly shifted to the breakthrough of HIV-1 gag VLPs, the breakthrough of dsDNA was detected by Picogreen assay. To detect if there was potential competitive binding between the VLPs and DNA, which might reduce the capacity for VLPs, the DBC was again determined by loading endonuclease pretreated and filtered culture supernatant. A comparable binding capacity of 1.6×10^{12} part/mL QA was determined, indicating that there is no competitive binding of VLPs and DNA. This result supports the application of the purification process cope without endonuclease pretreatment.

3.4. Evaluation of the optimized purification process

Using the optimized method that we defined from DBC and elution conditions, we performed confirmation runs where 160 mL filtered culture supernatant (equivalent to a total particle number of 1.0×10^{13} part/mL QA) was loaded at flow rates of 1 mL/min and 5 mL/min. In both cases yield was about 20% (Table 2) and the main HIV-1 gag VLP fraction contained a total number of 2.1×10^{12} and 2.2×10^{12} particles, respectively. The residual dsDNA levels were about 20–40% above the limits required for a licensed vaccine (10 ng dsDNA/dose), when we assume that one vaccination dose consist of 1.0×10^{9} particles (Table 2). When a flow rate of 5 mL/min was applied 2075 doses were purified within 47 min. In comparison the process performed at 1 mL/min, yielded in 2219 doses within 4 h (Table 2). With slight improvements or for example by implementation of an endonuclease treatment after chromatography it would be possible to reduce the DNA level to the values claimed by the authorities.

4. Conclusion

Monoliths serve as a method to tackle extremely challenging separation problems in the field of bionanoparticles. Enveloped VLPs are efficiently overproduced in CHO cells, but they are contaminated by hc proteins, hc DNA, and potentially by extracellular particles. This method is able to separate these main impurities including particles with different characteristic than HIV-1 gag VLPs and is in principle suited for purification of pandemic vaccines. The process at the current stage is a laboratory process but all process parameters have been developed, which are needed to scale up such a process. With a 1 mL monolith, at least 160 mL supernatant, equivalent to a total load of 1.0×10^{13} particles, were processed within less than one hour. In comparison, a maximum of 20 mL supernatant, equivalent to a total load of 9.3×10^{11} particles, could be purified by the existing density gradient centrifugation processes within 20 h resulting in about one-tenth of doses (230) compared to monoliths. Currently 8 L monoliths are commercially available and a 40 L monolith has been presented as an industrial prototype. With an 8 L monolith, about 10^7 doses could be purified and with the 40 L prototype about 5×10^7 doses. Our work provides a direction for how a pandemic vaccine could be efficiently purified.

Acknowledgements

The research leading to these results has received funding from the European Union Seventh Framework Programme (FP7/2007-2013) under grant agreement no 312004. This work has been also partly supported by the Federal Ministry of Science, Research and Economy (BMWFW), the Federal Ministry of Traffic, Innovation and Technology (bmvit), the Styrian Business Promotion Agency SFG, the Standortagentur Tirol and ZIT – Technology Agency of the City of Vienna through the COMET-Funding Program managed by the Austrian Research Promotion Agency FFG. We thank Gerhard Sekot for assisting with TEM pictures. P.A. was supported by the Austrian Science Fund (project BioToP; FWF W1224).

Appendix A. Supplementary data

Supplementary data associated with this article can be found, in the online version, at http://dx.doi.org/10.1016/j.chroma.2016.05.053.

References

[1] A.F. Rodrigues, H.R. Soares, M.R. Guerreiro, P.M. Alves, A.S. Coroadinha, Viral vaccines and their manufacturing cell substrates: new trends and designs in modern vaccinology, Biotechnol. J. 10 (2015) 1329–1344.
[2] R.S. Felberbaum, The baculovirus expression vector system: a commercial manufacturing platform for viral vaccines and gene therapy vectors, Biotechnol. J. 10 (2015) 702–714.
[3] F. Krammer, Emerging influenza viruses and the prospect of a universal influenza virus vaccine, Biotechnol. J. 10 (2015) 690–701.
[4] F. Krammer, S. Nakowitsch, P. Messner, D. Palmberger, B. Ferko, R. Grabherr, Swine-origin pandemic H1N1 influenza virus-like particles produced in insect cells induce hemagglutination inhibiting antibodies in BALB/c mice, Biotechnol. J. 5 (2010) 17–23.
[5] G.P. Pijlman, Enveloped virus-like particles as vaccines against pathogenic arboviruses, Biotechnol. J. 10 (2015) 659–670.
[6] T. Frensing, Defective interfering viruses and their impact on vaccines and viral vectors, Biotechnol. J. 10 (2015) 681–689.
[7] S.C. Lin, W.C. Liu, Y.F. Lin, Y.H. Huang, J.H. Liu, S.C. Wu, Heterologous prime-boost immunization regimens using adenovirus vector and virus-like particles induce broadly neutralizing antibodies against H5N1 avian influenza viruses, Biotechnol. J. 8 (2013) 1315–1322.

[8] C.L. Effio, J. Hubbuch, Next generation vaccines and vectors: designing downstream processes for recombinant protein-based virus-like particles, Biotechnol. J. 10 (2015) 715–727.
[9] P. Nestola, C. Peixoto, R.R.J.S. Silva, P.M. Alves, J.P.B. Mota, M.J.T. Carrondo, Improved virus purification processes for vaccines and gene therapy, Biotechnol. Bioeng. 112 (2015) 843–857.
[10] P.E. Cruz, C.C. Peixoto, K. Devos, J.L. Moreira, E. Saman, M.J.T. Carrondo, Characterization and downstream processing of HIV-1 core and virus-like-particles produced in serum free medium, Enzyme Microb. Technol. 26 (2000) 61–70.
[11] P. Pushko, P. Pumpens, E. Grens, Development of virus-like particle technology from small highly symmetric to large complex virus-like particle structures, Intervirology 56 (2013) 141–165.
[12] S. Welsch, B. Müller, H.G. Kräusslich, More than one door—Budding of enveloped viruses through cellular membranes, FEBS Lett. 581 (2007) 2089–2097.
[13] G. Raposo, W. Stoorvogel, Extracellular vesicles: exosomes, microvesicles, and friends, J. Cell Biol. 200 (2013) 373–383.
[14] J.W. Bess Jr., R.J. Gorelick, W.J. Bosche, L.E. Henderson, L.O. Arthur, Microvesicles are a source of contaminating cellular proteins found in purified HIV-1 preparations, Virology 230 (1997) 134–144.
[15] M. Hammarstedt, H. Garoff, Passive and active inclusion of host proteins in human immunodeficiency virus type 1 Gag particles during budding at the plasma membrane, J. Virol. 78 (2004) 5686–5697.
[16] A. Podgornik, S. Yamamoto, M. Peterka, N.L. Krajnc, Fast separation of large biomolecules using short monolithic columns, J. Chromatogr. B 927 (2013) 80–89.
[17] P. Gerster, E.M. Kopecky, N. Hammerschmidt, M. Klausberger, F. Krammer, R. Grabherr, C. Mersich, L. Urbas, P. Kramberger, T. Paril, M. Schreiner, K. Nöbauer, E. Razzazi-Fazeli, A. Jungbauer, Purification of infective baculoviruses by monoliths, J. Chromatogr. A 1290 (2013) 36–45.
[18] A. Jungbauer, R. Hahn, Polymethacrylate monoliths for preparative and industrial separation of biomolecular assemblies, J. Chromatogr. A 1184 (2008) 62–79.
[19] C. Tarmann, A. Jungbauer, Adsorption of plasmid DNA on anion exchange chromatography media, J. Sep. Sci. 31 (2008) 2605–2618.
[20] C.S. Burden, J. Jin, A. Podgornik, D.G. Bracewell, A monolith purification process for virus-like particles from yeast homogenate, J. Chromatogr. B 880 (2012) 82–89.
[21] L. Urbas, B.L. Jarc, M. Barut, M. Zochowska, J. Chroboczek, B. Pihlar, E. Szolajska, Purification of recombinant adenovirus type 3 dodecahedric virus-like particles for biomedical applications using short monolithic columns, J. Chromatogr. A 1218 (2011) 2451–2459.
[22] M. Zaveckas, S. Snipaitis, H. Pesliakas, J. Nainys, A. Gedvilaite, Purification of recombinant virus-like particles of porcine circovirus type 2 capsid protein using ion-exchange monolith chromatography, J. Chromatogr. B 991 (2015) 21–28.
[23] J. Urthaler, R. Schlegl, A. Podgornik, A. Strancar, A. Jungbauer, R. Necina, Application of monoliths for plasmid DNA purification: development and transfer to production, J. Chromatogr. A 1065 (2005) 93–106.
[24] M.W. Wolff, U. Reichl, Downstream processing of cell culture-derived virus particles, Expert Rev. Vaccines 10 (2011) 1451–1475.
[25] L. Cervera, S. Gutiérrez-Granados, M. Martínez, J. Blanco, F. Gòdia, M.M. Segura, Generation of HIV-1 Gag VLPs by transient transfection of HEK 293 suspension cell cultures using an optimized animal-derived component free medium, J. Biotechnol. 166 (2013) 152–165.
[26] C.M. Thompson, E. Petiot, A. Mullick, M.G. Aucoin, O. Henry, A.A. Kamen, Critical assessment of influenza VLP production in Sf9 and HEK293 expression systems, BMC Biotechnol. 15 (2015).
[27] W. Akahata, Z.Y. Yang, H. Andersen, S. Sun, H.A. Holdaway, W.P. Kong, M.G. Lewis, S. Higgs, M.G. Rossmann, S. Rao, G.J. Nabel, A virus-like particle vaccine for epidemic Chikungunya virus protects nonhuman primates against infection, Nat. Med. 16 (2010) 334–338.
[28] M. Li, P.T. Schmitt, Z. Li, T.S. McCrory, B. He, A.P. Schmitt, Mumps virus matrix, fusion, and nucleocapsid proteins cooperate for efficient production of virus-like particles, J. Virol. 83 (2009) 7261–7272.
[29] L. Deml, C. Speth, M.P. Dierich, H. Wolf, R. Wagner, Recombinant HIV-1 Pr55 gag virus-like particles: potent stimulators of innate and acquired immune responses, Mol. Immunol. 42 (2005) 259–277.
[30] B. Michen, T. Graule, Isoelectric points of viruses, J. Appl. Microbiol. 109 (2010) 388–397.
[31] A. Bedina Zavec, V. Kralj-Iglič, M. Brinc, T. Ficko Trček, Microvesicles as a new parameter for industrial bioprocess monitoring, Biotechnol. J. 10 (2015).
[32] A. Zeltins, Construction and characterization of virus-like particles: a review, Mol. Biotechnol. 53 (2013) 92–107.
[33] U.S. Department of Health and Human Services Food and Drug Administration Guidance for Industry, Bioanalytical Method Validation, in, Center for Drug Evaluation and Research (CDER) Center for Veterinary Medicine (CVM), 2001.
[34] P. Kramberger, M. Ciringer, A. Trancar, M. Peterka, Evaluation of nanoparticle tracking analysis for total virus particle determination, Virol. J. 9 (2012).
[35] B.K. Thakur, H. Zhang, A. Becker, I. Matei, Y. Huang, B. Costa-Silva, Y. Zheng, A. Hoshino, H. Brazier, J. Xiang, C. Williams, R. Rodriguez-Barrueco, J.M. Silva, W. Zhang, S. Hearn, O. Elemento, N. Paknejad, K. Manova-Todorova, K. Welte, J. Bromberg, H. Peinado, D. Lyden, Double-stranded DNA in exosomes: a novel biomarker in cancer detection, Cell Res. 24 (2014) 766–769.
[36] L.H. Lua, N.K. Connors, F. Sainsbury, Y.P. Chuan, N. Wibowo, A.P. Middelberg, Bioengineering virus-like particles as vaccines, Biotechnol. Bioeng. 111 (2014) 425–440.
[37] T. Vicente, A. Roldão, C. Peixoto, M.J.T. Carrondo, P.M. Alves, Large-scale production and purification of VLP-based vaccines, J. Invertebr. Pathol. 107 (2011) S42–S48 (Supplement).
[38] T. Vicente, M.F.Q. Sousa, C. Peixoto, J.P.B. Mota, P.M. Alves, M.J.T. Carrondo, Anion-exchange membrane chromatography for purification of rotavirus-like particles, J. Membr. Sci. 311 (2008) 270–283.
[39] F. Gharahdaghi, C.R. Weinberg, D.A. Meagher, B.S. Imai, S.M. Mische, Mass spectrometric identification of proteins from silver-stained polyacrylamide gel: a method for the removal of silver ions to enhance sensitivity, Electrophoresis 20 (1999) 601–605.
[40] C.R. Jiménez, L. Huang, Y. Qiu, A.L. Burlingame, In-gel digestion of proteins for MALDI-MS fingerprint mapping, in: Current Protocols in Protein Science, John Wiley & Sons, Inc., 2001.
[41] A. Shevchenko, M. Wilm, O. Vorm, M. Mann, Mass spectrometric sequencing of proteins from silver-stained polyacrylamide gels, Anal. Chem. 68 (1996) 850–858.
[42] M.A. Hayat, S.E. Miller, Negative Staining, McGraw-Hill, New York, 1990.
[43] L.K. Buehler, Cell membranes, in: Graland Science, Taylor and Francis Group, 2016.
[44] T.M. Pabst, G. Carta, pH transitions in cation exchange chromatographic columns containing weak acid groups, J. Chromatogr. A 1142 (2007) 19–31.

PUBLICATION V

Journal of Chromatography A, 1588 (2019) 77–84

Contents lists available at ScienceDirect

Journal of Chromatography A

journal homepage: www.elsevier.com/locate/chroma

Separation of virus-like particles and extracellular vesicles by flow-through and heparin affinity chromatography

Katrin Reiter[a], Patricia Pereira Aguilar[b], Viktoria Wetter[a], Petra Steppert[b], Andres Tover[c], Alois Jungbauer[a,b,*]

[a] Austrian Centre of Industrial Biotechnology, Vienna, Austria
[b] Department of Biotechnology, University of Natural Resources and Life Sciences, Vienna, Austria
[c] Icosagen AS, Tartumaa, Estonia

ARTICLE INFO

Article history:
Received 29 October 2018
Received in revised form
12 December 2018
Accepted 17 December 2018
Available online 18 December 2018

Keywords:
HIV-1 gag VLP
Exosomes
Capto Heparin
Capto Core 700
HEK 293

ABSTRACT

Separation of enveloped virus-like particles from other extracellular vesicles is a challenging separation problem due to the similarity of these bionanoparticles. Without simple and scalable methods for purification and analytics, it is difficult to gain deeper insight into their biological function. A two-step chromatographic purification method was developed. In the first step, virus-like particles and extracellular vesicles were collected and separated from smaller impurities in a flow-through mode. Benzonase® treated HEK 293 cell culture supernatant was directly loaded onto a column packed with core-shell beads. The collected flow-through was further purified using heparin affinity chromatography. In heparin affinity chromatography 54% of the total particle load were found in the flow-through, and 15% of the particles were eluted during the salt linear gradient. The particle characterization, especially particle size distribution and mass spectrometry data, suggests that extracellular vesicles dominate the flow-through fraction and HIV-1 gag VLPs are enriched in the elution peak. This is in part in contradiction to other protocols where the extracellular vesicles are recovered by binding to heparin affinity chromatography. The developed method is easily scalable to pilot and process scale and allows a fast accomplishment of this separation within one day.

© 2018 The Authors. Published by Elsevier B.V. This is an open access article under the CC BY license (http://creativecommons.org/licenses/by/4.0/).

1. Introduction

It has been shown that viruses and enveloped virus-like particles (VLPs) are co-expressed with other extracellular vesicles (EVs) [1–4]. We used HIV-1 gag VLPs produced in HEK 293 cells as model system to study the separation of these very similar bionanoparticles. Separation and discrimination between HIV-1 gag VLPs and EVs represent a major challenge due to morphological and biophysical similarities [5], often they contain the same molecular structures [6] and have similar size. For production of HIV-1 gag VLPs, the gag polyprotein is over-expressed in the cell, accumulates in the cell membrane and leads to spontaneous formation and budding of VLPs from the plasma membrane [7]. Thus, VLPs are covered with a lipid bilayer from the host cell membrane [8]. EVs comprise a heterogeneous particle mixture including different subtypes as exosomes and microvesicles [9]. Exosomes are released via exocytosis from multivesicular bodies, while microvesicles directly bud from the plasma membrane [10]. Both are involved in intercellular communication and allow cells to exchange proteins, lipids and genetic material [11].

HIV-1 gag VLPs range between 100–200 nm in diameter, some subtypes of EVs are in the same size range, especially exosomes (50–150 nm) and microvesicles (50–500 nm) [11–13]. A second obstacle in the separation process of these bionanoparticles arises from their comparable buoyant densities: 1.13–1.19 g/L for EVs [13–15] and 1.15–1.18 g/L for HIV-1 gag VLPs [15,16]. A further challenge in development of such separation process is the lack of specific biochemical markers on the surface or within the particles. A clear discrimination and separation between these bionanoparticles is hard to achieve, as both particles contain proteins from the lipid bilayer of the host cell, sharing many proteins enriched in the plasma membrane, like tetraspanins [17]. They also show high similarities in the composition of proteins present on the cell surface (integrins) and in the cytoplasm (heat shock proteins) [17], which is conclusive as these bionanoparticles use partly similar budding mechanisms. Typical purification methods such as density gradient centrifugation, ultrafiltration or size exclusion chromatog-

* Corresponding author at: Department of Biotechnology, University of Natural Resources and Life Sciences Vienna, Muthgasse 18, 1190, Vienna, Austria.
E-mail address: alois.jungbauer@boku.ac.at (A. Jungbauer).

https://doi.org/10.1016/j.chroma.2018.12.035
0021-9673/© 2018 The Authors. Published by Elsevier B.V. This is an open access article under the CC BY license (http://creativecommons.org/licenses/by/4.0/).

raphy, which are used for virus purification [18] and nanoparticle purification [19,20] are not recommended for efficient separation of EVs and VLPs. It has been shown that viruses [21–23] and VLPs [24] can be purified efficiently using heparin affinity chromatography, thus we used it as alternative method for VLP and EV separation. A direct purification in a single step using heparin affinity chromatography is not feasible due to the high amount of heparin binding proteins present in mammalian cell culture supernatants. Those protein impurities would directly compete with the bionanoparticles for the heparin binding sites, drastically reducing the resinś binding capacity. Therefore, we developed a two-step chromatographic process. The first step is a flow-through method based on the Capto Core 700 resin for collection of both particle types. Core-shell beads with an inert outer layer and a ligand activated octylamide core are used for initial purification of viruses and other bionanoparticles [25]. The beads are designed to have both, hydrophobic and positively charged properties with a molecular size cut-off of 700 kDa. Bionanoparticles, as HIV-1 gag VLPs and EVs exceed 700 kDa and cannot enter the core, while proteins, DNA fragments and other small cellular metabolites are able to penetrate into the core and bind to the octylamide ligands. Large entities directly flow through the column. Thus, this step allows removal of the majority of small impurities, including heparin-binding proteins and as the bead exterior is inactive it permits purification of VLPs and EVs. Capto Core 700 shows a particle size of ~90 μm. A pore size twice the diameter of the excluded molecules was assumed for our calculation. Pore size was estimated with 25 nm. For spherical proteins a 700 kDa protein has a size of 11.7 nm [26]. Using the estimated pore diameter of 25 nm, internal surface area with extraparticle porosity of 60% and 90% was 67.2 m^2/mL and 100.8 m^2/mL, respectively. For a more detailed calculation an exact electron microscopy would be necessary to get a dimension of the shell and the inner core. Compared to size exclusion chromatography, also very often applied for virus, VLP and nanoparticle purification, the capacity of core-shell beads is much higher. In size exclusion chromatography only about 30% of the total column volume can be loaded without further compromising the purity of the void fraction [27]. In case of the core-shell beads, due to the binding site in their core, several column volumes can be loaded improving productivity and robustness. Another advantage is that the flow-through material collected in the first chromatography step can be directly loaded onto the second chromatography column (Capto Heparin) for further purification.

We developed a novel purification strategy that allows the separation of EVs and VLPs based on flow-through mixed mode and affinity chromatography.

2. Material and methods

2.1. Chemicals and standards

All chemicals were of analytical grade, if not otherwise stated. Benzonase®, sodium chloride (NaCl), sodium hydroxide (NaOH), sodium dodecyl sulfate (SDS), 2-(N-morpholino)ethanesulfonic acid (MES), Tween-20, sulfuric acid (95–97%, H_2SO_4), uranyl acetate were purchased from Merck (Darmstadt, Germany).

4-(2-hydroxyethyl)-1-piperazineethanesulfonic acid (HEPES) (≥99.5%), 2-Propanol, bovine serum albumine (≥99.5%, BSA), 1–4 Dithiotreitol (DTT), EZBlue™ Gel Staining Reagent, Anti-mouse IgG (γ-chain specific)- alkaline phosphatase antibody (#3438), BCIP®/NBT solution, Triton X-100, SIGMAFAST™ OPD substrate tablet, glutaraldehyde solution (grade I), acetonitrile (MS grade), formic acid (98–100%) and iodoacetamide (≥99%) were purchased from Sigma Aldrich (St. Louis, MO, USA). HSP90 monoclonal antibody (#MA1-10372), anti-rabbit IgG (H + L) secondary antibody (#31460), anti-mouse IgG (H + L) superclonal secondary antibody (#A28177) and Super Signal™ West Femto Maximum Sensitivity Substrate were purchased from Thermo Fisher Scientific (Waltham, MA, USA). SeeBlue® Plus 2 Pre-stained Protein Standard and 4x LDS sample buffer were purchased from Invitrogen (Carlsbad, CA, USA). Coomassie Brilliant Blue G-250 dye was purchased from Bio-Rad Laboratories (Hercules, CA, USA), HIV-1 p24 antibody (ab9071) from Abcam (Cambridge, England), anti-human HSP70 antibody (EXOAB-Hsp70A-1) from System Biosciences (CA, USA), HIV-1 p24 Capsid Protein p24 ELISA Kit from Sino Biological (Wayne, USA) and trypsin from Promega (Madison, Wisconsin, USA).

2.2. Expression of HIV-1 gag VLPs in HEK 293 cell culture system

For production of HIV-1 gag VLPs, Icosagen Cell Factory OÜ proprietary 293 ALL (derived from 293-F, Thermo Fisher Scientific, Waltham, MA, USA) was used. For 1 L of VLP production, 450 mL of cell culture (3×10^6 cells/mL) was chemically transfected with HIV-gag expression vector (100 μg) using Reagent 007 (Icosagen AS, Tartumaa, Estonia) in BalanCD® HEK 293 media supplemented with 4 mM GlutaMAX (Thermo Fisher Scientific). The cell culture media volume was raised to the final volume by adding BalanCD® HEK 293 media supplemented with 4 mM GlutaMAX and feed. The culture was fed during the production with BalanCD® HEK 293 (total feed amount is 30% of the final media volume) for 7 days. Culture was harvested by centrifugation for 1000 g and 30 min and 0.01% NaN_3 was added.

2.3. Chromatographic system

All chromatographic experiments were performed with an Äkta Pure 25 M2 equipped with a sample pump S9 and a fraction collector F9-C (GE Healthcare, Uppsala, Sweden). Unicorn software 6.4.1 was used for data collection and analysis. Following parameters were monitored simultaneously: UV signals at 280 and 260 nm, conductivity and pH.

2.4. Preparative chromatography experiments

2.4.1. Flow-through chromatography of bionanoparticles with core-shell beads

For the flow-through chromatography, 100 mL of HEK 293 cell culture supernatant were treated with Benzonase® (purity grade II, Merck KgA, Darmstadt, Germany) at a final concentration of 150 U/mL for 2 h, at room temperature and moderate shaking. The endonuclease treatment was followed by a filtration step using a 0.8 μm syringe filter (Millex AA filter, Millipore Bedford, MA, USA). Benzonase® treated and filtered cell culture supernatant (100 mL) was loaded onto a XK 16/20 column packed with 5.4 mL of Capto Core 700 resin (GE Healthcare, Uppsala, Sweden). Buffer A consisted of 50 mM HEPES, pH 7.2 and buffer B of 50 mM HEPES, 2 M NaCl, pH 7.2. Before loading, the column was equilibrated for 5 column volumes (CV) with 6% B to enable the same conductivity as in the loading material. After loading, the column was washed with 6% B for 10 CV to ensure that all unbound species can leave the column before starting the elution step. Elution was performed by applying a step gradient of 100% B and regeneration was performed with 10 CV of 1 M NaOH and 10 CV of 30% 2-Propanol. The flow rate was 1.3 mL/min, ensuring a residence time of 4 min. For further investigation, 1 mL fractions were collected throughout the whole run and later pooled according to the chromatogram.

2.4.2. Separation of HIV-1 gag VLPs and EVs by heparin affinity

Flow-through fractions from the flow-through chromatography step were pooled and 20 mL were directly loaded onto a 2 mL XK

16/20 column packed with Capto Heparin resin (GE Healthcare, Uppsala, Sweden). Mobile phase A and B were the same as for the previous step. Elution was achieved using a salt linear gradient from 6 to 100% B in 20 CV, including a hold step at 100% B for 10 CV. The flow rate was 0.5 mL/min (4 min residence time). The column was regenerated using 10 CV of 1 M NaOH followed by 10 CV of 30% 2-Propanol. Fractions of 1 mL were collected and pooled according to the chromatogram.

2.5. Determination of total protein content and double stranded DNA content

For determination of total protein content, Bradford assay was used. It utilizes the binding of Coomassie Brilliant Blue G-250 dye (Bio-Rad Laboratories, Hercules, CA, USA) to the proteins. The assay was performed in a 96-well plate format according to the manufacturer's instructions. Calibration curve was obtained by diluting bovine serum albumin (BSA) standard with TE-buffer to a concentration range from 25 to 200 μg/mL.

Double stranded DNA (dsDNA) was determined by Quant-iT™ PicoGreen® dsDNA kit (Life Technologies, Waltham, MA, USA) in a 96-well plate format according to the manufacturer's instructions. Signals for protein and dsDNA content were measured by Genius Pro Plate Reader (Tecan, Männedorf, Switzerland).

2.6. Sodium dodecyl sulphate polyacrylamide gel electrophoresis (SDS-PAGE) and Western blot

SDS-PAGE was performed using reduced MES-SDS running conditions and NuPAGE® Bis/Tris Mini gels 4–12% (Invitrogen, Carlsbad, CA, USA). For protein denaturation, 45 μL of sample were treated with 15 μL of 4x LDS sample buffer and 1% (v/v) DTT, followed by heat denaturation for 20 min at 96 °C. SeeBlue® Plus 2 Pre-stained Protein Standard (Invitrogen, Carlsbad, CA, USA) was used as protein molecular weight marker. The following electrophoretic settings were used: 400 V, 200 mA, 50 min. Protein bands were stained using a Coomassie Brilliant Blue G-250 based EZBlue™ Gel Staining Reagent (Sigma Aldrich, St. Louis, MO, USA).

For Western blot analysis, proteins were blotted using the Trans-Blot® turbo system (Bio-Rad Laboratories, Hercules, CA, USA) and 0.2 μm nitrocellulose membranes (Whatman, Dassel, Germany). Blocking buffer contained 3% BSA and 0.1% (w/v) Tween-20. For the detection of the HIV-1 gag protein, membranes were blocked overnight at 4 °C and afterwards incubated for 2 h with primary mouse monoclonal antibody against HIV-1 p24 [39/5.4 A] (Abcam, Cambridge, England), diluted 1:1000 in PBS-T and containing 1% BSA. Anti-mouse IgG (γ-chain specific)-alkaline phosphatase antibody (#3438, Sigma Aldrich, St. Louis, MO, USA) diluted 1:1000 in PBS-T and containing 1% BSA was used as secondary antibody. For visualization of HIV-1 gag protein, the membrane was incubated in 10 mL premixed BCIP®/NBT solution (Sigma Aldrich, St. Louis, MO, USA) for 2–3 min. For the detection of heat shock proteins, anti-human HSP70 antibody (EXOAB-Hsp70A-1, System Biosciences, CA, USA) and HSP90 monoclonal antibody (MBH90AB, Thermo Fisher Scientific, Waltham, MA, USA) were used as primary antibodies. Membranes were blocked for 1 h in blocking buffer and incubated overnight at 4 °C with the primary antibody (1:1000 diluted in PBS-T containing 1% BSA). Afterwards the membrane was incubated for 1 h with the secondary antibody using a 1:4000 dilution (HSP70: anti-rabbit IgG (H + L) secondary antibody, HRP (31460) and HSP90: anti-mouse IgG (H + L) superclonal™ secondary antibody, HRP (A28177) both Thermo Fisher Scientific, Waltham, MA, USA). For chemiluminescent detection, Super Signal™ West Femto Maximum Sensitivity Substrate (Thermo Fisher Scientific, Waltham, MA, USA) was used as substrate and proteins were visualized by Lumi Imager (Boehringer Ingelheim, Ingelheim, Germany).

2.7. Nanoparticle tracking analysis (NTA)

For determination of the particle concentration and particle size distribution, nanoparticle tracking analysis (NTA) was used. Experiments were performed on a NanoSight NS300 (Malvern Instruments Ltd., Worcestershire, UK) with a blue laser module (488 nm) and a neutral density filter. Samples were diluted in particle-free water in order to obtain 20–100 particles per frame. In total, three different dilutions were measured per sample. Videos of 30 s were captured using a temperature of 25 °C. The camera level was adjusted manually, prior to the measurements. For determination of particle concentration, each dilution was measured 5 times. In total, 15 videos were analysed for each sample.

2.8. Enzyme-linked immunosorbent assay (ELISA)

HIV-1 p24 concentration was determined by HIV-1 p24 Capsid Protein p24 ELISA Kit (Sino Biological, Wayne, USA). In order to disrupt the particles and remove their lipid bilayer, samples were incubated with SNCR buffer [28] for 10 min at 70 °C, followed by an incubation with 1.5% Triton X-100 for 10 min at 100 °C. A linear calibration curve was obtained by serial dilution of provided positive control. A SIGMAFAST™ OPD substrate tablet (Sigma Aldrich, St. Louis, MO, USA) dissolved in 20 mL deionized water was used as substrate solution. The reaction was stopped adding 1.25 N H_2SO_4. The absorbance was measured at 492 nm with a reference wavelength at 630 nm with a Tecan Infinite 200 Pro (Tecan) reader.

2.9. Transmission electron microscopy (TEM)

For particle visualization, 30 μL of sample were adhered on a copper grid with 400-mesh size. Samples were incubated for 1 min at room temperature. After removal of excessive liquid, the samples were fixed with 2.5% glutaraldehyde solution for 15 min. Samples were washed three times with water and then stained in 1% uranyl acetate solution for 30 s. Excessive liquid was removed and the grids were air-dried. For the visualization a Tecnai G^2 200 kV transmission electron microscope (FEI, Eindhoven, The Netherlands) was used.

2.10. Proteomic analysis

Selected samples were digested in solution. Proteins were S-alkylated with iodoacetamide and digested with trypsin (Promega, Madison, WI, USA). Digested samples were loaded on a Thermo Acclaim PepMap300 RSLC C18 separation column (2 μm particle size, 150 x 0.075 mm) with a Thermo Acclaim PepMap μ-precolumn using 0.1% formic acid as the aqueous solvent. A gradient from 6% B (B: 80% acetonitrile) to 40% B in 45 min was applied, followed by a 10 min gradient from 40 to 90% B that facilitates elution of large peptides, at a flow rate of 0.3 μL/min. Detection was performed with a QTOF MS, Bruker maXis 4 G ETD (Bruker, MA, USA), equipped with the captive spray source in positive ion, DDA mode (= switching to MSMS mode for eluting peaks). MS-scans were recorded (range: 150–2200 Da) and the 6 highest peaks were selected for fragmentation. Instrument calibration was performed using ESI calibration mixture (Agilent Technologies, CA, USA).

The analysis files were converted (using Data Analysis, Bruker) to mgf files, which are suitable for performing a MS/MS ion search with ProteinScape 3.0 (Bruker, MASCOT embedded). The files were searched against the Uniprot database (http://www.uniprot.org) for all organisms and *homo sapiens* (taxonomy id: 9606). Only proteins identified with at least 2 peptides and a MASCOT score higher

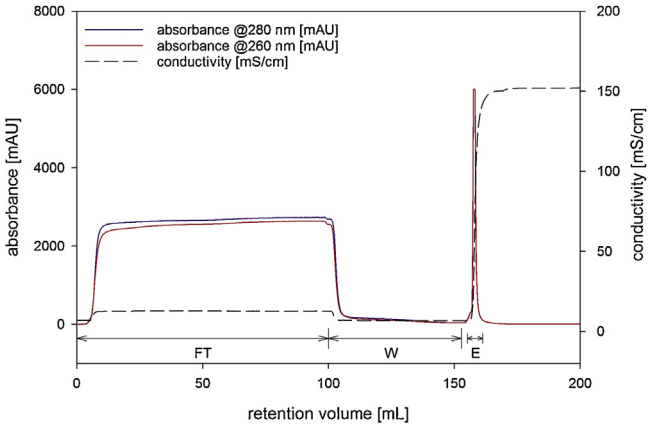

Fig. 1. Chromatogram of a flow-through chromatography run for the removal of small molecular weight impurities from 100 mL Benzonase® treated and 0.8 μm filtered HEK 293 cell culture supernatant, containing HIV-1 gag VLPs and host cell EVs. A 5.4 mL Capto Core 700 column was used. The residence time was 4 min. The column was equilibrated (before loading) and washed (after loading) with 50 mM HEPES, 120 mM NaCl, pH 7.2 buffer. Elution was achieved using 50 mM HEPES, 2 M NaCl, pH 7.2 buffer. FT: flow-through; W: wash; E: elution peak.

than 50 were accepted for further analysis. Alternatively the files were searched with GPM (X!Tandem algorithm embedded) against a human database containing HIV sequence data (downloaded from Uniprot - Oct. 2018).

2.11. Multiangle light scattering (MALS)

MALS measurements for the determination of the light scattering intensity were performed using an Ultimate 3000 HPLC system (Thermo Fisher, Waltham, MA, USA) with a quaternary LPG-3400SD pump, a WPS-3000TSL autosampler and a DAD 3000 UV-detector. Mobile phase consisted of 50 mM HEPES, 150 mM NaCl, pH 7.2. A sample volume of 30 μL was injected in bypass mode using a flow rate of 0.3 mL/min. All samples were measured in duplicates. MALS signals were acquired by the DAWN HELEOS 18-angle detector (Wyatt, Santa Barbara, CA, USA). For HPLC programming Chromeleon 7 software (Thermo Fisher, Waltham, MA, USA) was used. MALS data collection and analysis was performed with ASTRA software, version 6.1.2 (Wyatt, Santa Barbara, CA, USA).

3. Results and discussion

The aim of this work was the development of a chromatographic method to purify HIV-1 gag VLPs and separate them from host cell EVs. A two-step chromatographic method was developed. The first step, based on multimodal core-shell technology, was operated in flow-through mode and aimed to remove small impurities such as host cell proteins and DNA fragments. The second step, based on heparin affinity chromatography, was used to purify and separate VLPs and EVs and further reduce the impurity content.

3.1. Flow-through chromatography of bionanoparticles with core-shell beads

For the purification of HIV-1 gag VLPs and EVs, Benzonase® treated and filtered cell culture supernatant was loaded onto a lab scale column (5.4 mL) packed with Capto Core 700 resin (Fig. 1). A step gradient with 2 M NaCl was employed for elution and two different regeneration steps with 1 M NaOH and 30% 2-Propanol were used (Figure S1, Supplementary Material A). This method allowed the collection of particles in the flow-through (9.4×10^{10} particles/mL) with a yield of 73% and a total recovery of 75% (Table 1). Both, yield and recovery of this method are high when compared

Table 1
Mass balance of the flow-through chromatography run, using a 5.4 mL Capto Core 700 column. S: HEK 293 cell culture supernatant, L: loading material (Benzonase® treated and 0.8 μm filtered HEK 293 cell culture supernatant from batch 1); FT: flow-through; W: wash; E: elution peak; R1: regenerate 1 (1 M NaOH); R2: regenerate 2 (30% 2-Propanol).

	Volume [mL]	Particles [part/mL]	Recovery [%]	Total protein [μg/mL]	dsDNA [ng/mL]	p24 [ng/mL]
S	100.0	1.2E+11	-	491.5	1647.3	n.d.
L	100.0	1.3E+11	100.0	472.1	339.4	683.7
FT	100.0	9.4E+10	73.1	274.3	246.6	626.6
W	54.3	3.3E+09	1.4	49.7	< LLOQ	31.6
E	10.9	3.1E+09	0.3	228.4	156.8	33.7
R1	10.9	n.d.	n.a.	69.9	< LLOQ	< LLOQ
R2	10.9	n.d.	n.a.	1165.0	193.0	< LLOQ
Sum	-	-	**74.8**	-	-	-

n.d. - not determined.
n.a. - not applicable.
< LLOQ - lower than the lower limit of quantification.

to the ones obtained in other virus and VLP purification methods, such as ultracentrifugation and filtration techniques [29–31]. Furthermore, it was possible to achieve higher particle recovery in the flow-through (up to 95%) simply by increasing the loading volume (up to 225 mL) and/or by changing the column hardware (Table S1, Supplementary Material B). The increase in recovery by changing the column hardware, especially the column frits, suggests that particles are entrapped in the frits. This can occur by non-specific adsorption of the particles on the frit's surface or by entrapment of the particles in dead end pores. Additionally, the increase on the recovery by increasing the loading volume (maintaining the same hardware) suggests that particles non-specifically adsorb to other surfaces which can include the column hardware (column wall and tubing) as well as the chromatography station (pumps, tubing and detectors). Those surfaces have limited "binding-sites", resulting in a maximum number of particles that can be loss by unspecific adsorption. Consequently, as the loaded number of particles increases (by increasing the loading volume), the relative amount of particles that are lost by non-specific binding decreases leading to higher recoveries. For that reason, in this method, the loss of VLPs by non-specific adsorption when using industrially relevant loading volumes will not represent a significant loss in the process recovery.

The total protein concentration was reduced from 472.1 μg/mL in the loading material to 274.3 μg/mL in the flow-through, which corresponds to a depletion of 42% (Table 1). This reduction can also be observed in the SDS-PAGE (Fig. 2A) where the FT contains less bands than the loading material (L). Pooled fractions were further analysed by anti-p24 Western blot and p24 ELISA in order to detect and quantify HIV-1 gag protein. Additionally, an anti-HSP90 (EV marker) Western blot was used to detect the presence of heat shock protein 90. According to the p24 ELISA, 92% of the p24 content was collected in the FT. This result is supported by the p24 Western blot (Fig. 2B) as the band for the gag polyprotein (55 kDa) is present in the FT, almost absent in the elution (E) and absent in both regenerations (R1 and R2). The presence of heat shock protein 90 in the FT was confirmed by anti-HSP90 Western blot (Fig. 2C).

The cell culture supernatant was treated with Benzonase®, reducing the initial dsDNA concentration from 1647.3 μg/mL in the supernatant (S) to 339.4 μg/mL in the loading material (L, Table 1). Moreover, a dsDNA depletion of 27% was achieved during the flow-through chromatographic step, with a reduction in dsDNA from 339.4 μg/mL in the L to 246.6 μg/mL in the FT (Table 1). Together, a total depletion of 85% of dsDNA was achieved.

These results demonstrate the capability of the Capto Core 700 resin used in flow-through mode to pre-purify bionanoparticles with reduction on the total protein and dsDNA content. The product

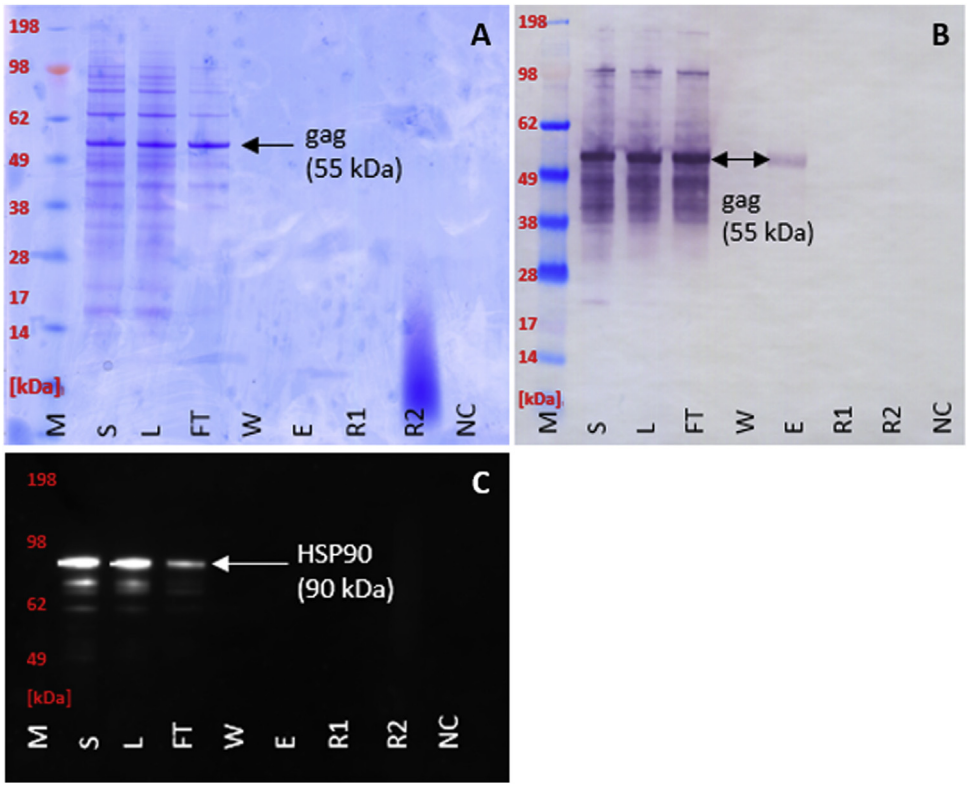

Fig. 2. Characterization of the pooled fractions from the flow-through chromatography run (Fig. 1): (A) SDS-PAGE; (B) p24 Western blot; (C) HSP90 Western blot. M: molecular weight marker; S: HEK 293 cell culture supernatant; L: loading material (Benzonase® treated and 0.8 μm filtered HEK 293 cell culture supernatant from batch 1); FT: flow-through; W: wash; E: elution peak; R1: regenerate 1 (1 M NaOH); R2: regenerate 2 (30% 2-Propanol); NC: negative control (cultivation media).

fraction of this step (FT) can then be further purified using heparin affinity chromatography.

3.2. Separation of HIV-1 gag VLPs and EVs by heparin affinity

Several studies have shown the potential of heparin affinity chromatography for the purification of EVs [32], viruses [21,22,33] and VLPs [24,34]. Additionally, it was shown that different EVs have different affinities to heparin ligands [32]. In our work, we explored the ability of heparin affinity chromatography to separate recombinant HIV-1 gag VLPs produced in HEK 293 cells from host cell EVs. For that purpose, a 2 mL Capto Heparin column was used. In order to avoid non-specific interactions due to the cation exchange properties of the heparin ligands [35], the column was equilibrated with 50 mM HEPES, 120 mM NaCl, pH 7.2 buffer prior to the sample loading. After equilibration, the column was loaded with part of the flow-through (20 mL) collected in the flow-through chromatography run. The sample loading was followed by a 10 CV wash step using the equilibration buffer. Elution was achieved using a 20 CV salt linear gradient from 120 to 2000 mM NaCl, including a 10 CV hold step at the end of the gradient (Fig. 3). The column was regenerated using 1 M NaOH for 10 CV, followed by 30% 2-Propanol for 10 CV (Figure S2, Supplementary Material A). Fractions of 1 mL were collected throughout the entire chromatographic run. All collected fractions were directly injected into a MALS detector using an HPLC in bypass mode. Since the intensity of scattered light is proportional to the number of particles in a certain volume [36–39], we used this fast offline method to detect the presence of particles in each one of the collected fractions (Fig. 3, LS area). Both, UV absorbance and light scattering intensity signals were used as sample pooling criteria. Pooled fractions (flow-through – FT and peak 1 – P1) were further analysed in order to quantify dsDNA (Picogreen assay), quantify and detect total and specific protein (Bradford assay, SDS-PAGE, Western blot, p24 ELISA and mass spectrometry) and quantify and characterize particles (NTA and TEM). The flow-through and/or elution of particles from the Capto Heparin column can be tracked by the light scattering signal. In Fig. 3, each bar on the graph represents the light scattering area (LS area) of each 1 mL fraction collected during the purification run. This area corresponds to the area under the curve of the light scattering peak obtained using the MALS detector and it is directly proportional to the scattered intensity. As a result, higher values of LS area represent higher particle concentration. Considering the LS area signal during the loading phase (Fig. 3, from 0 to 20 mL retention volume), despite particles start to breakthrough immediately after 1 CV loading, a slow breakthrough is observed. This suggests that while some particles bind to the heparin ligands, others are excluded from the column. This indicates that different particles have different affinity to the heparin ligands. Moreover, at the end of the loading phase (Fig. 3, at 20 mL) the LS area signal is still lower than the one measured for the loading material (data not shown), indicating that the column was not completely overloaded. The flow-through pooled sample (FT) included all the fractions collected from 1 CV after the column started to be loaded until the first 2.5 CV of the wash step (Fig. 3, from 2 to 25 mL retention volume), simultaneously ensuring that all unbound particles are contained in this sample and avoiding sample dilution.

The total amount of unbound particles (FT) was 5.4×10^{11}, corresponding to 54% of the loaded particles (Table 2). Despite most of the particles in this sample had a diameter of 160 nm (statistical mode measured by NTA), the particle size distribution was wide, ranging from about 100 to 500 nm in diameter (Figure S3, Supplementary Material A). This suggests the presence of a heterogeneous particle population, which is common in EV samples [12]. Additionally, the FT contained 24% of the total protein (equivalent to a protein amount of 0.7 mg), 64% of the dsDNA (equivalent to a

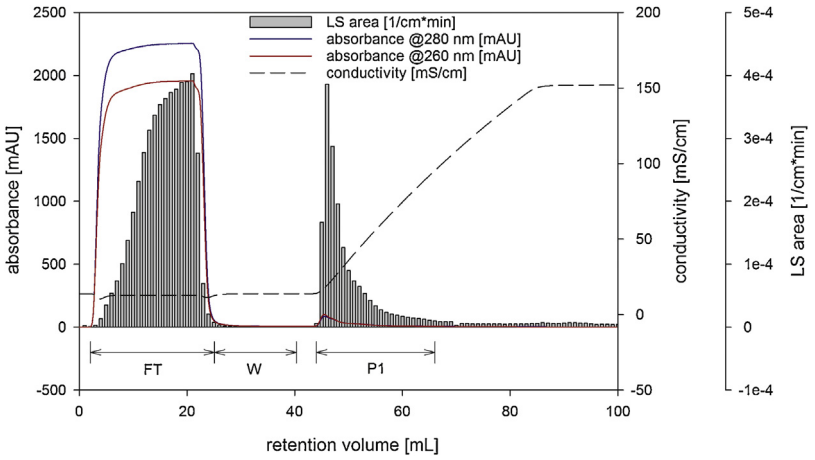

Fig. 3. Chromatogram of a heparin affinity chromatography run for the separation of HIV-1 gag VLPs and EVs. The column was loaded with 20 mL of a flow-through fraction from a flow-through chromatography run (in which the loading material was Benzonase® treated and 0.8 μm filtered HEK 293 cell culture supernatant from batch 2). A 2 mL Capto Heparin column was used. The residence time was 4 min. The column was equilibrated (before loading) and washed (after loading) with 50 mM HEPES, 120 mM NaCl, pH 7.2 buffer. Elution was achieved using a salt linear gradient from 120 to 2000 mM NaCl. FT: flow-through; W: wash; P1: elution peak 1; H: hold step (100% B).

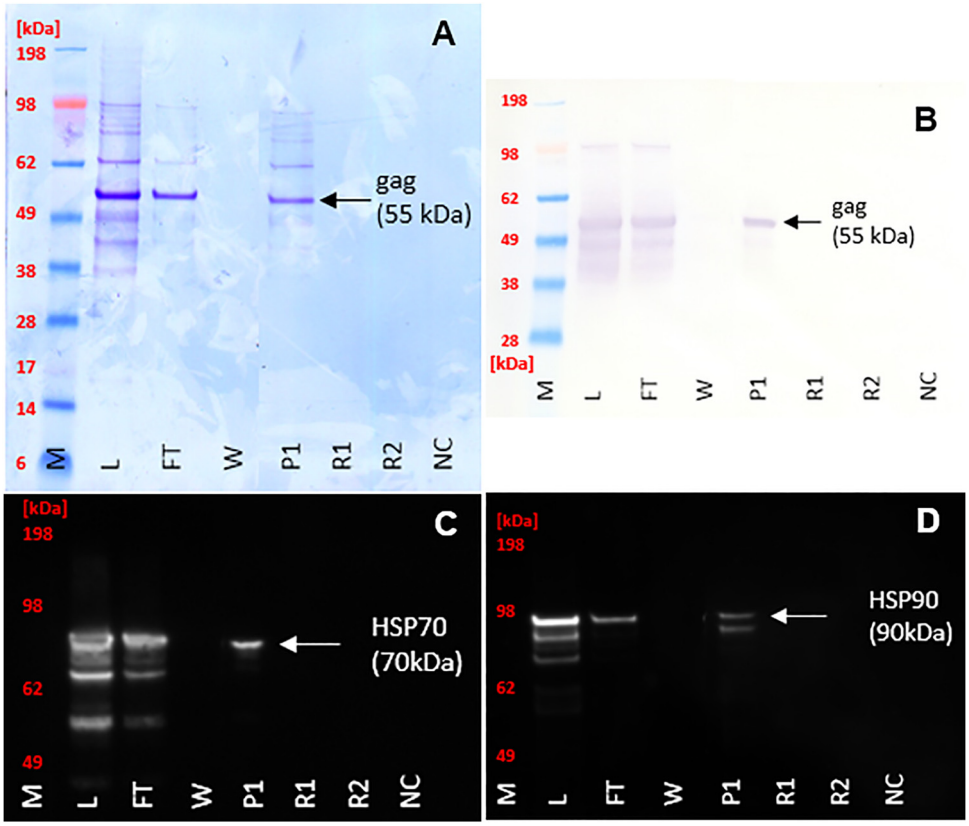

Fig. 4. Characterization of the pooled fractions from the heparin affinity chromatography run (Fig. 3): (A) SDS-PAGE; (B) p24 Western blot; (C) HSP70 Western blot; (D) HSP90 Western blot. M: molecular weight marker; L: loading material (flow-through fraction from a flow-through chromatography run); FT: flow-through; W: wash; P1: elution peak 1; R1: regenerate 1 (1 M NaOH); R2: regenerate 2 (30% 2-Propanol); NC: negative control (cultivation media).

dsDNA amount of 1.8 μg) and 66% of the HIV-1 gag protein (equivalent to a p24 amount of 3.6 μg). Bound particles start eluting from the column during the salt linear gradient at a conductivity of about 14 mS/cm (Fig. 3, at 44 mL). All fractions in the linear gradient elution with LS area higher than 1.0×10^{-5} cm^{-1} min^{-1} were included in the elution pooled sample (Fig. 3, P1, from 44 to 66 mL retention volume). A total amount of 1.5×10^{11} particles was found in P1, corresponding to 15% of the loaded particles (Table 2). Particle size analysis by NTA revealed that most of the particles in P1 have a diameter of 153 nm (statistical mode) and 80% of the particles had a diameter between 133 and 230 nm (D10 and D90, respectively). This suggests the presence of a more homogeneous particle population, when compared to the FT. Moreover, similar particle size distributions were previously demonstrated for HIV-1 gag VLPs [5]. Additionally, P1 contained 12% of the total protein (equivalent to a protein amount of 0.4 mg), 18% of the dsDNA (equivalent to a dsDNA amount of 0.5 μg) and 25% of the HIV-1 gag protein (equivalent to a p24 amount of 1.3 μg). Whereas the different particle size distribution of FT and P1 suggests the presence of different particle populations, the results obtained by SDS-PAGE, Western

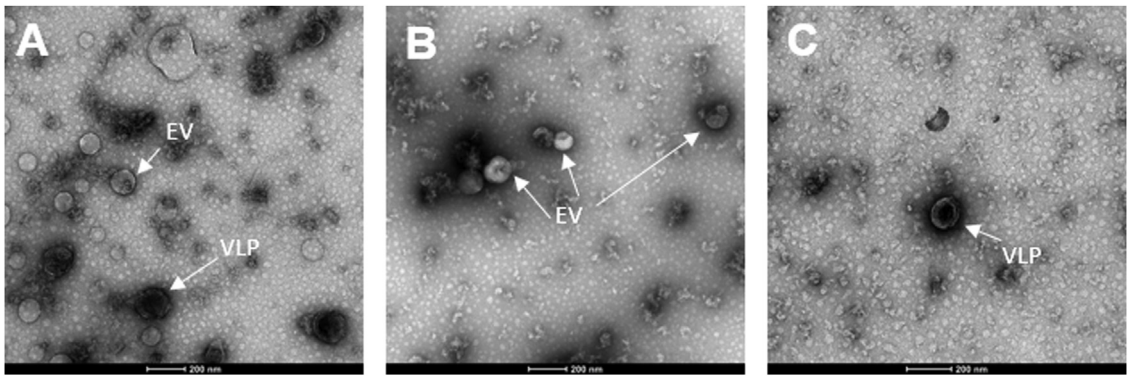

Fig. 5. Transmission electron microscopy pictures of the pooled fractions from the heparin affinity chromatography run (Fig. 3): (A) loading material; (B) flow-through; (C) elution peak 1. Scale bars correspond to 200 nm.

Table 2
Mass balance of the heparin affinity chromatography run for the separation of HIV-1 gag VLPs and EVs, using a 2 mL Capto Heparin column. L: loading material (flow-through fraction from a flow-trough chromatography run in which the loading material was Benzonase® treated and 0.8 μm filtered HEK 293 cell culture supernatant from batch 2); FT: flow-through; W: wash; P1: elution peak.

	Volume [mL]	Particles [part/mL]	Recovery [%]	Total protein [μg/mL]	dsDNA [ng/mL]	p24 [ng/mL]
L	20.0	5.0E+10	100.0	147.3	143.0	273.2
FT	23.0	2.4E+10	53.8	31.0	79.6	157.8
W	15.1	< LLOQ	n.a.	< LLOQ	< LLOQ	< LLOQ
P1	22.0	6.9E+09	15.1	16.5	22.7	61.0
Sum	–	–	**69.1**	–	–	–

n.a. - not applicable.
< LLOQ - lower than the lower limit of quantification.

blot and TEM do not disclose significant differences between those samples. In the SDS-PAGE, a band around 55 kDa indicates the presence of the gag protein in both samples (Fig. 4A, FT and P1). This is confirmed in the Western blot analysis (Fig. 4B). Additionally, HSP70 and HSP90 were used as indicator proteins for EVs [40,41] and the corresponding bands (70 kDa and 90 kDa) are also detected by Western blot analysis in both fractions (Fig. 4C and D). TEM pictures demonstrate the presence of intact spherical particles in both samples (Fig. 5A, B and Figure S4, Supplementary Material A).

In order to further characterize and discriminate the separated particle populations, proteomic analysis of FT and P1 pooled fractions was performed. From the total 348 identified proteins, 170 were present in both fractions, 62 only in FT and 116 only in P1 (Figure S5, Supplementary material C, FT_selected and P1_selected). We compared these proteins with the TOP 100 most identified proteins in EVs from the EVpedia database (evpedia.info). On one hand, 30% of the unique proteins in FT are part of the TOP 100 most identified proteins in EVs. On the other hand, only 6% of the unique proteins in P1 are in this list. Furthermore, 47% of the unique proteins in P1 are known to interact with the HIV-1 gag protein or have been found incorporated in HIV-1 gag viruses and virus-like particles (HIV-1 interactions in ncbi.nlm.nih.gov/gene). Considering both, particle size distribution and proteomic analysis, we conclude that in P1 HIV-1 gag VLPs are enriched and in FT a heterogeneous mixture of host cell EVs is present.

In order to perform an adequate comparison of the impurity and p24 contents (representative of the HIV-1 gag content) between both samples (FT and P1), the values obtained in the Bradford, Picogreen and p24 ELISA assays were normalized to 10^9 particles (as an hypothetical vaccination dose). The dsDNA content per dose was similar in both samples (FT: 3.4 ng/10^9 particles; P1: 3.3 ng/10^9 particles). These values already meet the requirements of the regulatory agencies (<10 ng residual dsDNA per dose) [42]. The total protein content and the p24 content were slightly higher in P1 (total protein: 2.4 μg/10^9 particles; p24: 8.8 ng/10^9 particles) compared to FT (total protein: 1.3 μg/10^9 particles; p24: 6.7 ng/10^9 particles).

Despite the recent efforts on the characterization of the role of EVs upon retroviral infection, as well as studies regarding the similarities in EVs and retroviruses biogenesis, so far no discriminative feature for these particles has been described except for high resolution imaging techniques such as cryo-EM. We used the combination of size distribution data and proteomic data to characterize the type of particles present in each sample. This method is simple and maybe useful for rapid isolation of extracellular vesicles.

4. Conclusion

This two-step chromatography method combining a core-shell multimodal flow-through and a heparin binding chromatography is able to separate the enveloped VLPs from EVs. The first step is mainly for the reduction of small molecular impurities, while the second step separates different particles. The method is scalable and allows a fast particle separation within one day. This is in contradiction to other protocols where the extracellular vesicles are recovered by binding to heparin affinity chromatography. The collection of the fractions must be performed with a detector such as nanoparticle tracking analysis or multiangle light scattering to track the particles. The UV signal is not sensitive enough for the particle detection. The method solves the crucial problem of VLP and EV separation and quantification on a scalable robust platform with chromatography. In comparison to other methods such as ultracentrifugation this opens the possibility for a large-scale production of VLPs and EVs as well as the development of a small scale HPLC based analytical method in the future.

Acknowledgements

This work has been supported by the Federal Ministry for Digital and Economic Affairs (bmwd), the Federal Ministry for Transport, Innovation and Technology (bmvit), the Styrian Business Promotion Agency SFG, the Standortagentur Tirol, Government of Lower Austria and ZIT - Technology Agency of the City of Vienna through the COMET-Funding Program managed by the Austrian Research Promotion Agency FFG. The funding agencies had no influence on the conduct of this research. Patricia Pereira Aguilar was supported by the Austrian Science Fund (project BioToP; FWF W1224). We want to thank Friedrich Altmann and Clemens Grünwald-Gruber for providing mass spectrometry data.

Appendix A. Supplementary data

Supplementary material related to this article can be found, in the online version, at doi:https://doi.org/10.1016/j.chroma.2018.12.035.

References

[1] S. Welsch, B. Müller, H.G. Kräusslich, More than one door - budding of enveloped viruses through cellular membranes, FEBS Lett. 581 (2007) 2089–2097.
[2] J.W. Bess, R.J. Gorelick, W.J. Bosche, L.E. Henderson, L.O. Arthur, Microvesicles are a source of contaminating cellular proteins found in purified HIV-1 preparations, Virology 230 (1997) 134–144.
[3] A. Arakelyan, W. Fitzgerald, S. Zicari, C. Vanpouille, L. Margolis, Extracellular vesicles carry HIV env and facilitate hiv infection of human lymphoid tissue, Sci. Rep. 7 (2017) 1695.
[4] P. Gluschankof, I. Mondor, H.R. Gelderblom, Q.J. Sattentau, Cell membrane vesicles are a major contaminant of gradient-enriched human immunodeficiency virus type-1 preparations, Virology 230 (1997) 125–133.
[5] P. Steppert, D. Burgstaller, M. Klausberger, P. Kramberger, A. Tover, E. Berger, K. Nöbauer, E. Razzazi-Fazeli, A. Jungbauer, Separation of HIV-1 gag virus-like particles from vesicular particles impurities by hydroxyl-functionalized monoliths, J. Sep. Sci. 40 (2017) 979–990.
[6] R. Cantin, J. Diou, D. Bélanger, A.M. Tremblay, C. Gilbert, Discrimination between exosomes and HIV-1: purification of both vesicles from cell-free supernatants, J. Immunol. Methods 338 (2008) 21–30.
[7] L. Deml, C. Speth, M.P. Dierich, H. Wolf, R. Wagner, Recombinant HIV-1 Pr55gag virus-like particles: potent stimulators of innate and acquired immune responses, Mol. Immunol. 42 (2005) 259–277.
[8] P. Steppert, D. Burgstaller, M. Klausberger, E. Berger, P.P. Aguilar, T.A. Schneider, P. Kramberger, A. Tover, K. Nöbauer, E. Razzazi-Fazeli, A. Jungbauer, Purification of HIV-1 gag virus-like particles and separation of other extracellular particles, J. Chromatogr. A 1455 (2016) 93–101.
[9] E. Willms, C. Cabañas, I. Mäger, M.J.A. Wood, P. Vader, Extracellular vesicle heterogeneity: subpopulations, isolation techniques, and diverse functions in cancer progression, Front. Immunol. 9 (2018) 738.
[10] R.A. Dragovic, C. Gardiner, A.S. Brooks, D.S. Tannetta, D.J. Ferguson, P. Hole, B. Carr, C.W. Redman, A.L. Harris, P.J. Dobson, P. Harrison, I.L. Sargent, Sizing and phenotyping of cellular vesicles using nanoparticle tracking analysis, Nanomedicine 7 (2011) 780–788.
[11] G. van Niel, G. D'Angelo, G. Raposo, Shedding light on the cell biology of extracellular vesicles, Nat. Rev. Mol. Cell Biol. 19 (2018) 213–228.
[12] G. Raposo, W. Stoorvogel, Extracellular vesicles: exosomes, microvesicles, and friends, J Cell. Biol. 200 (2013) 373–383.
[13] L.T. Brinton, H.S. Sloane, M. Kester, K.A. Kelly, Formation and role of exosomes in cancer, Cell Mol. Life Sci. 72 (2015) 659–671.
[14] F.T. Borges, L.A. Reis, N. Schor, Extracellular vesicles: structure, function, and potential clinical uses in renal diseases, Braz. J. Med. Biol. Res. 46 (2013) 824–830.
[15] E. Nolte-'t Hoen, T. Cremer, R.C. Gallo, L.B. Margolis, Extracellular vesicles and viruses: are they close relatives? Proc. Natl. Acad. Sci. U. S. A. 113 (2016) 9155–9161.
[16] J.J. Wang, R. Horton, V. Varthakavi, P. Spearman, L. Ratner, Formation and release of virus-like particles by HIV-1 matrix protein, AIDS 13 (1999) 281–283.
[17] S.J. Gould, A.M. Booth, J.E. Hildreth, The trojan exosome hypothesis, Proc. Natl. Acad. Sci. U. S. A. 100 (2003) 10592–10597.
[18] R. Khachatoorian, W. Cohn, A. Buzzanco, R. Riahi, V. Arumugaswami, A. Dasgupta, J.P. Whitelegge, S.W. French, HSP70 copurifies with zika virus particles, Virology 522 (2018) 228–233.
[19] P. Satzer, M. Wellhoefer, A. Jungbauer, Continuous separation of protein loaded nanoparticles by simulated moving bed chromatography, J. Chromatogr. A 1349 (2014) 44–49.
[20] M.Y. Konoshenko, E.A. Lekchnov, A.V. Vlassov, P.P. Laktionov, Isolation of extracellular vesicles: General methodologies and latest trends, Biomed. Res. Int. 2018 (2018), 8545347.
[21] R. Spannaus, C. Miller, D. Lindemann, J. Bodem, Purification of foamy viral particles, Virology 506 (2017) 28–33.
[22] M. Nasimuzzaman, J.C.M. van der Loo, P. Malik, Production and purification of baculovirus for Gene therapy application, J Vis. Exp. (Apr 9) (2018) 134.
[23] M. Nasimuzzaman, D. Lynn, J.C. van der Loo, P. Malik, Purification of baculovirus vectors using heparin affinity chromatography, Mol. Ther. Methods Clin. Dev. 3 (2016) 16071.
[24] R. Minkner, R. Baba, Y. Kurosawa, S. Suzuki, T. Kato, S. Kobayashi, E.Y. Park, Purification of human papillomavirus-like particles expressed in silkworm using a bombyx mori nucleopolyhedrovirus bacmid expression system, J. Chromatogr. B Analyt. Technol. Biomed. Life Sci. 1096 (2018) 39–47.
[25] T. Weigel, T. Solomaier, A. Peuker, T. Pathapati, M.W. Wolff, U. Reichl, A flow-through chromatography process for influenza A and B virus purification, J. Virol. Methods 207 (2014) 45–53.
[26] H.P. Erickson, Size and shape of protein molecules at the nanometer level determined by sedimentation, gel filtration, and electron microscopy, Biol. Proced. Online 11 (2009) 32–51.
[27] P. Kramberger, L. Urbas, A. Štrancar, Downstream processing and chromatography based analytical methods for production of vaccines, gene therapy vectors, and bacteriophages, Hum. Vaccin Immunother. 11 (2015) 1010–1021.
[28] J. Schüpbach, Z. Tomasik, M. Knuchel, M. Opravil, H.F. Günthard, D. Nadal, J. Böni, S.H.C. Study, S.H.M.C.C. Study, Optimized virus disruption improves detection of HIV-1 p24 in particles and uncovers a p24 reactivity in patients with undetectable HIV-1 RNA under long-term HAART, J. Med. Virol. 78 (2006) 1003–1010.
[29] T. Vicente, C. Peixoto, M.J. Carrondo, P.M. Alves, Purification of recombinant baculoviruses for gene therapy using membrane processes, Gene Ther. 16 (2009) 766–775.
[30] C. Peixoto, M.F. Sousa, A.C. Silva, M.J. Carrondo, P.M. Alves, Downstream processing of triple layered rotavirus like particles, J. Biotechnol. 127 (2007) 452–461.
[31] C. Ladd Effio, T. Hahn, J. Seiler, S.A. Oelmeier, I. Asen, C. Silberer, L. Villain, J. Hubbuch, Modeling and simulation of anion-exchange membrane chromatography for purification of Sf9 insect cell-derived virus-like particles, J. Chromatogr. A 1429 (2016) 142–154.
[32] L. Balaj, N.A. Atai, W. Chen, D. Mu, B.A. Tannous, X.O. Breakefield, J. Skog, C.A. Maguire, Heparin affinity purification of extracellular vesicles, Sci. Rep. 5 (2015) 10266.
[33] P. Du, S. Sun, J. Dong, X. Zhi, Y. Chang, Z. Teng, H. Guo, Z. Liu, Purification of foot-and-mouth disease virus by heparin as ligand for certain strains, J. Chromatogr. B Analyt. Technol. Biomed. Life Sci. 1049-1050 (2017) 16–23.
[34] M. Zaveckas, S. Snipaitis, H. Pesliakas, J. Nainys, A. Gedvilaite, Purification of recombinant virus-like particles of porcine circovirus type 2 capsid protein using ion-exchange monolith chromatography, J. Chromatogr. B Analyt. Technol. Biomed. Life Sci. 991 (2015) 21–28.
[35] S. Xiong, L. Zhang, Q.Y. He, Fractionation of proteins by heparin chromatography, Methods Mol. Biol 424 (2008) 213–221.
[36] P. Steppert, D. Burgstaller, M. Klausberger, A. Tover, E. Berger, A. Jungbauer, Quantification and characterization of virus-like particles by size-exclusion chromatography and nanoparticle tracking analysis, J. Chromatogr. A 1487 (2017) 89–99.
[37] P.J. Wyatt, Measurement of special nanoparticle structures by light scattering, Anal. Chem. 86 (2014) 7171–7183.
[38] K. Kamide, T. Dobashi, Chapter 7 - light scattering, in: Physical Chemistry of Polymer Solutions, Elsevier Science, Amsterdam, 2000, pp. 377–442.
[39] S. Podzimek, W. John, Sons, Light Scattering, Size Exclusion Chromatography, and Asymmetric Flow Field Flow Fractionation : Powerful Tools for the Characterization of Polymers, Proteins and Nanoparticles, A John Wiley & Sons, Inc., Hoboken, 2011.
[40] J. Kowal, G. Arras, M. Colombo, M. Jouve, J.P. Morath, B. Primdal-Bengtson, F. Dingli, D. Loew, M. Tkach, C. Théry, Proteomic comparison defines novel markers to characterize heterogeneous populations of extracellular vesicle subtypes, Proc. Natl. Acad. Sci. U. S. A. 113 (2016) E968–977.
[41] Y. Yoshioka, Y. Konishi, N. Kosaka, T. Katsuda, T. Kato, T. Ochiya, Comparative marker analysis of extracellular vesicles in different human cancer types, J. Extracell Vesicles 2 (2013).
[42] U.S. Department of Health and Human Services Food and Drug Administration Guidance for Industry, Bioanalytical Method Validation, Center for Drug Evaluation and Research (CDER) Center for Veter inary Medic ine (CVM), 2001.

Supplementary Material A

Separation of virus-like particles and extracellular vesicles by flow through and heparin affinity chromatography

Katrin Reiter[1], Patricia Pereira Aguilar[2], Viktoria Wetter[1], Petra Steppert[2], Andres Tover[3], Alois Jungbauer[1,2]

[1] Austrian Centre of Industrial Biotechnology, Vienna, Austria
[2] Department of Biotechnology, University of Natural Resources and Life Sciences, Vienna, Austria
[3] Icosagen AS, Tartumaa, Estonia

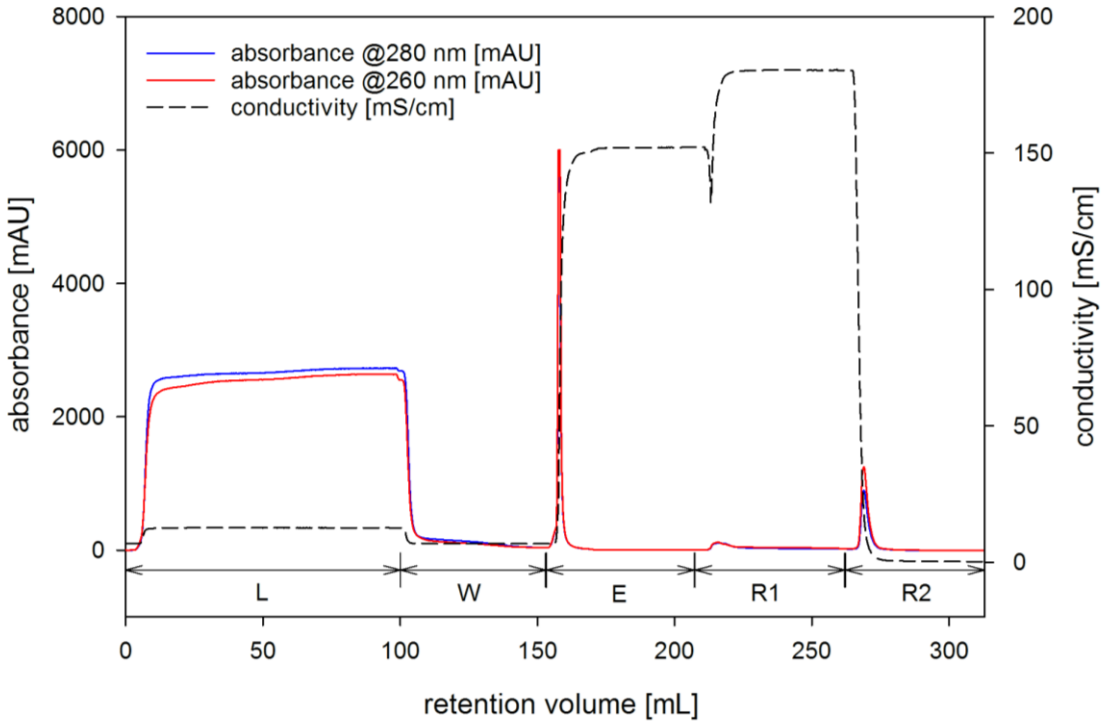

Figure S1: Chromatogram of a flow-through chromatography run for the removal of small molecular weight impurities from 100 mL Benzonase® treated and 0.8 µm filtered HEK 293 cell culture supernatant, containing HIV-1 gag VLPs and host cell EVs. A 5.4 mL Capto Core 700 column was used. The residence time was 4 min. The column was equilibrated (before loading) and washed (after loading) with 50 mM HEPES, 120 mM NaCl, pH 7.2 buffer. Elution was achieved using a 50 mM HEPES, 2 M NaCl, pH 7.2 buffer. L: load; W: wash; E: elution; R1: regeneration with 1 M NaOH; R2: regeneration with 30% 2-Propanol.

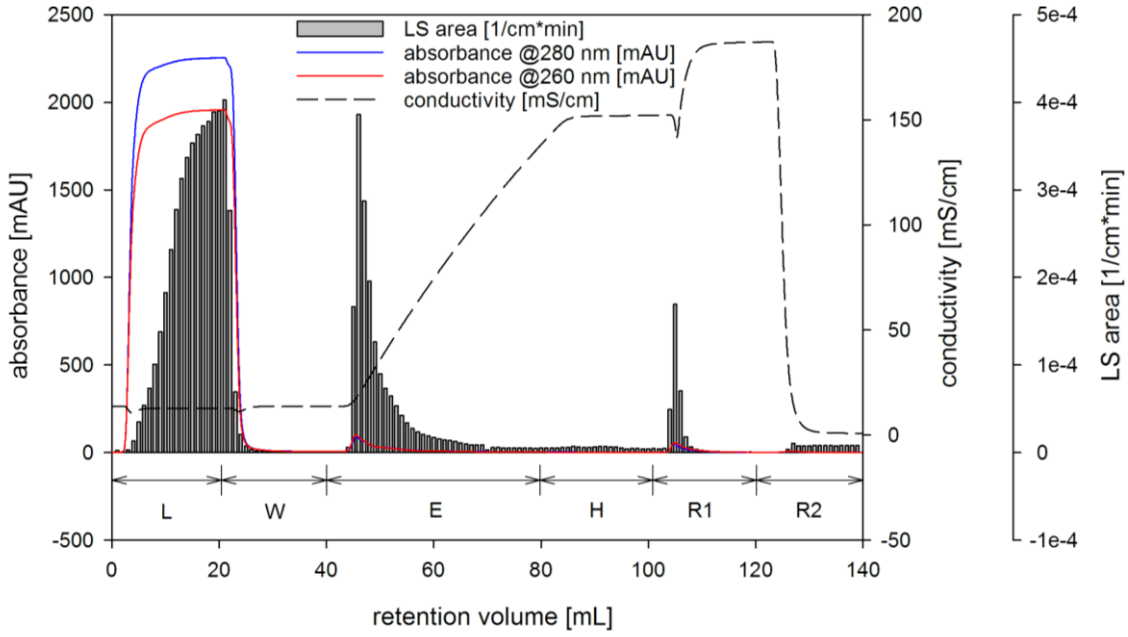

Figure S2: Chromatogram of a heparin affinity chromatography run for the separation of HIV-1 gag VLPs and EVs. The column was loaded with 20 mL of a flow-through fraction from a flow-through chromatography run (in which the loading material was Benzonase® treated and 0.8 µm filtered HEK 293 cell culture supernatant from batch 2). A 2 mL Capto Heparin column was used. The residence time was 4 min. The column was equilibrated (before loading) and washed (after loading) with 50 mM HEPES, 120 mM NaCl, pH 7.2 buffer. Elution was achieved using a salt linear gradient from 120 to 2000 mM NaCl. L: load; W: wash; E: elution; H: hold step (100% B); R1: regeneration with 1 M NaOH; R2: regeneration with 30% 2-Propanol.

Table S1: Mass balance of the heparin affinity chromatography run for the separation of HIV-1 gag VLPs and EVs, using a 2 mL Capto Heparin column. L: loading material (flow-through fraction from a flow-through chromatography run in which the loading material was Benzonase® treated and 0.8 µm filtered HEK 293 cell culture supernatant from batch 2); FT: flow-through; W: wash; E: complete elution step.

	Volume [mL]	Particles [part/mL]	Recovery [%]	Total protein [µg/mL]	dsDNA [ng/mL]	p24 [ng/mL]
L	20.0	5.0E+10	100.0	147.3	143.0	273.2
FT	23.0	2.4E+10	53.8	31.0	79.6	157.8
W	15.1	< LLOQ	0.0	< LLOQ	< LLOQ	< LLOQ
E	60.3	2.8E+09	16.7	28.2	< LLOQ	< LLOQ
Sum	-	-	**70.5**	-	-	-

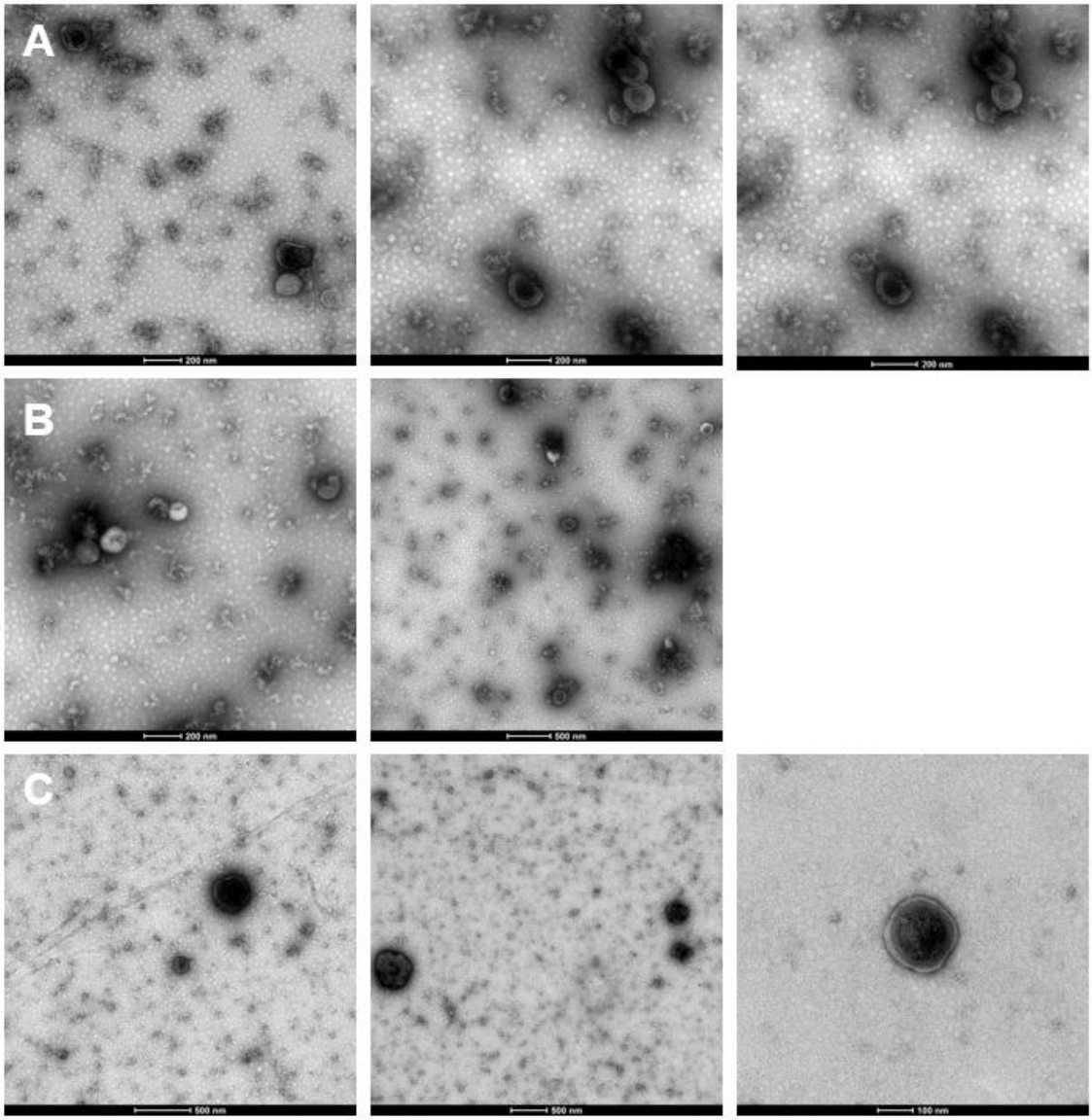

Figure S3: Transmission electron microscopy pictures of the pooled samples from the heparin affinity chromatography run. (A) loading material; (B) flow-through; (C) elution peak (P1).

(A)

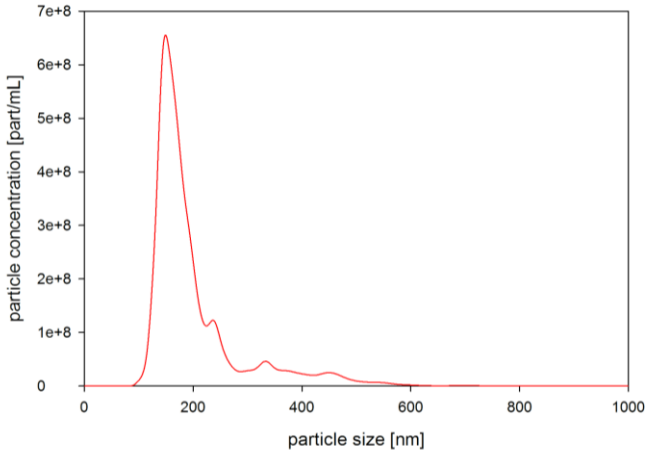

(B)

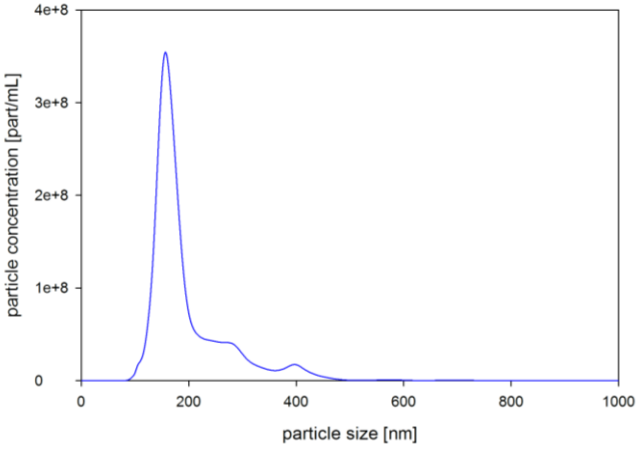

(C)

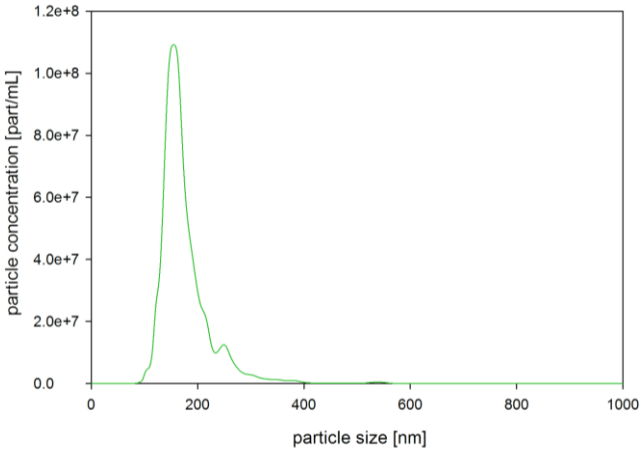

Figure S4: Particle size distribution, measured by nanoparticle tracking analysis, of the pooled samples from the heparin affinity chromatography run. (A) loading material; (B) flow-through; (C) elution peak (P1).

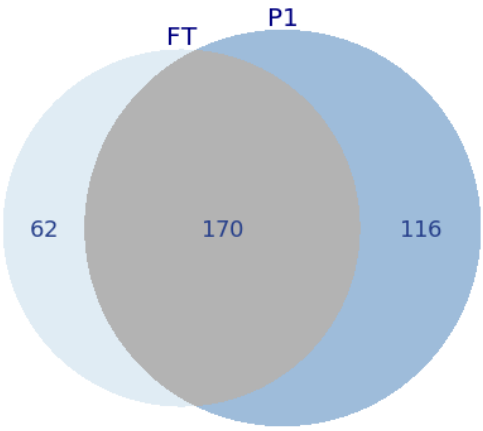

Figure S5: Comparison of proteins identified by mass spectrometry in the flow-through (FT) and elution peak (P1) of the heparin affinity chromatography run.

Supplementary Material B

Separation of virus-like particles and extracellular vesicles by flow through and heparin affinity chromatography

Katrin Reiter[1], Patricia Pereira Aguilar[2], Viktoria Wetter[1], Petra Steppert[2], Andres Tover[3], Alois Jungbauer[1,2]

[1] Austrian Centre of Industrial Biotechnology, Vienna, Austria
[2] Department of Biotechnology, University of Natural Resources and Life Sciences, Vienna, Austria
[3] Icosagen AS, Tartumaa, Estonia

Influence of column hardware and bed support on particle recovery

1. Materials and Methods

Different column hardware and bed supports (frits/nets) were tested in order to evaluate their impact on particle recovery due to potential particle entrapment or non-specific adsorption. Tricorn 10/20 (GE Healthcare, Uppsala, Sweden) and XK 16/20 chromatography columns (GE Healthcare) were used as column hardware. For the Tricorn 10/20 columns, two different types of frits were used, a Tricorn 10 filter (GE Healthcare) with 7 µm porosity, made of polyethylene and a Tricorn 10 Coarse filter (GE Healthcare) with 25 µm porosity, made of Vyon™, a high-density polyethylene. The XK 16/20 chromatography column was used with the provided net with 10 µm porosity, made of polypropylene and polyamide. All columns were packed with the multimodal flow-through chromatography resin Capto Core 700 (GE Healthcare). Both Tricorn 10/20 columns had a column volume of 1.7 mL. The XK 16/20 column volume was 10 mL. Benzonase® treated and 0.8 µm filtered HEK 293 cell culture supernatant was used as loading material. Buffer A consisted of 50 mM HEPES, pH 7.2 and buffer B of 50 mM HEPES, 2 M NaCl, pH 7.2. Columns were equilibrated with 6% B to ensure same conductivity as in the loading material. After loading, the column was washed with the equilibration buffer. Elution was performed by applying a step gradient of 100% B. Residence time was 4 min for all columns.

2. Results

As VLPs and EVs range between 30-500 nm in diameter they can get entrapped in the column frit/net. We used different column hardware and types of frits for investigation of this possibility. Table S1 shows the particle recovery for each combination of column hardware and frits tested. For determination of particle recovery, the particle concentration was measured by nanoparticle tracking analysis. Comparing the Tricorn 10/20 columns using two different types of frits, an increase in particle recovery from 66% to 74% was observed for the frit with larger pores (7 µm compared to 25 µm). Using the XK 16/20 column we were able to further increase the particle recovery up to 97%, despite the 10 nm porosity referred by the manufacturer. We assume that such an increasing recovery is due to the change of the bed support from frit to net. Although some unspecific absorption can still occur in the nets, the entrapment of particles in dead end pores is avoided.

This results show the importance of the selection of the hardware and its impact on particle recovery for downstream processing of enveloped bionanoparticles.

Table S1: Influence of column hardware and bed support material on particle recovery

Column hardware	Bed support	Material	Loading volume [CV]	Column volume [mL]	Particle recovery [%]
Tricorn 10/20	Tricorn 10 Filter (porosity: 7 µm)	Polyethylene	29	1.7	65
Tricorn 10/20	Tricorn 10 Coarse Filter (porosity: 25 µm)	Vyon™	29	1.7	73
XK 16/20	Net ring (porosity: 10 µm)	Polypropylene, Polyamide	22.5	10.0	97

PUBLICATION VI

Separation of influenza virus-like particles from baculovirus by polymer grafted anion-exchanger

Journal:	*Journal of Separation Science*
Manuscript ID	Draft
Wiley - Manuscript type:	Original Paper
Date Submitted by the Author:	n/a
Complete List of Authors:	Reiter, Katrin ; Austrian Centre of Industrial Biotechnology Pereira Aguilar, Patricia; BOKU, Department of Biotechnology Joseph, Judith ; Austrian Centre of Industrial Biotechnology Grammelhofer, Dominik; Austrian Centre of Industrial Biotechnology Steppert, Petra; University of Natural Resources and Life Sciences, Vienna, Biotechnology Jungbauer, Alois; Univeersity of Natural Resources and Applied Life Sciences, Department of Biotechnology
Keywords:	Anion exchange chromatography, downstream processing, HIV-1 gag, insect cells, vaccine

SCHOLARONE™
Manuscripts

For submission to Journal of Separation Science

Separation of influenza virus-like particles from baculovirus by polymer grafted anion-exchanger

Katrin Reiter[1], Patricia Pereira Aguilar[1,2], Dominik Grammelhofer[1], Judith Joseph[1], Petra Steppert[2], Alois Jungbauer[1,2*]

[1] Austrian Centre of Industrial Biotechnology, Vienna, Austria

[2] Department of Biotechnology, University of Natural Resources and Life Sciences, Vienna, Austria

*Corresponding author

Univ.Prof. Dipl.-Ing. Dr.nat.techn. Alois Jungbauer

Department of Biotechnology

University of Natural Resources and Life Sciences Vienna,

Muthgasse 18, 1190 Vienna

Phone: +43 1 47654-79083

Fax: +43 1 47654-79009

E-mail: alois.jungbauer@boku.ac.at

For Review Only

23 **List of Abbreviations**

AcMNPV	Autographa californica multicapsid nucleopolyhedrovirus
AIEX	Anion exchange chromatography
BEVS	Baculovirus expression vector system
CV	Column volume
DBC	Dynamic binding capacity
DO	Dissolved oxygen
dsDNA	Double-stranded deoxyribonucleic acid
DTT	1,4-Dithiotreitol
EV	Extracellular vesicles
FDA	Food and drug administration
FT	Flow-through
Gp64	Glycoprotein 64
H1	Hemagglutinin 1
HEPES	4-(2-hydroxyethyl)-1-piperazineethanesulfonic acid
HIV-1	Human immunodeficiency virus-1
LS	Light scattering
LLOQ	Lowest limit of quantification
MALS	Multiangle Light Scattering
MES	2-(N-moprholino)ethanesulfate acid
NaCl	Sodium chloride
NaOH	Sodium hydroxide
NTA	Nanoparticle Tracking Analysis

For Review Only

PBS	Phosphate buffered saline
TCID50	Tissue Culture Infective Dose 50
TEM	Transmission Electron Microscopy
TMAE	Trimethylammoniumethyl
VLP	Virus-like particle

Keywords: Anion exchange chromatography; downstream processing; HIV-1 gag, insect cells, vaccine

For Review Only

Abstract

The baculovirus expression vector system is a very powerful tool to produce virus-like particles and gene-therapy vectors, but the removal of co-expressed baculovirus has been a major barrier for wider industrial use. We used chimeric HIV-1 gag influenza-HA VLPs produced in *Tnms*42 insect cells using the baculovirus insect cell expression vector system as model VLPs. A fast and simple purification method for these VLPs with direct capture and purification within one chromatography step was developed. The insect cell culture supernatant was treated with endonuclease and filtered, before it was directly loaded onto a polymer grafted anion exchanger and eluted by a linear salt gradient. A 4.3 log clearance of baculovirus from VLPs was achieved. The absence of the baculovirus capsid protein (vp39) in the product fraction was additionally shown by HPLC-MS. When considering a vaccination dose of 10^9 particles, 4200 doses can be purified per L pre-treated supernatant, meeting the requirements for vaccines with <10 ng dsDNA/dose and 3.4 µg protein/dose in a single step. The process is simple with a very low number of handling steps and has the characteristics to become a platform for purification of these types of VLPs.

For Review Only

1. Introduction

The insect-cell baculovirus expression vector system (BEVS) has been widely used for industrial manufacturing of vaccines [1, 2] and gene therapy vectors [3]. The major challenge for effective downstream processing of virus-like particles (VLPs) produced using BEVS is the co-expression of baculovirus and other extracellular vesicles (EVs) alongside VLPs [4, 5]. VLPs based on the HIV-1 gag construct are spherical nanoparticles with a diameter between 100-200 nm, surrounded by a lipid envelope [6-9]. Baculoviruses are rod-shaped, enveloped double-stranded DNA (dsDNA) viruses with a particle size of 30-70 nm in diameter and 200-400 nm in length [10, 11]. During budding from the host cell, baculovirus nucleocapsids obtain a host cell-derived envelope which is enriched with the baculovirus major envelope glycoprotein gp64 [12, 13]. The nucleocapsid core is composed mainly by the major capsid protein vp39, which encapsulates the viral genome and is used as specific marker for the presence of baculovirus [14]. Separation and discrimination of VLPs and baculovirus is challenging due to their overlap in size and buoyant densities [15]. Therefore, efficient separation of these particles cannot be performed by density gradient centrifugation or size exclusion chromatography [16-18]. Additionally, these strategies often do not fulfill the purity specifications of VLP/vaccine preparations for human application. VLPs and baculovirus show similar composition of membrane proteins as both particles bud directly from the plasma membrane of the

For Review Only

host cell. It has been shown, that enveloped VLPs based on the HIV-1 gag construct produced in BEVS display viral or cellular membrane proteins on their surface and can also carry the baculovirus encoded major envelope glycoprotein gp64 [19-21]. This complicates the purification of these types of particles even more and thus, detailed characterization of samples is only possible by using a combination of several analytical methods. The first VLP-based vaccine produced in the BEVS was a vaccine against cervical cancer [22], approved in 2009 [23], but this a protein particle and therefore substantially different to baculovirus. Similar, the recombinant hemagglutinin-based trivalent influenza vaccine FluBlok approved by FDA in 2013 [24], is protein based and thus very different to baculovirus. We used HIV-1 gag influenza H1 VLPs expressed in *Tnms*42 insect cells as model system. These chimeric VLPs are enveloped VLPs composed of the HIV-1 gag capsid protein and the influenza A virus derived hemagglutinin (HA) H1. H1 is one of the subtypes of the major influenza surface glycoprotein HA, to which antibodies are able to bind resulting in the agglutination of virus particles and consequently, enabling virus neutralization [25]. Therefore, HA is immune dominant and the main antigen in the VLPs [26], besides the HIV-1 gag capsid protein. We developed a downstream process based on anion-exchange chromatography (AIEX) for capture and purification of HIV-1 gag H1 VLPs using Fractogel®-TMAE as stationary phase. Fractogel®-TMAE is a polymer-grafted ion exchange medium, consisting of synthetic

For Review Only

methacrylate porous beads with long linear polymer chains (“tentacles”), carrying the functional groups, Trimethylammoniumethyl (TMAE). These so-called “tentacles” are covalently attached to the hydroxyl groups of the matrix, increasing the surface area and number of ligands available for binding. Fractogel®-TMAE shows a particle size of 40-90 µm and a pore size of approximately 80 nm [27]. This work presents the establishment of an AIEX method, based on polymer-grafted media, to successfully separate HIV-1 gag H1 VLPs from co-expressed baculovirus produced using *Tnms*42 insect cells. The use of Fractogel®-TMAE allowed the capture and purification of enveloped VLPs, including separation of VLPs and baculovirus and reduction of host cell proteins and DNA in a single step. The developed method is suitable for fast and simple downstream processing of enveloped VLPs produced using insect-cell BEVS and allows the direct loading of endonuclease treated cell culture supernatant onto the column.

For Review Only

2. Material and Methods

2.1. Chemicals and Standards

All chemicals were of analytical grade, if not otherwise stated. Sodium chloride (NaCl), sodium hydroxide (NaOH), sodium dodecyl sulfate (SDS), 2-(N-moprholino)ethanesulfate acid (MES), Tween-20, sulfuric acid (95-97%, H_2SO_4), uranyl acetate were purchased from Merck (Darmstadt, Germany).

4-(2-hydroxyethyl)-1-piperazineethanesulfonic acid (HEPES) (≥99.5%), 2-Propanol, bovine serum albumine (BSA) (≥99.5%), 1,4-Dithiotreitol (DTT), Anti-mouse IgG (γ-chain specific)- alkaline phosphatase antibody (#3438), BCIP®/NBT solution, Triton X-100, glutaraldehyde solution (grade I), acetonitrile (MS grade), formic acid (98-100%) and iodacetamide (≥ 99%) were purchased from Sigma Aldrich (St. Louis, MO, USA). Anti-rabbit IgG (H+L) secondary antibody (**#**31460), anti-mouse IgG (H+L) superclonal secondary antibody (**#**A28177) were purchased from Thermo Fisher (Waltham, MA, USA). SeeBlue® Plus 2 Pre-stained Protein Standard and 4x LDS sample buffer were purchased from Invitrogen (Carlsbad, CA, USA). C-LEcta Denarase® was purchased from VWR (Radnor, PA, USA), HIV-1 p24 antibody (ab9071) and ACV5 (ab49581*)* from Abcam (Cambridge, England), influenza A virus H1N1 HA (GTX127357) from GeneTex (Irvine, CA, USA) and trypsin from Promega (Madison, Wisconsin, USA).

For Review Only

2.2 Production of HIV-1 gag H1 VLPs

Preculture

For the cultivation of HIV-1 gag H1 VLPs, *Tnms*42 cells were kept in exponential growth phase at 27 °C in shaker flasks at 100 rpm. The cells were grown in serum-free medium (Hyclone SFM4Insect, GE Healthcare) supplemented with 0.1% Kolliphor P188 (Sigma-Aldrich, St. Louis, MO, USA). Viable cell counts were determined by trypan blue exclusion using an automated cell counter (TC20 Bio-Rad Laboratories, Hercules, CA, USA). For each experiment, cells were taken from adherent culture, transferred to suspension with a starting cell density of $0.5x10^6$ cells/mL, and grown to desired cell numbers. All precultures with *Tnms*42 cells were supplemented with heparin sodium (1:1000, Sigma Aldrich St. Louis, MO, USA) to avoid cell clumping.

Benchtop bioreactor cultivations

Production was performed in a 10 L single use bioreactor (BioBLU 10c, Eppendorf) equipped with one pitched-blade impeller (3 blades; 45 °). The temperature was set to 27 °C and the pH maintained at 6.4±0.05 using 25% (v/v) phosphoric acid and 7.5% (w/v) sodium bicarbonate. The dissolved oxygen (DO) level was maintained at 30%. Cells were inoculated at a cell density of $1x10^6$ cells/mL and cultivated in the bioreactor for 1 day prior to infection. Cell count in the bioreactor was determined, and the vessel was infected with the respective amount of baculovirus (MOI = 5) and diluted back to $1x10^6$ cells/mL.

For Review Only

Clarification

Cell culture supernatant was harvested after 66 h and a viability of 54% and clarified by low-speed centrifugation at 200 g for 30 min and 0.01% NaN_3 was added to inhibit microbial growth. Culture was either stored in the cold room at 4 °C or was frozen at -80 °C for long time storage.

2.3 Chromatographic workstation

All chromatographic experiments were performed with an Äkta Pure 25 M2, equipped with a sample pump S9 and a fraction collector F9-C (GE Healthcare, Uppsala, Sweden). Unicorn software 6.4.1 was used for data collection and analysis. During the purification runs, UV absorbances (280, 260 and 214 nm) and conductivity were monitored simultaneously.

2.4 Capture and purification of HIV-1 gag H1 VLPs using Fractogel®-TMAE

*Tnms*42 supernatant containing HIV-1 gag H1 VLPs and baculovirus was incubated with c-LEcta Denarase® (purity >99%,VWR, Radnor, PA, USA) at a final concentration of 185 U/mL for 2 hours, at 37 °C and moderate shaking. The endonuclease treatment was followed by a filtration step using Sartopure® PP3 filter elements (Sartorius Stedim Biotech GmbH, Germany) with a pore size of 3 µm. The purification process for the VLPs was performed by loading 28 CV (501 mL) of the endonuclease treated and filtered cell culture supernatant onto a XK 16/20 column packed with

For Review Only

17.9 mL of Fractogel® EMD TMAE Hicap (M) resin referred in the text as Fractogel®-TMAE (Merck, Darmstadt, Germany). Buffer A consisted of 50 mM HEPES (pH 7.2) and buffer B of 50 mM HEPES, 2 M NaCl (pH 7.2). A flow rate of 3.6 mL/min was used troughout the whole purification run to ensure a residence time of 5 min. In order to have the same conductivity as in the loading material, the column was equilibrated with 5% B for 5 CV. After loading, the column was washed for 6 CV with equilibration buffer (5% B) to remove all unbound material. Column-bound material was eluted using a salt linear gradient from 5-60% B in 25 CV, followed by a regeneration step at 100% B for 4 CV. The column was then sanitized with 0.5 M NaOH for 3 CV. Flow-through (FT) fractions were collected with a volume of 100.2 mL (in total 5 fractions). Elution fractions were collected in 1.6 mL fractions in a 96 deep well plates, further analysed by at-line HPLC-MALS [28] and then pooled according to the chromatogram and stored at 4°C until further use.

2.5 Determination of total protein content and double stranded DNA (dsDNA) content

Total protein and dsDNA quantification was done as previously described in [6]. Briefly, for quantification of the total protein the Bradford Assay was used in 96-well microplate format according to the manufacturer's instructions. Calibration curves were obtained by diluting bovine serum albumin (BSA) standard with TE-buffer to concentrations ranging from 25-

For Review Only

200 µg/mL. dsDNA was determined by Quant-iT™ PicoGreen® dsDNA kit (Life Technologies, Waltham, MA, USA) in 96-well microplate format according to the manufacturer's instructions. Signals for protein (595 nm) and dsDNA content ($\lambda_{excitation}$ = 480 nm, $\lambda_{emission}$ = 520 nm) were measured by Tecan Infinite® 200 Pro (Tecan, Männedorf, Switzerland).

2.6 Sodium dodecyl sulphate polyacrylamide gel electrophoresis (SDS-PAGE) and Western blot

SDS-PAGE was performed as previously described in [6]. Protein bands were stained using silver staining. All solutions used and a full protocol for the silver stain are described in the Supplementary Material A, Protocol for Silver Stain.

For Western blot analysis, proteins were blotted as already described in [6]. For detection of the VLPs capsid protein HIV-1 p24 (*[39/5.4A],* Abcam, Cambridge, England) was used. The detection of the VLPs membrane protein H1 influenza A virus H1N1 HA (GTX127357, GeneTex, Irvine, CA, USA) was used. The primary antibodies were diluted 1:1000 in PBS-T containing 1% BSA (=incubation buffer). Anti-mouse IgG (γ-chain specific)-alkaline phosphatase antibody (#3438, Sigma Aldrich, St. Louis, MO, USA) diluted 1:1000 in incubation buffer was used as secondary antibody. For the detection of the baculovirus capsid protein a primary antibody against vp39 was used. For the detection of the membrane glycoprotein gp64 a primary antibody against ACV5 was used (*ab49581*,

For Review Only

Abcam, London, UK). The antibody against vp39 was diluted 1:50, ACV5 was diluted 1:1500 in incubation buffer for 2 h followed by a secondary antibody incubation with anti-mouse IgG (γ-chain specific)-alkaline phosphatase antibody (Sigma Aldrich, St. Louis, MO, USA), diluted 1:1000 also in incubation buffer. For visualization, the membranes were incubated in 10 mL premixed BCIP®/NBT solution (Sigma Aldrich, St. Louis, MO, USA) for 2-3 minutes. Results were evaluated by visual estimation.

2.7 Nanoparticle Tracking Analysis (NTA)

The determination of the particle concentration and particle size distribution by nanoparticle tracking analysis (NTA) was performed as described in [6], using a NanoSight NS300 (Malvern Instruments Ltd., Worcestershire, UK) with a blue laser module (488 nm) and a neutral density filter. Samples were diluted in particle-free water in order to obtain 20-100 particles per frame. In total, three different dilutions were measured per sample. All measurements were performed at 25 °C and videos of 30 s were captured. All particles and a selected particle size range especially for detection of VLPs between 100-200 nm were considered for sample evaluation. Capture settings (shutter and gain) were adjusted manually, prior to the measurements. For determination of particle concentration, each dilution was measured 5 times. In total, 15 videos were analysed for each sample with the NTA 2.3 Analytical software.

For Review Only

2.8 Tissue Culture Infective Dose 50 (TCID50) on Spodoptera frugiperda 9 (Sf9) cells

Quantification of infectious baculovirus titer was performed with TCID50 on Sf9 cells. Sf9 cells in exponential phase were diluted to $0.4x10^6$ cells/mL, 100 µL of this dilution were dispensed into each well of a 96-well plate and incubated for at least 1 h at 27°C to allow cell attachment. Each sample was done in duplicates. Samples were pre-diluted with HyClone medium (Hyclone SFM5Insect, GE Healthcare) 1:10, in the plates 1:5 dilutions were performed. Virus dilutions were transferred to the 96-well plates with the attached Sf9 cells. A volume of 30 µL of each virus dilution was added to each well. Plates were incubated at 27°C for at least 7 days. After incubation, the plates were inspected under the Leica DM IL LED Inverted Laboratory Fluorescence Microscope (Leica Microsystems, Wetzlar, Germany). Each well with any sign of infection was counted as a positive well.

2.9 Transmission Electron Microscopy (TEM)

TEM analysis was used for particle visualization, especially to analyze the presence, integrity and morphology of particles present across the entire purification run. Sample preparation was performed by negative staining with 1% uranyl acetate as described in [6]. Images were taken using a

For Review Only

Tecnai G2 200 kV transmission electron microscope (FEI, Eindhoven, The Netherlands).

2.10 Protein identification and peptide analysis using LC-ESI-MS

Protein identification and peptide analysis was done as already described in [6]. The files were searched against the SwissProt database (https://www.ebi.ac.uk/uniprot) against *Trichopulsia* ni (taxonomy ID: 7111) and with special focus on proteins for detection of Autographa california nuclear polyhedrosis (AcNPV, taxonomy ID: 46015), Human immunodeficiency virus-1 (taxonomy ID: 11676, strain: HIV-1 HXB2) and Influenza A virus (taxonomy ID: 11320, strain: A/Puerto Rico/8/1934).

2.11 High Performance Liquid Chromatography-Multiangle Light Scattering (HPLC-MALS)

At-line MALS measurements for the determination of the light scattering intensity were performed using an Ultimate 3000 HPLC system (Thermo Fisher, Waltham, MA, USA) with a quaternary LPG-3400SD pump, a WPS-3000TSL autosampler and a DAD 3000 UV-detector. Mobile phase consisted of 50 mM HEPES, 100 mM NaCl, pH 7.2. A sample volume of 50 µL was injected in bypass mode using a flow rate of 0.3 mL/min. All samples were measured in duplicates. MALS signals were acquired by the DAWN HELEOS 18-angle detector (Wyatt, Santa Barbara, CA, USA). For HPLC programming Chromeleon 7 software (Thermo Fisher, Waltham,

For Review Only

MA, USA) was used. MALS data collection and analysis was performed with ASTRA software, version 6.1.2 (Wyatt, Santa Barbara, CA, USA).

2.12 HPLC Size Exclusion Chromatography coupled with MALS (HPLC-SEC-MALS)

Relevant samples were analysed by HPLC-SEC-MALS in order to determine particle compositon and estimate purity. All experiments were performed using the HPLC system mentioned in 2.11 with the Chromeleon 7 software (Thermo Fisher Scientific, Waltham, MA, USA) for method programming, control and data aquisition. A TSKgel G5000PWXL column (300.0 mm x 7.8 mm i.d.) combined with a TSKgel PWXL guard column (40.0 mm x 6.0 mm i.d.) (Tosoh Bioscience, Stuttgart, Germany) was used. A volume of 50 µL of each sample was injected. The flow rate was 0.3 mL/min. Isocratic elution was performed with 50 mM HEPES, 100 mM NaCl, pH 7.2. UV signals at 280 and 260 nm were recorded by the Chromeleon software and light scattering signal was acquired with a DAWN HELEOS 18-angle detector (Wyatt, Santa Barbara, CA, USA) with the Astra Software 5.3.4 (Wyatt, Santa Barbara, CA, USA). Data evaluation was performed in Astra 6.1.2.

For Review Only

3. Results and Discussion

A downstream process based on strong anion-exchange chromatography (AIEX) using Fractogel®-EMD TMAE Hicap (M) as stationary phase was developed for capture and separation of enveloped HIV-1 gag H1 VLPs from baculovirus. The results of the VLP capture and purification are described in 3.1 and the purity and particle content of the main particle containing fractions are compared in 3.2.

3.1 Purification of HIV-1 gag H1 VLPs using Fractogel®-TMAE

To estimate the dynamic binding capacity (DBC), a 1 mL Fractogel®-TMAE prepacked MiniChrom column 8 × 20 mm (Merck KGaA, Darmstadt, Germany) was overloaded with clarified and endonuclease pretreated *Tnms*42 cell culture supernatant. Light scattering (LS) signal of the flow-through (FT) fractions during the loading phase show particle breakthrough after approximately 30 mL, equivalent to 30 CV (Supplementary Material B, Figure S1, Fraction FT1). In order to avoid product loss due to overloading, the 17.9 mL Fractogel®-TMAE column was loaded with 28 CV. Accordingly, 501.0 mL of clarified, endonuclease pretreated and filtered *Tnms*42 supernatant were directly loaded onto the column. A salt linear gradient from 100-1000 mM NaCl over 25 CV allowed the elution of bound particles from the column (Figure 1). Collected fractions were analysed by at-line MALS [6]. Sample pooling was performed considering both, UV absorbance and LS area [8, 28, 29].

For Review Only

For the pooled samples, dsDNA was determined by Picogreen Assay (Table 1 and Supplementary Material B, Table S1), total protein was quantified by Bradford Assay (Table 1 and Supplementary Material B, Table S1) and specific protein contents were accessed by SDS-PAGE (Figure 2A), Western Blots (Figure 2B) and mass spectrometry (Supplementary Material C). Particle content (Table 1 and Supplementary Material B, Table S1) and particle size distribution (Figure 3) were measured by NTA and quantification of infectious baculovirus titer by TCID50 (Supplementary Material B, Table S2). The combination of these data allowed the evaluation of the process performance in terms of recovery and purity. Yield cannot be calculated in a direct manner, because there is no method to specifically quantifiy the VLPs in the crude material in presence of baculovirus and many process related impurities. Additionally, biochemcial markers targeting specific proteins are not VLP specific once they would also measure free protein in solution that did not assemble into VLPs. Treatment of the supernatant with endonuclease allowed a depletion of 57% dsDNA from 1583.6 ng/mL in the supernatant to 683.8 ng/mL in the loading material (Table 1). For specific detection of VLPs and baculovirus, we used Western blot analysis against the proteins HIV-1 p24 (band at 55 kDa) and baculovirus vp39 (band at 39 kDa), respectively, because these are the main capsid proteins. Additionally, influenza A virus H1N1 hemagglutinin (band at 64 kDa) and the baculovirus major envelope glycoprotein gp64 (band at 59 kDa) were used

For Review Only

to detect membrane proteins for VLP and baculovirus, respectively. However, membrane proteins were identified in all particle containing fractions (Figure 2B), which was expected once the different particles share the same budding mechanism at the cell membrane. Particle concentration measured by NTA reaveals, that E2 and E3 contain the majority of the eluted particles (Table 1). These results were supported by the HPLC-SEC-MALS measurements, in which particles elute in the void volume of the column after a retention time of 20 min and the highest light scattering (LS) signals can be observed for E2 and E3 (Figure 4). Considering the LS data, particles were also concentrated from the loading material to E2 and E3 (Figure 4). The UV280 data of the analytical SEC measurements was evaluated in order to infer about the purity level of the main elution fractions E2 and E3 (Supplementary Material B, Figure S2). Moreover, when looking at the UV280 data in E2 and E3, the reduced signal indicates reduction in impurity content. Also, a different protein pattern between E2 and E3 can be observed on the SDS-PAGE (Figure 2A), indicating the elution of different particle populations. On the SDS-PAGE in lane E3 a very dense band at 39 kDa (Figure 2A) which is not visible in E2, suggests the elution of baculovirus. Considering the Western blot results against HIV-1 p24 and baculovirus vp39, in E2 a dense band against the capsid protein p24 is visible while only a faint band for vp39 is present (Figure 2B). This indicates the enrichment of VLPs and separation from baculovirus in E2. Contrariwise, in E3 the vp39 band is denser

For Review Only

indicating the elution of baculovirus. VLP enrichment in E2 and starting co-elution of baculovirus can also be confirmed by TEM pictures (Figure 2C - Figure 2E). Since E2 and E3 are not resolved peaks (Figure 1), the separation of VLPs and baculovirus could be improved by either using a narrower pooling criteria or by optimizing the elution gradient. Elution of VLPs in E2 is further supported by NTA results (Table 1), which showed that E2 contained 20% of the loaded particles (100-200 nm). Particle size distribution showed that the particles in E2 had a mean diameter of 158.4 nm, the typical diameter of VLPs based on the HIV-1 gag construct [8] (Figure 3). Additionally, 81% of the particles in E2 have a diameter between 100-200 nm (NTA), while in E3 particles have a slightly wider particle size distribution (Figure 3) with mean size of 161.3 nm, which can be explained by the co-elution of baculovirus. This supports the findings of the Western blot analysis (Figure 2B). Proteomic analysis was performed by LC-ESI-MS in order to identify specific proteins in the main particle containing fractions. Considering E2 and E3, in total 145 and 161 proteins were identified against the host *Trichopulsia ni* database, respectively (Supplementary Material C). Additionally, a search against the specific strains used for HIV-1, influenza and baculovirus was performed. As shown by the Western blot analysis, both membrane proteins (H1 and gp64) were detected in both samples (E2 and E3). In E2, the capsid protein HIV-1 gag (specific for VLP) was identified again confirming the Western blot results. Additionally, 6 different proteins from baculovirus

For Review Only

(AcMNPV) were present in E2, indicating co-elution, however, since the peaks are not fully resolved and MS is a very sensitive detection method this is expected. In E3, 15 proteins specific for baculovirus were identified, including the major capsid protein vp39, which was not detected in E2 (Supplementary Material C). A purification run with *Tnms*42 cell culture supernatant previously stored at -80°C was performed and showed the same elution profile as the purification run performed using fresh material (Supplementary Material, Figure S3). First, a pure fraction of VLPs is eluting in E2.1 and in E3, baculovirus starts to co-elute, which can be confirmed by Western blot analysis performed against the specific capsid proteins p24 and vp39 (Supplementary Material B, Figure S4). After thawing, the loading material infectivity regarding baculovirus was $3.0x10^6$ TCID50/mL (Supplementary Material B, Table S2). After purification, a virus clearance of log 4.3 and 3.2 was achieved for E2.1 (main VLP fraction) and E3 (VLP-baculovirus co-elution), respectively. Considering the particle size distribution, Western blot profiles, proteomic data, TEM pictures and TCID50 values of the main particle containing fractions, we conclude that a HIV-1 gag H1 VLPs enriched fraction elutes in E2, and baculovirus co-elution starts in E3.

3.2 Purity of VLPs

Total protein, dsDNA and particle contents of E2 and E3 were determined and normalized per vaccine dose (10^9 particles) in order to allow the

For Review Only

comparison of the main particle fractions regarding its purity. The total protein content per dose was 3.4 µg/dose for E2 and 6.3 µg/dose for E3 (Figure 5). The dsDNA content per dose was similar for both fractions (3.4 ng/dose for E2 and 4.3 ng/dose for E3, Figure 5) and already meet the requirements of the regulatory agencies with <10 ng residual dsDNA per dose [30]. Performance of the purification run was calculated based on the number of vaccination doses per L loading material. We were able to purify 4200 vaccination doses per L pre-treated *Tnms*42 cell culture supernatant using a 17.9 mL Fractogel® -TMAE column.

4. Concluding Remarks

In our work we demonstrate that polymer-grafted anion-exchangers are capable of efficiently capture chimeric HIV-1 gag influenza H1 VLPs directly from clarified and endonuclease treated insect cell culture supernatant. Moreover, this method allowed the separation of the VLPs from process related impurities such as host cell proteins and dsDNA, and most importantly from baculovirus, in a single step. A reduction of 94% total protein and 98% dsDNA was achieved for the main product fraction. When considering 10^9 particles as a vaccination dose, purified influenza VLPs already meet the requirements of the regulatory agencies with <10 ng residual dsDNA. Per L pre-treated cell culture supernatant we were able to process 4200 vaccination doses with Fractogel®-TMAE. The process is simple with a very low number of handling steps and has the

For Review Only

characteristics to become a platform for purification of these types of VLPs.

Acknowledgements

This work has been supported by the Federal Ministry for Digital and Economic Affairs (bmwd), the Federal Ministry for Transport, Innovation and Technology (bmvit), the Styrian Business Promotion Agency SFG, the Standortagentur Tirol, Government of Lower Austria and ZIT - Technology Agency of the City of Vienna through the COMET-Funding Program managed by the Austrian Research Promotion Agency FFG. The funding agencies had no influence on the conduct of this research. Pereira Aguilar was supported by the Austrian Science Fund (project BioToP; FWF W1224). We acknowledge Fritz Altmann and Clemens Grünwald Gruber for provinding the MS data of the elution fractions.

Conflict of Interest

The authors have declared no conflict of interest.

For Review Only

References

[1] Mena, J. A., Kamen, A. A., Insect cell technology is a versatile and robust vaccine manufacturing platform. *Expert Rev Vaccines* 2011, *10*, 1063-1081 DOI: 10.1586/erv.11.24.

[2] Krammer, F., Schinko, T., Palmberger, D., Tauer, C., Messner, P., Grabherr, R., Trichoplusia ni cells (High Five) are highly efficient for the production of influenza A virus-like particles: a comparison of two insect cell lines as production platforms for influenza vaccines. *Mol Biotechnol* 2010, *45*, 226-234 DOI: 10.1007/s12033-010-9268-3.

[3] Meghrous, J., Aucoin, M. G., Jacob, D., Chahal, P. S., Arcand, N., Kamen, A. A., Production of recombinant adeno-associated viral vectors using a baculovirus/insect cell suspension culture system: from shake flasks to a 20-L bioreactor. *Biotechnol Prog* 2005, *21*, 154-160 DOI: 10.1021/bp049802e.

[4] Margine, I., Martinez-Gil, L., Chou, Y. Y., Krammer, F., Residual baculovirus in insect cell-derived influenza virus-like particle preparations enhances immunogenicity. *PLoS One* 2012, *7*, e51559 DOI: 10.1371/journal.pone.0051559.

[5] Smith, G. E., Flyer, D. C., Raghunandan, R., Liu, Y., Wei, Z., Wu, Y., Kpamegan, E., Courbron, D., Fries, L. F., Glenn, G. M., Development of influenza H7N9 virus like particle (VLP) vaccine: homologous A/Anhui/1/2013 (H7N9) protection and heterologous A/chicken/Jalisco/CPA1/2012 (H7N3) cross-protection in vaccinated mice

For Review Only

challenged with H7N9 virus. *Vaccine* 2013, *31*, 4305-4313 DOI: 10.1016/j.vaccine.2013.07.043.

[6] Reiter, K., Aguilar, P. P., Wetter, V., Steppert, P., Tover, A., Jungbauer, A., Separation of virus-like particles and extracellular vesicles by flow-through and heparin affinity chromatography. *J Chromatogr A* 2018 DOI: 10.1016/j.chroma.2018.12.035.

[7] Steppert, P., Burgstaller, D., Klausberger, M., Berger, E., Aguilar, P. P., Schneider, T. A., Kramberger, P., Tover, A., Nobauer, K., Razzazi-Fazeli, E., Jungbauer, A., Purification of HIV-1 gag virus-like particles and separation of other extracellular particles. *Journal of chromatography. A* 2016, *1455*, 93-101 DOI: 10.1016/j.chroma.2016.05.053.

[8] Steppert, P., Burgstaller, D., Klausberger, M., Tover, A., Berger, E., Jungbauer, A., Quantification and characterization of virus-like particles by size-exclusion chromatography and nanoparticle tracking analysis. *Journal of chromatography. A* 2017, *1487*, 89-99 DOI: 10.1016/j.chroma.2016.12.085.

[9] Steppert, P., Burgstaller, D., Klausberger, M., Kramberger, P., Tover, A., Berger, E., Nobauer, K., Razzazi-Fazeli, E., Jungbauer, A., Separation of HIV-1 gag virus-like particles from vesicular particles impurities by hydroxyl-functionalized monoliths. *Journal of separation science* 2017, *40*, 979-990 DOI: 10.1002/jssc.201600765.

For Review Only

513 [10] Clem, R. J., Passarelli, A. L., Baculoviruses: sophisticated pathogens
514 of insects. *PLoS Pathog* 2013, *9*, e1003729 DOI:
515 10.1371/journal.ppat.1003729.
516 [11] Wang, Q., Bosch, B. J., Vlak, J. M., van Oers, M. M., Rottier, P. J.,
517 van Lent, J. W. M., Budded baculovirus particle structure revisited. *J*
518 *Invertebr Pathol* 2016, *134*, 15-22 DOI: 10.1016/j.jip.2015.12.001.
519 [12] Oomens, A. G., Wertz, G. W., The baculovirus GP64 protein mediates
520 highly stable infectivity of a human respiratory syncytial virus lacking its
521 homologous transmembrane glycoproteins. *J Virol* 2004, *78*, 124-135 DOI:
522 10.1128/jvi.78.1.124-135.2004.
523 [13] Grabherr, R., Ernst, W., Oker-Blom, C., Jones, I., Developments in the
524 use of baculoviruses for the surface display of complex eukaryotic
525 proteins. *Trends Biotechnol* 2001, *19*, 231-236 DOI: 10.1016/s0167-
526 7799(01)01610-9.
527 [14] Katsuma, S., Kokusho, R., A Conserved Glycine Residue Is Required
528 for Proper Functioning of a Baculovirus VP39 Protein. *J Virol* 2017, *91*
529 DOI: 10.1128/JVI.02253-16.
530 [15] Summers, M. D., Volkman, L. E., Comparison of biophysical and
531 morphological properties of occluded and extracellular nonoccluded
532 baculovirus from in vivo and in vitro host systems. *J Virol* 1976, *17*, 962-
533 972.

For Review Only

[16] Vicente, T., Roldão, A., Peixoto, C., Carrondo, M. J., Alves, P. M., Large-scale production and purification of VLP-based vaccines. *J Invertebr Pathol* 2011, *107 Suppl*, S42-48 DOI: 10.1016/j.jip.2011.05.004.

[17] Song, J. M., Choi, C. W., Kwon, S. O., Compans, R. W., Kang, S. M., Kim, S. I., Proteomic characterization of influenza H5N1 virus-like particles and their protective immunogenicity. *J Proteome Res* 2011, *10*, 3450-3459 DOI: 10.1021/pr200086v.

[18] Krammer, F., Grabherr, R., Alternative influenza vaccines made by insect cells. *Trends Mol Med* 2010, *16*, 313-320 DOI: 10.1016/j.molmed.2010.05.002.

[19] Chaves, L. C. S., Ribeiro, B. M., Blissard, G. W., Production of GP64-free virus-like particles from baculovirus-infected insect cells. *J Gen Virol* 2018, *99*, 265-274 DOI: 10.1099/jgv.0.001002.

[20] Buonaguro, L., Tagliamonte, M., Tornesello, M. L., Buonaguro, F. M., Developments in virus-like particle-based vaccines for infectious diseases and cancer. *Expert Rev Vaccines* 2011, *10*, 1569-1583 DOI: 10.1586/erv.11.135.

[21] Valley-Omar, Z., Meyers, A. E., Shephard, E. G., Williamson, A. L., Rybicki, E. P., Abrogation of contaminating RNA activity in HIV-1 Gag VLPs. *Virol J* 2011, *8*, 462 DOI: 10.1186/1743-422X-8-462.

[22] Monie, A., Hung, C. F., Roden, R., Wu, T. C., Cervarix: a vaccine for the prevention of HPV 16, 18-associated cervical cancer. *Biologics* 2008, *2*, 97-105.

For Review Only

[23] Harper, D. M., Impact of vaccination with Cervarix (trade mark) on subsequent HPV-16/18 infection and cervical disease in women 15-25 years of age. *Gynecol Oncol* 2008, *110*, S11-17 DOI: 10.1016/j.ygyno.2008.06.029.

[24] Treanor, J. J., El Sahly, H., King, J., Graham, I., Izikson, R., Kohberger, R., Patriarca, P., Cox, M., Protective efficacy of a trivalent recombinant hemagglutinin protein vaccine (FluBlok®) against influenza in healthy adults: a randomized, placebo-controlled trial. *Vaccine* 2011, *29*, 7733-7739 DOI: 10.1016/j.vaccine.2011.07.128.

[25] Gallagher, J. R., McCraw, D. M., Torian, U., Gulati, N. M., Myers, M. L., Conlon, M. T., Harris, A. K., Characterization of Hemagglutinin Antigens on Influenza Virus and within Vaccines Using Electron Microscopy. *Vaccines (Basel)* 2018, *6* DOI: 10.3390/vaccines6020031.

[26] Kang, S. M., Kim, M. C., Compans, R. W., Virus-like particles as universal influenza vaccines. *Expert Rev Vaccines* 2012, *11*, 995-1007 DOI: 10.1586/erv.12.70.

[27] Pereira Aguilar, P., Schneider, T. A., Wetter, V., Maresch, D., Ling, W. L., Tover, A., Steppert, P., Jungbauer, A., Polymer-grafted chromatography media for the purification of enveloped virus-like particles, exemplified with HIV-1 gag VLP. *Vaccine* 2019, *37*, 7070-7080 DOI: 10.1016/j.vaccine.2019.07.001.

[28] Pereira Aguilar, P., González-Domínguez, I., Schneider, T. A., Gòdia, F., Cervera, L., Jungbauer, A., At-line multi-angle light scattering detector

For Review Only

for faster process development in enveloped virus-like particle purification. *J Sep Sci* 2019, *42*, 2640-2649 DOI: 10.1002/jssc.201900441.

[29] Wyatt, P. J., Measurement of special nanoparticle structures by light scattering. *Anal Chem* 2014, *86*, 7171-7183 DOI: 10.1021/ac500185w.

[30] Drug, U. S. D. o. H. a. H. S. F. a., Industry, A. G. f., 2001.

For Review Only

588 **Figure Captions**

589 Figure 1

590 Chromatographic purification of HIV-1 gag H1 VLPs from baculovirus
591 produced in *Tnms*42 insect cells with Fractogel®-TMAE using a linear
592 gradient elution from 100-1000 mM NaCl (Buffer A: 50 mM HEPES, pH
593 7.2; Buffer B: 50 mM HEPES, 2 M NaCl, pH 7.2). Loading material (28 CV,
594 501 mL) was endonuclease treated and filtered (3 µm). Grey bars
595 represent the area under the curve of the light scattering intensity (LS)
596 measurements performed on MALS detector. FT1-FT5: flow-through
597 fractions 1-5, E1-E7: elution fractions 1-7, R: regeneration (100% B), CIP:
598 cleaning in place (0.5 M NaOH).

599

600 Figure 2

601 (A) SDS-PAGE, (B) Western blot analysis and of the pooled fractions from
602 the purification run represented in Figure 1. (C), (D), and (E) electron
603 microscopy micrographs of loading material (L) and main elution fractions
604 E2 and E3, respectively. M: molecular weight marker, L: loading material
605 (endonuclease treated and filtered), FT: pooled flow-through, E1-E5:
606 elution fractions 1-5.

607

608 **Error! Reference source not found.**

For Review Only

Particle size distribution measured by Nanoparticle Tracking Analysis of loading material (L) and the main particle containing fractions E2 (VLP containing fraction) and E3 (VLP and coelution of baculovirus).

Figure 4

Analysis of the loading material (L) and the main elution fractions E2 and E3 from the purification run represented in Figure 1 by analytical size exclusion chromatography coupled to MALS.

Error! Reference source not found.: Purity of the loading material (L) and the main particle elution fractions E2 and E3 from the Fractogel®-TMAE purification run calculated based on µg protein and ng dsDNA/dose and baculovirus clearance based on TCID50/mL and log reduction.

For Review Only

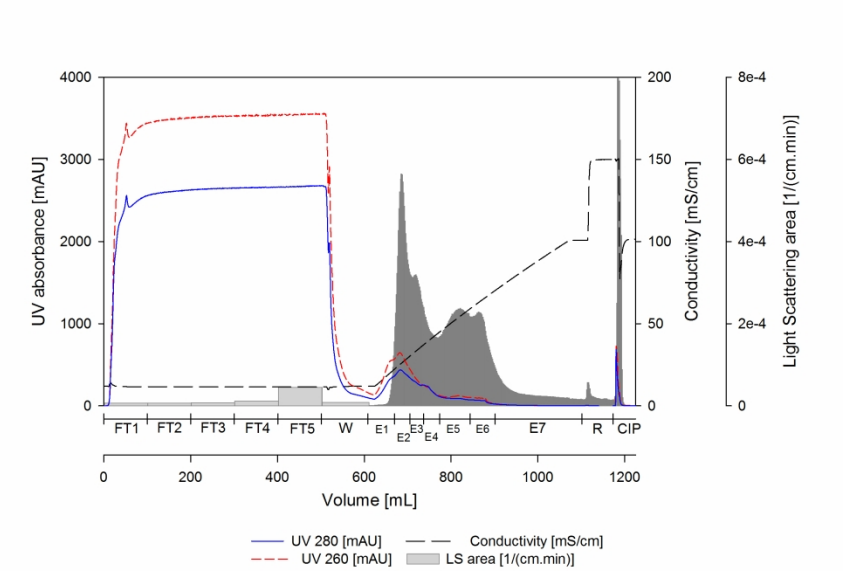

Figure 1
Chromatographic purification of HIV-1 gag H1 VLPs from baculovirus produced in Tnms42 insect cells with Fractogel®-TMAE using a linear gradient elution from 100-1000 mM NaCl (Buffer A: 50 mM HEPES, pH 7.2; Buffer B: 50 mM HEPES, 2 M NaCl, pH 7.2). Loading material (28 CV, 501 mL) was endonuclease treated and filtered (3 µm). Grey bars represent the area under the curve of the light scattering intensity (LS) measurements performed on MALS detector. FT1-FT5: flow-through fractions 1-5, E1-E7: elution fractions 1-7, R: regeneration (100% B), CIP: cleaning in place (0.5 M NaOH).

209x296mm (300 x 300 DPI)

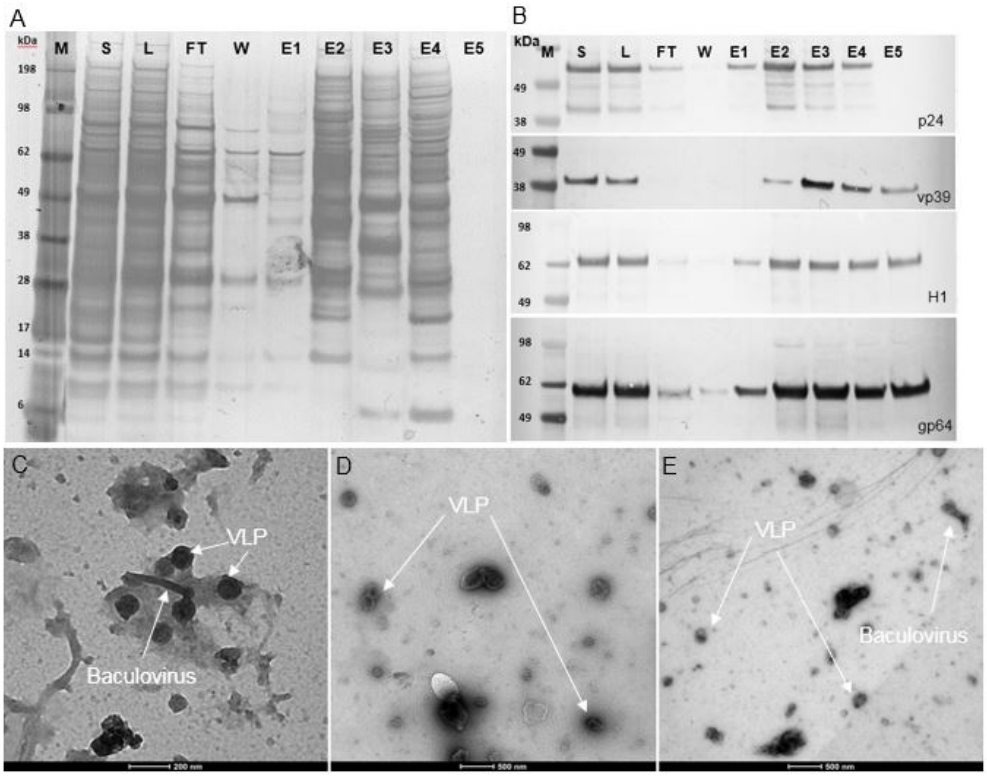

Figure 2
(A) SDS-PAGE, (B) Western blot analysis and of the pooled fractions from the purification run represented in Figure 1. (C), (D), and (E) electron microscopy micrographs of loading material (L) and main elution fractions E2 and E3, respectively. M: molecular weight marker, L: loading material (endonuclease treated and filtered), FT: pooled flow-through, E1-E5: elution fractions 1-5.

180x141mm (96 x 96 DPI)

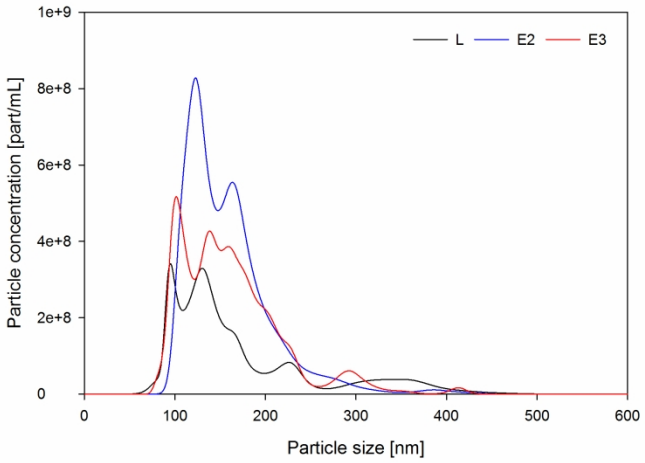

Figure 3
Particle size distribution measured by Nanoparticle Tracking Analysis of loading material (L) and the main particle containing fractions E2 (VLP containing fraction) and E3 (VLP and coelution of baculovirus).

215x279mm (300 x 300 DPI)

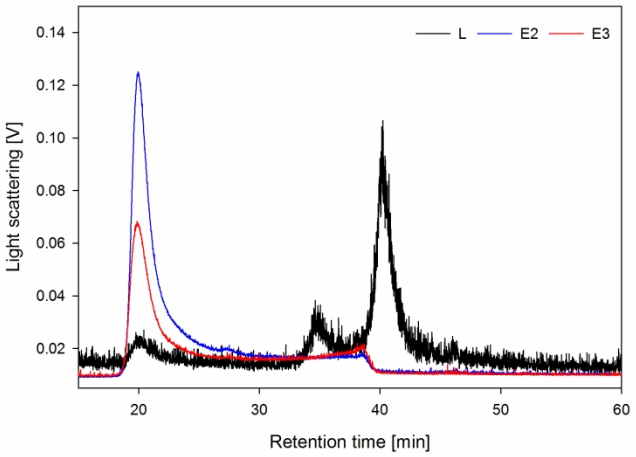

Figure 4
Analysis of the loading material (L) and the main elution fractions E2 and E3 from the purification run represented in Figure 1 by analytical size exclusion chromatography coupled to MALS.

215x279mm (300 x 300 DPI)

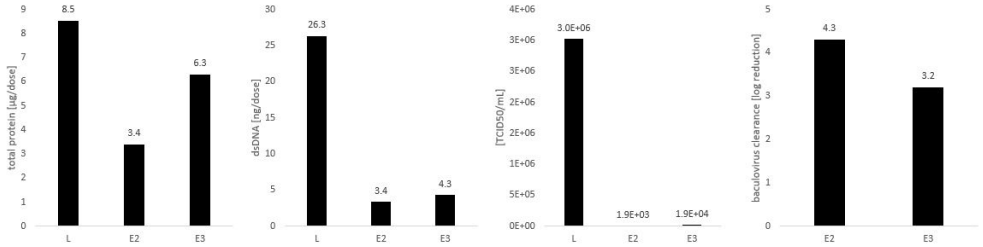

Figure 5: Purity of the loading material (L) and the main particle elution fractions E2 and E3 from the Fractogel®-TMAE purification run calculated based on µg protein and ng dsDNA/dose and baculovirus clearance based on TCID50/mL and log reduction.

309x80mm (96 x 96 DPI)

Table 1: Mass balance of the purification run for HIV-1 gag H1 VLPs on a 17.9 mL Fractogel®-TMAE column by linear gradient elution. Loading material was c-LEcta Denarase® and 3 µm filtered *Tnms*42 cell culture supernatant. S: *Tnms*42 cell culture supernatant, L = loading material, E2-E3 = elution fractions 2-3 (main particle containing fractions)

sample	volume [mL]	particles (1-1000nm) [part/mL]	recovery [%]	particles (100-200nm) [part/mL]	recovery [%]	total protein [µg/mL]	dsDNA [ng/mL]
S	501.0	-	-	-	-	249.5	1583.6
L	501.0	2.6E+10	100%	1.8E+10	100%	221.6	683.8
E2	35.2	6.0E+10	16%	4.9E+10	20%	204.9	204.2
E3	32.0	4.0E+10	10%	2.9E+10	10%	252.0	173.1

For Review Only

Supplementary Material A

Separation of influenza virus-like particles from baculovirus by polymer grafted ion-exchangers

Katrin Reiter[1], Patricia Pereira Aguilar[1,2], Dominik Grammelhofer[1], Judith Joseph[1], Petra Steppert[2], Alois Jungbauer[1,2*]

[1] Austrian Centre of Industrial Biotechnology, Vienna, Austria

[2] Department of Biotechnology, University of Natural Resources and Life Sciences, Vienna, Austria

*Corresponding author

Univ.Prof. Dipl.-Ing. Dr.nat.techn. Alois Jungbauer

Department of Biotechnology

University of Natural Resources and Life Sciences Vienna,

Muthgasse 18, 1190 Vienna

Phone: +43 1 47654-79083

Fax: +43 1 47654-79009

E-mail: alois.jungbauer@boku.ac.at

Supplemenatary Material A, Protocol for Silver Stain

Solutions

Fixing Solution **30 min +**

Ethanol (96%)	500 mL
Acetic Acid (100%)	100 mL
RO-Water	Fill to 1 L

Incubation Solution **30 min +**

	For 1 L	**One gel (50 mL)**
Ethanol (96%)	300 mL	15 mL
Na-acetate (waterfree)	68 g	3.4 g
Thiosulfate-pentahydrate ($Na_2S_2O_3.5H_2O$)	2 g	0.1 g
RO-Water	Fill to 1 L	Fill to 50 mL
Add before use:		
Glutaraldehyde (50% in water (5.6 M)	2.5 mL	125 µL

wash 3x5 min

Silver Solution **20 min**

	For 1 L	**One gel (50 mL)**
Silver nitrate ($AgNO_3$)	1 g	50 mg
RO-Water	Fill to 1 L	Fill to 50 mL

Add before use:		
Formaldehyde 35%	200 µL	10 µL

wash 2-3x

Developing Solution **~ 5 min**

	For 1 L	One gel (150 mL)
Sodium carbonate (Na_2CO_3)	25 g	3.75 g
RO-Water	Fill to 1 L	Fill to 150 mL
Add before use:		
Formaldehyde 35%	100 µL	15 µL

Stop Solution **10 min**

EDTA/Triplex	14.6 g
RO-Water	Fill to 1 L

Silver Staining

- All steps have to be performed on a lab shaker, the fluid should cover the gel (~30 mL)
- Put the gel into an appropriate container and add 50 mL Fixing solution for at least 30 minutes if the Gel isn't already fixed
- The **Glutaraldehyd/Formaldehyd** is added to 50 mL of the Solution in a Greiner tube right before use
- Incubate it **30 minutes** in 50 mL **Incubation Solution**
- Wash **3 times for 5 minutes** in RO-Water
- Incubate **20 minutes** in 50 mL **Silver Solution**
- **Rinse shortly 2-3 times** with water to remove the Silver Solution
- Incubate in 50 mL **Developing Solution** for approximately ~ **5 minutes** until the protein bands are clearly visible. Change the Developing Solution every 2-3 minutes to get better results.
- Incubate the gel min. **10 min** in 50 mL **Stop Solution** to stop the reaction. (gel can be kept in stop solution until scanning)
- Scan the gel and store the data.

Supplementary Material B

Separation of influenza virus-like particles from baculovirus by polymer grafted ion-exchangers

Katrin Reiter[1], Patricia Pereira Aguilar[1,2], Dominik Grammelhofer[1], Judith Joseph[1], Petra Steppert[2], Alois Jungbauer[1,2*]

[1] Austrian Centre of Industrial Biotechnology, Vienna, Austria

[2] Department of Biotechnology, University of Natural Resources and Life Sciences, Vienna, Austria

*Corresponding author

Univ.Prof. Dipl.-Ing. Dr.nat.techn. Alois Jungbauer

Department of Biotechnology

University of Natural Resources and Life Sciences Vienna,

Muthgasse 18, 1190 Vienna

Phone: +43 1 47654-79083

Fax: +43 1 47654-79009

E-mail: alois.jungbauer@boku.ac.at

Figure S1

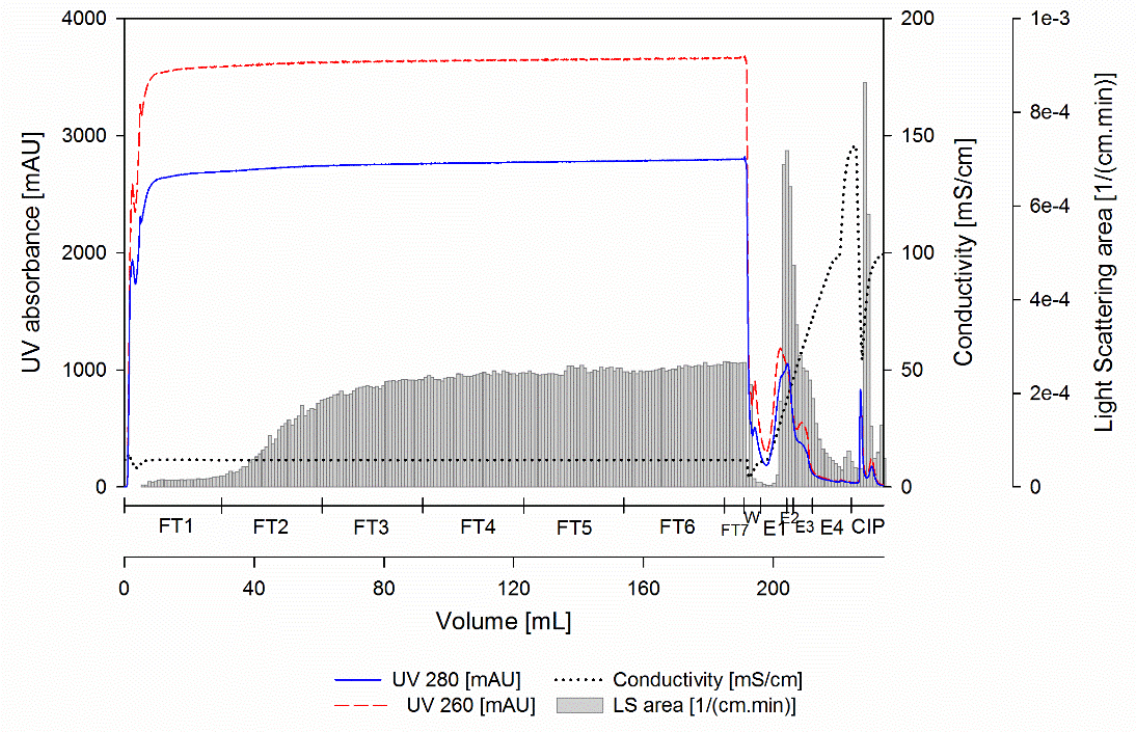

Figure S1: Chromatographic purification of HIV-1 gag H1 VLPs from baculovirus produced in *Tnms*42 insect cells with a 1 mL Fractogel®-TMAE prepacked MiniChrom column 8 × 20 mm (Merck KGaA, Darmstadt, Germany), using a linear gradient elution from 100-1000 mM NaCl (Buffer A: 50 mM HEPES, pH 7.2; Buffer B: 50 mM HEPES, 2 M NaCl, pH 7.2). Column was overloaded with 191 CV. The loading material was endonuclease treated and filtered (3 µm). Grey bars represent the area under the curve of the light scattering intensity (LS) measurements performed on MALS detector. FT1-FT7: flow-through fractions 1-7, E1-E4: elution fractions 1-4, CIP: cleaning in place (0.5 M NaOH).

Figure S2

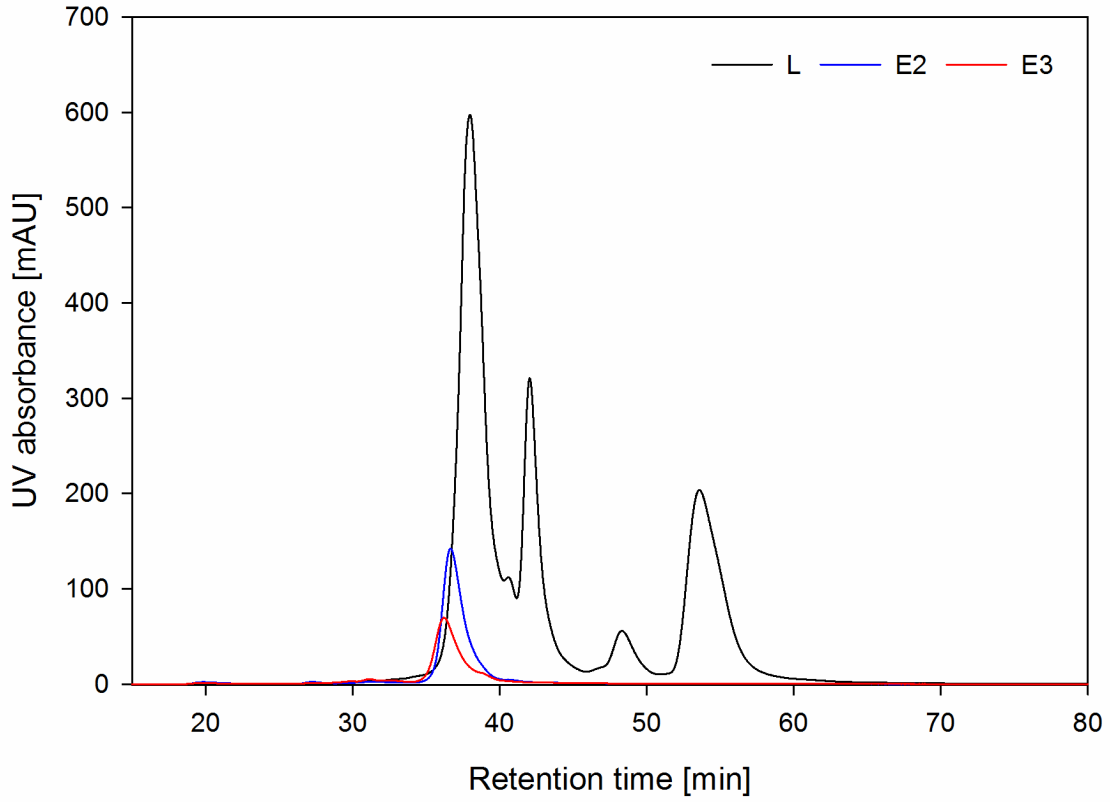

Figure S2: UV280 absorbances for analysis of the loading material (L) and the main elution fractions E2 and E3 from the purification run represented in Figure 1 by HPLC-SEC.

96 Figure S2

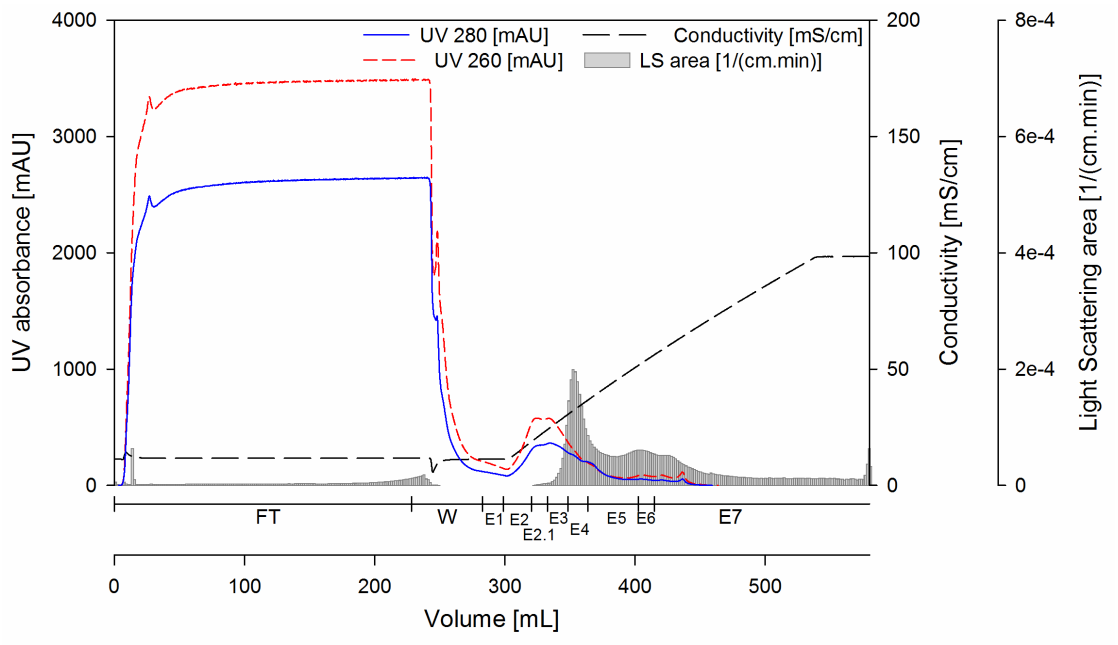

97

98

Figure S2: Chromatographic purification of HIV-1 gag H1 VLPs from baculovirus produced in *Tnms*42 insect cells on a 9.5 mL Fractogel®-TMAE column, using a linear gradient elution from 100-1000 mM NaCl (Buffer A: 50 mM HEPES, pH 7.2; Buffer B: 50 mM HEPES, 2 M NaCl, pH 7.2). Column was loaded with 25 CV. The loading material previously stored at -80°C, was thawed, endonuclease treated and filtered (3 µm). Grey bars represent the area under the curve of the light scattering intensity (LS) measurements performed on MALS detector. FT: flow-throug, E1-E7: elution fractions 1-7

109 Figure S3

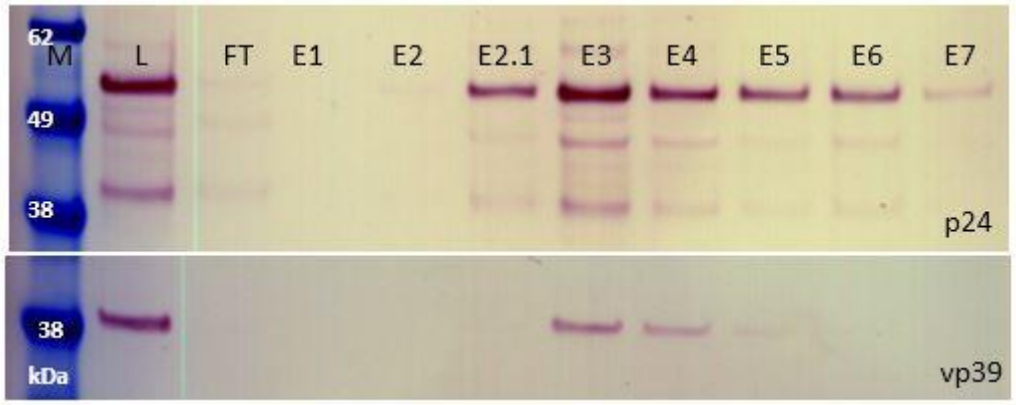

110

111

Figure S3: Characterization of the pooled fractions from the Fractogel®-TMAE repetition run using *Tnms*42 cell culture supernatant represented in Figure S3. Western blots against the specific capsid proteins HIV-1 p24 and vp39 for VLP and baculovirus detection, respectively. M: molecular weight marker, L: loading material (c-LEcta Denarase® treated and filtered), FT: flow-through, E1-E7: elution fractions 1-7.

120 Table S1: Total mass balance of the purification run using Fractogel®-
121 TMAE for the separation of HIV-1 gag H1 VLPs and baculovirus, using a
122 17.9 mL packed column. S: Tnms42 cell culture supernatant containing
123 HIV-1 gag H1 VLPs and BV, L: loading material (endonuclease treated
124 and filtered); FT1-5: flow-through fractions 1-5; W: wash; E1-E7: elution
125 fractions 1-7, R: regeneration (100% B), CIP: cleaning-in-place (0.5 M
126 NaOH).

sample	volume [mL]	particles (1-1000nm) [part/mL]	*r*ecovery [%]	particles (100-200nm) [part/mL]	recovery [%]	total protein [µg/mL]	dsDNA [ng/mL]
S	501	-	-	-	-	249.5	1583.6
L	501	2.60E+10	100%	1.80E+10	100%	221.6	683.8
FT1	100.2	1.30E+09	1%	9.40E+08	1%	77.6	199.6
FT2	100.2	1.30E+09	1%	9.40E+08	1%	119.8	325.6
FT3	100.2	1.60E+09	1%	1.20E+09	1%	99.2	345.6
FT4	100.2	1.20E+09	1%	9.30E+08	1%	114.8	338.4
FT5	100.2	3.90E+08	0%	9.70E+07	0%	123.2	369.5
W	107.4	5.90E+08	0%	3.54E+09	0%	< LLOQ	87.4
E1	60.8	1.50E+09	1%	1.30E+09	1%	55	41.5
E2	35.2	6.00E+10	16%	4.90E+10	19%	204.9	204.2
E3	32	4.00E+10	10%	2.90E+10	10%	252	173.1
E4	36.8	1.40E+10	4%	9.30E+09	4%	158.1	115
E5	70.4	1.30E+10	7%	8.50E+09	7%	192.7	460.5
E6	57.6	5.90E+09	3%	3.60E+09	2%	210.1	837.5
E7	199.5	5.00E+08	1%	2.90E+08	1%	< LLOQ	39.1
R	71.6	n.d.	n.d.	n.d.	n.d.	< LLOQ	< LLOQ
CIP	52.8	n.d.	n.d.	n.d.	n.d.	81.2	< LLOQ
Sum			**45%**		**48%**		

127

128 n.d.: not determined

129 < LLOQ: under the lowest limit of quantification

130

131 Table S2: Characterization of the pooled fractions from the Fractogel®-
132 TMAE repetition represented in Figure S3. L: loading material
133 (endonuclease treated and fitlered), E2.1 and E3: main elution fractions

sample	volume [mL]	virus infectivity [TCID50/mL]	log reduction
L	236.3	3.0E+06	-
E2.1	12.8	1.9E+03	4.3
E3	16.0	1.9E+04	3.2

134